PNL--8476

DE93 006820

FINAL REPORT

1/12-SCALE PHYSICAL MODELING EXPERIMENTS IN SUPPORT OF TANK 241-SY-101 HYDROGEN MITIGATION

J. A. Fort
J. A. Bamberger
J. M. Bates
C. W. Enderlin
M. R. Elmore

January 1993

Prepared for
the U.S. Department of Energy
under Contract DE-AC06-76RLO 1830

Pacific Northwest Laboratory
Richland, Washington 99352

SUMMARY

Scaled experiments were performed to support the Tank 241-SY-101 Hydrogen Mitigation Project. The experiments were conducted in a 1/12-scale model of the tank using a 1/12-scale model of the proposed mixing pump. A similarity analysis of sludge mobilization and slurry suspension was used to scale the experiments. The analysis yielded nine dimensionless parameters. The scaling parameters define the desired simulant properties required to conduct these 1/12-scale experiments, as well as the operating parameters for the mixer pumps. No attempt was made to duplicate waste chemical behavior or gas release. The simulant was chosen to emulate the fluid dynamical and rheological behavior only.

A number of simplifying assumptions were made in the design of this experiment. Among those were that tank internals, other than the mixing pump itself, would have a negligible effect on the flow field; neither would the centering of the model pump assembly in the tank instead of an 8 percent radial offset as proposed for the full-scale tests. Another assumption was that the crust layer would have a similarly negligible affect on the flow field. Specific limitations of this work include

1. an imperfect knowledge of tank 241-SY-101 waste properties
2. simulants were two phase (solid particulate and liquid); no gas phase was included to enable modeling of that parameter
3. differences existed between some model and full-scale dimensionless parameters.

Item 1 of these will improve with further characterization. Item 2 makes this experiment conservative from the standpoint of mobilization; a settled solids layer permeated with gas would be easier to break up with a fluid jet. However, even if the distribution of gas was known, this distribution would be extremely difficult to simulate experimentally. The item 3 limitation could be overcome with more time to improve the simulant recipes. In general, the dimensionless parameter differences are conservative.

Three types of scaled experiments were performed: flow visualization, model validation, and operating parameter. The flow visualization experiments

examined transient and steady-state tank flow fields for fixed jets. The model validation tests were used to gather detailed velocity and concentration measurements in water and simulants using fixed mixing jets. The operating parameter tests mimicked the proposed pump operation in tank 241-SY-101 and were used to investigate solids mobilization and suspension for mixing jets rotated in fixed increments about the tank centerline.

The scaling analysis was used to extrapolate the operating parameter test results to the full-scale tank. This led to the following conclusion: To the extent that this scaled experiment duplicated tank 241-SY-101 (gas phase was not simulated), it may be inferred that operation of the proposed mixing pump at full speed (88 ft/s jet velocity) would suspend a minimum of 66 percent of the tank solids, and settled sludge would be dislodged, at least intermittently, from the entire tank floor. This is based on an operating sequence of 104 min in successive 30-degree sectors of the full-scale tank with a 7-min pump rest time between assembly rotations. This prediction should be tempered by the knowledge that, as stated above, tank 241-SY-101 is not perfectly modeled by this experiment.

ACKNOWLEDGMENTS

The work described in this report was conducted for the Tank 241-SY-101 Hydrogen Mitigation Project. The project manager is J. W. Lentsch (Westinghouse Hanford Company). Direction and project management support was provided by M. R. Kreiter and J. C. Colson, both of Pacific Northwest Laboratory.

M. S. Greenwood and J. L. Mai supported the ultrasonic concentration measurements and data reduction and provided the description of the technique in Appendix A. The authors especially wish to thank K. D. Hinkle, Pacific Northwest Laboratory, for the many and timely contributions that allowed the tests to run smoothly.

CONTENTS

FIGURES

TABLES

NOMENCLATURE

A	area
cP	centipoise
DAS	data acquisition system
em	electromagnetic
Fr	Froude number
Fr_d	densimetric Froude number
$f_{s0}(\epsilon_s)$	functional variation of settling velocity with concentration
$f_\mu(\Delta,\epsilon_s)$	functional dependence of viscosity
g	acceleration caused by gravity
H_t	height of fluid in tank
m	mass
N_ρ	density ratio
N_τ	stress ratio
PNL	Pacific Northwest Laboratory
r	radial position
Re_H	Reynolds number based on fluid height in the tank
RS	received signal
S.G.	specific gravity
T_0	period of jet oscillation
V	volume
V_s	particle settling velocity ratio
V_{s0i}	velocity at which an individual solid waste particle would settle if immersed in a fluid with reference mixture viscosity μ_{eo}
W_0	jet nozzle exit velocity

WHC	Westinghouse Hanford Company
wt%	weight percent
z	vertical position

Greek Letters

Δ	local fluid strain rate
ϵ_s	mean solids volume fraction
η_t	inverse time parameter
θ	angular position
μ_e	effective viscosity
μ_{e0}	effective mixture viscosity measured at the mean tank solids volume fraction and reference strain rate
ρ_j	jet density
ρ_l	supernatant (liquid) density
ρ_m	mixture density
ρ_s	solids density
τ_{ss}	shear strength

1.0 INTRODUCTION

Hanford tank 241-SY-101 is a 75-ft-dia double-shell tank that contains approximately 1.1 M gal of radioactive fuel reprocessing waste. Core samples have shown that the tank contents are separated into two main layers, a particle laden supernatant liquid at the top of the tank and a more dense slurry on the bottom. Two additional layers may be present, one being a potentially thick sludge lying beneath the slurry at the bottom of the tank and the other being the crust that has formed on the surface of the supernatant liquid. The supernatant is more commonly referred to as the convective layer and the slurry as the non-convective layer. The tank dimensions and distribution of tank contents are shown in Figure 1.1.

Tank 241-SY-101 is well known for its brief episodic releases of hydrogen gas in potentially flammable concentrations. These releases, otherwise known as burps, may be of sufficient volume that the lower flammability limit is exceeded for brief periods of time in the tank free space (above the waste) after the event (Babad et al. 1992). Purge air rapidly dilutes the hydrogen to safe levels, but the short-term hazard is enough to have tank 241-SY-101 labelled as the U.S. Department of Energy's top safety concern. Accumulation of gas (partly hydrogen) in the non-convective layer is suspected to be the key mechanism behind the gas burp phenomena, and several mitigation schemes are being developed to encourage a more uniform gas release rate (Benegas 1992).

The first mitigation scheme planned for testing is hydraulic agitation with horizontal mixing jets suspended into the slurry layer from the tank dome. The pump and jet nozzle arrangement for this test is illustrated in Figure 1.1. Design of the mixer pump system requires testing to determine the operating parameters necessary to mobilize the settled solids and maintain the solids in suspension. Examples of operating parameters include jet nozzle diameter, jet flow rate, and required duration and sequence of jet nozzle operation at specified positions. Testing is also necessary to support

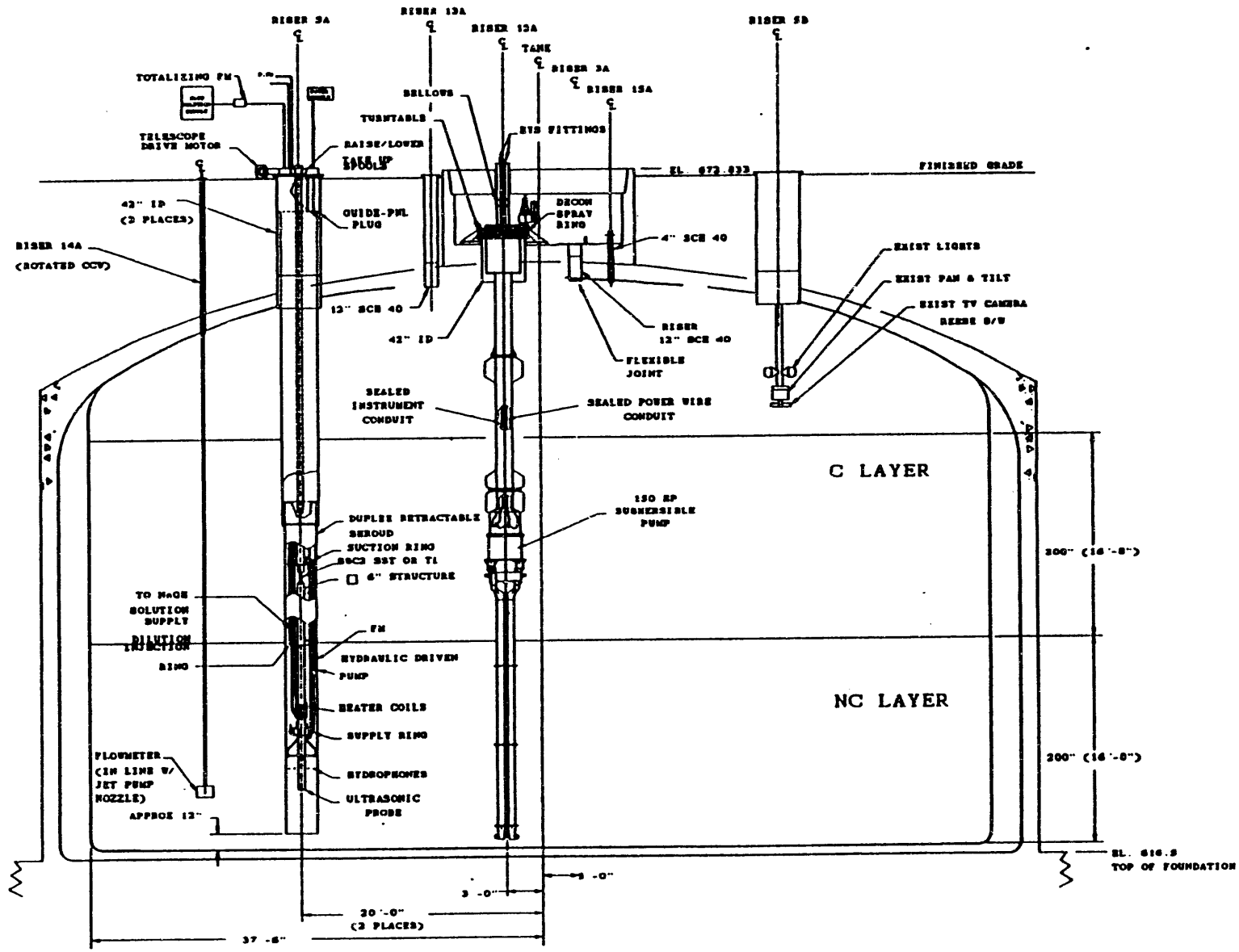

FIGURE 1.1. Tank 241-SY-101 Configuration for Hydrogen Mitigation Test (from WHC-SD-WM-FDC-022, Rev. 0, pg. 2-2)

ongoing analytical and numerical modeling of this mitigation concept. Full-scale experiments are not practical because a suitable testing facility does not exist. Therefore, reduced-scale tests were performed.

The value of the information obtained from these reduced-scale experiments depends on the effective use of scaling analysis in the experimental design. The results of a scaling analysis are included in this report to identify the required scaled test parameters and to provide a basis for extrapolating results to a full-scale condition. Limitations of the scaling laws are also discussed. The biggest limitation is the uncertainty regarding tank 241-SY-101 waste contents properties.

1.1 OBJECTIVES

To support the full-scale hydraulic mitigation test, scaled experiments were performed to satisfy two objectives:

1. provide an experimental database for numerical model validation
2. establish operating parameter values required to mobilize the settled solids and maintain the solids in suspension.

As will be shown, it is difficult to extrapolate reduced-scale parameter values to the full-scale tank. This is because of uncertainties in waste properties and the inability to model the gas phase in the scaled experiment.

1.2 SCOPE OF WORK

Three sets of scaled experiments were performed: 1) experiments to visualize jet flow patterns, 2) experiments to provide data sets for code validation, and 3) dynamically scaled experiments to provide data to determine full-scale operating parameters from scaled tests. This report describes the experiments conducted in Pacific Northwest Laboratory's (PNL)[a] 1/12-scale facility.

(a) Operated for the U.S. Department of Energy by Battelle Memorial Institute under Contract DE-AC06-76RLO 1830.

With two exceptions, the experiments are geometrically scaled representations of the full-scale mixing pump design proposed in July 1992 and are based on the understanding of tank 241-SY-101 waste properties at that time. Using this minimal knowledge of the waste properties of tank 241-SY-101, simulants were developed for both liquid and solid waste, each with the desired characteristics determined in the scaling analysis. The gas phase of the waste was not simulated in the experiments.

The two exceptions to geometric similarity are 1) the jet nozzle assembly was positioned at the tank centerline for all 1/12-scale experiments, and 2) tank internals were excluded (other than the mixing pump). The tank center position was used despite the full-scale mixer pump location being 3-ft (8 percent radial) offset from the centerline of the 75-ft-dia tank, as shown in Figure 1.1. This small offset is estimated to have little influence on flow patterns in the tank induced by the mixer pump dual-opposed jets. A pair of flow visualization tests in water (one with the mixer pump positioned at the tank centerline, the other with an offset mixer pump) was performed to verify this assertion. The centerline position provided a plane of symmetry through the tank centerline, thereby reducing the computational modeling grid by 50 percent. The excluded tank internals consisted of velocity, density, and temperature instrument trees (VDTTs) and multiple instrument trees (MITs) that are contained in 3-in. pipes.

1.3 ORGANIZATION OF REPORT

The summary and conclusions of the tests are given in Section 2. Section 3 discusses the experimental approach including the similarity analysis used to determine test parameters. The instrumentation and the measuring techniques applied during testing are described in Section 4. The results of all of the tests are presented in Section 5. Section 6 is a list of references.

A prototypic ultrasonic concentration probe developed at PNL was used to take concentration profiles during testing. The theory and operation of the ultrasonic probe is explained in Appendix A. The data from all of the tests conducted are included in Appendix B. Appendix C describes the uncertainties associated with both the experimental and reduced data. The mixing efficiency

based on the particle size distributions being suspended in the supernatant is discussed in Appendix D. At the completion of the 1/12-scale testing the jet nozzles showed evidence of erosion. Post-tests were conducted to help determine if the erosion had any effect on the test results; results of these tests are included in Appendix E.

2.0 CONCLUSIONS

Three types of tests were performed: flow visualization, model validation, and operating parameter. The flow visualization experiments examined transient and steady-state tank flow fields for fixed location jets. The model validation tests were used to gather detailed velocity and concentration measurements in water and simulants using fixed (nonrotating) mixing jets. The operating parameter tests mimicked the proposed pump operation in tank 241-SY-101 and were used to investigate solids mobilization and suspension for jets rotated in fixed increments about the tank centerline. Observations from these scaled experiments include the following:

- Flow Visualization (in water)
  - Jets were turbulent and well balanced for all cases studied.
  - Centerline versus offset pump tests gave similar results and supported performing remainder of tests with a centered mixer pump.
  - Transient test results are useful for code validation.
- Flow Visualization (in simulant)
  - Supernatant layer was generally too cloudy for effective visualization.
  - Techniques are available for improving supernatant layer clarity.
  - Observations of the settled solids interface during a start-up transient showed that the mixing action was always confined within the slurry layer.
- Model Validation (in water)
  - Velocity profile datasets were successfully collected.
  - Pitot probes and electromagnetic probes gave comparable results.
  - An abrupt downward shift in the elevation of the peak jet velocity was observed at a jet velocity of approximately 50 ft/s.
- Model Validation (in simulant)
  - pitot probes were not usable because of variations in reference leg pressure resulting from density gradients in the tank.

- Electromagnetic probes were successfully used to measure velocities in the simulant.

- The abrupt downward shift in the jet was the same as in the water tests, except that this phenomenon occurred at higher velocities.

- Considering measurement uncertainty, no significant differences were observed between steady-state, centerline velocity profiles for water and simulant.

- A 15 ft/s jet velocity was not capable of clearing settled sludge off the tank floor all the way to the tank wall.

- The 15-ft/s jet velocity produced a stratified flow field at the steady state; 25-ft/s and higher jet velocities always circulated solids to the tank surface.

· Operating Parameter

  - The slurry interface rose more slowly for the rotated jets used in these tests than for the fixed location jets used in the model validation tests.

  - Solids suspension was more effective for the rotated jets used in these tests than for the fixed location jets used in the model validation tests.

  - Percent solids suspended with a 25-ft/s jet was 66 to 72 percent in the high viscosity simulant and 59 to 67 percent in the low viscosity simulant.

  - Percent solids suspended with a 50-ft/s jet was 74 to 81 percent in the low viscosity simulant.

  - A 25-ft/s jet velocity was adequate to clear settled solids from the tank floor all the way to the tank wall for both simulants.

The scaling analysis was used to relate the reduced scale results to the full scale to determine implications for tank 241-SY-101. Operating parameter test results led to the following conclusion.

To the extent that this scaled experiment duplicated tank 241-SY-101, it may be inferred that operation of the proposed mixing pump at full speed (88-ft/s jet velocity) would suspend a minimum[a] of 66 percent of the tank

---

(a) The assumption is that a greater suspension of solids would be achieved in the gas permeated settled layer in tank 241-SY-101 than was achieved without gas in these scaled experiments.

solids, and settled sludge would be dislodged, at least intermittently, from the entire tank floor. This is based on an operating sequence in the full-scale tank of 104 min in each successive 30-degree sector of the tank with a pump rest time of 7 min between assembly rotations. These operating times result in one complete rotation of the mixing jet assembly in a 24-h period. This prediction should be tempered by the knowledge that tank 241-SY-101 is not perfectly modeled by this experiment.

From the model validation test results, it may be concluded that the abrupt downward shift of the jet observed during scaled-model testing is not expected to impact mixing in the full scale because this phenomena would occur at jet velocities in excess of the proposed mixing pump's capabilities.

3.0 EXPERIMENTAL APPROACH

Hydraulic mixing techniques are proposed to mitigate gas accumulation in tank 241-SY-101. The basic assumption underlying the concept of hydraulic mitigation is that mobilization or maintained suspension of settled solids that accumulate at the bottom of the tank will prevent gas accumulation. Engineering of proposed hydraulic technology will require testing to determine the operating parameters required to mobilize the solids and to maintain these solids in suspension. Full-scale testing is extremely expensive and difficult to implement; therefore, scaled tests were designed to assess the merit of the proposed mixing technique and to provide data to support numerical and analytical modeling.

A necessary compromise in the scaled experiment was to exclude a gaseous phase in the simulated waste. This is justified by the assumption that a greater suspension of solids would be achieved in the gas-permeated settled layer in tank 241-SY-101 than was achieved without gas in these scaled experiments. Therefore, this compromise is conservative in terms of predicting solids suspension in the full-scale tests.

Experiments were designed to be conducted in an existing model of a 75-ft-dia, double-shell tank, constructed to 1/12 scale. The similarity analysis that supports design of these experiments is discussed in Section 3.1. Properties of tank 241-SY-101 contents on which the tests are based, including the mixing pump parameters, are provided in Section 3.2. Parameters for the 1/12-scale experiment with measured physical and rheological properties of the waste simulant are discussed in Section 3.3.

3.1 SIMILARITY ANALYSIS

Mitigating gas accumulation in tank 241-SY-101 will require two stages of action: 1) mobilizing of the sludge layer at the bottom of the tank and 2) maintaining these solids in suspension until slurry is removed from the tank. Mobilization may be accomplished by a natural overturn caused by a gas-release event; however, maintaining solids in suspension will be required after the event ceases. Separate physical mechanisms are involved in solids mobilization and suspension.

Liljegren[a] developed a scaling law analysis to describe hydraulic mitigation of tank 241-SY-101. The analysis was based on the theory of similitude, which requires geometric, kinematic, and dynamic similarity between the prototype and scale model. Geometric similarity dictates that all linear dimensions of the model must relate to the prototype by a constant scale factor. Kinematic similarity dictates that velocities at any two points in the similar tanks must be in the same direction and all velocities will relate by a constant scale factor; likewise, for dynamic similarity, the force distribution must scale linearly between the prototype and model.

3.1.1 Dimensionless Parameters

Liljegren[a] defined nine matching parameters to ensure hydrodynamic similarity between fluid motion in scaled experiments and in tank 241-SY-101. These parameters are used to define simulant properties and operating conditions required to conduct scaled experiments. Four parameters define the simulant properties; five parameters define the jet operating conditions. These parameters are summarized in Table 3.1.

3.1.1.1 Mean Solids Volume Fraction

Mean solids volume fraction, ϵ_s, influences the magnitude of density variations in the tank and defines the volume percent of solids in the tank.

3.1.1.2 Functional Variation of Settling Velocity with Concentration

Functional variation of settling velocity with concentration, $f_{so}(\epsilon_s)$, describes how settling velocity varies with concentration and affects the settling velocity ratio.

(a) Based on a 1992 draft PNL report by L. M. Liljegren entitled Similarity Analysis Applied to the Design of Scaled Tests of Hydraulic Mitigation Methods for 241-SY-101.

TABLE 3.1 Summary of Dimensionless Parameters

Parameter	Definition
ϵ_s	mean solids volume fraction
$f_{so}(\epsilon_s)$	functional variation of settling velocity with concentration
$f_\mu(\Delta,\epsilon_s)$	functional dependence of viscosity
N_ρ	density ratio
Fr	Froude number
V_s	particle settling velocity ratio
η_t	inverse time parameter
N_τ	stress ratio
Re	Reynolds number

3.1.1.3 Functional Dependence of Viscosity

Functional dependence of viscosity, $f_\mu(\Delta,\epsilon_s)$, defines how viscosity changes with concentration and strain rate. The effective viscosity (μ_e) obeys the general form

$$\mu_e = \mu_{e0}\, f_\mu(\Delta,\, \epsilon_s) \qquad (3.1)$$

where μ_{e0} = effective mixture viscosity measured at the mean tank solids volume fraction (ϵ_s) and the arbitrarily selected reference strain rate $\Delta = W_0/H_t$

W_0 = jet nozzle exit velocity

H_t = height of fluid in tank.

3.1.1.4 Density Ratio

Density ratio, N_ρ, describes the density difference between the solids and the mixture and appears in both mixture continuity and momentum equations.

$$N_\rho = (\rho_s - \rho_l)/\rho_m \quad (3.2)$$

where ρ_s = solids density

ρ_l = supernatant (liquid) density

ρ_m = $\rho_l + (\rho_s - \rho_l)\ \epsilon_s$ = mixture density.

3.1.1.5 Froude Number

Froude number, Fr, describes the general effect of density differences on jet motion.

$$Fr = W_0/(g\ H_t)^{0.5} \quad (3.3)$$

where g = acceleration caused by gravity.

The Froude number describes the ability of the jet to carry solids to the upper regions of the tank. The importance of the densimetric Froude number (Fr_d) was identified by Fossett et al. (1949) and Fossett and Prosser (1951) during an experiment designed to study the effect of the Reynolds number on mixing using jets. Qualitative observations indicated that both the jet density (ρ_j) ratio, $(\rho_j - \rho_m)/\rho_m$, and Reynolds number have a dramatic effec on the motion of a jet. When the Froude number of the dense jet was low, the jet could not rise to the upper regions of the tank. When a surface crust is absent, the Froude number also describes the degree of surface rippling.

3.1.1.6 Settling Velocity Ratio

Settling velocity ratio, V_s, describes the tendency of suspended particles to settle.

$$V_s = V_{s0i}/W_0 \quad (3.4)$$

where V_{s0i} = velocity at which an individual solid waste particle would settle if immersed in a fluid with reference mixture viscosity μ_{eo}.

3.1.1.7 Inverse Time Parameter

Inverse time parameter, η_t, describes the effect of the time dependence of the jet on the behavior of tank contents.

$$\eta_t = H_t/(T_0\ W_0) \tag{3.5}$$

where T_0 = period of jet oscillation.

3.1.1.8 Stress Ratio

Stress ratio, N_τ, describes the ability of the jet to erode settled slurry; it represents the ratio of dynamic pressure of the jet to the shear stress of the sludge.

$$N_\tau = (\rho_m\ W_0^2)/\tau_{ss} \tag{3.6}$$

3.1.1.9 Reynolds Number

Reynolds number, Re_H, based on height of fluid in the tank describes the degree of turbulence in the tank.

$$Re_H = (\rho_m\ W_0\ H_t)/\mu_{e0} \tag{3.7}$$

where μ_{e0} = effective mixture viscosity.[a]

3.2 FULL-SCALE TANK (241-SY-101) PARAMETERS

Together with the scaling analysis, parameter values for the full-scale tank (241-SY-101) form the basis for the scaled experiment. Relevant full-scale parameters are summarized in this section, and are grouped according to geometry, waste properties, and proposed mixing pump operation. Dimensionless parameters are calculated from tank 241-SY-101 data and are presented last.

(a) Measured at a mean tank solids volume fraction and the reference strain rate.

This information was obtained from a number of sources, including discussions with other project personnel. Documents are referenced when available.

3.2.1 Tank and Mixing Pump Geometry

The full-scale tank dimensions and relative placement of the mixing pump were shown in Figure 1.1. The pump suction is in the convective layer at the base of the submerged pump. Fluid is discharged equally between two opposed nozzles near the tank floor. Geometric parameters used for modeling the full-scale tank and mixing pump are listed in Table 3.2.

3.2.2 Waste Properties

The waste in tank 241-SY-101 has been characterized as having three layers. Beginning at the bottom of the tank these layers are 1) non-convective, 2) convective, and 3) crust. Reynolds estimated the depth of the non-convective layer as between 160 and 170 in., the top of the convective layer as 370 in., and the top of the crust at 410 in.[(a)] Average values were used for modeling purposes: 165 in. for the depth of the non-convective layer and 400 in. for the total depth.

TABLE 3.2. Full-Scale Tank and Mixing Pump Geometrical Parameters

Parameter	Value
tank inside diameter	75 ft
nozzle diameter	2.6 in.
height of nozzle centerline	32 in.
tank/pump centerline offset	3 ft
pump centerline to nozzle exit	14.4 in.
pump suction height	264 in.

(a) Dan Reynolds, "Layers in 101-SY", WHC memo to Jeff Grover, April 14, 1992.

The use of tank 241-SY-101 physical and rheological properties in the design of a scaled experiment is discussed by Liljegren.[a] The analysis was based on core sample analyses conducted by J. M. Tingey.[b][c] A summary of waste properties used for tank 241-SY-101 is given along with the previously mentioned layer depths in Table 3.3.[d]

TABLE 3.3. Tank 241-SY-101 Waste Properties

Parameter	Value
particle diameter	12 to 150 μm
solids density	2.31 g/cm^3, (calculated using Tingey's data with 0.44 packing factor)
convective layer density	1.46 g/cm^3
mixture density	1.59 g/cm^3
convective layer viscosity	13 cP @ 65°C
sludge shear strength	4000 dynes/cm^2
particle settling velocity	0.7 in./hr, calculated for 12 μm 113 in./hr, calculated for 150 μm
non-convective layer depth	165 in.
total waste depth	400 in.

(a) Based on the draft PNL report by L. M. Liljegren footnoted on pg. 3.2.

(b) Draft PNL report by J. M. Tingey entitled Physical Characterization of Tank 101-SY Core Samples from Window C, February 1992.

(c) Draft PNL report by J. M. Tingey entitled Rheological Properties of Waste from Tank 101-SY, May 1992.

(d) Particle size distribution was measured from a variety of samples. These data are listed and discussed in WHC-SD-WM-DTR-024, Rev 0, pp. 7-16, 7-17, and F-1 to F-22. 12 μm was chosen as an average value; 150 μm represents an upper bound.

The convective layer and mixture densities are averages for Tingey's measurements from six core sample segments spanning the tank depth. Solids density is calculated using average values of convective layer and centrifuged solids density, together with an estimate of the mean solids volume fraction for the centrifuged solids. Liljegren[a] estimated this volume fraction for uniformly sized close-packed spheres; this value is 0.74. To refine this estimate the packing fractions of two samples of Minusil-30[b] and two samples of kaolin of known weight percent (wt%) solids were determined from centrifuged solids. For these cases based on an initial wt% solids of 31 percent, the volume packing fractions of Minusil-30 samples were 0.50 and 0.47 and kaolin samples were each 0.40; an average of the four samples provides an average volume fraction of 0.44. This value is consistent with some observations made by analysts at Westinghouse. Their findings show that "centrifuged solids contain a substantial fraction of interstitial liquid, generally more than half, by weight."

The convective layer viscosity is an average of measurements Tingey made for the samples taken above 171 in. in the tank. Because the convective layer contains roughly 10 volume percent solids, the convective layer viscosity is greater than the pure liquid value, but it is also considerably less than the bulk viscosity for the entire tank. Allemann has estimated a convective layer liquid viscosity of 11 cP and a mixed slurry viscosity of between 100 and 200 cP for the non-convective layer.[c]

The shear strength given in Table 3.3 is Tingey's measurement for Segment 22, which is in the sludge layer within 19 in. of the tank bottom. Finally, the particle settling velocity is calculated using two representative particle diameters, 12 and 150 μm, and the 13 cP convective layer viscosity.

(a) Based on the draft PNL report by L. M. Liljegren footnoted on pg. 3.2.

(b) Sized SiO_2, manufactured by U.S. Silica Co., Pacific, Missouri.

(c) R. T. Allemann, "Viscosity and Shear Strength of 241-SY-101 Slurry," memo to M. R. Kreiter, Pacific Northwest Laboratory, June 3, 1992.

3.2.3 Proposed Mixing Pump Operating Parameters

The mitigation operating parameters for the full-scale mixer pump are defined in the proposed test plan.[a] The pump is to be started at 200 rpm at one position and then raised to the full pump speed of 1180 rpm in 200 rpm increments. This condition is maintained until a steady hydrogen concentration is measured or for a minimum of 1 h. With the pump speed reduced to 200 rpm, the pump and nozzle assembly is then rotated 30 degrees and the process repeated, as it is again at 30-degree increments around the tank centerline. Upon completing the first tank sweep, the pump is stopped and the tank allowed to rest for 24 h. In subsequent tank sweeps, the precautionary incremental increase in pump speed at each position is eliminated and the pump is started at full speed. Jet velocities corresponding to the range of pump speeds are 15 ft/s at 200 rpm and 88 ft/s at the full-speed value of 1180 rpm.

The actual test procedure will likely be different but, because the changes cannot be anticipated, this proposed procedure was used in the design of the experiment.

3.2.4 Dimensionless Parameters

Full-scale values of the dimensionless parameters can be calculated using equations from Section 3.1.1 and the tank 241-SY-101 geometry and property values listed above. Table 3.4 gives dimensionless parameter values for two jet velocities representing the minimum and maximum values in the full-scale test.

Calculation of the first five parameters in Table 3.4 is straight forward. Calculation of mean solids volume fraction is less direct. This parameter is not measured directly when samples from tank 241-SY-101 are characterized. Volume of settled solids, volume of centrifuged solids and wt% water are measured and reported. Not enough information is available from this data to directly calculate the solids volume fraction; however, the value can be bounded. Physical packing limitations exist; therefore, the solids volume fraction must be less than the volume fraction of centrifuged solids.

(a) T. M. Burke, "Draft Test Plan for Tank 101-SY Mitigation-by-Mixing Test," 23230-92-TMB-010, memo to M. R. Kreiter, Pacific Northwest Laboratory, April 22, 1992.

TABLE 3.4. Dimensionless Parameter Values Based on Tank 241-SY-101

Parameter	15 ft/s jet velocity	88 ft/s jet velocity
Froude Number, Fr	0.46	2.7
Reynolds Number, Re_H	5.6×10^6	33×10^6
stress ratio, N_τ	83	2856
settling velocity ratio, V_s	1.1×10^{-6} to 1.8×10^{-4}	1.9×10^{-7} to 3.0×10^{-5}
density ratio, N_ρ	0.53	0.53
mean solids volume fraction, ϵ_s	0.18	0.18

As stated in Section 3.2.2, the volume fraction of centrifuged solids has been estimated as 0.44. Based on this volume fraction and the measured value of volume percent centrifuged solids for tank 241-SY-101, the average estimated solids volume fraction is calculated to be 18 percent.[(a)]

3.3 1/12-SCALE EXPERIMENT PARAMETERS

Nominal parameter values for the 1/12-scale experiment are established in this section. Relevant parameters are grouped according to geometry, waste properties, and proposed mixing pump operation.

3.3.1 Tank and Mixing Pump Geometry

Geometrical parameters used for modeling the 1/12-scale tank and mixing pump are listed in Table 3.5. Differences between nominal and actual values are explained in Section 5.0.

(a) Estimated solids volume fraction = (packing fraction) (volume % centrifuged solids).

TABLE 3.5. 1/12-Scale Tank and Mixing Pump Geometrical Parameters

Parameter	Value
tank inside diameter	75 in.
nozzle diameter	2.6/12 = 0.217 in.
height of nozzle centerline	32/12 = 2.667 in.
tank/pump centerline offset	3 in. for some flow visualization tests, centered for remainder of tests
pump centerline to nozzle exit	14.4/12 = 1.20 in.
pump suction height	264/12 = 22.0 in.

3.3.2 Nominal Waste Simulant Properties

In the discussion that follows, tank 241-SY-101 waste properties cited in Table 3.2 are used with results from the scaling analysis to propose values for the 1/12-scale experiments. The basic approach is to match all nine dimensionless parameters to the full-scale values. This section is labelled "nominal" waste properties because it may not be feasible to obtain materials with these properties. Actual property values obtained in the waste simulants are given in Section 5.1.

3.3.2.1 Mean Solids Volume Fraction

To perform scaled experiments, mean solids volume fraction, ϵ_s, must be equal in tank 241-SY-101 and the 1/12-scale tank. As listed in Table 3.4, the full-scale value is 0.18; therefore,

$$\epsilon_{s,x} = \epsilon_{s,SY} = 0.18 \tag{3.8}$$

where subscript x refers to the 1/12-scale experiment and subscript SY refers to tank 241-SY-101.

3.3.2.2 Component Densities

If $\epsilon_{s,x}$ matches at 1/12 scale and in tank 241-SY-101, the requirement of matched density ratio can be expressed by matching ρ_s/ρ_l, the density ratio of solids to liquid. From Section 3.2,

$$N_{\rho,SY} = 0.53$$

This is based on

$$\epsilon_{s,x} = \epsilon_{s,SY} = 0.18$$

$$\rho_{s,SY} = 2.31 \text{ g/cm}^3$$

$$\rho_{l,SY} = 1.46 \text{ g/cm}^3$$

$$\rho_{m,SY} = 1.59 \text{ g/cm}^3$$

The 1/12-scale simulant was based on Minusil-30 as the particulate. The solids density of Minusil-30 is 2.65 g/cm^3. Therefore, based on a mean solids volume fraction of 0.18 and a density ratio of 0.53, the mixture density and liquid density are calculated to be

$$\rho_{s,x} = 2.65 \text{ g/cm}^3$$

$$\rho_{l,x} = 1.67 \text{ g/cm}^3$$

$$\rho_{m,x} = 1.85 \text{ g/cm}^3$$

Unfortunately, liquid densities of 1.67 g/cm^3 are not practical. Saturated aqueous solutions of heavy metal salts can approach 1.5 g/cm^3, but these are hazardous materials and cannot be easily handled or disposed of. The approach followed instead, was to match the target mixture viscosities and settled layer shear strength and accept the resulting liquid density.

3.3.2.3 Viscosity

The difficulties of selecting a simulant viscosity are discussed by Liljegren[(a)]. "In principle similarity may be achieved at any scale provided that slurries with suitable properties may be manufactured. ... In practice, certain arbitrary properties are difficult to achieve. It is anticipated that achieving a simulant with the appropriate viscosity will impose the primary impediment to performing tests in an appropriate sized

---

(a) Based on the draft PNL report by L. M. Liljegren footnoted on pg. 3.2.

tank. Other similarity criteria may be difficult to achieve such as the need to match the correct settling velocity, but the difficulties in achieving them are not affected by the experimental scale."

Table 3.3 gives the viscosity of the convective layer as 13 cP at 65°C, and the mixture density as 1.59 g/cm^3; the corresponding kinematic viscosity is 8.2 x 10^{-6} m^2/s. Matching Froude and Reynolds numbers, similarity could be achieved in a 1/12-scale tank with a kinematic viscosity of 0.2 x 10^{-6} m^2/s. Assuming that the density of the simulant is also 1.59 g/cm^3, this would require a simulant viscosity of 0.3 cP.

This viscosity is low relative to common fluids. For example, the viscosity of water is approximately 1 cP at 20°C. The challenge involved in making a 0.3 cP simulant is made even more daunting when considering that the simulant must include a representative fraction of suspended solids.

Since achieving the desired viscosity is clearly not practical, Liljegren[(a)] recommends using two distinct viscosities, such as 3 and 10 cP, while holding other simulant properties constant. The behavior at desired viscosity will then be obtained by extrapolation. The viscosity values will be used to adjust the values obtained for particle settling velocity, which also depends on viscosity. The method used in extrapolation will be discussed in Section 5.4.4.

3.3.2.4 Functional Dependence of Viscosity

Likewise the 1/12-scale functional dependence of viscosity on concentration and shear rate must match that of tank 241-SY-101. The simulant and tank 241-SY-101 mixture should exhibit the same rheology. The supernatant in tank 241-SY-101 exhibits Newtonian rheology. The sludge exhibits Bingham plastic behavior.

3.3.2.5 Particle Diameter

The following method was used to estimate the required particle diameter:

(a) Based on the draft PNL report by L. M. Liljegren footnoted on pg. 3.2.

1. Scale the particle settling velocity. Based on the combined requirements of matched settling velocity ratio and Froude number, particle settling velocity scales by

$$V_{s0,x} = V_{s0,SY}(1/12)^{0.5} \qquad (3.9)$$

2. Calculate $V_{s0,SY}$. Base this calculation on μ_{SY} = 13 cP, $\rho_{m,SY}$ = 1.5 g/cm^3. Perform two calculations based on $d_{p,SY}$ = 12 μm and 150 μm. The value for a 12-μm-dia particle was given in Table 3.3 as 0.72 in./h. For a 150-μm-dia particle in the same fluid, the particle settling velocity is 113 in./h.

3. Calculate $V_{s0,x}$. Using Equation (3.9)

$$V_{s0,x} = V_{s0,SY}(1/12)^{0.5} = 0.2887\ V_{s0,SY}$$

The corresponding settling velocity range of $V_{s0,x}$ = 0.21 in./h to 33 in./h is required for tests at 1/12 scale.

4. Calculate the particle diameter for the 1/12-scale experiments. Base this calculation on matching N_ρ, $\epsilon_{s,x}$, and a solids density for Minusil-30 of 2.65 g/cm^3. Use two simulant viscosities, μ_x = 3 cP and 10 cP.[(a)]

Particle diameter ranges for 1/12-scale simulant as follows:

3 cP ==> $d_{p,x}$ = 2.9 to 36 μm corresponds to $d_{p,SY}$ = 12 to 150 μm for tank 241-SY-101

10 cP ==> $d_{p,x}$ = 5.3 to 66 μm corresponds to $d_{p,SY}$ = 12 to 150 μm for tank 241-SY-101

5. Determine how the Minusil mimics particle diameters in tank 241-SY-101.

Minusil-30 with $d_{p,x}$ = 10.5 μm represents settling velocities for particle diameters ranging from $d_{p,SY}$ = 24 to 44 μm. Minusil-30 particulate produces particles that scale to be within the measured particle diameter range in tank 241-SY-101. This was conservative for the smaller diameter

---

(a) Draft PNL report by M. R. Powell, C. L. Fow, G. A. Whyatt, P. A. Scott, and C. M. Ruecker entitled Proposed Test Strategy for the Evaluation of Double-Shell Tank Sludge Mobilization, p. 3.38, November 1990.

particles in tank 241-SY-101, because larger diameter particles have a greater settling velocity. Likewise, Minusil-30 is not conservative for the larger particles.

3.3.2.6 Functional Variation of Settling Velocity with Concentration

The functional variation of settling velocity with concentration for the 1/12 scale must match that of tank 241-SY-101. It is anticipated that for equal solids volume fractions, the variation of settling with concentration will be similar in each simulant. No additional steps to match this parameter will be taken.

3.3.2.7 Shear Strength

If Froude number is matched, the stress ratio N_τ scales as

$$(\tau_{ss}/\rho_m)_x = (\tau_{ss}/\rho_m)_{SY} \ (1/12) \qquad (3.10)$$

Based on $\tau_{ss,\ SY} = 4000$ dyne/cm^2 from Table 3.3 and densities

$\rho_{m,SY} = 1.59$ g/cm^3

$\rho_{m,x} = 1.85$ g/cm^3

the following is obtained

$\tau_{ss,x} = 388$ dyne/cm^2

This value will change based on the mixture density obtained for the 1/12-scale simulant. It is important to match this parameter exactly.

3.3.2.8 Property Summary for 1/12-Scale Experiments

Nominal property values for 1/12-scale experiments are summarized in Table 3.6.

3.3.3 Operating Parameters

The operating sequence proposed for the full-scale test was used in the design of the small-scale operating parameter test. The main exception was

TABLE 3.6. Summary of Nominal Property Values for 1/12-Scale Experiments

Parameter	Value
mean solids volume fraction	0.18
shear strength	388 dynes/cm^2, calculated from density parameter and solid and supernatant densities. Use mixture density of 1/12-scale simulant to obtain final value for shear strength.
viscosity	3 and 10 cP, this parameter is adjustable as long as two distinct values are obtained.
density parameter	0.53
solids density	2.65 g/cm^3 for Minusil-30
supernatant density	1.67 g/cm^3
mixture density	1.85 g/cm^3
solids diameter	2.8 to 65 μm

that pump speed was not varied at each jet position; instead tests at several fixed pump speeds were run. The procedure is given in detail in Section 5.4.1.

3.3.3.1 Jet Velocity

Velocities are obtained by matching the 1/12 scale and tank 241-SY-101 Froude number. Froude number is matched by scaling the nozzle exit velocity (W_0).

$$W_{0,x} = W_{0,SY}(1/12)^{0.5} \tag{3.11}$$

As noted in Section 3.2.3, 100 percent of design flow rate in tank 241-SY-101 gives a jet velocity, $W_{0,SY}$ = 88 ft/s. By Equation (3.11), this scales to $W_{0,x}$ = 25.4 ft/s at 1/12 scale. For the minimum planned flow rate in tank 241-SY-101, $W_{0,SY}$ = 15 ft/s. This scales to $W_{0,x}$ = 4.33 ft/s at 1/12 scale.

3.3.3.2 Time Scaling

Time is scaled using the inverse time parameter, η_t. This is used to determine the jet oscillation period, on cycle, off cycle and rest time. When Froude number is matched

$$T_{0,x} = T_{0,SY}(1/12)^{0.5} \tag{3.12}$$

This operating period will be scaled based on the operating time selected for tank 241-SY-101.

4.0 MEASUREMENTS AND INSTRUMENTATION

The existing 1/12-scale facility, measurements, and instrumentation used in the experiments are described in this section.

4.1 1/12-SCALE TEST FACILITY

The experiments were performed in a 1/12-scale model of a double-shell tank located in the 336 building/300 area of the Hanford Site.[a] The tank can be configured to represent component arrangements in actual waste tanks using models of internal components such as air-lift circulators, steam coils, radiation dry wells, and other tank hardware. The present configuration neglects all internals except for the mixer pump assembly. The tank, made of 304L stainless steel, is illustrated in Figure 4.1 with the mixing pump installed.

The 1/12-scale mixing pumps model the operation of the prototype tank mixing pump in tank 241-SY-101. An assembly drawing of the model mixing pump is presented in Figure 4.2. To simulate the operation of the prototype mixing pump, a circulation pump draws the slurry from the upper portion of the tank and discharges the slurry through the mixing pump annulus and out two diametrically opposed nozzles. The suction location can duplicate the same vertical location as the prototype mixing pump, but its horizontal position is slightly offset from centerline (approximately 2 in.). The nozzles are removable to accommodate design variations. A cross-sectional drawing of the nozzles used in the present tests is given in Figure 4.3.

The test facility can accommodate six mixing pumps, each with two nozzles. The Moyno circulation pump will deliver up to 25 gpm at 207 ft of head. The mixing height above the floor can be varied. Also, the mixing pump can rotate or oscillate at speeds up to 8 rpm.

(a) Description of the 1/12-scale tank facility taken from a strategy plan by Bamberger et al. entitled Strategy Plan: A Methodology to Predict the Uniformity of Double-Shell Tank Waste Slurries Based on Mixing Pump Operations, December 1990.

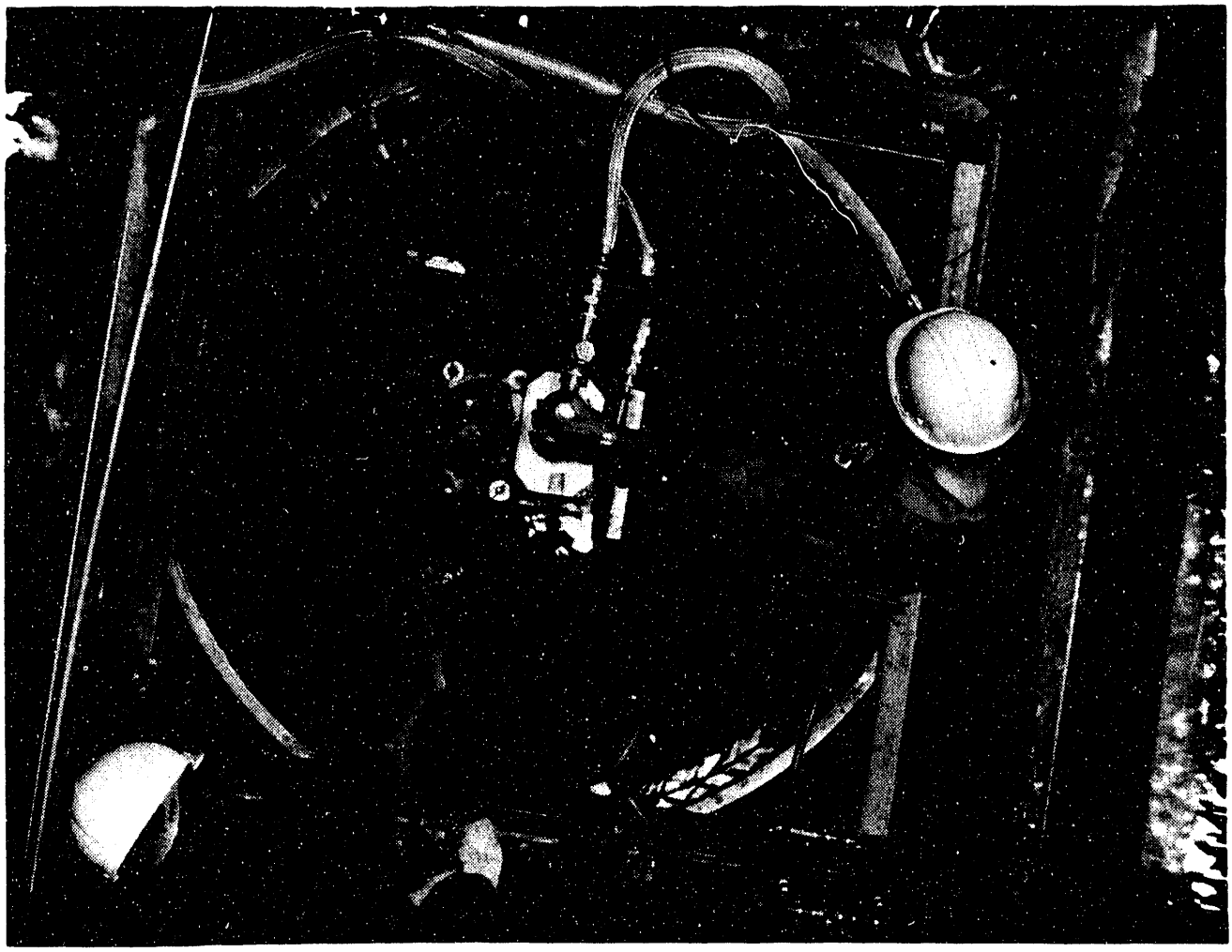

FIGURE 4.1. 1/12-Scale Tank With Mixing Pump Model

The facility is equipped to prepare waste simulants with facility components including makeup tank, holding tank, and circulation and transfer pumps. These components are shown along with manifolding and facility flow controls in Figure 4.4. The makeup tank is equipped with an agitator to mix the simulant prior to transfer to the scaled waste tank. The makeup tank is instrumented with load cells to measure slurry ingredients, as well as the

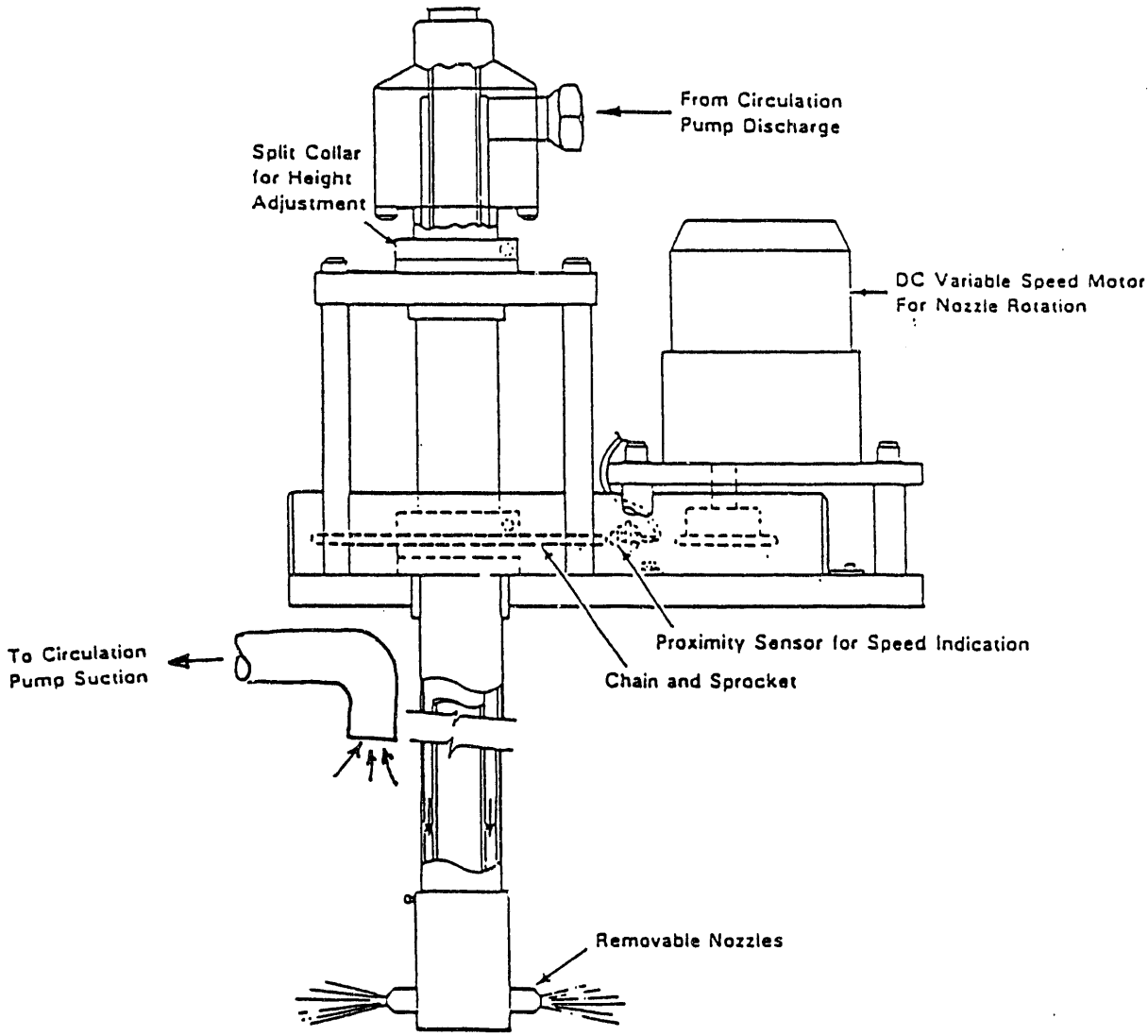

FIGURE 4.2 Mixing Pump Model Configuration

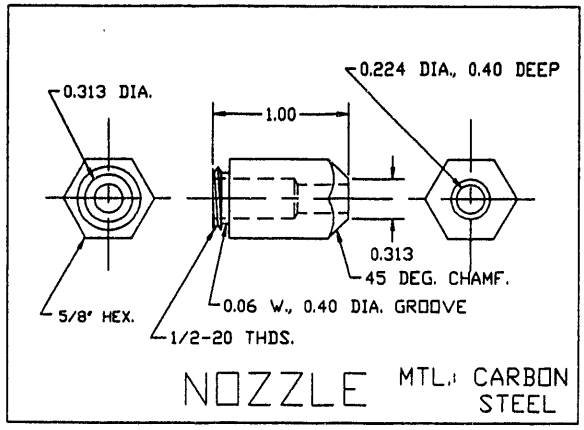

FIGURE 4.3 Jet Nozzle Configuration

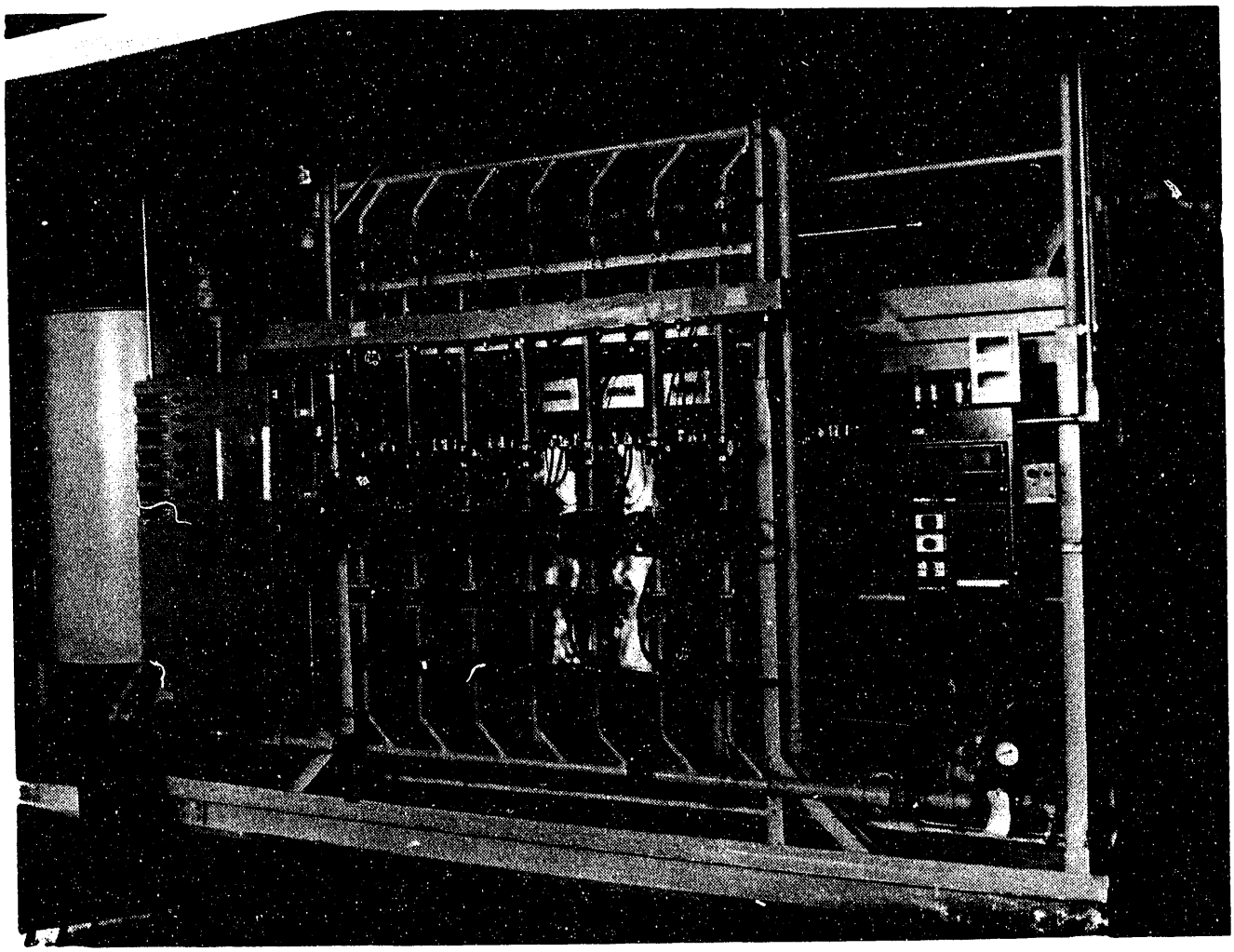

FIGURE 4.4 1/12-Scale Facility and Auxiliary Tanks

mass of slurry transferred into and retrieved from the 1/12-scale tank. A centrifugal pump with a capacity of 50 gpm at 50 ft of head is used to transfer slurries throughout the test facility.

4.2 INSTRUMENTATION

Process variables to be measured include temperature and flow rate.

4.2.1 Temperature

Three thermocouples will be used to monitor temperature: 1) at the inlet to the pump, 2) along the tank wall at the height of the jet centerline,

and 3) along the tank wall at an elevation of 25 in. These measurements will detect any tank temperature stratification and temperature differences between the jet and the tank.

4.2.2 Flow Rate

Flow rate is measured in the process line. The flow is assumed to be split equally between the two nozzles. This can be visually checked by review of the transient dye injection videos and quantified by centerline velocity measurements at the same location in both jets.

4.2.3 Jet Velocity

Jet velocity profiles were measured to determine the bulk motion of the jet including the centerline velocity, the vertical centerline profile (as can be best determined with available instrumentation), and the vertical and horizontal velocity components at the tank wall.

Pitot probes and electromagnetic flowmeters were used to measure the jet velocity profiles.

4.2.3.1 Pitot Probes

Two types of pitot probes have been designed: one with a horizontal inlet to measure the axial component of the jet velocity, and another with a vertical inlet to measure the vertical component of the jet velocity along the tank wall. The probes were manufactured using chamfered 3/16-in. tubing with a 0.016-in. wall. Reference pressure was taken at a tap in the tank bottom.

Three pressure transducers are available to switch between these probes:

- 0 to 1000 in. H_2O, measures velocities to 52 ft/s
- 0 to 250 in. H_2O, measures velocities to 26 ft/s
- 0 to 20 in. H_2O, measures velocities to 5 ft/s.

The first two transducers could be used to measure the horizontal component of velocity along the centerline near the nozzle. The third transducer could be used to measure jet velocities at more distant jet locations. Resolution is expected to be a problem for transverse velocities

near the tank wall, where dynamic pressures fall below 1 in. of water (corresponding to a measured velocity in water of less than 1.6 ft/s).

4.2.3.2 Electromagnetic Flowmeters

The electromagnetic flowmeters are Marsh-McBirney's Flo-Mate Model 2000. These probes are designed to measure fluid velocities in open channel flows. These 1.5-in.-dia probes were more intrusive than the pitot probes, but have the benefit of directly measuring velocity. This is important in slurry flows where local density is difficult to measure. The electromagnetic flowmeters also have the advantage of improved accuracy over a greater flow range. Specifications for the electromagnetic flowmeter are given in Table 4.1.

4.2.4 Density/Concentration

Three different instruments/techniques were used to measure slurry density.

4.2.4.1 Statham

The Statham Model MD-3018 density transmitter is typically used to measure drilling mud density. It infers an average density from a static head measurement. The static head difference is measured between two diaphragms spaced 10 in. apart. Because of this large averaging distance, this instrument was used to track density changes at a single position in the upper portion of the tank.

TABLE 4.1. Specifications for Electromagnetic Flowmeter

Parameter	Specification
Manufacturer/model	Marsh-McBirney/Flo-Mate Model 2000
Range	-0.5 to 20 ft/s
Zero stability	±0.05 ft/s
Accuracy	±2% of reading + zero stability

4.2.4.2 Discrete Samples

A manual probe was developed to take discrete mass samples from various elevations in the tank. The probe consisted of a syringe (with a volume of 10 cm^3) mounted on an extension rod. To operate, the probe was manually placed at the desired tank cylindrical coordinate (r, θ, z), the remote actuator pulled, and a sample taken. The probe was removed from the vessel and the contents were transferred into a tared 10-ml graduated cylinder. By measuring the mass of the contents in the cylinder (m) and observing the filled volume (V), the sample density (ρ_m) could be calculated

$$\rho_m = m/V \tag{4.1}$$

4.2.4.3 Ultrasonic Probe

An experimental ultrasonic probe being developed to measure concentration in real time across a fixed separation distance was evaluated during these experiments.[a] The probe consists of two ultrasonic sensors: a transmitter that transmits a signal through a liquid/slurry medium, and a receiver that records the transmitted signal. The signal attenuation is proportional to the volume fraction of solids in the liquid. The probe was configured to measure concentration across a 4-in. separation distance. The probe sensors (each about 1-in. in diameter) were mounted horizontally.

Although the probe configuration was not optimized; useful real-time concentration measurements were obtained. The theory to support the probe methodology, calibration, and operation is described in Appendix A.

4.2.5 Measurement and Test Equipment

Measurement and test equipment used during these experiments are listed in Table 4.2.

(a) The probe is being developed to support the Double-Shell Tank Retrieval project uniformity experiments. Proof-of-principal evaluation of the technique has been completed using a non-optimized probe design.

TABLE 4.2. M&TE Control Listing

Project/Activity No. 17667 QA Plan No. MCS-036
Scaled Experiments to Support Mitigation by Mixing in Tank 214-SY-101, Impact Level III

Line Item	Control #	M&TE Description
1		Type J Thermocouple T wall, jet centerline
2		Type J Thermocouple T wall, elevation 25 in.
3		Type J Thermocouple T jet, in pump supply line
4	HEDL 999-80-02-012	Electronic Transmitter Honeywell Y41104 Pressure, 0 to 1000 in. H_2O
5	HEDL 999-80-02-009	Electronic Transmitter Honeywell Y41104 Pressure, 0 to 250 in. H_2O
6	HEDL 999-80-02-008	Electronic Transmitter Honeywell Y41104 Pressure, 0 to 20 in. H_2O
7	HEDL 374-06-03-001	Mettler H51 Balance
8		Model Magnetic Flowmeter, Krone
9		Model Load Cell #1
10		Model Load Cell #2
11		Model Load Cell #3
12		Model Statham Densitometer, #1

TABLE 4.2. (contd)

Line Item	Control #	M&TE Description
13		Model Statham Densitometer, #2
14		Model 201 Marsh-McBirney, Inc. Portable water flowmeter
Instrumentation that Supports the Ultrasonic Probe		
15		PNL prototype Ultrasound probe
Instrumentation Used for Simulant Characterization		
16	HEDL 394-06-01-001	Mettler Electronic Balance, PC-4400
17	HEDL 441-06-01-001	Mettler Electronic Balance, PC-180
18	U-121	Canon-Fenske Capillary Viscometer Model #50
19	282-C	Canon-Fenske Capillary Viscometer Model #100
20	WA69469	HAAKE Rotational Viscometer, RV-100 Model #50
21		Type J Thermocouple

5.0 RESULTS

Three sets of scaled experiments were performed: 1) flow visualization, 2) model verification, and 3) operating parameter. The flow visualization tests used a dye tracer in the mixing jets to study flow patterns in water. The model verification tests involved collecting detailed velocity measurements of the steady tank flow field for a fixed jet position; these datasets will then be used for numerical model verification. The operating parameter tests focused on the ability of an incrementally rotated jet to mobilize and maintain suspension of settled solids.

This section begins with results of the simulant development, then follows with highlights of each test type. The balance of the data are given in the Appendix B.

5.1 SIMULANT DEVELOPMENT

Simulants were developed at bench-scale to provide the slurry characteristics necessary to conduct scaled experiments. These properties were summarized in Table 3.6. The priority for matching these properties is 1) mean solids volume fraction, 2) shear strength, 3) viscosity, 4) density parameter (obtained by matching solids density, supernatant density, and mixture density), and 5) particle diameter/settling velocity.

5.1.1 Simulant Properties

Two simulants are required to conduct these experiments, one with a high viscosity (near 10 Cp) and one with a lower viscosity (near 3 cP). The simulants were water based (to provide the lower viscosity). SiO_2 flour was used to simulate the settled solids; Minusil-30 was chosen for its availability and also because it can develop a variable shear strength that increases with time. Minusil-30 has a mean particle diameter of about 10 μm based on volume density, and 1.25 μm based on number density. The particle diameter and density combined to provide a settling velocity in the desirable range. Salt was added to the recipe to stabilize the shear strength. Sugar was added to vary the viscosity.

5.1.1.1 Simulant Recipes

The recipe for each simulant is listed in Table 5.1.

5.1.1.2 Physical Properties

The physical properties of bench-scale samples of the two simulants are given in Table 5.2. Several shear strength measurements of the simulants were taken; these are denoted by batch designations A, B, and C in the table. Other physical property measurements were not as variable as shear strength. These properties may differ from those in the tank because of differences in recipe and conditions (e.g., increased static head effect on shear strength).

5.1.1.3 Dimensionless Parameters

Dimensionless parameters can be calculated using the simulant properties given in Table 5.2. The results are compared with those for tank 241-SY-101 in Table 5.3. The tank 241-SY-101 dimensionless parameter values were initially presented in Table 3.4.

TABLE 5.1. Simulant Recipe

	High Viscosity Simulant		Low Viscosity Simulant	
Element	Wt%	Recipe, lbm[(a)]	Wt%	Recipe, lbm[(b)]
Minusil-30, SiO_2	33	2620	33	2193
Sugar	20	1586	2	191
Salt	2	159	2	144
Water	45	3586	63	4470
Total	100	7951	100	6998

(a) Manufactured 105 percent of mass required to fill 1/12-scale vessel to allow for simulant volume in piping and residual in makeup tank.

(b) Recipe manufactured with 100 percent of solids fraction and 105 percent of supernatant fraction to account for residual fluid left in lines and in makeup tank.

TABLE 5.2. Physical Properties of the Simulants

	High Viscosity		Low Viscosity	
	Desired	Obtained	Desired	Obtained
Mean solids volume fraction	0.18	0.18	0.18	0.17
Shear stress,[a] dyne/cm^2	388	[b]298	388	[b]266
Batch A				
After 5 h		285		
After 16 h		341		
Batch B				
After 8 h		190		
After 23 h		360		
Batch C				
After 9 h				440
After 16 h				490
Solids density, g/cm^3	2.65	2.65	2.65	2.65
Supernatant density, g/cm^3	1.67	1.1	1.67	(est.)1
Mixture density, g/cm^3	1.85	1.42	1.85	1.27
Viscosity, cP	10.00	7.8	2.0	2.5
Settling velocity, in./h	0.21	1.7	0.21	5.4

(a) The desired value must be calculated based on the resultant value of mixture density.

$(\tau_{ss}/\rho_m)_x = (\tau_{ss}/\rho_m)_{SY}$ (1/12) = 209.6 dyne-cm/g

Based on $\tau_{ss,\ SY}$ = 4000 dyne/cm^2, $\rho_{m,\ SY}$ = 1.59 g/cm^3, and $\rho_{m,\ x}$ = 1.85 g/cm^3

$\tau_{ss,\ x}$ = 388 dyne/cm^2

(b) Calculated as follows

$\tau_{ss,\ x} = \rho_{m,\ x}$ (209.6 dyne-cm/g)

where $\rho_{m,\ x}$ = the actual value obtained for the simulant.

TABLE 5.3. Range of Dimensionless Parameters

Parameter	1/12-Scale Tank		Full-Scale Tank 241-SY-101	
	High viscosity	Low viscosity	Prototype at min. W_o	Prototype at max. W_o
jet velocity, W_o	25.4 ft/s	25.4 ft/s	15 ft/s	88 ft/s
Froude Number, Fr	2.7	2.7	0.46	2.7
Reynolds Number, Re_H	1.2×10^6	3.3×10^6	5.6×10^6	33×10^6
stress ratio, N_τ	2833	2534	83	2856
settling velocity ratio, V_s	1.5×10^{-6}	5×10^{-6}	1.1×10^{-6}, [a] 1.8×10^{-4}	1.9×10^{-7}, 3.0×10^{-5}
density ratio, N_ρ	1.09	1.3	0.53	0.53
mean solids volume fraction, ϵ_s	0.18	0.18	0.18	0.18

(a) Range calculated for particle diameters of 12 and 150 μm; see Section 3.2.2.

Dimensionless parameters for both mean solids volume fraction and settled solids shear strength matched between the simulant and tank 241-SY-101 waste. The range in viscosity is near the 3 to 10 cP desired. The density parameter was not well matched because it was not practical to produce (and dispose of) a sufficiently dense supernatant liquid. It is not clear whether or not this is conservative. The settling velocity ratio was a good compromise between the range of full-scale values. Improved size characterization of tank 241-SY-101 solids particle size is needed to make a final assessment.

The differences in individual parameters shown in Table 3.4 also impact the ability to determine the influence of Reynolds number. Ideally, the only difference between the two simulants would be their viscosity; this would

allow a comparison of Reynolds number for two tests with otherwise identical conditions. Unfortunately, the differences in settling velocity and density ratio complicate any interpretation of Reynolds number affect. This ideal could only be achieved with differences in particle size and supernatant composition for the two simulants. The present simulant pair represents a necessary compromise in this ideal.

5.1.1.4 Simulant Properties as a Function of Solids Concentration

To facilitate comparison between the ultrasonic measurement of particle concentration and the other two methods of determining the particle concentration, physical properties of density and viscosity were measured over a range of 0 to 50 wt% solids. This was done for both the low and high viscosity simulants (see Table 5.4). Simulant recipes follow:

In this method the supernatant composition remained constant; the wt% of solids varied from 0 wt% to 50 wt%. The recipes specified in Table 5.1 were used to formulate each of the samples.

TABLE 5.4. Simulant Recipes for Property Measurements

	Supernatant Composition	
Component	High Viscosity	Low Viscosity
Sugar	20/67 = 30 wt%	2/67 = 3 wt%
Salt	2/67 = 3 wt%	2/67 = 3 wt%
Water	45/67 = 67 wt%	63/67 = 94 wt%

Component	High Viscosity, wt%					Low Viscosity, wt%				
Minusil	10	20	30	40	50	10	20	30	40	50
Supernate	90	80	70	60	50	90	80	70	60	50
	3									
Sugar	27	24	21	18	15	3	2	2	2	2
Salt	3	2	2	2	2	3	2	2	2	2
Water	60	54	47	40	34	84	76	66	56	48

Based on these recipes, the supernatant composition remained constant as wt% solids were varied from 0 to 50 percent. This method produced mixtures with compositions similar to those observed during the tests; i.e., fully settled with 0 wt% solids at the top of the tank, fully mixed at 33 wt% solids throughout the tank (see Figure 5.1), and stratified with 50 wt% solids near the bottom of the tank.

5.1.2 1/12-Scale Simulant Physical and Rheological Property Measurements

The properties to be characterized during the experiments are listed in Table 5.5. All measurements were performed in accordance with PNL Technical Procedure PNL-ALO-501 (Scheele 1992). All measurements were made at ambient temperature unless specified otherwise. The ambient temperature was recorded at the time of each measurement.

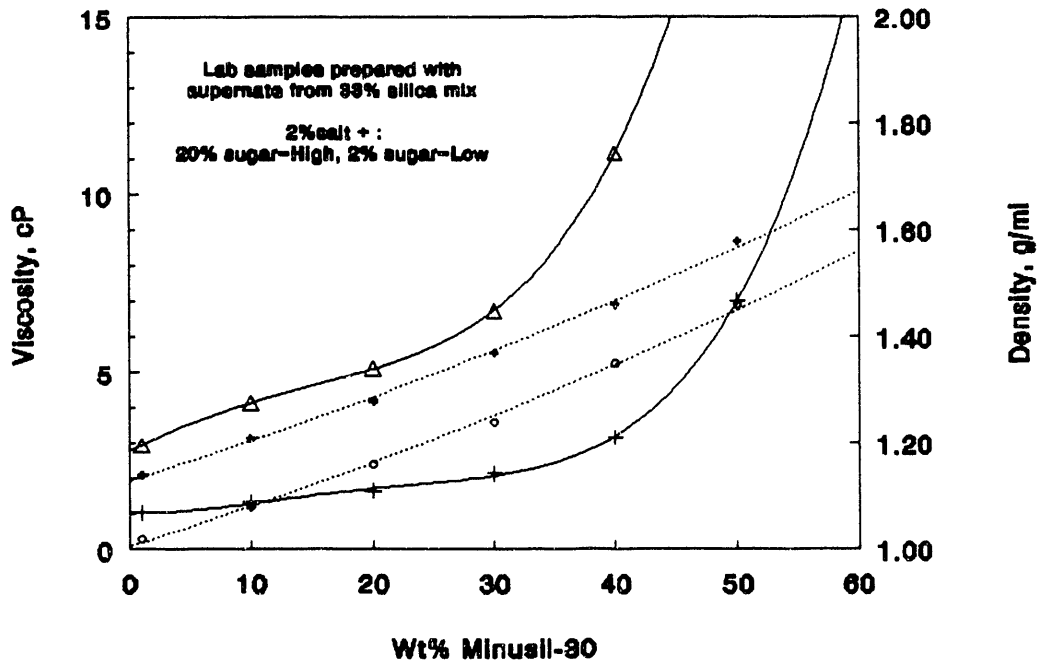

Simulant	Density Symbol	Viscosity Symbol
Low Viscosity	°	+
High Viscosity	+	Δ

FIGURE 5.1. Density and Viscosity as a Function of Wt% Solids for the High and Low Viscosity Simulants

TABLE 5.5. Simulant Physical and Rheological Property Measurements

1. **Density**	
· dry solids	Measure prior to makeup of simulant H.
· centrifuged solids	Measure after makeup of simulants H and L, prior to start of the initial test based on each simulant and after completion of all tests with each simulant.
· supernatant	Measure after makeup of simulants H and L, prior to start of the initial test based on each simulant and after completion of all tests with each simulant.
2. **Viscosity**	
· supernatant	Measure after makeup of simulants H and L, prior to start of the initial test based on each simulant and after completion of all tests with each simulant.
· bulk slurry	Measure as a function of wt% solids at 0%, 10%, 20%, 30%, 40%, and 50% for simulant H and L. This measurement can be performed at any time and is not specifically tied to the run time.
3. **Particle size range and distribution**	Measure after makeup of simulants H and L, prior to start of the initial test based on each simulant and after completion of all tests with each simulant. Use the supernatant liquid to suspend the particulate samples.
4. **Particle settling velocity**	Measure after makeup of simulants H and L, prior to start of the initial test based on each simulant and after completion of all tests with each simulant.
5. **Shear strength**	Measure after simulant makeup, prior to start of each individual test run for each simulant. Initially samples of simulant will be removed from the test tank and measured using the Haake viscometer located in the 324 building. These measurements will be compared with samples allowed to settle in bottles for the same period of time. If no difference occurs, the out-of-tank method will be used.
6. **Discrete samples**	Measure the wt% solids for samples taken using a syringe to characterize concentration during experiments with simulants H and L.
7. **Ultrasonic measurement of concentration**	Concentration will be measured using the ultrasonic probe. This measurement will be performed during both steady-state and transient operation. The measurements will be compared with the discrete samples.

5.2 FLOW VISUALIZATION TESTS

This first series of tests include a check of facility operation and flow visualization with dye injection in clear water. The purposes of these tests are

- observe the flow patterns generated within the tank to investigate the effect of offset jet nozzle assembly position
- observe the flow patterns for steady-state and start-up jets.

Checkout of test equipment and instrumentation demonstrated readiness of systems needed for subsequent tests. Current traceable calibrations are required for all instrumentation. Tests are summarized in the test matrix in Table 5.6.

5.2.1 Test Procedure

The visualization tests were performed with geometrically scaled parameters as called out on the test data sheet. For the first test, the jet nozzle assembly was positioned at the center of the tank. The procedure for transient tests is listed as follows:

1. Fill the tank with water to the specified depth (scaled fluid height H_t).
2. Allow tank contents to reach a quiescent state (confirm by tracer) and record tank temperature.

TABLE 5.6. Test Matrix for Flow Visualization Tests

Test Number	Jet Velocity, ft/s	Transient	Steady State	Offset Pump	Completed
1	25		✓		(a)
2	25	✓			✓
3	25	✓		✓	✓
4	25	✓			(b)

(a) Done at jet velocity of 15 ft/s.

(b) Done with low viscosity simulant with fully settled solids and a clear supernatant liquid layer.

3. Tracer ready. For tracer (dilute latex paint) injection, this was accomplished by charging the jet nozzle assembly with the dilute paint mixture.

4. Initiate video recording from vertical position above tank with field of view including the full tank contents. Initiate recording of loop flow rate and other data acquisition.

5. Start jet mixing pump from dead stop and allow to reach preset flow rate.

6. Operate until flow field reaches steady-state conditions, or until further visualization is no longer effective.

7. Shut down the video and flow loop.

Tests were also run to investigate the steady-state flow field. In these cases, steps 1 through 7 were repeated, replacing step 5 with the following:

5. Initiate flow through jet mixing pump and allow flow to reach steady-state conditions. Initiate flow of tracer through jet mixing pump.

The final test was performed with the pump assembly placed off of the tank centerline to duplicate placement in the full-scale tank. The procedure was otherwise unchanged for the steady-state case.

5.2.2 Transient Test Results

The transient test started from a zero flow condition and went to a maximum nozzle exit velocity of 16 ft/s in 20 seconds. The dye injection showed the plumes leaving the nozzles widening at a constant rate (a constant jet angle of expansion was maintained) as it approached the tank wall. The two jets appeared symmetrical throughout the test. The plume leaving the nozzle did not appear to fall or rise as it approached the wall. Upon reaching the wall, the plume fanned out symmetrically along the wall. There was significant flow in both the vertical and circumferential directions. The plume stayed close to the wall as it spread out.

After reaching the surface, the plume traveled back towards the center of the tank. The plume appeared to have significant depth as it moved back towards the center. At the water surface, the plume front was perpendicular to the jet axis and reached across the entire tank. After the two plume fronts met in the center of the tank the whole tank was cloudy from the dye.

In general, the concentration was definitely not uniform across the tank but no distinguishable flow patterns were observed.

5.2.3 Steady-State Test Results

The two steady-state tests were conducted at nozzle exit velocities of 25 ft/s. The tests differed in the location of the nozzles. One test was conducted with the nozzles centered in the tank. The second test had the nozzles positioned 3 in. south of the tank center along the jets' axes. For both tests, the nozzle centerline height was 2.625 in.

No major differences were observed between the two tests. The most noticeable difference was the time at which the initial jet plumes reached the tank wall. For the centered test both plumes reached the wall simultaneously. The plumes of the off-center test reached the wall at different times with the plume from the closer nozzle impacting the wall first.

The centered and off-centered tests had dye injection times of approximately 8 and 6 seconds, respectively. The initial plume fronts of both steady-state tests were basically identical. As in the transient test, the plumes were symmetrical and spread with a uniform jet angle. After reaching the wall, the plume again spread evenly along the wall; however, the thickness of the plume along the wall appeared thinner compared to that of the transient test. The plume rose to the surface and propagated back towards the tank center as observed during the transient test, only without the depth seen in the transient case. The plumes met in the tank middle along the entire plume fronts.

In the steady-state tests it was possible to observe the end of the plume. The tail ends of the plume were shaped the same as the leading fronts. It climbed up the tank wall and then traveled in a straight line perpendicular to the jet axis towards the tank centerline. As the plume end passed across the top of the tank, it was possible to see the tank bottom. The plume of dye had traveled out to the tank wall, up the wall, across the top, and moved downward in the tank middle with very little dye mixed into the semi-stagnant areas of the tank. It was then possible to observe the reentrainment of the dye into the jet. The plume again traveled in the same manner as before only

more of the paint became mixed into the stagnant areas of the tank. Upon the second entrainment, the dye plume's trailing edge was not clearly visible.

In the case of the centered nozzles, it was possible to observe at the surface a third plume of high concentration dye rise up from along the tank wall and travel through the cloudy water. After this, the tank had become to opaque to make further observations.

5.2.4 Observations in Simulant

Flow visualization was not generally possible in the simulant because it was opaque. This was especially true of the high viscosity simulant because allowed settling times were inadequate to settle out the fine solids. However, the interfacial waves between the supernate and slurry layer could be seen when the interface was within 1 in. of the surface. Particle settling velocities were much higher in the low-viscosity simulant and the supernate was, at times, quite clear.

An informal test was performed in the low viscosity simulant to assess the potential for success of a videotaped test. The results were very interesting, but unfortunately supernatant liquid clarity could not be restored for a formal test. A list of log book notations made during this informal test and a summary of observations is included under test FVLS/1 in Appendix B.

5.3 MODEL VALIDATION TESTS

Numerical model validation is required for the circular tank geometry and for non-Newtonian fluid behavior, specifically for highly viscous, solid-liquid mixtures with yield stress. These tests differ from the operating parameter tests in the previous section primarily in the duration of the test and in the number of quantitative measurements performed.

Tests performed to provide the validation data included three different working fluids: water, high viscosity simulant, and low viscosity simulant. Water was used in initial tests to provide baseline test results as well as check out the test equipment and instrumentation.

Two jet velocities were used for each working fluid: the first was based on the maximum full-scale pump flow, and the second was used for comparison with WHC's 1/10-scale test results. The jet velocity used in this experiment was scaled using the same methodology as in the operating parameter tests. Geometrical scaling was used for all dimensional parameters. The six tests are represented in the test matrix in Table 5.7.

5.3.1 Test Procedure

The test performed for each of these six cases consisted of a startup transient of the mixing jets and continued until a steady-state condition was achieved. The criteria for steady-state simulant tests was a nonincreasing mixture density at a height of 24.8 in. above the tank floor. For the water tests, the criteria for steady state was unchanging velocity measurements at several points that showed that the average velocity was constant or by waiting a conservative amount of time (as determined during flow visualization testing).

Measured parameters common to all working fluids include fluid temperature, jet flow rates, and in-tank fluid velocity flow field mapping. Pretest measurements were made to verify equal flow to both nozzles. At a minimum, transient measurements with the simulants consisted of jet centerline velocities at several axial positions between the nozzle exit and tank wall.

TABLE 5.7. Test Matrix for Model Validation Tests

Test Number	Jet Velocity, ft/s	Simulant Type	Completed
1	25.0	water	✓
2	50.0	water	Completed at 45 and 55 ft/s to bracket wall jet behavior.
3	25.4	high μ	✓
4	50.0	high μ	
5	25.4	low μ	✓
6	50.0	low μ	✓

Flow field mapping was performed at steady state. Measured parameters unique to the simulant tests include concentration and shear strength. The number and location of the concentration measurements needed to be adequate to assess the amount of mobilized solids. This was accomplished using

- discrete samples to measure concentration
- density measurement
- ultrasonic concentration probe to measure real-time concentration in a fixed location.

5.3.2 Water Tests

An observation was made at the start of the model validation tests in water that was confirmed in the high viscosity simulant and again in the low viscosity simulant: there is a critical jet velocity above which the jet abruptly shifts downward toward the floor of the tank. That is not to say that floor jet behavior was unexpected; despite the jet nozzle being 12 nozzle diameters away from the floor, the tank radius is sufficient for the jet to be influenced by the floor. What was unexpected was the sensitivity of this behavior to slight changes in jet velocity. This observed phenomena will be referred to as 'jet attachment' throughout the remainder of the report.

The jet attachment phenomena was first observed in comparison tests of the electromagnetic (EM) and pitot probes for velocity measurement. One probe type was placed on nozzle centerline in one jet; the other probe type was similarly placed in the opposite jet. Jet flow rate was increased in steps until both instruments indicated a sudden downward shift in fluid velocity. A reduction in the flow rate recovered the former measured velocity. Figures B.1 and B.2 in Appendix B illustrate this. The behavior was repeatable and was measured in both jets by different instruments. The change was highly sensitive to jet flow rate; as little as a 10 percent change in jet flow rate resulted in a 40 percent reduction in measured velocity.

One observation of this unexpected behavior was a sudden and dramatic shift upstream of the jet attachment point on the tank floor. As the jet shifts toward the floor, the probe left in a fixed position measures velocities away from the jet centerline. Measured velocity profiles confirm

this as shown for three radial locations in Figure 5.2. At the highest velocity, a noticeable shift in peak velocity has already occurred 10 in. from the jet. This is surprising in that this radial position is only 45 jet nozzle diameters and the jet begins at nearly 12 diameters off of the tank floor. This shift in jet attachment location was accompanied by a marked increase in jet-generated audible noise in the 1/12-scale tests. The loud noise emanating from the tank was apparently caused by the impact of the high velocity turbulent jet on the unsupported tank floor.

The location of floor attachment could have a significant impact on the effectiveness of jet mixing in waste tanks. This is because floor attachment is accompanied by faster lateral jet growth and a rapid deterioration in peak jet velocities beyond the attachment point. Mobilization of the settled solids will be enhanced locally, but the jet may not have an effect near the tank walls. Of course, if this change in attachment occurs at a jet flow rate beyond the capacity of the pump (as indicated by scaling analysis), this observation is not relevant. The jet attachment behavior is discussed again in the simulant test results (Sections 5.3.3 and 5.3.4) and in the extrapolation to full scale (Section 5.4.4).

The intent of the EM/pitot comparison test was to check the agreement between the EM and pitot probe instruments for velocity measurements. In addition to evidence of the jet attachment behavior mentioned previously, Figures B.1 and B.2 in Appendix B show good agreement between the two instruments. The instantaneous measurements in Figure B.2 show the EM probe giving slightly higher velocities. They also show a remarkable measurement-to-measurement agreement considering that the probes are in two separate jets. Such behavior cannot be attributed to random turbulence because it would be different for each jet. Instead this is the likely result of pulsatile discharge from the Moyno circulation pump.

Velocity profiles were measured in both jets with a common instrument to verify jet symmetry. The results given in Figure B.3 show a slightly lower peak velocity in one jet, but the difference is insignificant relative to the measurement uncertainty (see Section 5.5).

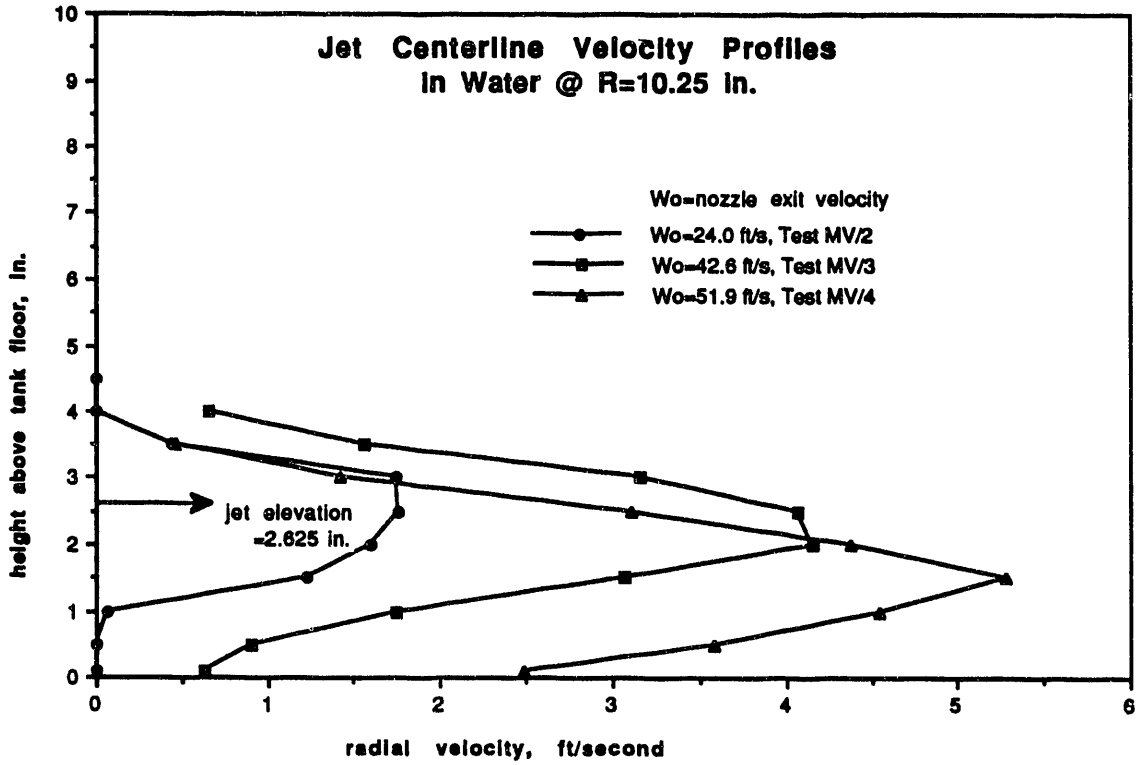

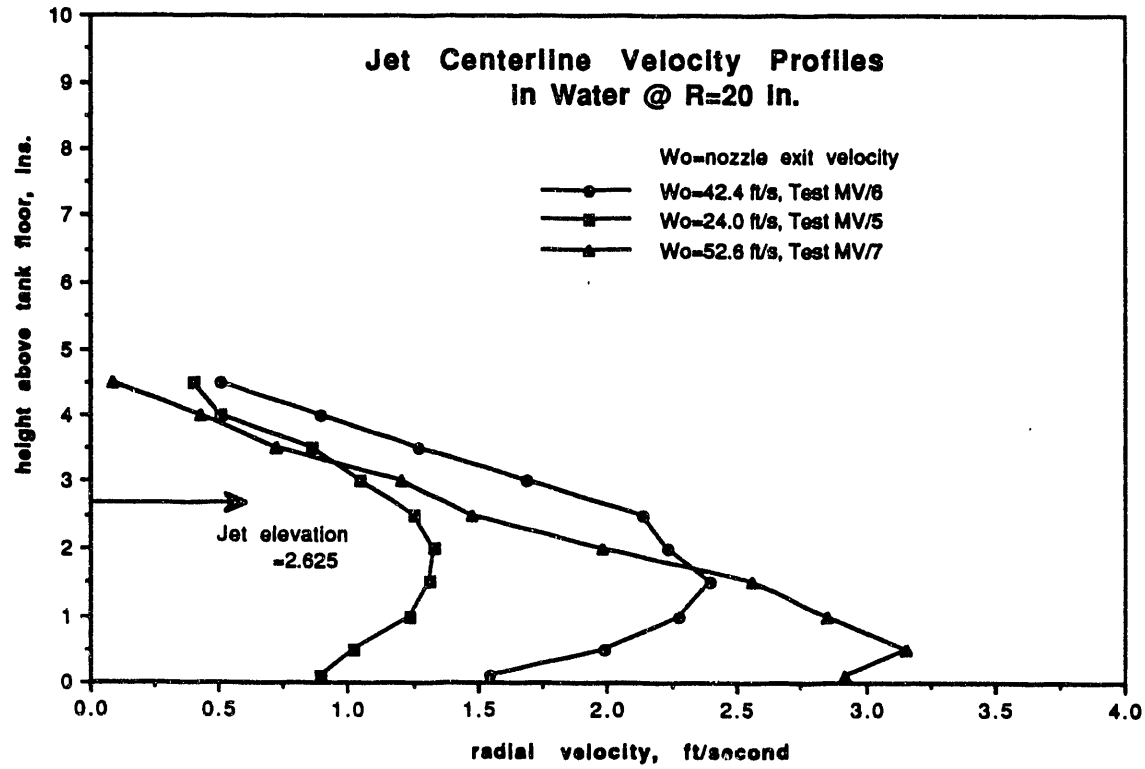

FIGURE 5.2. Centerline Jet Velocity Profiles Showing Wall Attachment

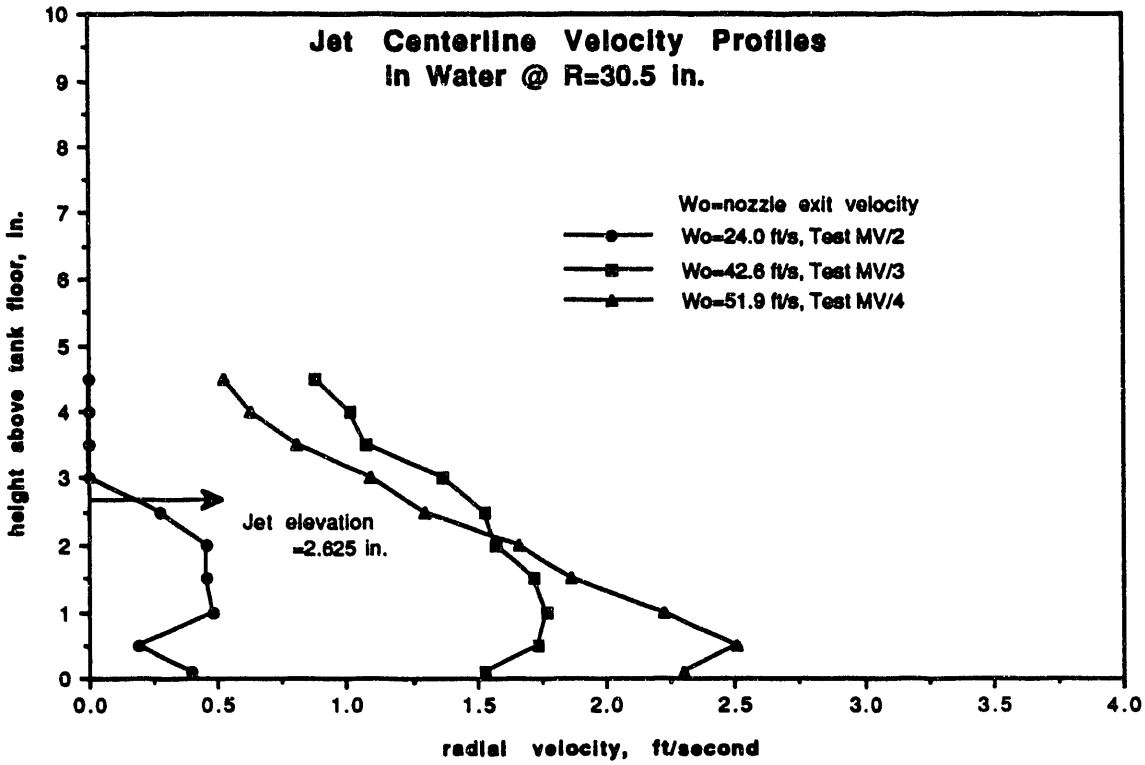

FIGURE 5.2. (contd)

In addition to velocity profiles taken through the jet centerline, measurements were also made of fluid velocities away from the jet stagnation region at the wall. Traverses away from the jet centerline and adjacent to the wall gave a measure of the azimuthal velocity distribution. An example is shown in Figure 5.3. A measurement traverse was also made of the vertical velocity component above the jet stagnation point. An example of this traverse is shown in Figure 5.4. The data points in Figure 5.4 that deviate from a smooth velocity profile are most likely caused by the uncertainty associated with velocity probe positions. Refer to Appendix C for a description of the experimental uncertainties.

5.3.3 High Viscosity Simulant Tests

Tests in the high viscosity simulant were made with two jet velocities, 25 ft/s and 15 ft/s. The higher value scales to 88 ft/s in the full scale, which is the maximum proposed jet velocity in tank 241-SY-101. The lower value scales to 53 ft/s, and represents 60 percent of capacity.

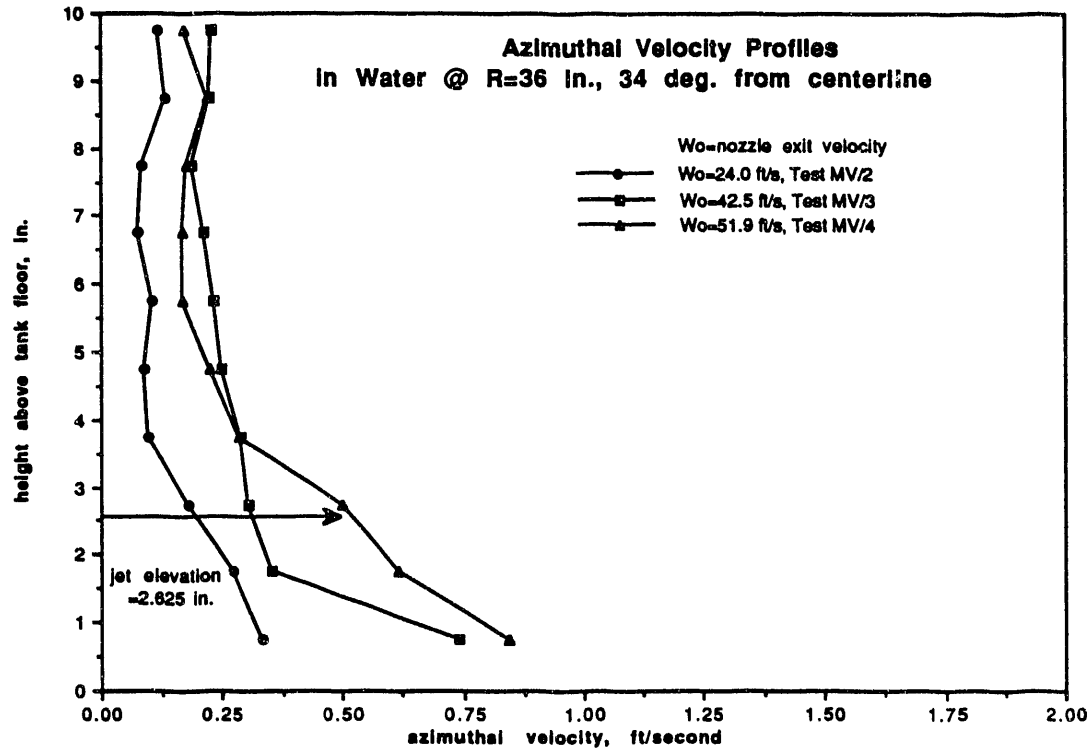

FIGURE 5.3. Azimuthal Velocity Profiles in Water

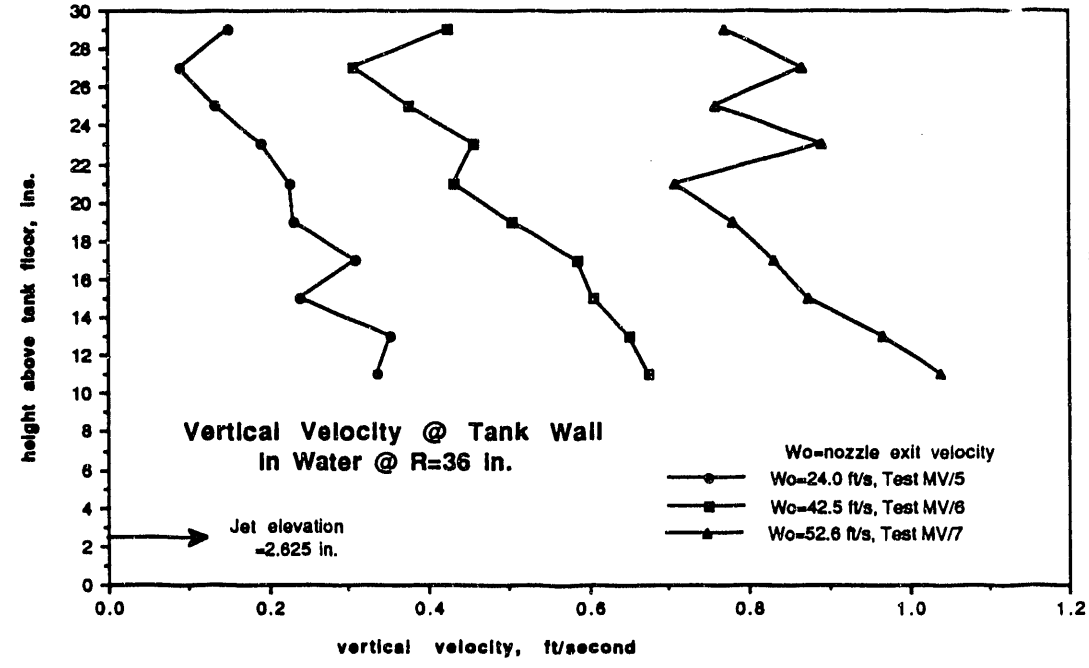

FIGURE 5.4 Vertical Velocity Profiles in Water

5.3.3.1 25 ft/s Jet Velocity

Simulant tests were relatively uneventful until the slurry interface rose sufficiently to give readings on the various instrumentation. An early indication of jet progress was given by locating a velocity probe on nozzle centerline at some distance from the jet. The probe was placed prior to the solids settling and was essentially cast in place. As the jet eroded its way through the settled solids, it eventually reached the buried probe; this is referred to as the breakthrough time. Figure B.11 shows that the breakthrough time for the 25-ft/s jet was approximately 14 min.

The interface height variation with time is given in Table B.2. At the start of the test, the interface was 7 in. below the surface. This does not mean that the material below this interface was settled sludge. There was a settled sludge layer on the tank bottom, but the region in between was a slurry where the solids phase was still settling. A principal goal in modeling the full-scale tank was to simulate the shear strength of the settled solids. The shear strength of the settled solids in this simulant increased with time and desired values could be met or exceeded in typical overnight settling times (see Test No. MVS/2 measurements, Appendix B). Unfortunately, this was not sufficient time for all of the solids to settle. The result was that tests were conducted in a tank that had not yet reached a steady or equilibrium state. Although this was not ideal, the test results can still be used for model validation if the initial density distribution is included (see for example, Figure B.12). The low viscosity simulant with its higher settling velocity was better in these respects.

The interface reached the surface in 3 h and 20 min. Velocity profiles were recorded through the jet centerline at 1 h, 2½ h, and 5 h. The results are given in Figure 5.5. No significant difference is apparent between these profiles. Azimuthal and vertical velocity profiles are included in Figure B.22. All velocity measurements in simulant were made with the EM probes. In simulant, the pitot probes suffered from an ever changing reference pressure and no convenient means was available for a local measurement of density. The EM probes measured velocity directly and therefore did not require the local density measurement.

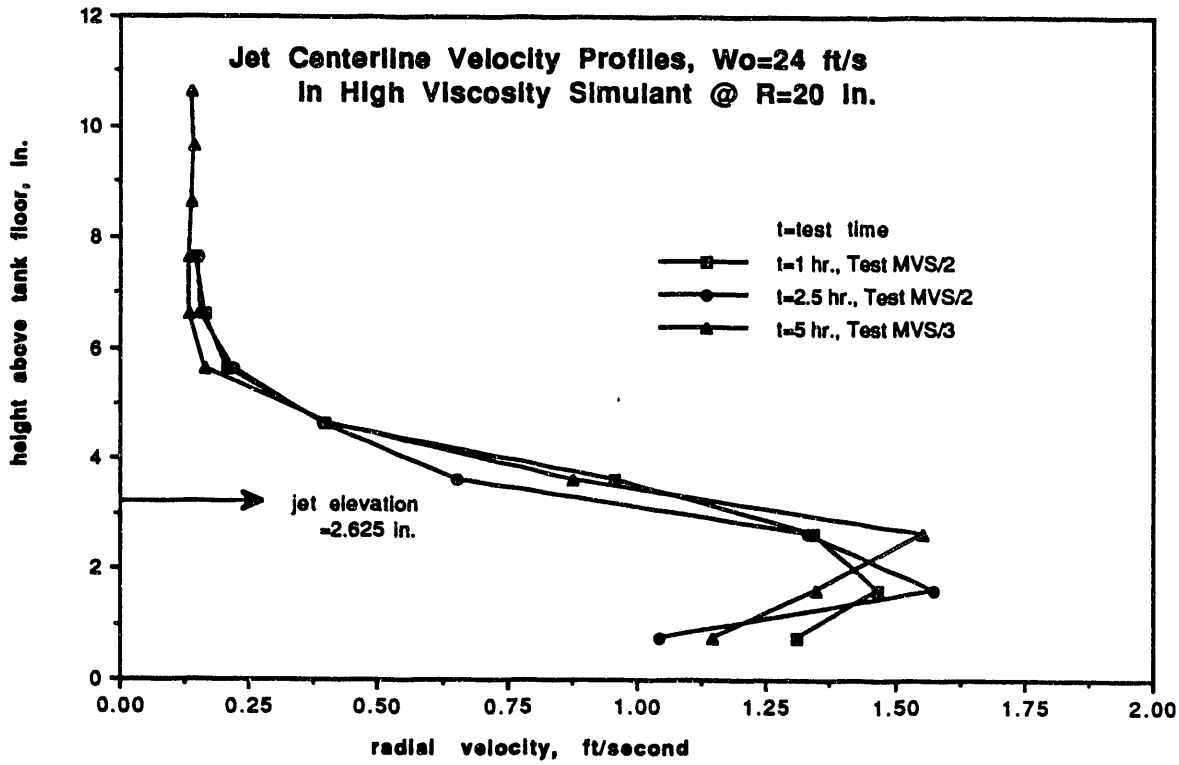

FIGURE 5.5 Jet Centerline Velocity Profiles for High Viscosity Simulant

A check near the end of the tests showed that the jets had dislodged settled solids from the tank floor all the way to the wall. The cleared area began in front of the nozzles and grew to 10 to 12 in. in width near the wall. Though not measured, there remained a substantial layer of settled solids in areas not directly impacted by the jet. In this and subsequent tests, it was apparent that a certain fraction of the material removed from in front of the jets was redeposited on the adjacent sludge. Only a portion was mobilized into the upper regions of the tank. Discrete concentration measurements given in Table B.5 were used to obtain a value for percent of solids suspended at steady state. Using a measured mixture density of 1.31 g/cm^3 and supernatant liquid and fully mixed simulant densities of 1.1 and 1.42 g/cm3, respectively, the solids suspension was 66 percent.

5.3.3.2 15 ft/s Jet Velocity

This test demonstrated that a pair of 15-ft/s fixed position jets was insufficient to mobilize the sludge at full tank radius. The jets dug a 1- to 2-in.-wide channel that did not penetrate beyond the buried velocity probes. A period of 1 h and 10 min was required to break through to the buried probe at a radius of 26.5 in. (see Figure B.18). The interface never made it to the tank surface; in fact, it continued to fall until reaching an apparent steady value at a depth of just over 7 in. This was because the solids in the upper regions of the tank continued to settle. It also indicated that the flow induced by the jets was stratified, or confined to the lower portions of the slurry. The equilibrium height attained by the interface was not limited to the pump suction height; it was 11 in. below the surface.

5.3.3.3 Jet Attachment

Similar to the water tests, a jet velocity was found where the jet attached to the floor very near the nozzle. This occurred at a jet velocity of 59 ft/s, appreciably higher than the roughly 50 ft/s value obtained in water. Note that because this scales to 200+ ft/s in the full-scale tank compared to the prescribed maximum expected velocity of 88 ft/s, the wall attachment behavior does not look like an issue for the proposed tank 241-SY-101 mixing test. Tests in low viscosity simulant will provide an assessment of any influence of Reynolds number on this conclusion.

5.3.4 Low Viscosity Simulant Tests

Low viscosity simulant tests were performed at 25 ft/s and 50 ft/s. The test at 50 ft/s was performed for comparison with experiments in the 1/10-scale tank facility.

5.3.4.1 25 ft/s Jet Velocity

For the low viscosity simulant, the overnight settling time was sufficient to settle out most of the solids. Table B.8 shows that the interface starts out at a depth of 20 in. After initiating the test, the interface raised rapidly for the first hour, then asymptotically approached the surface until finally reaching it at 7½ h.

Developing centerline velocity profiles at 16 and 27 in. are shown in Figure 5.6. The velocities are all positive at 16 in. and are non-changing after the first measurement at 1.25 h. This is consistent with the discrete concentration measurements and with fact that the interface is near the surface (within 3 in.). At 27 in., the consistently negative velocities in the upper portion of the measured profiles indicate a recirculation region. The extent of the recirculation cell cannot be determined from the limited data.

The solids suspension for this case was 59 percent. This value was calculated from the measured mixture density of 1.16 g/cm^3, the 1 g/cm^3 centrifuged supernatant density, and the 1.27 g/cm^3 bulk mixture density. This is a significantly lower solids suspension than the 66 percent reached in the high viscosity simulant at the same velocity. The difference can be attributed to the higher settling velocity in the low viscosity simulant.

5.3.4.2 50 ft/s Jet Velocity

Steady-state velocity profiles were measured after completing the test at 25 ft/s without allowing the contents to settle. Transient data are therefore not available for this jet velocity. The measured velocity profiles are shown in Figure B.26. The increase in jet velocity resulted in a mixed fraction of solids of 0.67.

5.3.4.3 Jet Attachment

The jet attachment behavior observed in water and in high viscosity simulant was also observed in the low viscosity simulant. The critical jet velocity of between 63 and 69 ft/s was higher than in the other two cases. The measured velocity profiles at 16 and 27 in. from the jet are shown in Figure 5.7. Jet attachment is evident from the velocities measured at the height of 3/4 in. The profile shape is the same as that measured in water.

5.3.5 Comparisons Between All Fluids

Several comparisons can be made between the model validation test results for all fluids investigated:

- No discernable difference was observed in the centerline velocity profiles at steady state.

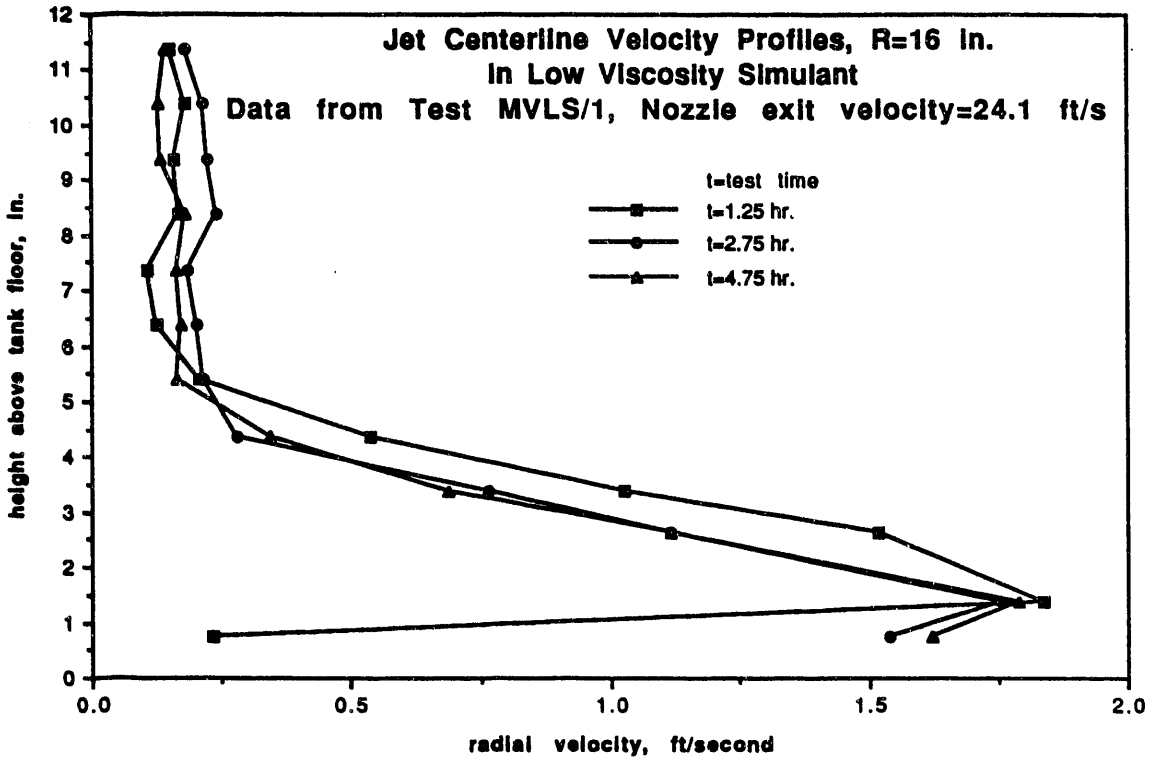

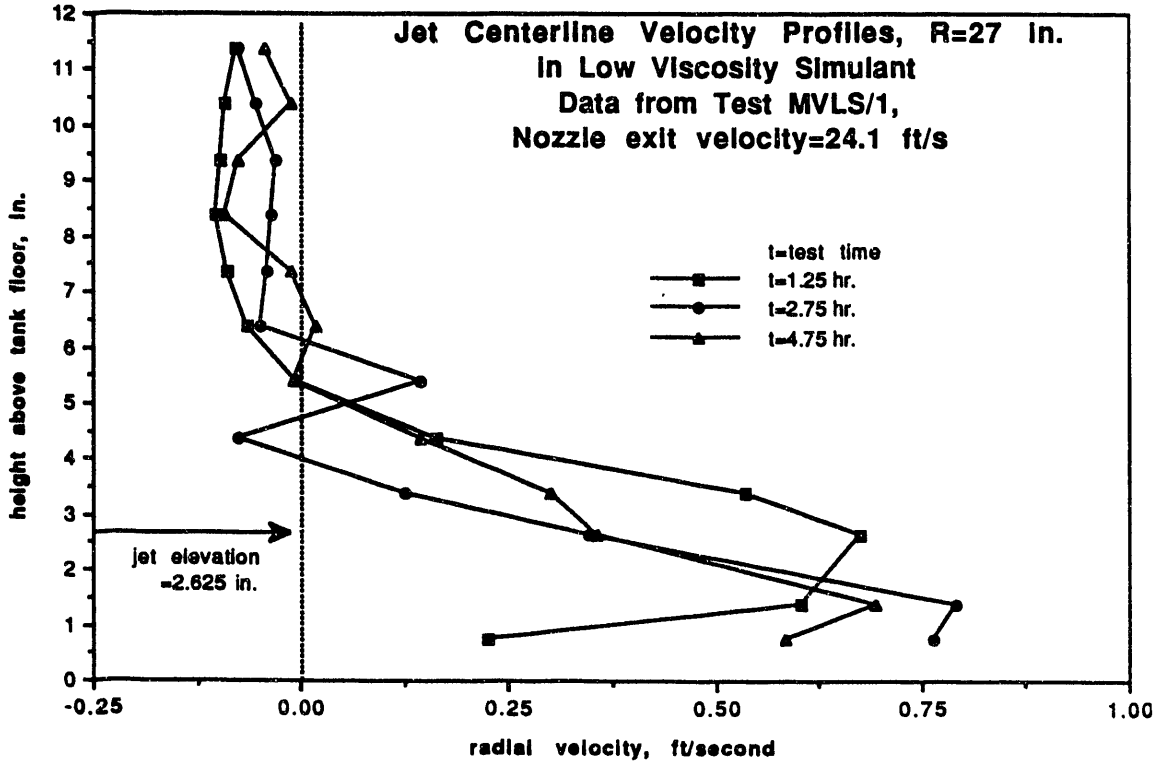

FIGURE 5.6. Developing Centerline Velocity Profiles for Low Viscosity Simulant at 25 ft/s Jet Velocity

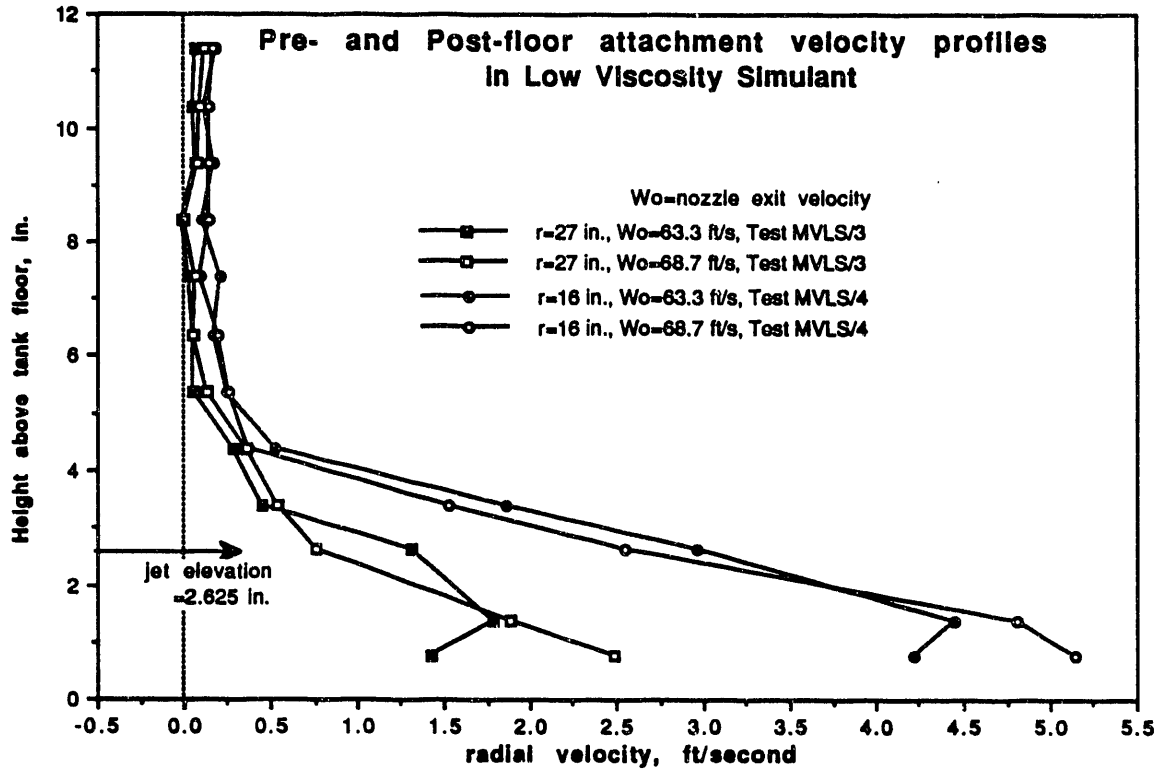

FIGURE 5.7. Centerline Velocity Profiles for Jet Attachment in Low Viscosity Simulant

- Magnitudes of azimuthal velocity profiles are higher for water than in simulant.
- Comparisons of vertical velocity profiles for water and simulant are inconsistent with trends observed in the azimuthal profiles.

Figure 5.8 is included as evidence for the first point. Allowing for differences in measurement location and considering experimental uncertainty, we cannot distinguish between the profiles shown. Although there is no significant difference in the steady-state profiles, there must be substantial differences in the developing profiles when the interface is near the bottom. As witnessed during testing, activity is confined beneath the slurry interface in simulant tests; for water, fluid flows uniformly away from the stagnation point and is subject only to the shape of the tank and surface boundaries. None of the developing jet profiles recorded here include measurements when the interface is near the tank floor.

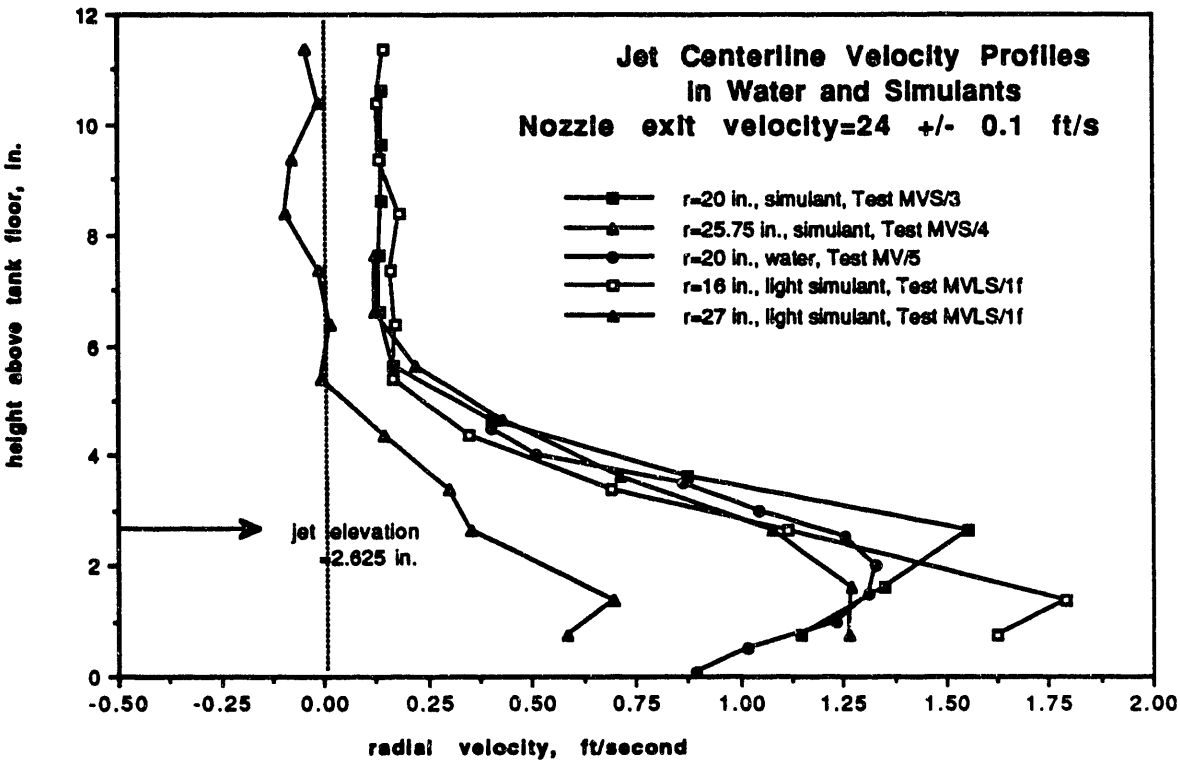

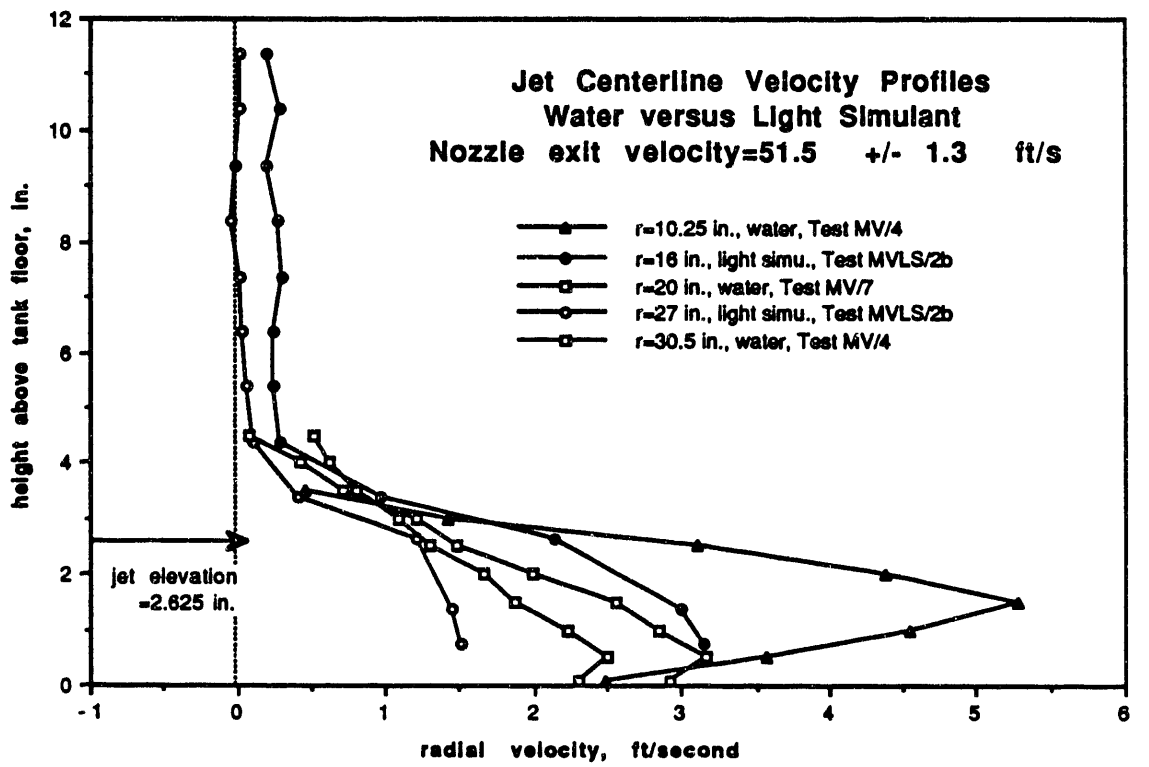

FIGURE 5.8. Comparison of Water and Simulant Centerline Velocity Profiles

Both plots in Figure 5.9 indicate a higher azimuthal velocities for water than for simulant for comparable jet velocities at the nozzle. Considering conservation of mass, higher azimuthal velocities should imply lower vertical velocities. However, the measured velocity profiles in Figure 5.10 are contradictory on this point, one indicating lower vertical velocities and the other indicating higher. This may be the result of too few velocity measurements that do not yield a complete picture of the flow field.

5.4 OPERATING PARAMETER TESTS

The purpose of this set of experiments is to provide input to the mixer pump design and tank 241-SY-101-SY test plan regarding mixing jet operating parameters. Scale model results will be extrapolated to full scale using Liljegren's scaling methodology. Parameters of primary interest include

- jet velocity
- operating time at each angular position required to achieve a desired amount of solids in suspension
- rest time allowable for maintaining a specific minimum percentage of solids in suspension

where rest time is defined as the pause in jet operation after stepping through all specified angular jet positions.

The initial test matrix that addresses jet velocity for each fluid is included in Table 5.8. A fixed operating time of 30 min and a fixed rest time of 2 min were used for these tests. Results are described in this section for the three tests that were completed.

5.4.1 Test Procedure

For this series of tests, the degree of mixing was determined using density measurements at two locations. Durations of the mixing and shutoff times were recorded along with flow rate versus time on the data acquisition system.

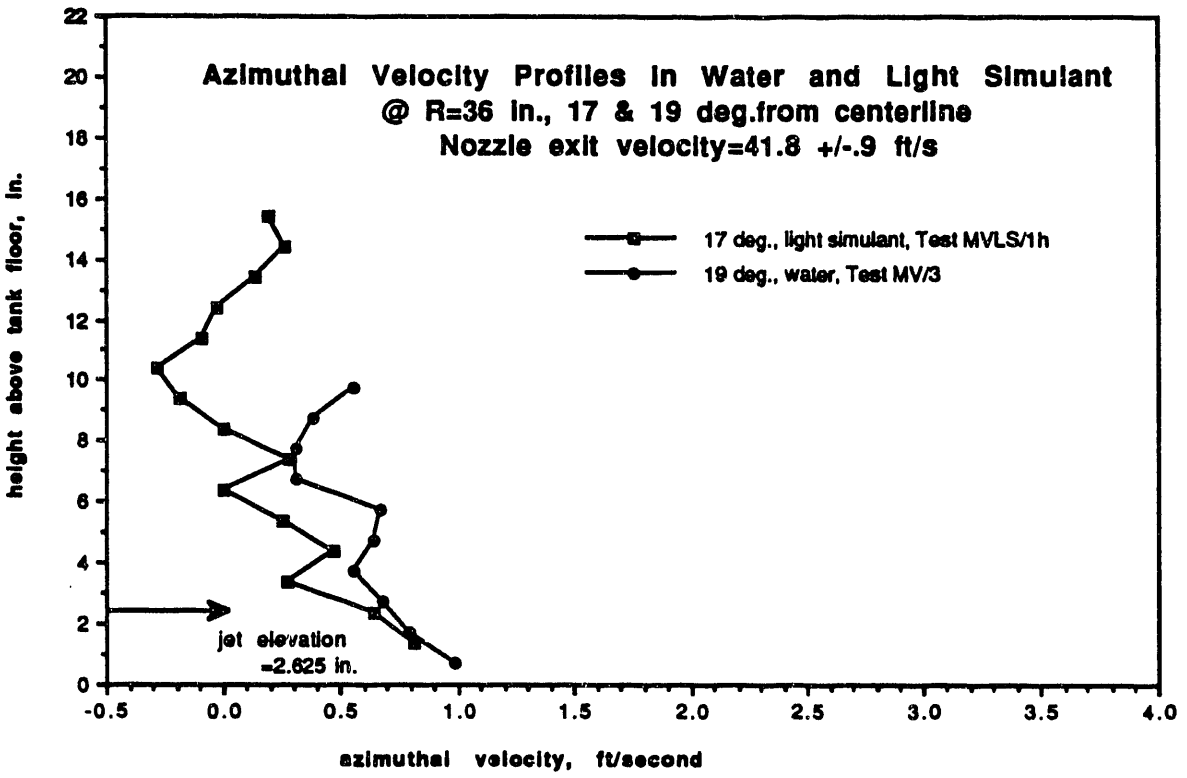

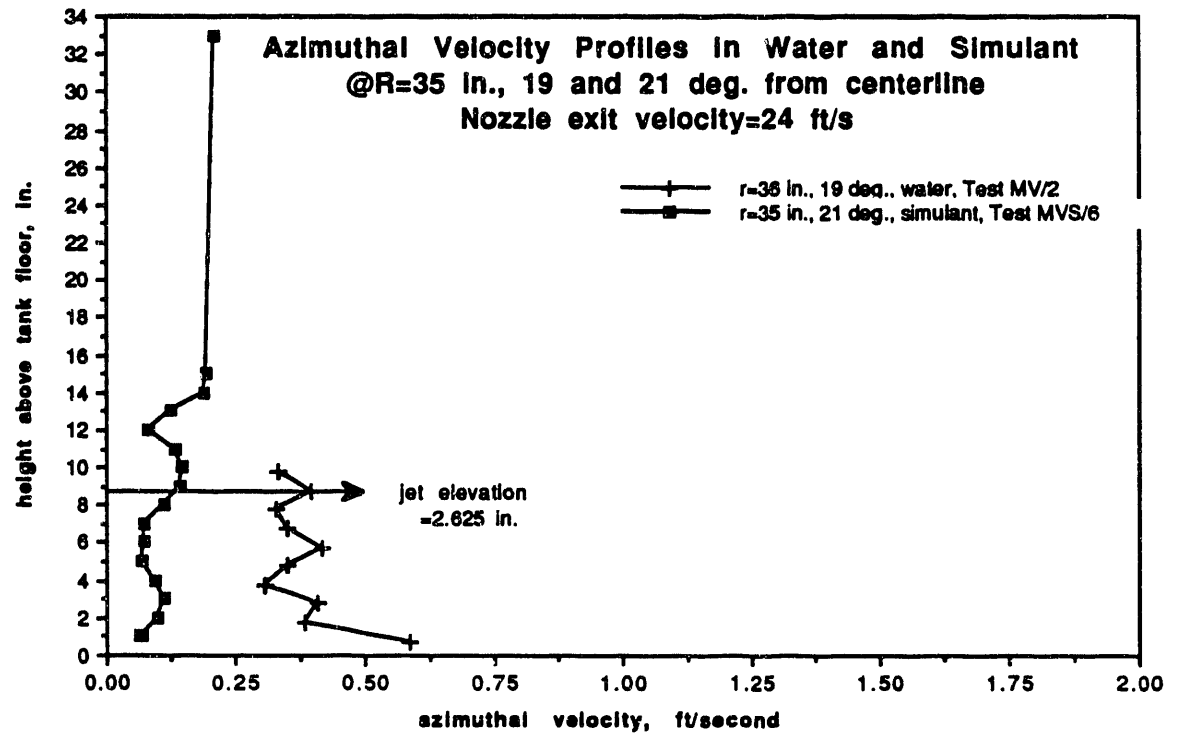

FIGURE 5.9. Comparison of Water and Simulant Azimuthal Velocity Profiles

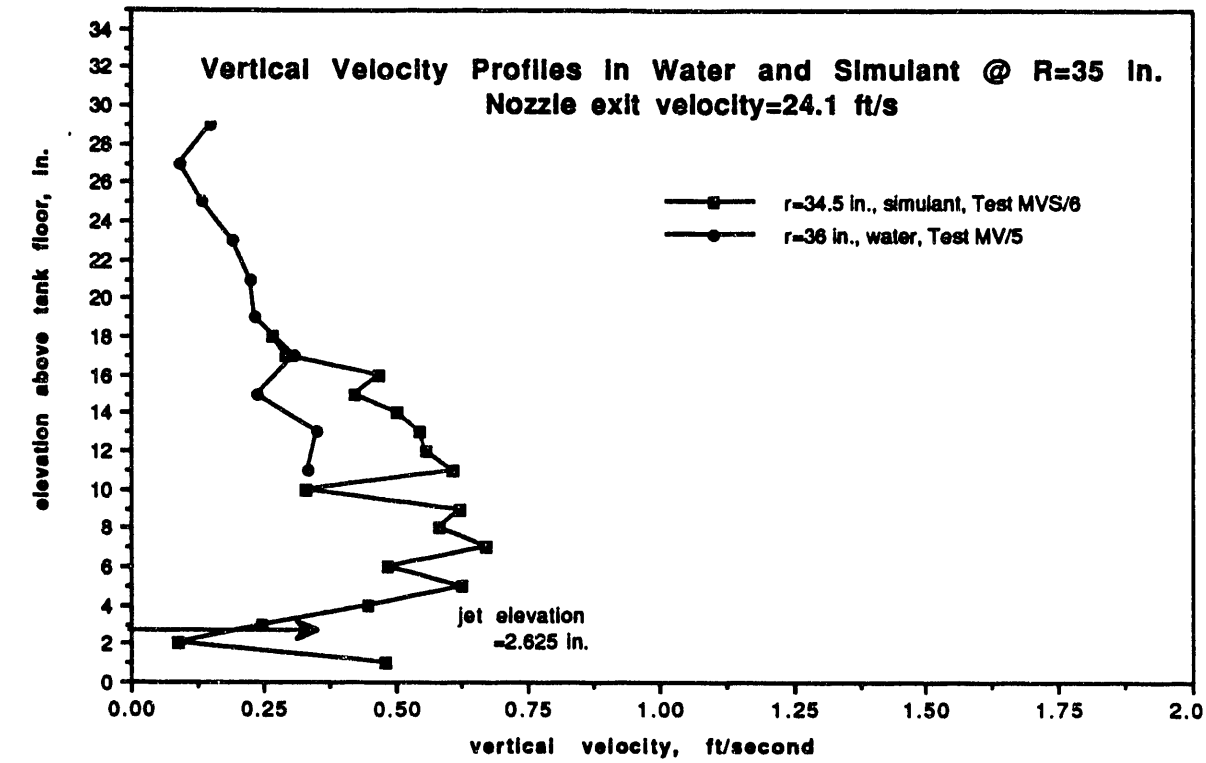

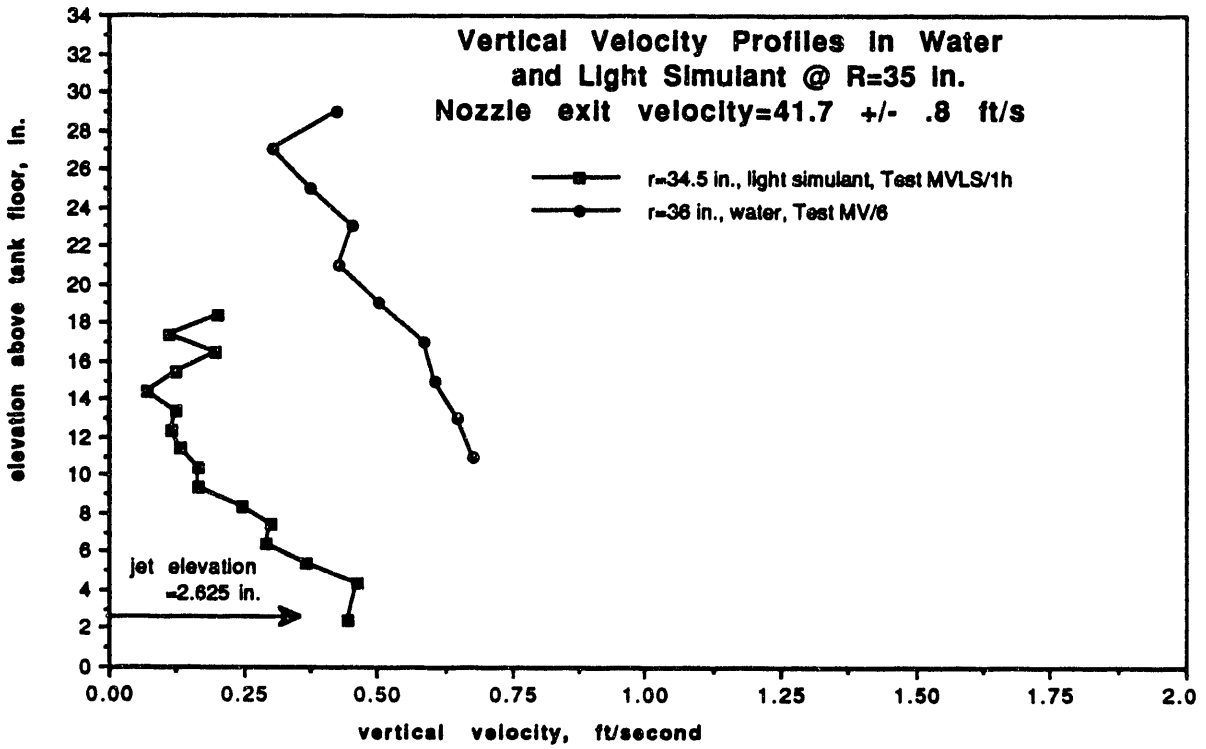

FIGURE 5.10. Comparison of Water and Simulant Vertical Velocity Profiles

TABLE 5.8. Test Matrix for Operating Parameter Tests

Test Number	Jet Velocity ft/s	Jet Nozzle Diameter, in.	Nozzle Height, in.	Simulant Type	Completed
1	15.0	0.217	2.67	high μ	
2	25.4	0.217	2.67	high μ	✓
3	50.0	0.217	2.67	high μ	
4	15.0	0.217	2.67	low μ	
5	25.4	0.217	2.67	low μ	✓
6	50.0	0.217	2.67	low μ	✓

The jets were operated for a fixed amount of time at each angular position. The test procedure includes the following steps:

1. Record the initial jet orientation.
2. Allow solids in tank to settle overnight.
3. Measure and record the initial supernatant density and shear strength of the settled solids.
4. Check the liquid level in the tank and measure the height of the settled solids.
5. Initiate the data acquisition system.
6. Start the pump.
7. Measure and record density at 1 min intervals.
8. Cease jet operation after 30 min.
9. Rotate the jets by 30 degrees.
10. Repeat steps 6 through 9 until the nozzles have been rotated at 30-degree increments a total of 180 degrees and record the hold time required to perform each jet rotation. Maintain jet interrupt time between moves at 2 min.
11. Reposition the jet nozzles back to the zero degree setting and immediately resume a second pass around the tank by repeating steps 6 through 10.

The test was stopped after a steady value of mixture density was reached.

5.4.2 High Viscosity Simulant Tests

Only one test was performed with the high viscosity simulant; it used a 25 ft/s jet velocity. It is interesting to compare the slurry interface rise rate for this test (Table B.10) with that for a fixed jet (Table B.4). It is clear that the interface rises more slowly for the moving jet than for the fixed jet. For example, point 5 in. beneath the surface is reached at 1 h 10 min for the fixed jet, but not until 2 h and 55 min for the moving jet). Despite this, the solids suspension is more effective for the moving jet. This greater efficiency should be expected, however the difference is not great: 66 percent for the fixed location jet versus 66 to 72 percent for the moving jet. Of more importance for tank mitigation was the observation that settled solids were mixed all the way to the wall at this jet velocity, even if they were not mobilized to the upper portions of the tank.

Figure B.31 shows a plot of mixture density versus jet position and time for this test. Small peaks in density were measured immediately after each repositioning of the jet. The mixture density rises steadily until finally reaching a steady value after about 4 h.

5.4.3 Low Viscosity Simulant Tests

5.4.3.1 25-ft/s Jet Velocity

As for the high viscosity test, the interface rises faster for the fixed jet (Table B.8) than for the moving jet (Table B.12). Likewise, the solids suspension was higher for the moving jet (59 percent for the fixed jet versus 59 to 67 percent for the moving jet).

The bottom of the tank was probed after one complete rotation of the jets to determine the depth of the sludge. The sludge layer was approximately ¼-in. deep at the initial jet position (0 degrees) just after moving the jet to the next position (30 degrees). At 90 degrees from the initial jet position, the sludge was 1¼-in. deep. All these measurements were made at 15 to 20 in. from the tank center. This shows the relative amounts and distribution of solids on the tank floor after extended operation.

Interface height and mixture density are shown plotted against jet position in Figures B.36 and B.37. The same peaking behavior is not seen at

each jet reposition because fewer datapoints were recorded for this test. The same trends are indicated as those for the high viscosity test. The comparison of interface height and mixture density in Figure 5.11 shows that the steady value of mixture density coincides with the interface reaching the tank surface (33⅛ in.).

5.4.3.2 50 ft/s Jet Velocity

The interface breaks the surface in 24 min when a 50-ft/s jet velocity is used. Interface data for a fixed jet position is not available for a comparison. The degree of solids suspension can be compared with the fixed jet case and is consistent with findings at lower velocities: solids suspension is higher for the moving jet (74 to 81 percent) than for the fixed jet (67 percent).

5.5 EXTRAPOLATION TO FULL SCALE

Extrapolation of the previously described scale model test results to the full scale, or prototype, is straightforward. As described in Section 3.3.3, prototype velocities are obtained by multiplying the model velocities by the square root of the tank scale, or 3.46. Time is scaled by the same parameter. For example, the sequence for the operating parameter tests at full scale would be 30 x 3.46, or 104 min of jet operating time in each tank sector, with a rest time of 2 x 3.46, or 7 min.

Conclusions drawn from this extrapolation should be tempered by the knowledge that tank 241-SY-101 is not perfectly modeled by this experiment. As noted in Section 5.1.1.3, the simulant dimensionless parameters do not match the full-scale tank's in all respects, and our knowledge of tank 241-SY-101 properties is imprecise. Also the gas phase is not modeled. However, because of the experimental conditions, we believe that our results are conservative; that is, if a given percentage of solids is mobilized and suspended in the scaled experiment, an even greater percentage of solids should be mobilized and suspended in tank 241-SY-101.

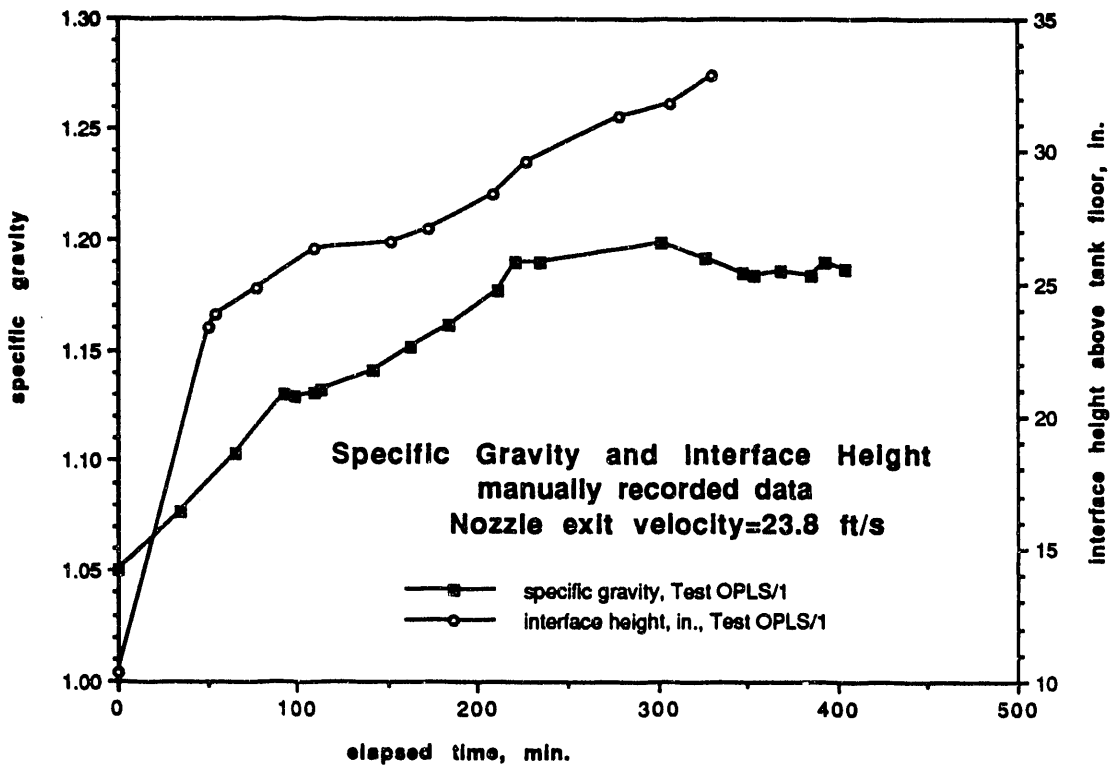

FIGURE 5.11. Comparison of Interface Height with Mixture Density for Low Viscosity Simulant Operating Parameter Test

5.6 MEASUREMENT UNCERTAINTY

Of all the measured and calculated data, the values with the greatest uncertainty are those defining the velocity probes' position. Because of the instrument support and traversing method used, the uncertainty in the velocity probes' horizontal and vertical positions were ±0.75 in. and ±0.25 in., respectively. These uncertainties are considered to contribute to the largest error in the velocity profiles. Because the horizontal profiles contain steep velocity gradients, a slight shift in probe location can result in a significant change in measured velocity. This contributes to the scatter in the data for velocity profiles such as that in Figures 5.4 and 5.10. From the horizontal profiles taken during post-testing (see Appendix E), it was observed that a 0.75-in. shift in a probe's horizontal position at a radius of 10 in. in water could result in a velocity variance of up to 50 percent.

Appendix C describes the uncertainties for all of the data. Table C.1 summarizes the uncertainties for the final reduced data reported.

6.0 REFERENCES

Babad, H., G. D. Johnson, D. A. Reynolds, and D. M. Strachan. 1992. "The Hydrogen Program: The Present Understanding of the Cyclic Venting Tanks." Proceedings of the International Topical Meeting on Nuclear and Hazardous Waste Management Spectrum '92. Vol 1, pp. 712-716. American Nuclear Society, Inc., La Grange Park, Illinois.

Benegas, T. R. 1992. "Tank 101-SY Hydrogen Mitigation Test Functional Design Criteria." WHC-SD-WM-FDC-022, Westinghouse Hanford Company, Richland, Washington.

Fossett, H. 1951. "The Action of Free Jets in the Mixing of Fluids." Trans. Inst. Chem. Engr. 29:322.

Fossett, H. and Prosser. 1949. "The Application of Free Jets to the Mixing of Fluids in Bulk." Proc. I. Mech. E. 160:224-251.

Herting, D. L., D. B. Bechtold, B. A. Crawford, T. L. Welsh, L. Jensen. 1991. Laboratory Characterization of Samples Taken in May 1991 from Hanford Waste Tank 241-SY-101, WHC-SD-WM-DTR-024, Rev. 0, p. 3-5. Westinghouse Hanford Company, Richland, Washington.

Scheele, R. D. 1992. Laboratory Procedure for Measurement of Physical Properties and Rheological Properties of Solutions, Slurries and Sludges. PNL-ALO-501, Rev. 0. Pacific Northwest Laboratory, Richland, Washington.

APPENDIX A

ULTRASONIC CONCENTRATION PROBE

APPENDIX A

ULTRASONIC CONCENTRATION PROBE

A.1 THEORY

Consider ultrasonic waves striking an area (A) of thickness dx. Let n be the number of particles per unit volume and σ be the cross section of each particle for the absorption of ultrasound (note that this is not the same as the geometric cross section). Then the absorption area resulting from all of these particles is n A dx σ. The change in intensity dI (after passing through dx) divided by the intensity I incident upon the layer is equal to the absorption area divided by the area A:

$$dI/I = -n \; A \; \sigma \, dx/A \tag{A.1}$$

The negative sign indicates that the intensity decreases. When this is integrated over a distance L, we obtain

$$I = I_o \; \exp(-n \, \sigma \, L) \tag{A.2}$$

However, transducers measure pressure (p) not intensity. Because intensity is proportional to the pressure squared, we obtain

$$p = p_o \; \exp(-n \, \sigma \, L/2) \tag{A.3}$$

The pressure p_o is proportional to the voltage V_o when the system is filled with distilled water, and p is proportional to the voltage V when the system is filled with simulant. Therefore,

$$V = V_o \; \exp(-n \, \sigma \, L/2) \tag{A.4}$$

$$V/V_o = \exp(-n \, \sigma \, L/2) \tag{A.4a}$$

$$\ln V/V_o = -n \, \sigma \, L/2 \tag{A.5}$$

Therefore, if V/V_o is plotted on a log-scale versus the concentration of the simulant in particles/volume, one should obtain a straight line having a slope equal to $-\sigma L/2$. L can be measured in the experiment; therefore, the absorption cross section σ can be determined.

The concentration of the simulant is often expressed in wt%, which is defined as the weight of the compound divided by the total weight of the compound plus water times 100%. The mass of the compound (M_c) is given by

$$M_c = N M_p \tag{A.6}$$

where N is the number of particles and M_p is the mass of each particle. Let V_w be the volume of water and V_s be the volume of the slurry. Because V_s may be only slightly different from V_w, we obtain

$$V_s = V_w(1 + f) \tag{A.7}$$

where f is some fraction that must be measured.

The wt% C is given by

$$C = N M_p / (N M_p + \rho_w V_w) \text{ X } 100\% \tag{A.8}$$

where ρ is the density of distilled water. Dividing numerator and denominator by V_s, we obtain

$$C = n M_p / [n M_p + \rho_w / (1 + f)] \text{ X } 100\% \tag{A.9}$$

Solving for n we find

$$n = [\rho_w / \{M_p(1 + f)\}] \{C / (100 - C)\} \tag{A.10}$$

Let us define n′ as follows:

$$n' = C / [(100 - C) (1 + f)] \tag{A.11}$$

Substituting Equations (A.10) and (A.11) into Equation (A.5) we obtain

$$\ln V/V_o = - [\sigma L \rho_w / 2 M_p] n' \qquad (A.12)$$

A.2 PROBE DESIGN

A probe developed to demonstrate the proof-of-principal of the ultrasonic measurement technique for the double-shell tank retrieval project was used in these tests. The probe consists of parallel and coaxial transducers mounted 4 in. apart and suspended in the tank by a rod.

The transmitter (send transducer) sends a swept-frequency pulse (0.1 to 3.0 Mhz) through the slurry to be received by the receiver (receive transducer). The pulse, whose duration can be made to range from 0.1 ms to 10 s, is actually a train of sinusoidal bursts whose frequencies increase successively to sweep the desired frequency range. The signal received by the second transducer is nothing more than these sinusoidal bursts that have been attenuated by the slurry. A peak detector is used to capture the amplitudes of each sinusoidal burst; the bursts are then displayed in real time on a Macintosh IIc. The first plot in Figure A.1 is an example of several sweeps of the received signal (RS), which was recorded at a sampling frequency of 100 Hz.

A.3 PROCEDURE

Every measurement actually began as a recording of several sweeps of the RS because some individual sweeps contained unexplained voltage spikes, which were perhaps caused by the electronics. One of the more uniform sweeps was later chosen to be analyzed as the actual data. The second plot in Figure A.1 is the sweep windowed in the first plot (note filled circles), but the amplitude has been adjusted to account for a gain that was introduced by a receiver/amplifier. The width of the sweep corresponds to the frequency range so that the points marked on the second plot indicate the amplitude of the RS at our chosen frequencies.

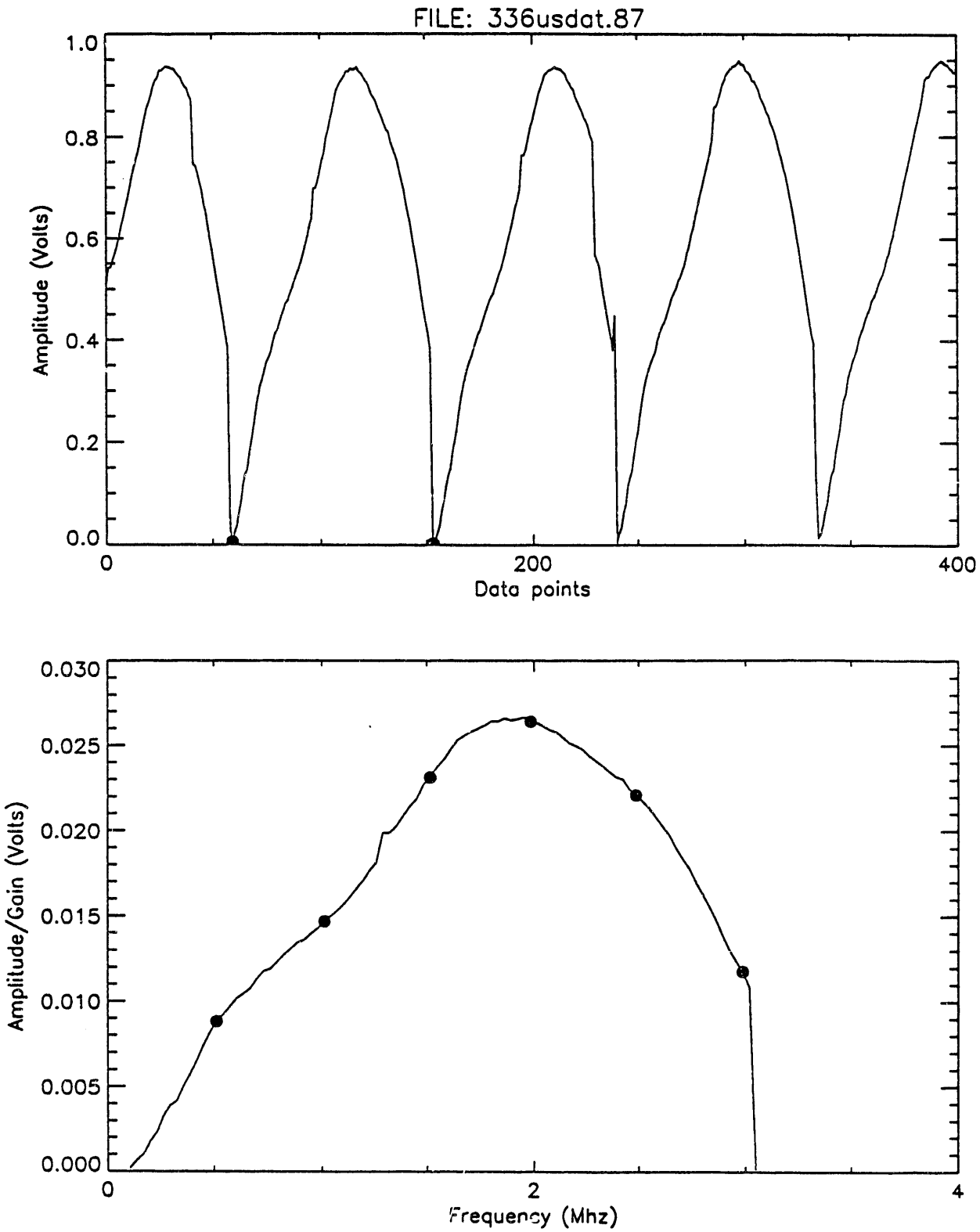

FIGURE A.1. Attenuated Ultrasonic Signal Captured by Receiver

To ensure that we were choosing the amplitudes at the proper frequencies, we also simultaneously recorded a voltage ramp that controlled, and was proportional to, the frequencies in the sweep range. Once a sweep was chosen, the appropriate ramp waveform was used to determine the point on the RS that corresponds to the chosen frequencies. For example, a point on the ramp that is half the amplitude of the ramp peak occurs simultaneously with the frequency that is halfway through the sweep range. Every time a RS and ramp were recorded, a new data file was created; in the end, 320 data files had been created, including those used for calibration.

The measurements were made for a high-viscosity slurry and a low-viscosity slurry, the viscosity being controlled by the amount of sugar and water added to the slurry. We began by taking two types of measurements in the high-viscosity slurry:

1. Before and after the jet was turned on, we recorded the RS every 5 min while the probe remained fixed at a certain height in the slurry.

2. Before and after the jet was turned on, we recorded the RS at several heights by lowering the probe into the slurry in 5-in. increments. We called this "taking a traverse," and we usually took several traverses a day.

Because we were interested in how the wt% profile of the slurry changed in time, we decided that the traverses were the more useful measurement. Therefore, during the high-viscosity measurements, we stopped taking data at a fixed height and took only traverses for the rest of the experiment.

A.4 DATA ANALYSIS

The first step was to convert the Macintosh-Excel[(a)]-formatted data to DOS[(b)]-formatted data that could be read into a SUN Sparcstation[(c)]. This conversion was accomplished using a program called Apple File Exchanger.[(a)] Next, a file was created on the SUN that contained information about all of the data files, including file name, the attenuation used when recording the

---

(a) Apple Computer, Inc., Cupertino, California.
(b) International Business Machines Corporation, Boca Raton, Florida.
(c) Sun Microsystems, Mountain View, California.

signal, the time of the recording, the height of the probe, etc. This file was used by several PV-WAVE[a] programs to analyze and plot the data. A program called slur336.pro[b] plots several of the RS sweeps and allows the user to use the cursor to choose a sweep that has the least amount of noise and the fewest odd spikes (see Figure A.1). The amplitudes at these frequencies are then written to an output file to be used by other programs to convert these voltage amplitudes to wt% and to plot the height versus wt%.

A.5 CALIBRATION

To convert voltages to wt%, calibration lines were generated for each of the two types of slurry. The RS was recorded for several known values of wt%, and straight lines were generated for frequencies of 0.5, 1.0, 1.5, 2.0, 2.5, 3.0 MHz. These calibration lines and data are plotted in Figures A.2 and A.3; Tables A.1 and A.2 list the coefficients for the straight lines provided by PV-WAVE for each of the two viscosities.

Note that, except for at 3.0 MHz, the slopes increase as the frequency increases. While the steepest slope provides best wt% resolution, it also implies that the amplitude of the RS at that frequency is greatly reduced at high wt%. Thus, by choosing the calibration line at 2 MHz, a compromise was made so that we achieved good resolution as well as an adequate wt% range. The amplitudes at 2 MHz were used to determine the wt%.

A.6 DISCUSSIONS AND CONCLUSIONS

This project was the first actual test of our ultrasonic probe outside of the laboratory, and the preliminary results shown in the above plots indicate that the probe is a viable method of determining wt% in certain slurries. We expected the wt% to increase or decrease at certain points in the tank, and our probe captured those changes repeatedly. There are, however, a few further points that should be mentioned.

(a) Precision Visuals Incorporated, Boulder, Colorado.
(b) slur336.pro was written especially to analyze this data by Joe Mai, Norcus student.

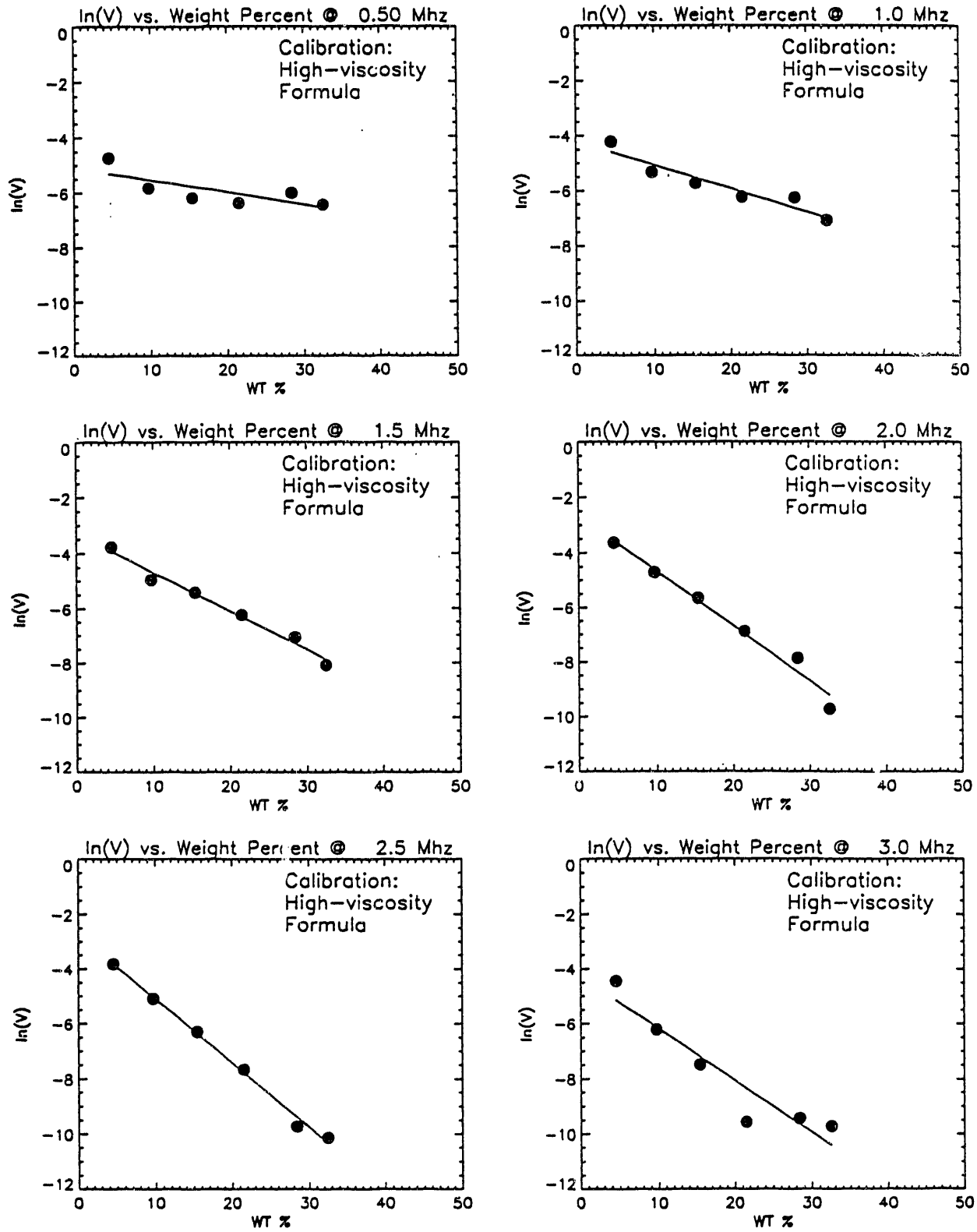

FIGURE A.2. Calibration Curves for High Viscosity Simulant

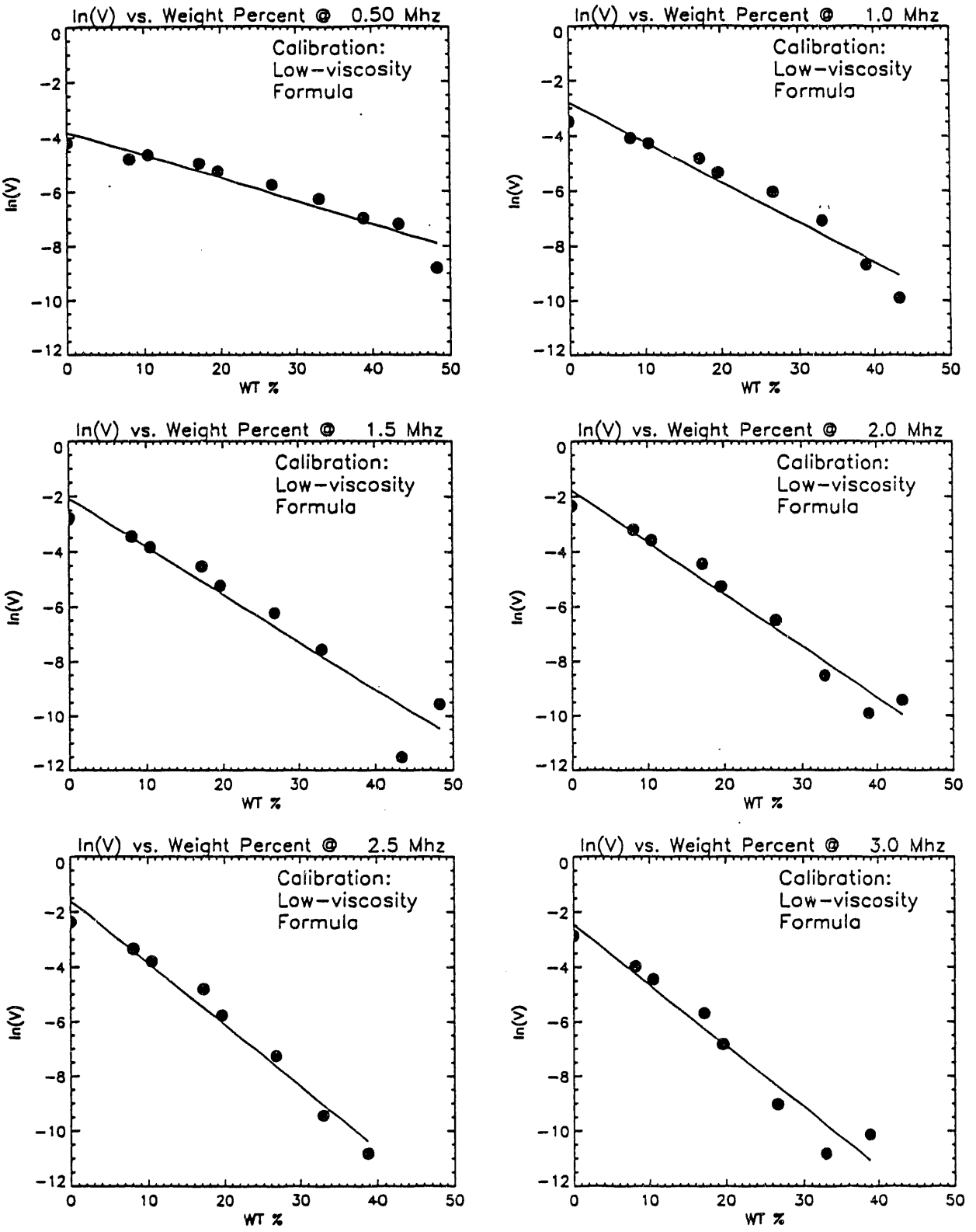

FIGURE A.3. Calibration Curves for Low Viscosity Simulant

TABLE A.1. Calibration Coefficients for High Viscosity Simulant

Frequency, MHz	Slope, ln(V)/wt%	Intercept, ln(V)
0.5	-0.046	-5.09
1.0	-0.085	-4.20
1.5	-0.141	-3.27
2.0	-0.202	-2.65
2.5	-0.232	-2.77
3.0	-0.188	-4.30

TABLE A.2. Calibration Coefficients for Low Viscosity Simulant

Frequency, MHz	Slope, ln(V)/wt%	Intercept, ln(V)
0.5	-0.085	-3.83
1.0	-0.145	-2.79
1.5	-0.174	-2.07
2.0	-0.189	-1.76
2.5	-0.226	-1.59
3.0	-0.222	-2.45

1. Although we were able to note general trends in the tank, we have been estimating the uncertainty of the wt% to be a few percent. We found in previous work with an aluminum-silicate slurry that the uncertainty is about 5 to 10 percent, but this slurry may behave differently. A determination of the actual uncertainty is important and should be quantified.

2. The wt% profile of the tank over time determined by the ultrasonic probe should have a correlation with the independent measurements of other fluid properties, such as the fluid flow rates and densities, that were taken simultaneously. At the time of this writing, the fact that the other measurements show the same general changes in wt% as our probe was known, but whether or not individual measurements at certain times and heights indicate the same wt% was not known.

3. The actual particle size(s) needs to be determined, and if there are variations in size, new calibration runs must be made for each size.

4. Some of the possible sources of uncertainty in our measurements are

   a) The wt% was calculated assuming that the supernatant liquid particle concentration remained constant, which may not have always been the case.

   b) Although, the peak detector was calibrated and inspected prior to this test, its output has a small error when compared to the amplitude of the input signal. However, because our calibration was made with this error in existence, our results should be repeatable.

   c) The MR101 receiver that amplified the RS has some varying uncertainties in its gain settings.

   d) As mentioned previously, the RS sometimes contained strange voltage spikes superimposed on the actual signal. We avoided using RS sweeps that contained these spikes, but they are still a source of uncertainty.

   e) During calibration, we discovered that the slurry can dry on the faces of the transducers if left out of the tank. If the faces of the transducers are not properly wiped before they are inserted in the tank, spurious signals can result.

   f) The height of the probe was taken as the distance between the bottom of the sleeves that hold the transducers and the bottom of the tank, but the axis of the sound beam travelled at a slightly higher height. Also, the U-shaped bar that held the transducers apart may have rotated out of its usually vertical plane as we pushed the probe into the thick sludge layer.

Because this probe is still in an experimental stage, some of these uncertainties are to be expected. As the probe is updated and made more efficient, the uncertainties will become more manageable and quantifiable.

APPENDIX B

DATA PACKAGES FOR ALL TESTS

APPENDIX B

DATA PACKAGES FOR ALL TESTS

Table B.1 presents a list of all tests performed along with their primary attributes. Data packages are included in this appendix in the order that the tests appear in Table B.1.

TABLE B.1. Tests Performed

Test Type TT/#	Simulant Type	Jet Velocity, ft/s	Transient	Steady State
FV/1	water	25		✓
FV/2	water	25		✓
FV/3	water	15	✓	
FVLS/1	low μ	25	✓	
IC/1	water	10 to 65	✓	
JC/1	water	50		✓
MV/2,5	water	25.4		✓
MV/3,6	water	45		✓
MV/4,7	water	55		✓
MVS/1,2	high μ	25.4	✓	
MVS/3,4	high μ	25.4		✓
MVS/5	high μ	15	✓	
MVLS/1	low μ	25.4	✓	✓
MVLS/2	low μ	50		✓
MVLS/3	low μ	63		✓
MVLS/4	low μ	69		✓
OPS/1	high μ	25.4	✓	
OPLS/1	low μ	25.4	✓	
OPLS/2	low μ	50	✓	

Abbreviation Legend: FV - flow visualization; MV - model validation; OP - operating parameter tests; IC - instrument comparison; JC - jet comparison; S - distinguishes simulant from water tests; and L - distinguishes low from high viscosity simulant.

B.1 SENSOR POSITIONS

Angular Position The tank is assumed to be symmetrical. (This was validated during instrumentation comparison testing.) The 0-degree position is the north-south centerline of the tank; this corresponds to the jets' axes. For the model validation tests, angular position is measured in either a clockwise or counter clockwise direction; therefore, angular position varies from 0 to 90 degrees. Angular position for the operations tests is measured from the 0-degree axis in a clockwise direction, the same direction the jets are rotated, and varies from 0 to 180 degrees.

Radial Position Radial measurements are taken from the tank center except on the centerline. Jet centerline measurements are measured from the tip of the nozzle (1.9 in. from the tank center).

Velocity Profiling Positions

Seven locations within the tank were selected for obtaining velocity measurements. The seven locations consisted of three jet centerline, two vertical wall, and two azimuthal (circumferential) measurement positions. Vertical velocity profiling was performed at each position except position No. 7. The specific location of some measurement positions varied among tests because of the test apparatus and instrumentation sizes and configurations The seven positions are described below.

Velocity Position 1 This position is located in the jet centerline, 0 degrees, at a radius of 10 in. and measures the jet's axial component. This position was used during freshwater model validation tests but not for tests with simulant. The pitot probes could not be utilized during simulant tests and the size of the electro-magnetic meter probes is to obstructive to allow for accurate readings at that close of distance to the nozzle.

Velocity Position 2 This position is located in the jet centerline, 0 degrees, at radii of 16 and 20 in. and measures the jet's axial component. This position was used for both simulant and freshwater tests.

Velocity Position 3 This position is located in the jet centerline, 0 degrees, at radii of between 25.75 and 28.5 in. and measures the jet's axial component. This position was used for both simulant and freshwater tests.

Velocity Position 4 This position is located near the tank wall at 0 degrees and radii of 36 and 35 in. (true radius). The smaller

radius was used for simulant tests. The higher conductivity of the simulant made it necessary to move the electromagnetic meter probes away from the metal tank wall to avoid interference. This position was used to measure vertical velocities.

Velocity Position 5 This position measures the azimuthal velocities near the tank wall. This position is located at 19 degrees and 21 degrees and radii of 36 and 35 in. As with position 4, the 35-in. radius was used for simulant tests.

Velocity Position 6 This position measures the azimuthal velocities near the tank wall. This position is located at 34 degrees and a radius of 36 in. Because of the low velocities observed while testing with water, position 6 was not used for simulant tests.

Velocity Position 7 This position is located at 12 degrees and a radius of 36 in. No profiling is performed at this position. The probe is held in a fixed position 17 in. above the tank floor. This position is used to measure wall velocities at an angle of approximately 27 degrees to the vertical centerline plane. This angle was created by directing the probe at the centerline on the tank floor.

Syringe Sampling Positions

Two locations were used for taking syringe samples to be used in determining concentration profiles. The two positions were designated north (N) and west (W). Unlike the velocity positions, which are considered the same in all four quarter sections of the tank, the syringe positions refer to a unique location in the tank. A description of the two positions follows.

North This position is at 0 degrees (north side of tank) and a radius of approximately 20 in. (true radius). This position was used for both model validation and operation tests. For model validation tests the position coincides with the jet. For operations tests it coincides with the 0 degrees and 180 degrees jet positions.

West This position is at 90 degrees (west side of tank) and a radius of approximately 20 in. This position was used for both model validation and operation tests. For operation tests, this position coincides with the 90 degrees jet position.

Statham Position The Statham was located in the southwest quarter of the tank at 47 degrees, a radius of 26 in., and a height of 24.8 in. The Statham measures the average density over a 10-in. vertical height. Statham measurements were averaged over the tank height range of 19.8 to 29.8 in.

B.2 FLOW VISUALIZATION TESTS

B.2.1 Water-Based Tests

Flow visualization testing consisted of three tests, one start up transient and two steady-state flow conditions. Approximately 200 cc of dye consisting of 1 part white latex paint and 9 parts water were mixed in a small pressure vessel. The vessel was pressurized with air, and the dye injected into the flow just upstream of the mixer jet assembly. The tests were video taped using three cameras. One camera filmed from above the entire tank. A second camera positioned above the tank focused on just the north jet. The third camera filmed the north wall of the tank from an angle to record the vertical rise of the dye plume. The video cameras recorded time and were synchronized with the data acquisition system (DAS) via audio signals. The DAS recorded flow rate and temperature.

The geometric dimensions of the test set up were the same as for all other tests except for the diameter of the nozzles. The nozzles used for the flow visualization tests had a diameter of 0.217 in. The diameter of the nozzles used for all other testing was 0.224 in. The test fluid was tap water.

B.2.1.1 Transient Tests

The transient test was conducted for model validation purposes and did not attempt to model any particular flow ramp up. The steady-state flow rate of the transient test was 16 ft/s. The dye injection lasted approximately 16 s. The jet assembly was centered in the tank.

The video of the transient test can be obtained from Westinghouse Hanford Company, Information Resource Management Division, Audio Visual Department, Tape No. 3422, Reel No. 5.

B.2.1.2 Steady-State Tests

The major difference between the two steady-state tests was the position of the jet assembly. The nozzle was centered in the tank. In the other test the jet assembly was positioned 3 in. south of tank center along the jets' axes. The flow rate for both tests was 25 ft/s. Dye injection time for the centered and off-centered tests was 8 and 6 s, respectively.

The video of the steady-state tests can be obtained from Westinghouse Hanford Company, Information Resource Management Division, Audio Visual Department, Tape No. 3422, Reels No. 1 and 2.

B.2.2 Simulant-Based Tests

Test FVLS/1, performed July 28, 1992, was a flow visualization test in low viscosity simulant. The purpose of the test was to observe the behavior of the settled solids layer when the jets were impulsively started and maintained at a velocity of roughly 25 ft/s. This was an informal test with no video or DAS record.

Observations: The supernate was clear to a depth of 24 in. at the start of the test. When the pump was started, a 1-in.-high wave was initiated at the tank center and travelled to the tank wall remaining concentric with the tank wall at all times (this was interesting because the disturbance centers are approximately 4 in. apart). The sludge interface appeared to be lifted by this initial wave, maybe 1 in., but this was difficult to tell from the vantage point above the tank. Immediately following the pump start and release of the surface wave, a surface disturbance formed in front of both jets. These disturbances were the dominant feature in the remainder of the 30-min test; they grew in size, sometimes stopped and reappeared, and slowly moved outward to the tank wall, but did not change otherwise.

The disturbance that formed in the front of each nozzle was in the form of a turbulent, roiling surface that might be compared to that formed when a garden hose is placed just under a water surface and the water is allowed to flow vertically upward. This disturbance rose above the otherwise level interface, with a height estimated at less than 1 in. The initial size of the disturbances was 6 to 8 in. across; this grew to maybe 12 to 14 in. by the

time the disturbance reached the wall. The disturbances were intermittent, sometimes stopping for a fraction of a minute; this intermittency was independent for the two disturbances. The likely explanation for this behavior was that the jet erosion process included periods where the jet was eroding the lower levels of the settled layer; the overburden of the upper levels of the sludge layer prevented the deflected jet from being seen at the surface.

As the disturbances moved outward, their progress was unsteady and inconsistent. The disturbances finally reached the tank wall in about 30 min, at which time the test was stopped. As noted below, the interface had risen to a depth of 20 in., a change of 4 in. during the course of the test.

Measurements: Supernatant density measured with the Statham was 1.049 g/cm^3 at the start of the test. Combined jet flow rate was 5.78 gpm for a jet velocity of 23.5 ft/s. The supernatant density and jet flow rate was unchanged at 21 min into the test, at which point the disturbance was two-thirds or three-quarters of the distance to the wall. After 28 min, the slurry interface was at 20 in. below the surface.

B.3 FACILITY CHECKOUT TESTS

B.3.1 Instrument Comparison Tests

A series of tests was performed to compare velocity measurement instrumentation, including pitot probes and electromagnetic probes. The two probes were located in opposing jets on jet nozzle centerline at equal distances from the tank centerline. Velocities were measured while varying flow rate over the expected test range. Measured velocities for probes located 10 in. from tank centerline are given in Figure B.1. Averaged data for the entire test is shown first, followed by instantaneous data for a selected interval. Similar data for probes located 25 in. from tank centerline are shown in Figure B.2.

B.3.2 Jet Comparison Tests

To verify a uniform jet from each nozzle, identical probes were used to measure velocity profiles in the two jets. Results for vertical traverses through the jets at 10 and 25 in. from tank centerline are shown in Figure B.3.

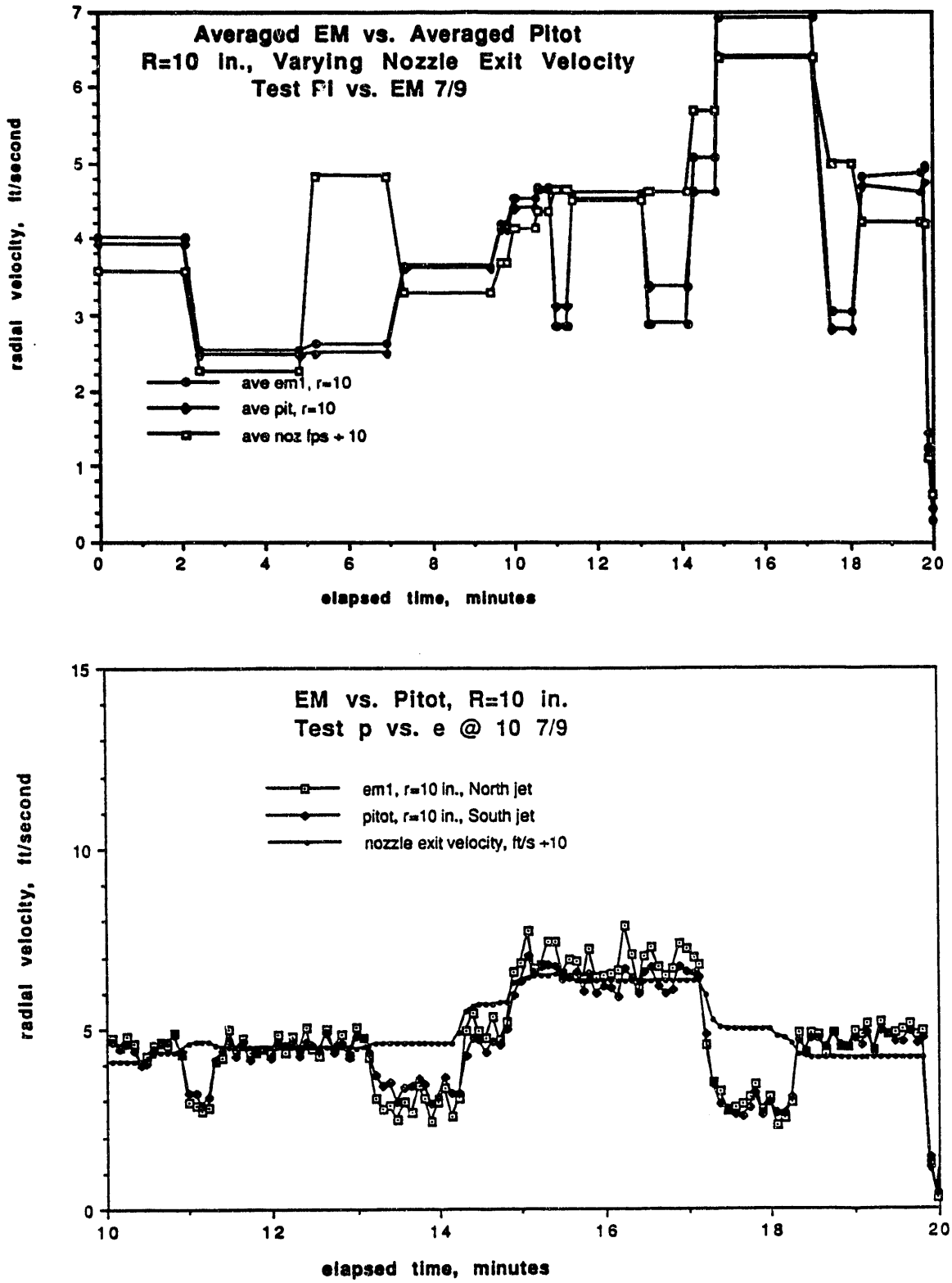

FIGURE B.1. Velocity Histories Measured in Test IC/1 at R=10 in.

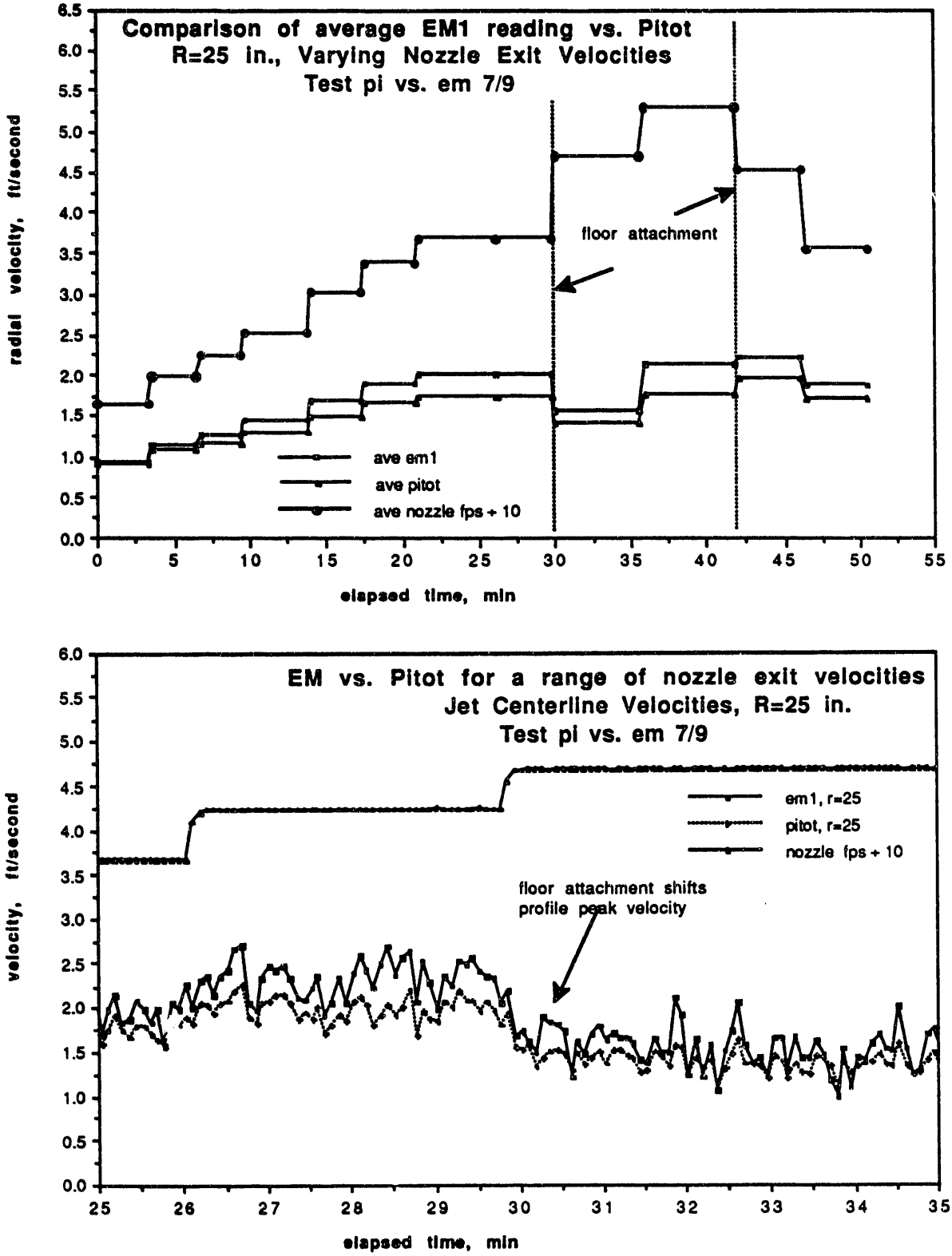

FIGURE B.2. Velocity Histories Measured in Test IC/1 at R=25 in.

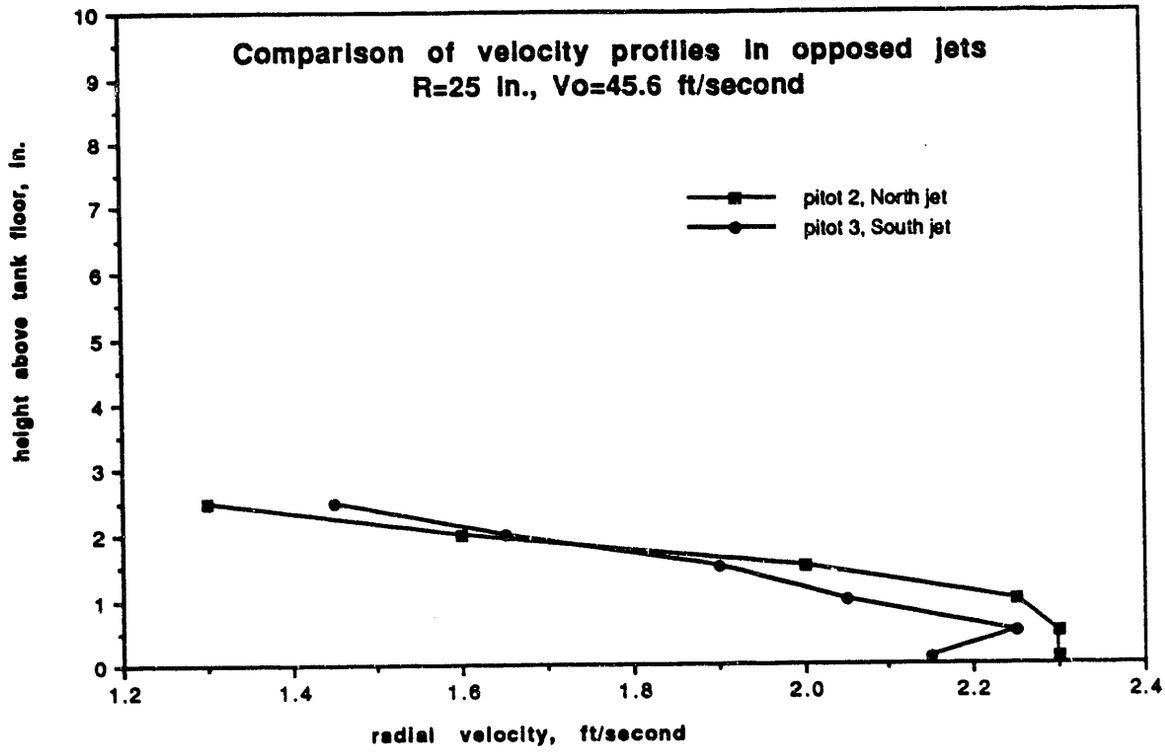

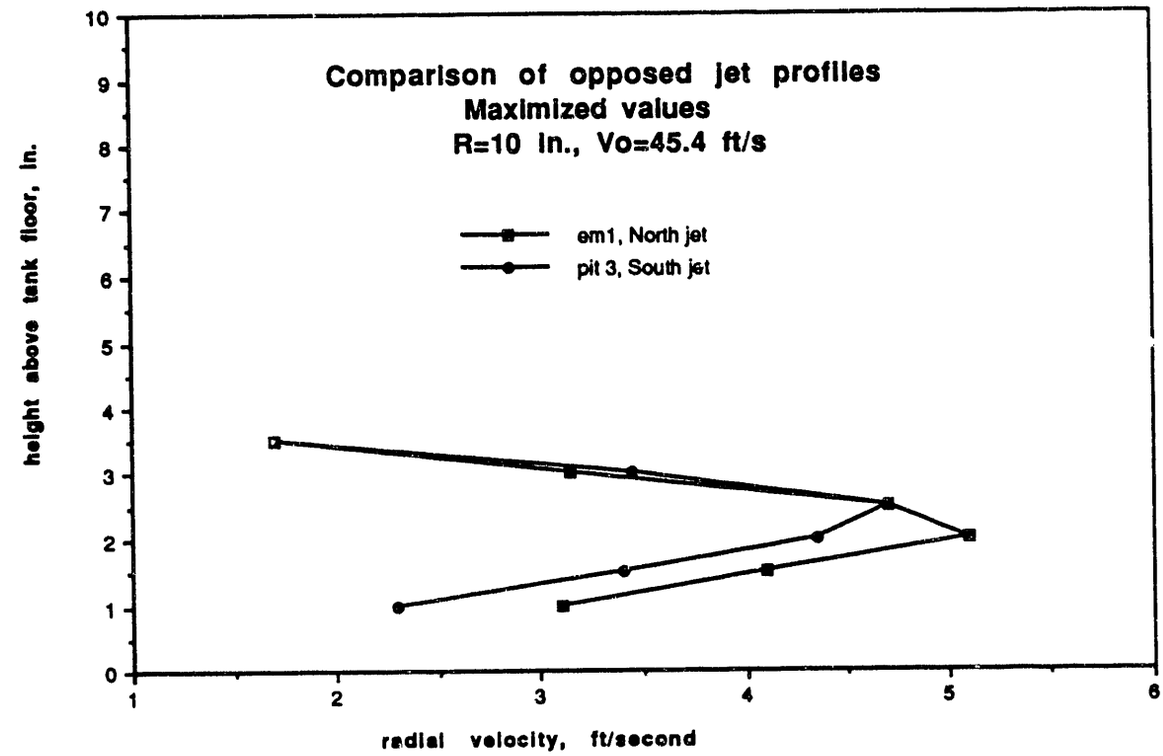

FIGURE B.3. Velocity Profiles Measured in Test JC/1

B.4 MODEL VALIDATION TESTS

A series of model validation test results is discussed in this section for both water-based and high viscosity simulant-based tests.

B.4.1 Water-Based Tests

Test No. MV/2 **Test Date:** July 10, 1992

Description: Freshwater velocity profiling at 25.4 ft/s. Locations 1, 3, 5, and 6 traversed.

Measurements: Velocity profiles are shown in Figure B.4.

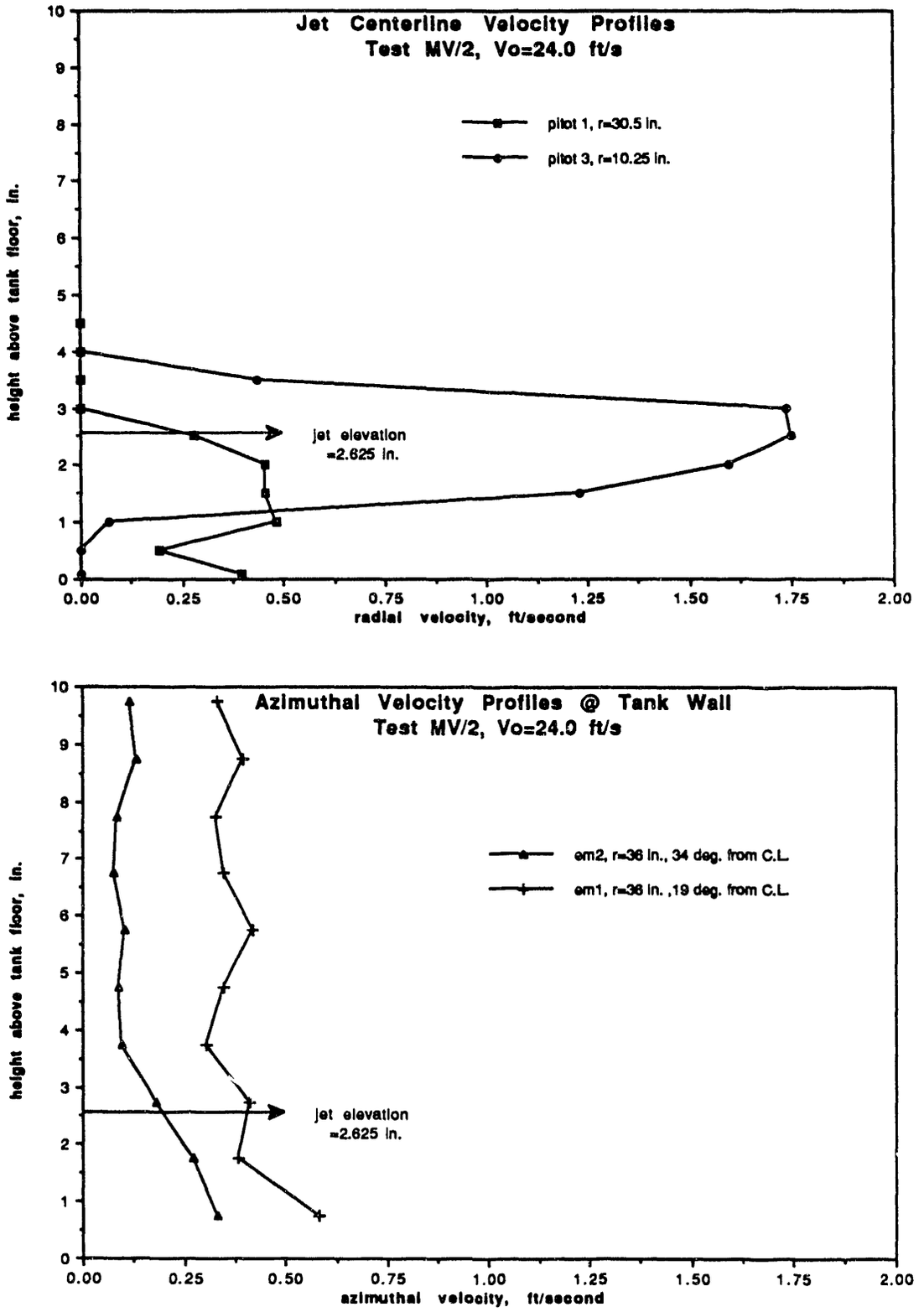

FIGURE B.4 Velocity Profiles Measured in Test MV/2

Test No. MV/3 **Test Date:** July 10, 1992

Description: Freshwater velocity profiling at 45 ft/s. Locations 1, 3, 5, and 6 traversed.

Measurements: Velocity profiles are shown in Figure B.5.

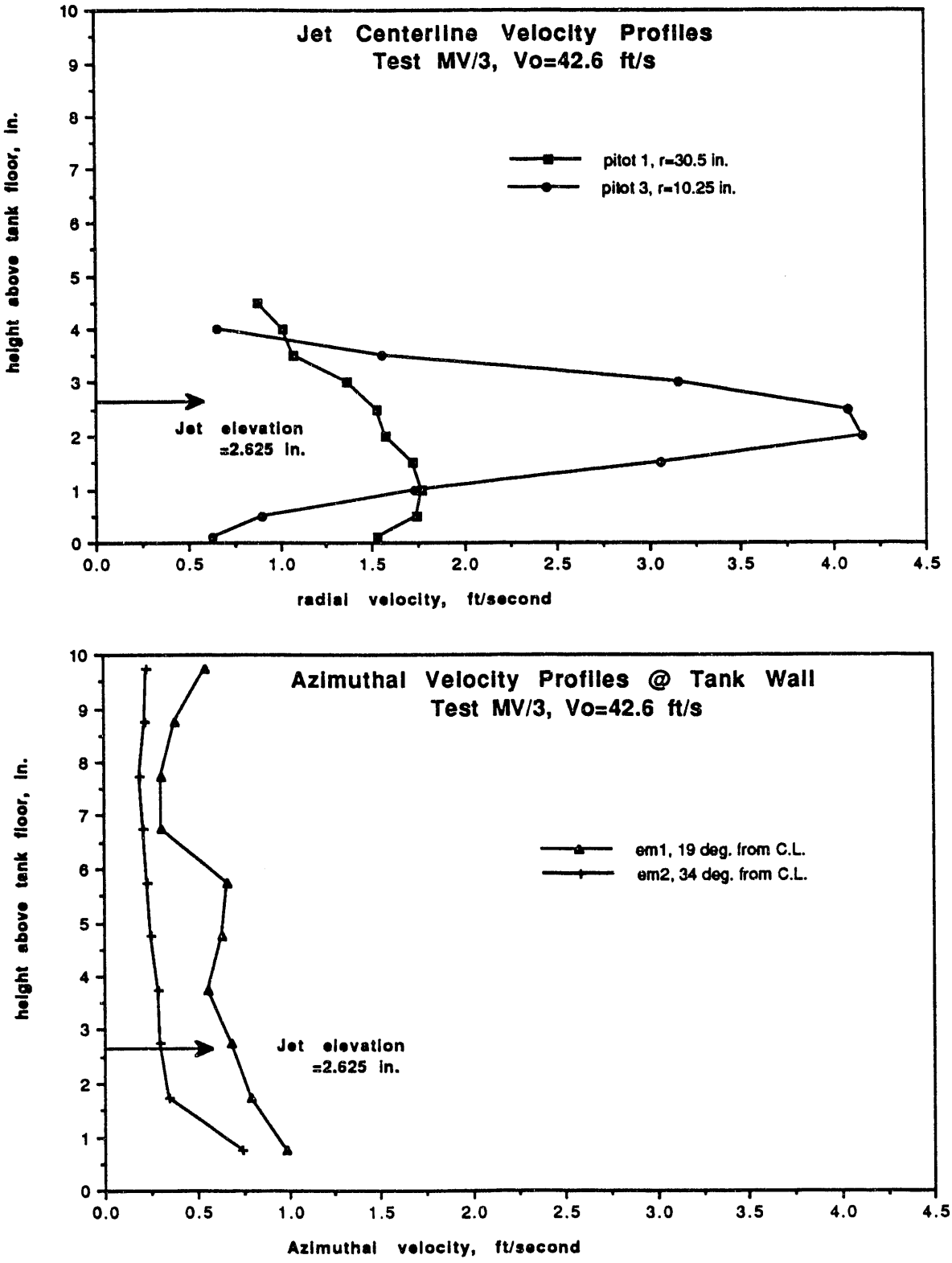

FIGURE B.5 Velocity Profiles Measured in Test MV/3

Test No. MV/4 **Test Date:** July 10, 1992

Description: Freshwater velocity profiling at 55 ft/s. Locations 1, 3, 5, and 6 traversed.

Measurements: Velocity profiles are shown in Figure B.6.

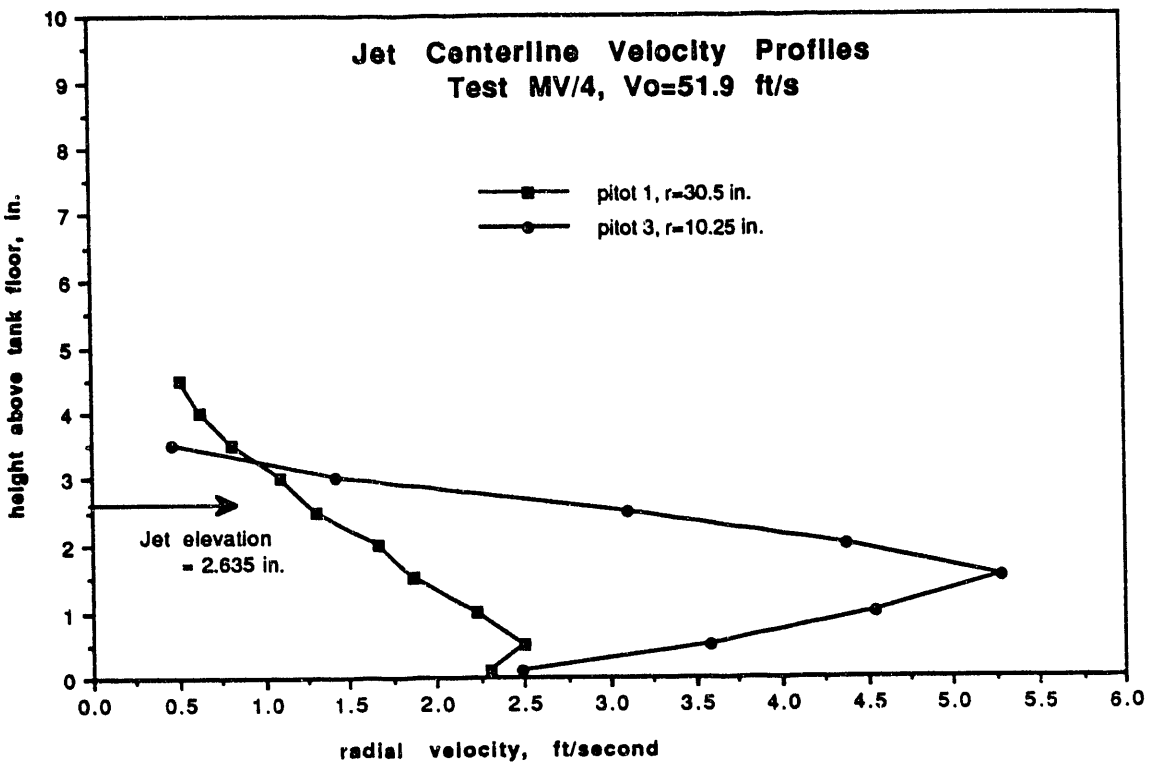

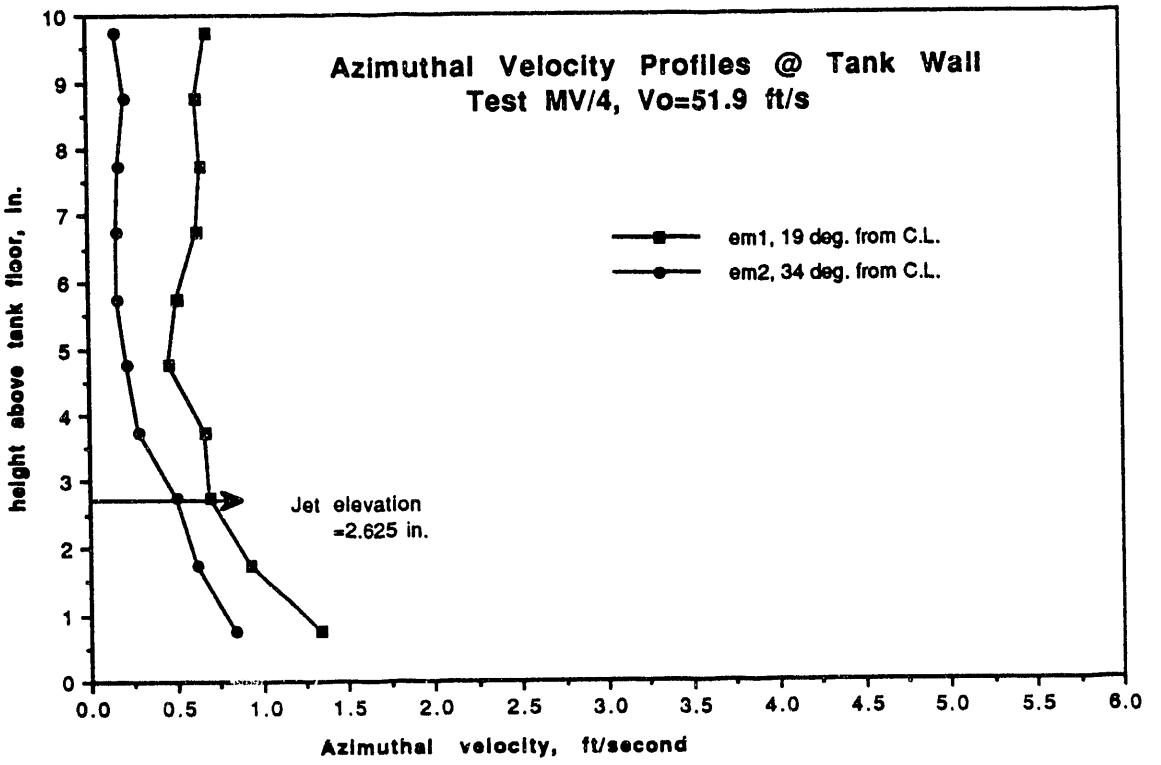

FIGURE B.6 Velocity Profiles Measured in Test MV/4

Test No. MV/5 **Test Date:** July 10, 1992

Description: Freshwater velocity profiling at 25.4 ft/s. Locations 2 and 4 traversed. Location 7 held fixed.

Measurements: Velocity measurements at location 7 are given in Table B.2. Velocity profiles at locations 2 and 4 are shown in Figure B.7.

TABLE B.2. Position 7 Velocity Data at 24 ft/s

Sampling Time min:sec	EM 1 Velocity Reading 90 sec averages (ft/s)
1:30	.42
5:35	.44
8:35	.41
10:45	.41
13:20	.42
16:35	.41
19:20	.43
22:50	.41
27:10	.46
29:30	.43

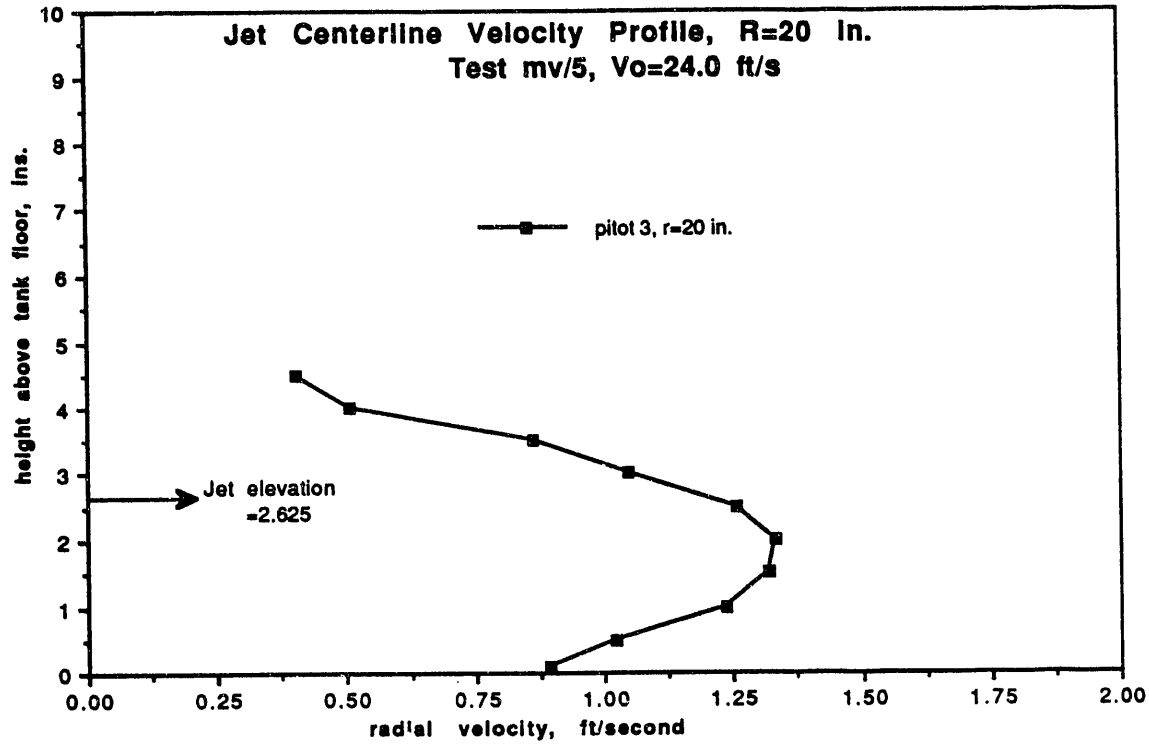

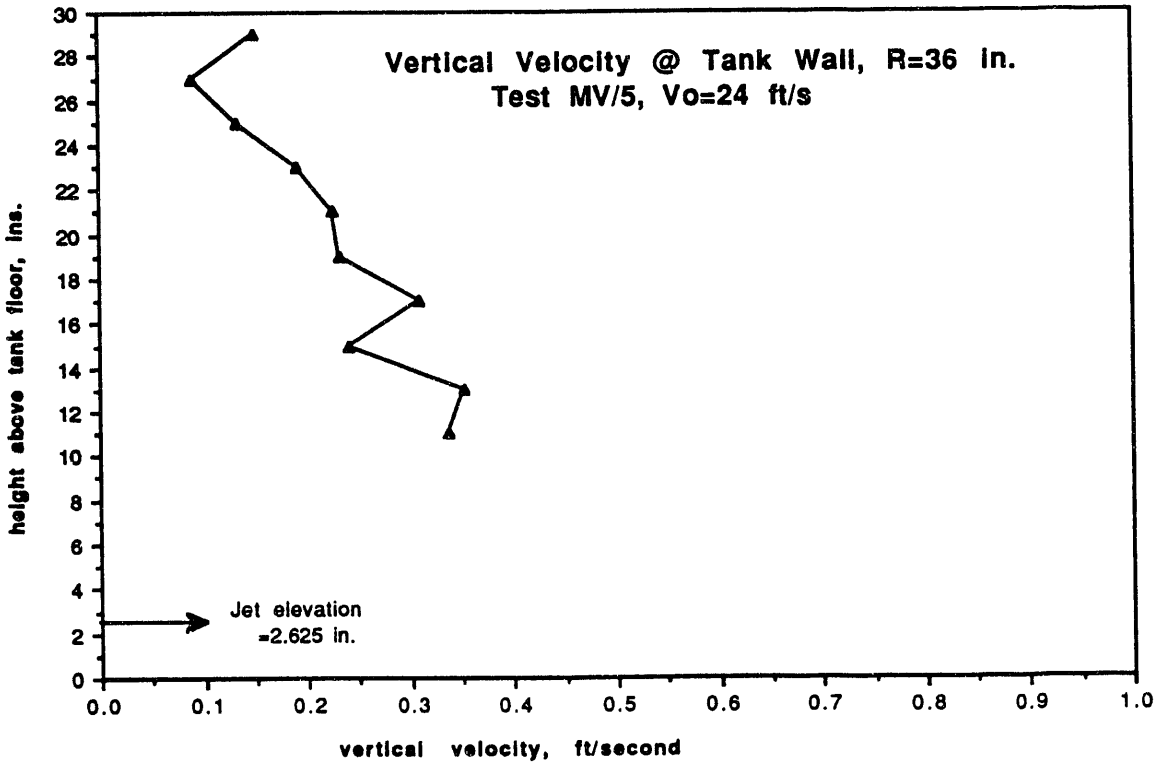

FIGURE B.7. Velocity Profiles Measured in Test MV/5

Test No. MV/6 **Test Date:** July 10, 1992

Description: Freshwater velocity profiling at 45 ft/s. Locations 2 and 4 traversed. Location 7 held fixed.

Measurements: Velocity measurements at location 7 are given in Table B.3. Velocity profiles at locations 2 and 4 are shown in Figure B.8.

TABLE B.3. Position 7 Velocity Data at 42.5 ft/s

Sampling Time min:sec	EM 1 Velocity Reading 90 sec averages (ft/s)
3:05	.78
6:40	.76
8:50	.76
11:10	.79
14:15	.78
16:35	.76
19:30	.7
22:05	.77
24:50	.78
28:55	.80

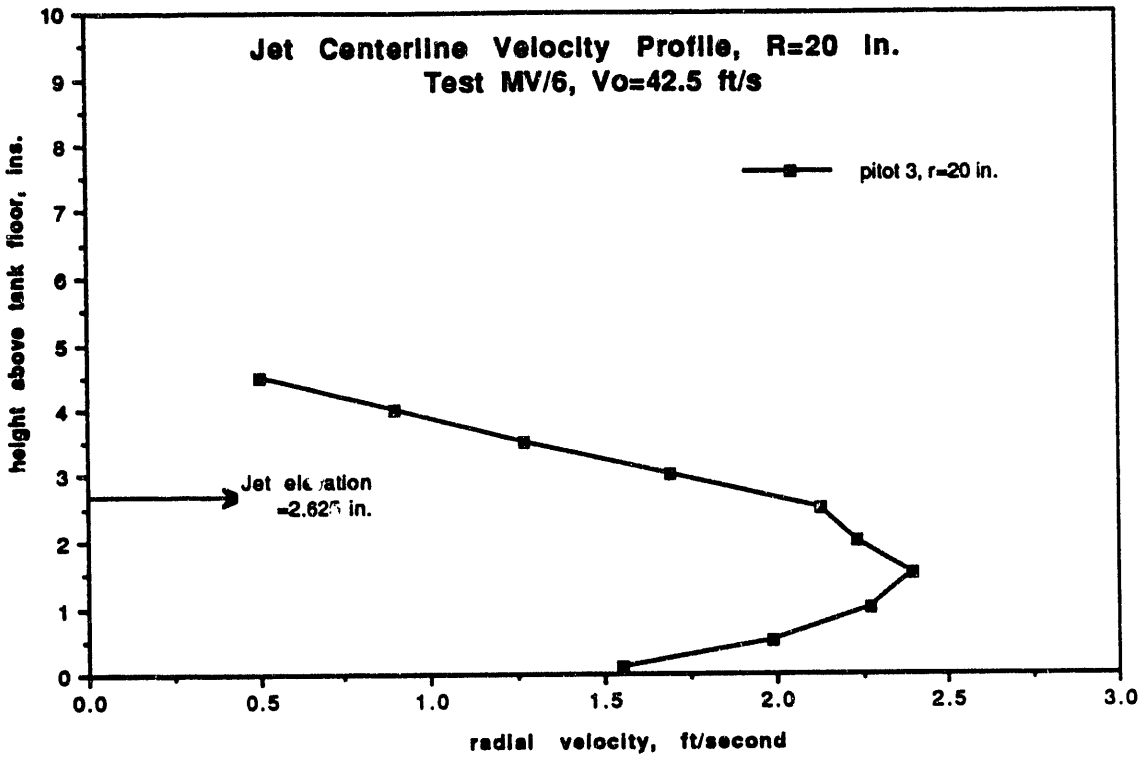

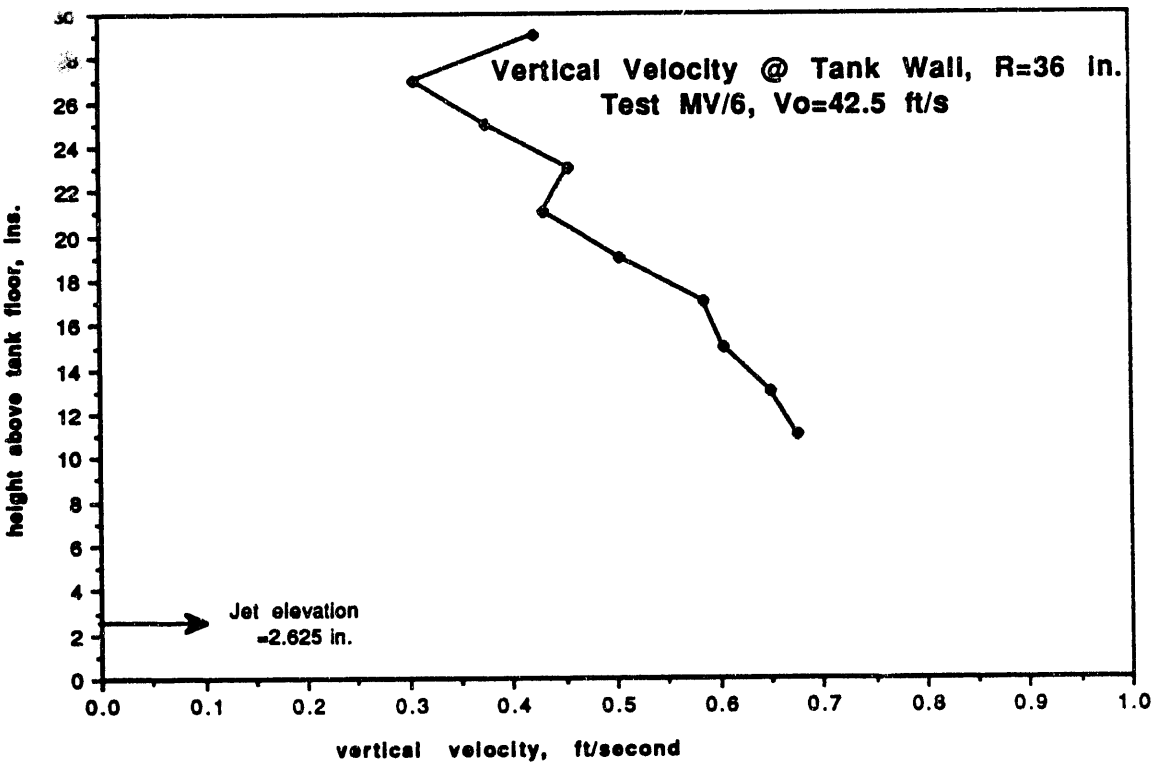

FIGURE B.8. Velocity Profiles Measured in Test MV/6

Test No. MV/7 **Test Date:** July 10, 1992

Description: Freshwater velocity profiling at 55 ft/s. Locations 2 and 4 traversed. Location 7 held fixed.

Measurements: Velocity measurements at location 7 are given in Table B.4. Velocity profiles at locations 2 and 4 are shown in Figure B.9.

TABLE B.4. Position 7 Velocity Data at 52.6 ft/s

Sampling Time min:sec	EM 1 Velocity Reading 90 sec averages (ft/s)
1:30	1.11
3:35	1.12
5:30	1.11
7:50	1.12
10:00	1.14
12:25	1.10
14:30	1.10
18:10	1.10
21:30	1.07
23:55	1.14

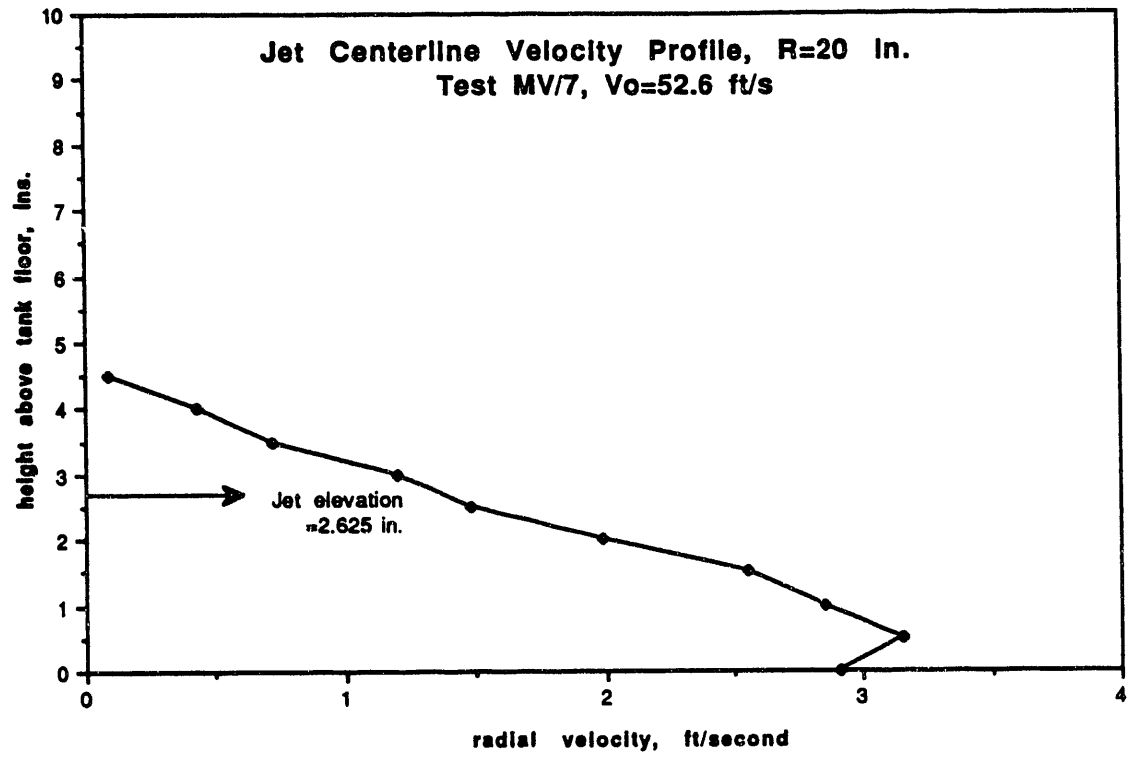

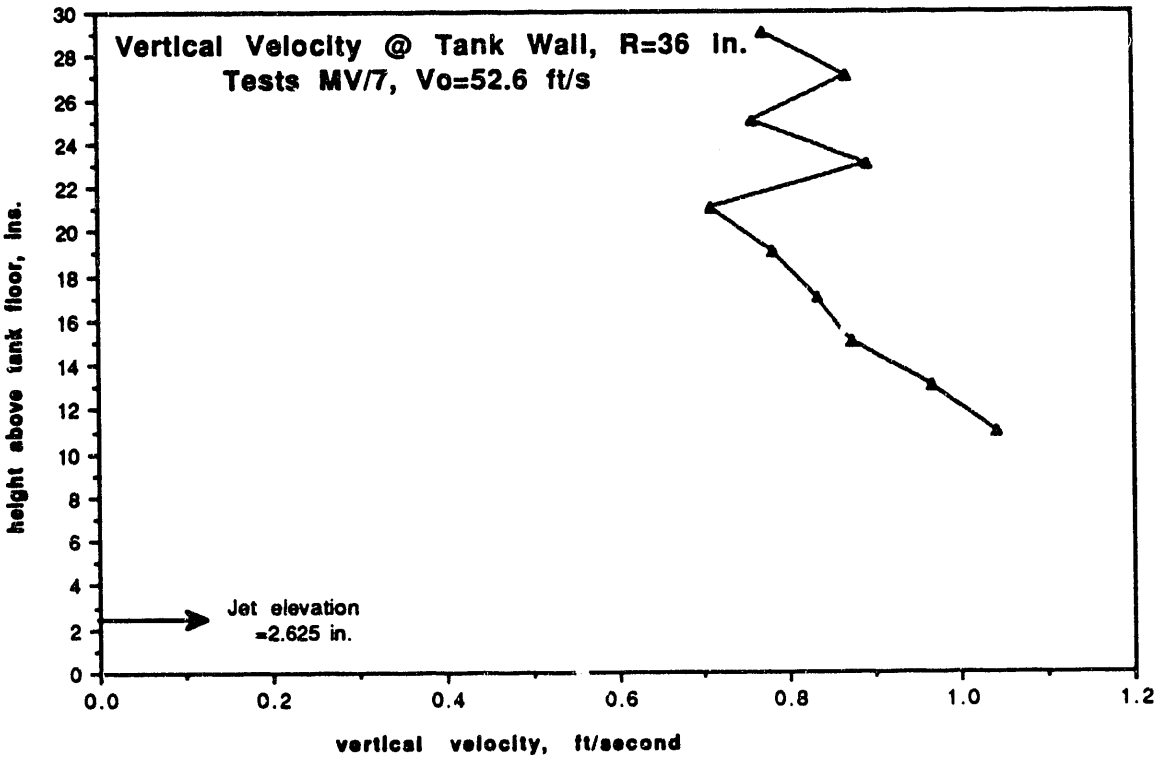

FIGURE B.9. Velocity Profiles Measured in Test MV/7

B.4.2 High Viscosity Simulant-Based Tests

Test No. MVS/1 **Test Date:** July 13, 1992

Description: Start-up transient with high viscosity simulant. Transient velocity data taken at locations 2, 4, and 5. Density profiles measured at N and W locations.

Observations: Supernate is opaque and therefore does not allow visual observations until sludge interface is within 1 to 2 in. of the surface. At this point, the interface is seen as a location of vigorous activity in the form of internal waves. Turbulent mixing appears to be confined to the region beneath the interface; the region above is nearly quiescent. Even when the interface is within ½-in. of the surface, the internal waves have no apparent influence on the surface. The internal wave amplitudes are on the order of ¼-in.

Measurements:

Sludge Interface Location - The tank contents had been allowed to settle for approximately 16 h after a complete mixing of the tank contents. Table B.5 shows the elapsed time and measurements of the slurry interface heights for MVS/1.

TABLE B.5. Slurry Interface Heights Measured in MVS/1

Elapsed Time hr:min	Interface Depth Below the Surface
0:00	7
1:40	2¾
1:55	2 - 2¼
2:20	1¾
2:40	1½
3:00	½ to ¾
3:13	@ surface

Discrete Concentration Data

Density as a function of elevation from the tank bottom was characterized after the tank contents settled overnight (see Table B.6). A sludge layer was observed at 3.33 in. from the tank bottom, with a density of 1.65 g/cm^3. The middle two samples at elevations of 13.33 and 23.33 in. were both clouded with particulate. The upper sample at an elevation of 32.33 in. was clear without visible particulate.

Four samples were taken near the Statham densitometer to compare readings with it. These densities were relatively constant at 1.37 g/cm^3.

TABLE B.6. Discrete Concentration Data Taken in MVS/1

Elapsed Time, min	Mixing Pump Orientation, degree	Probe Elevation from Tank Bottom, in.							Probe Location
		32.33	29.33	28.33	23.33	17.33	13.33	3.33	
		Density, g/cm^3							
~0	0	1.136			1.376		1.397	1.650	north
1:40	0			1.376					
	0			1.360					west
2:40	0		1.369		1.368	1.372			west
					1.364				
4:00	0			1.347	1.361				north
	0			1.359	1.345				

Test No. MVS/2 **Test Date:** July 14, 1992

Description: Start-up transient with 25.4 ft/s nominal jet velocity and high viscosity simulant. Transient velocity data taken at locations 2 and 4 with EM meters. Vertical traverses taken during transient. Density profiles measured at N and W locations.

Observations: Jets appear to be clearing sludge from tank floor all the way to the tank wall. Width of cleared area is 10 to 12 in. close to the wall. These observations were made by running a probe along the tank floor while feeling for changes in contour.

Measurements:

Velocity Data - Jet centerline profiles for the developing flow field are given for MVS/2 in Figure B.10. The time for the jet to break through to the buried EM probe is roughly 14 min, as illustrated in Figure B.11.

Shear Strength of Settled Layer - Shear strength measurements were taken on two samples retrieved from the settled solids layer. At approximately 7:00 p.m. on July 13, two cup samplers were inserted into the tank at the tank bottom. Prior to insertion, the tank had been mixed at a combined jet flow rate of 15 gpm for 15 min. Sample #1 was located in the plane of the north jet at a radius of 20 in. Sample #2 was located in the plane perpendicular to the west jet, also at a radius of 20 in. The tank was allowed to settle overnight. The samples were removed at approximately 8:00 a.m. on July 14, which gave a settling time of about 11 h.

Measurements were taken soon after carrying the cup samples to the laboratory in 324 Building. The samples were disturbed and showed virtually no shear strength. One sample (#1) was left overnight with the shear vane in place and shear strength was again measured the next morning (~15 h after the first). The shear vane was then carefully placed into the other sample (#2) to minimize disruption of the sludge and shear strength was then measured. Values obtained were as follows:

Sludge Sample #1890 dynes/cm^2
Sludge Sample #24700 dynes/cm^2

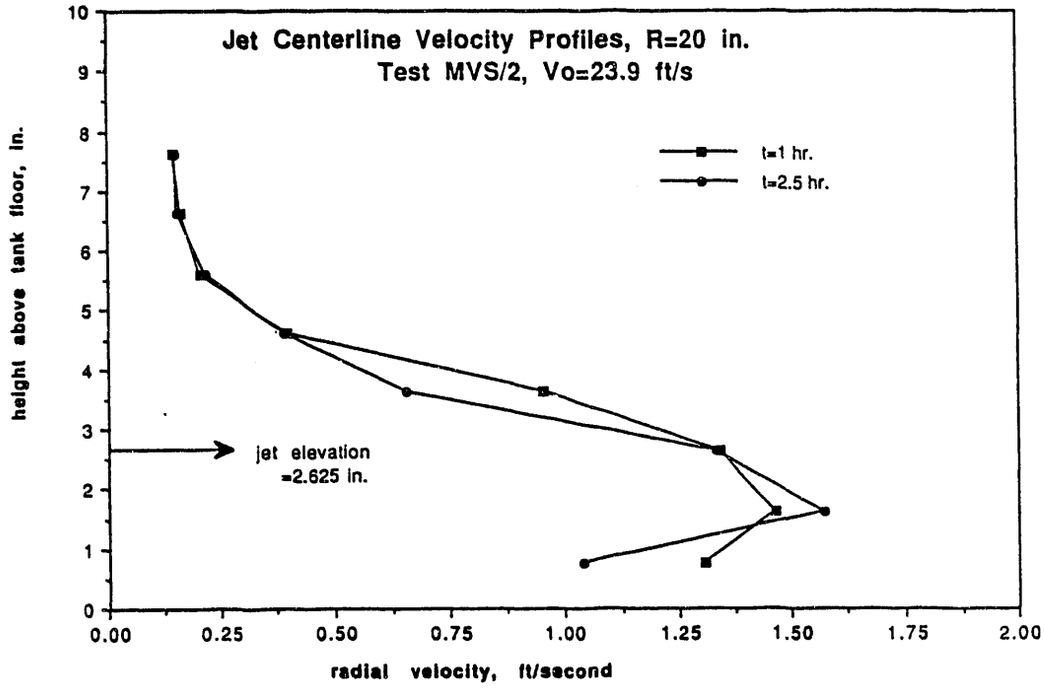

FIGURE B.10. Jet Centerline Velocity Profiles from MVS/2

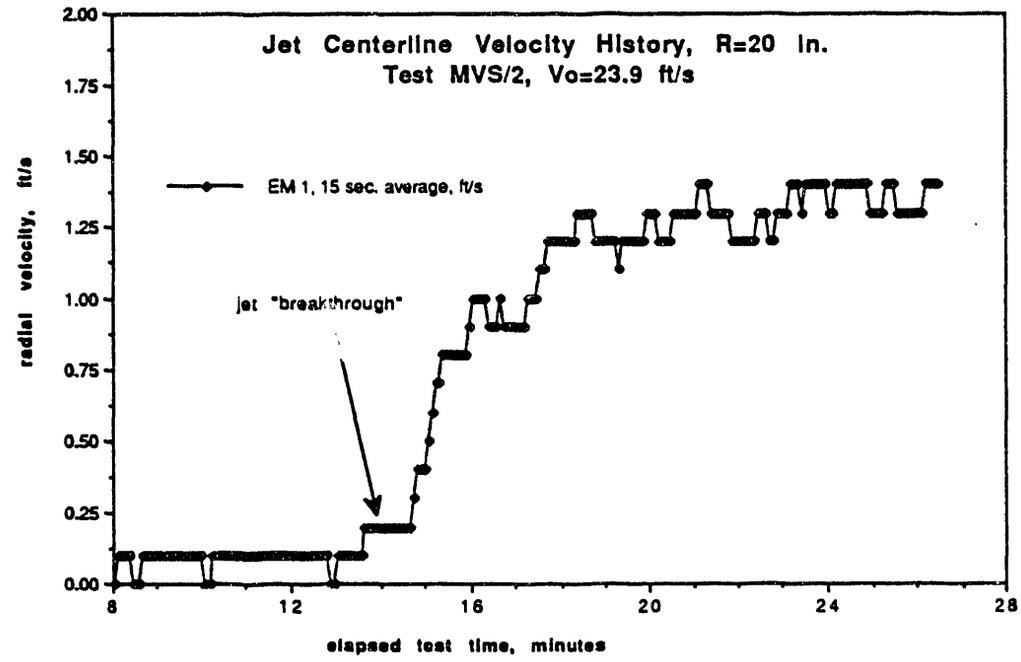

FIGURE B.11. Jet Centerline Velocity History from MVS/2

The shear strengths of both are higher than expected. Sample #2 was taken 90 degrees from the jet path. On July 13, the mixer pump was operated continuously. This may have caused sludge to accumulate in this location, providing a deeper layer of settled sludge than found in Sample #1. Monte Elmore suggests that it is probable that the sludge layer consolidates much more in the tank than in bottle samples made up in the laboratory. Also the samples were taken only in the sludge layer; therefore, the simulant density was not at the tank average when settling occurred.

Sludge Interface Location - The tank contents had been allowed to settle for approximately 19 h after a complete mixing of the tank contents. Table B.7 shows the elapsed times and measurements of the slurry interface heights for MVS/2.

TABLE B.7. Slurry Interface Heights Measured in MVS/2

Elapsed Time hr:min	Interface Depth Below the Surface
0:00	7
0:48	6
1:10	4¾
2:45	1¾
3:20	@ surface

Discrete Concentration Data - Data taken in MVS/2 are shown in Table B.8.

TABLE B.8 Discrete Concentration Data Taken in MVS/2

Elapsed Time, min	Mixing Pump Orientation, degree	Probe Elevation from Tank Bottom, in.				Probe Location
		28.33	23.33	13.33	3.33	
		Density, g/cm^3				
~0	0	1.277	1.339	1.327	1.716	north
130	0	1.315	1.324	1.376	1.655	
210	0	1.322	1.305	1.360	1.318	
~0	0	1.274	1.334	1.323	1.736	west
85	0	1.332	1.340	1.347	1.752	
220	0	1.308	1.304	1.313	1.726	

These data are shown plotted in Figure B.12.

Ultrasonic Concentration Data - Figure B.13 shows the change in wt% over time of the slurry at 23.5 in. from the bottom of the tank. Note that the wt% slowly decreased during the time shown.

Figure B.14 shows the results of two traverses; one at about 10:20 a.m. and one at about 2:40 p.m. after 170 min of operation. The first traverse, which was taken before the jet was turned on and after the tank had been allowed to settle overnight, indicates that the very top of the slurry (height = 30 to 33 in. from the bottom) contained relatively few solid particles while the very bottom of the tank (height = 0 in.) contained a large number of solid particles. The heights between the top and the bottom indicate a general increase in wt% as the probe was moved lower, although the point at about 10 in. from the bottom deviates from this trend.

The second traverse shows that the top of the tank became slightly more concentrated with stirring. The rest of the tank, except the lowest point, also increased in wt% and moved toward a uniform wt%. The lowest point, about 3 in. higher than the lowest point in the first traverse, seems to indicate an increase in wt% between the two traverses, which is not expected (the lowest point should be decreasing in wt% as time passes). But because wt% above

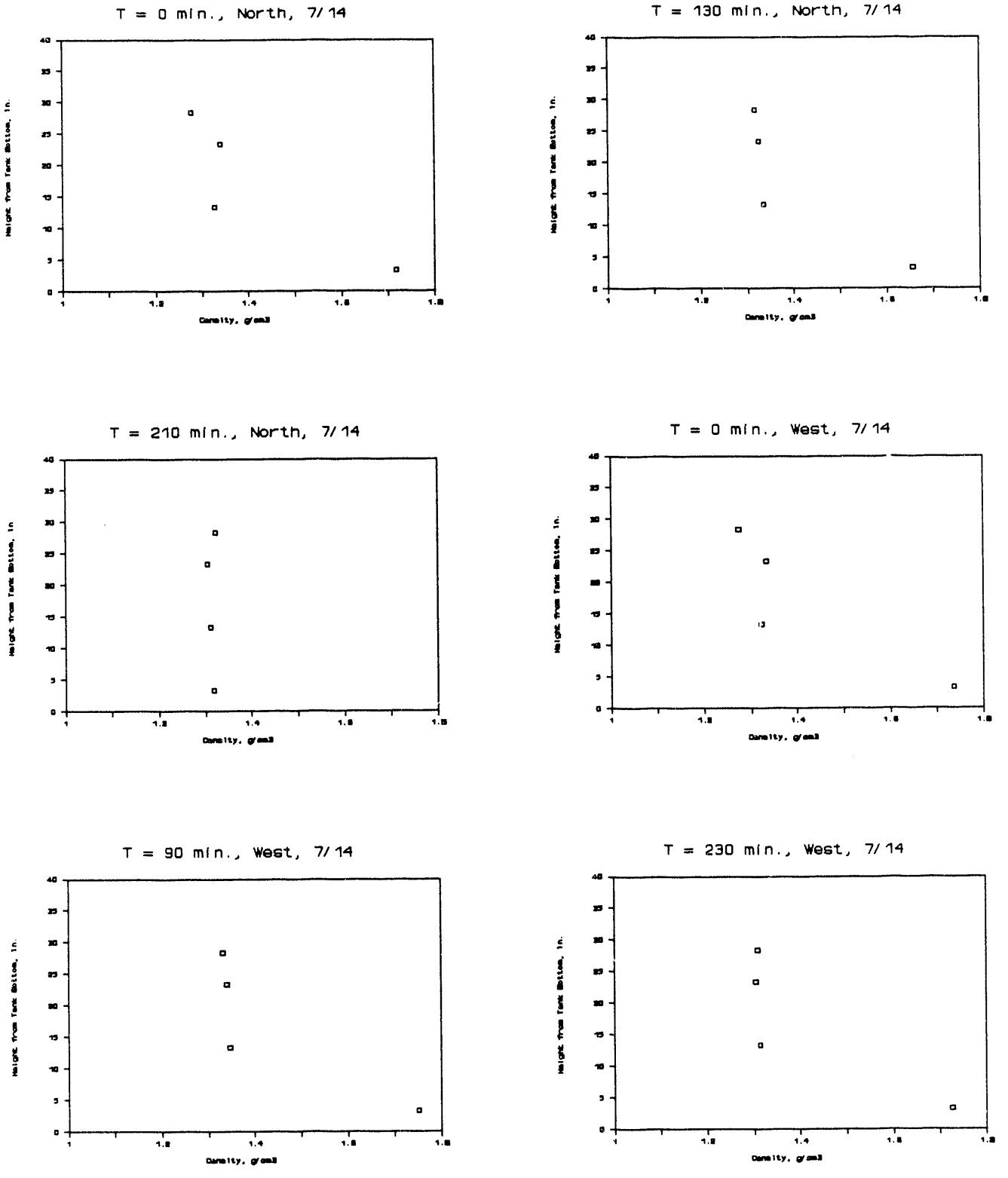

FIGURE B.12. Discrete Concentration Plots from MVS/2

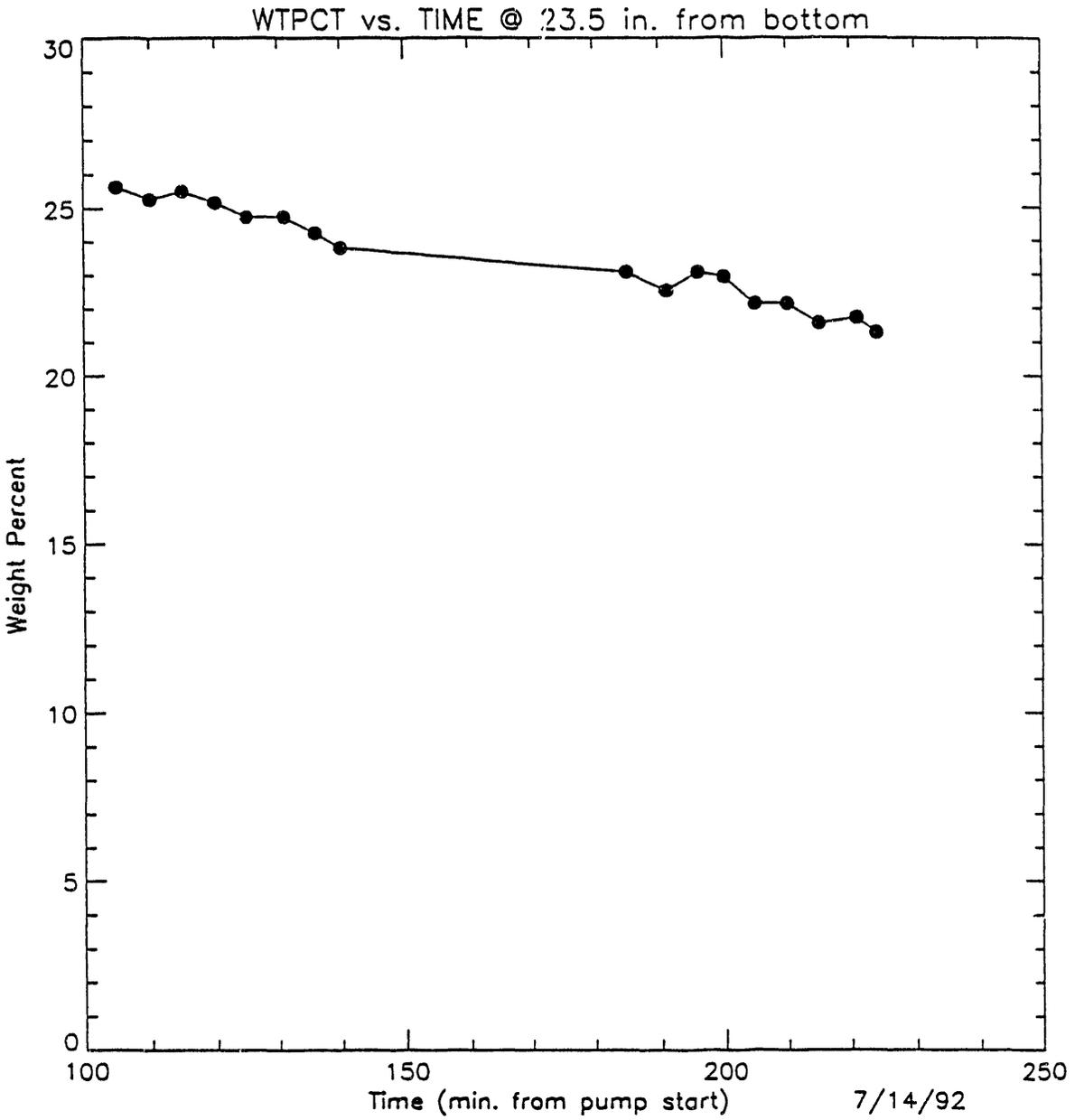

FIGURE B.13. Wt% Solids Versus Time at a Height of 23.5 in.

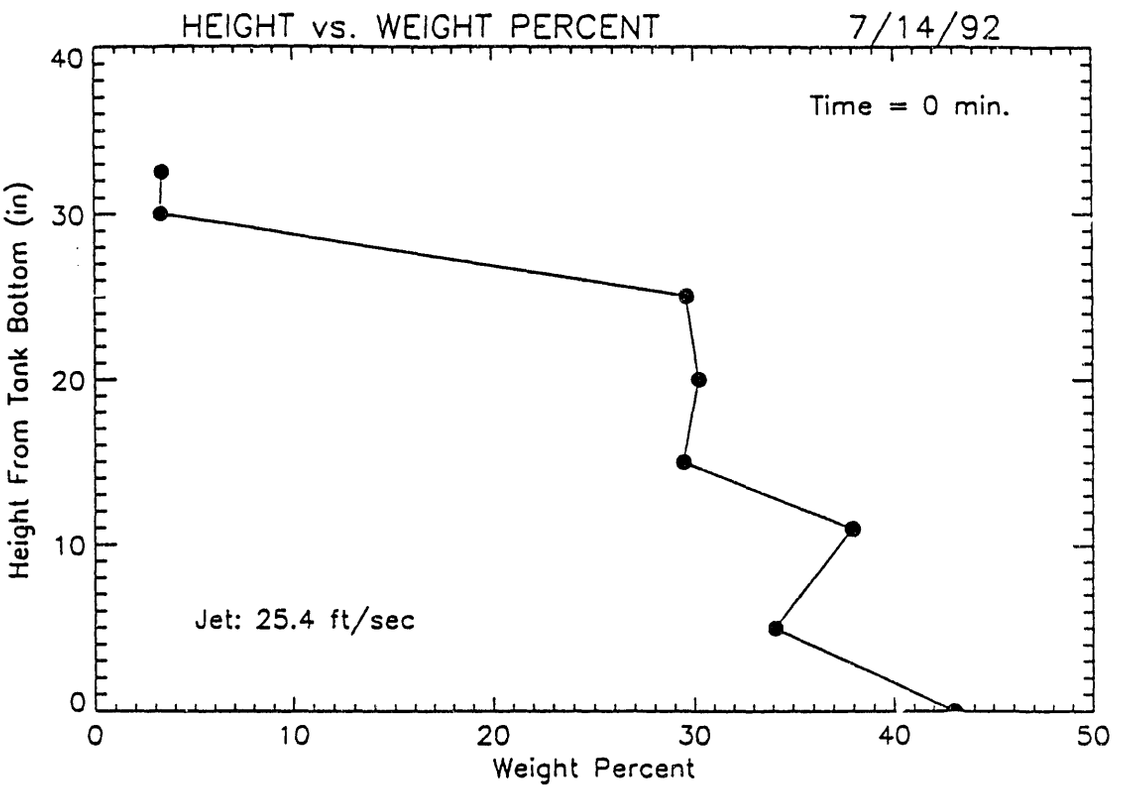

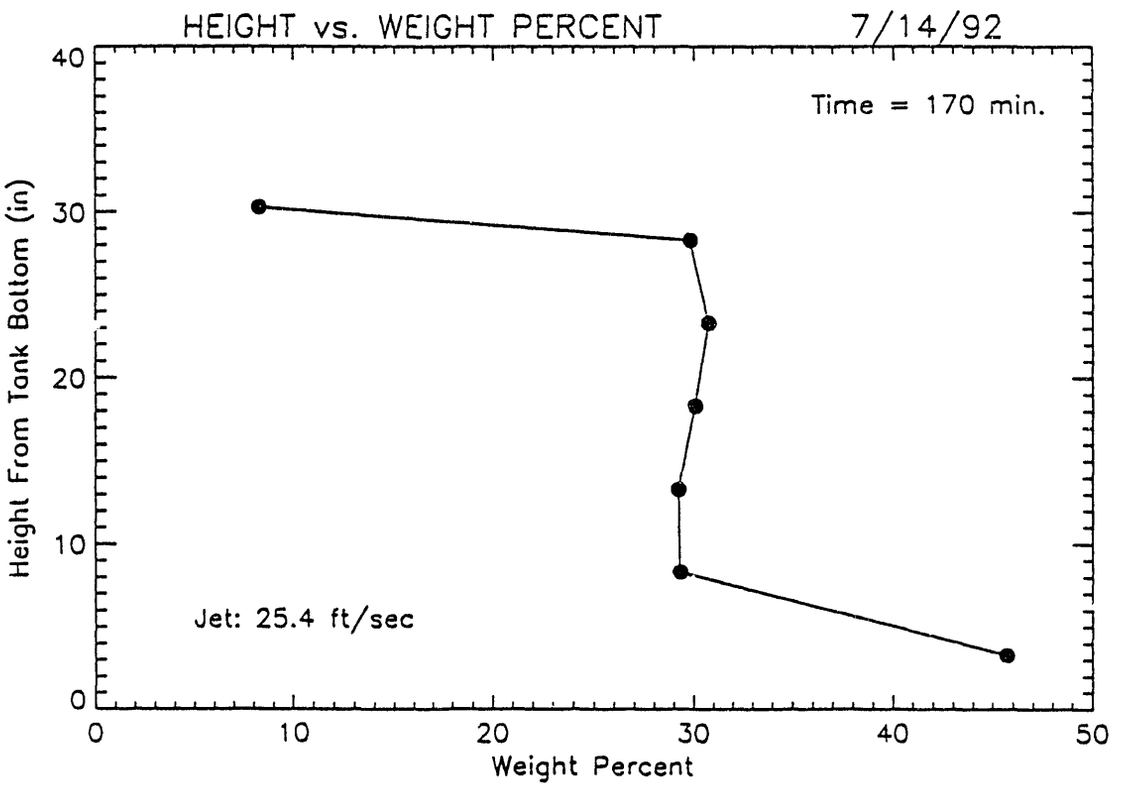

FIGURE B.14. Height Versus Wt% Solids for MVS/2

35 percent correspond to very small voltages (about the magnitude of the RS noise), the two points actually cannot be distinguished from one another by wt%; that is, they both say no more than the wt% is above 35 percent.

Test No. MVS/3 **Test Date:** July 14, 1992

Description: Steady-state test in high viscosity simulant with 25.4 ft/s jet velocity. Velocity profiling at locations 2 and 4.

Measurements: Velocity profiles are shown in Figure B.15.

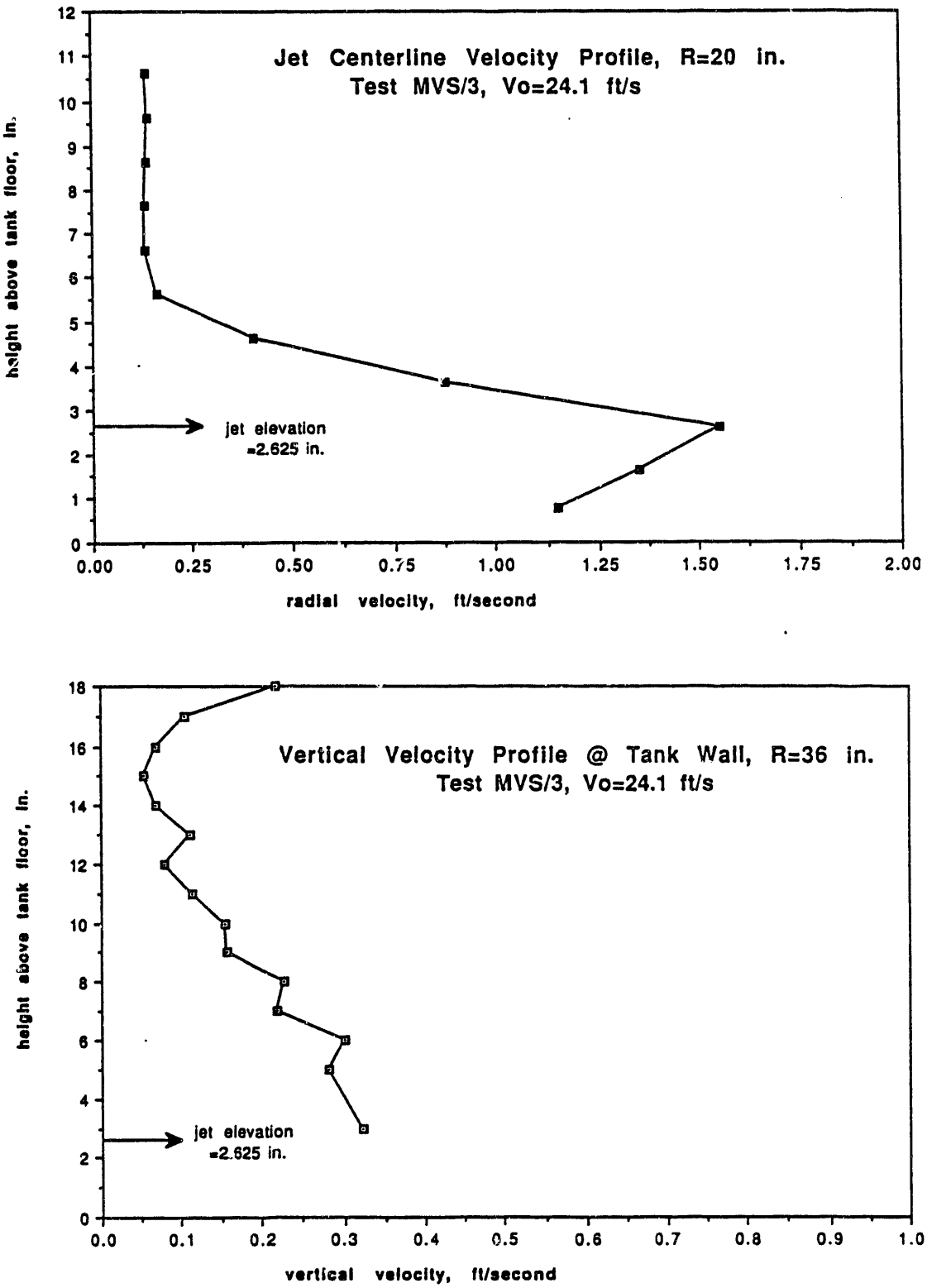

FIGURE B.15. Velocity Profiles Measured in Test MVS/3

Test No. MVS/4 **Test Date:** July 14, 1992

Description: Steady-state test in high viscosity simulant with 25.4 ft/s jet velocity. Velocity profiling at locations 3 and 5.

Measurements: Velocity profiles are shown in Figure B.16.

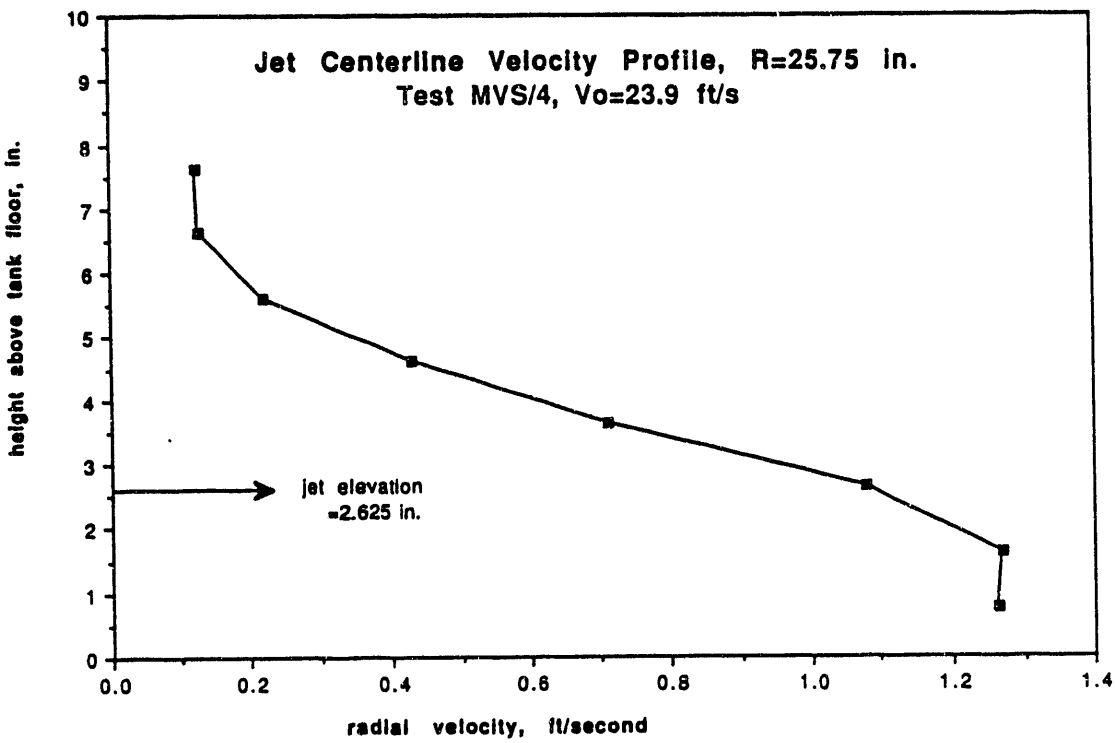

FIGURE B.16 Velocity Profiles Measured in Test MVS/4

Test No. MVS/5 **Test Date:** July 15, 1992

Description: Start-up transient with high viscosity simulant and 15 ft/s jet velocity. Transient velocity data taken at location 3 in both jets. Density profiles measured at N and W locations.

Observations: The influence of the mixing jet never reached the surface of the tank in this 9-h test. In fact, the slurry interface continued to fall throughout the test. This continued settling was caused by suspended fines in the supernate that did not reach the solids layer in the time between tests.

The extent of floor cleaning was checked after 8 h of jet operation. Narrow channels had been cut in front of each jet. On one side, a 1- to 1½-in.-wide channel extended out to the location of the buried EM probe and stopped there. On the other side, the channel was initially the same 1½-in. width. It widened to 3 to 4 in. at the buried pitot probe, and did not penetrate further. The pitot and EM probes were at 20 and 25 in. from the tank centerline, respectively.

Measurements:

Velocity Data - Jet centerline profiles for the developing flow field are given for MVS/5 in Figure B.17. The time for the jet to break through to the buried EM probe is just over 70 min, as illustrated in Figure B.18.

Sludge Interface Location - The tank contents had been allowed to settle for approximately 13 h after a complete mixing of the tank contents. The interface had settled to 7 in. below the surface. Approximately 2 in. of excess supernate was decanted prior to beginning the test. Results are illustrated in Table B.9.

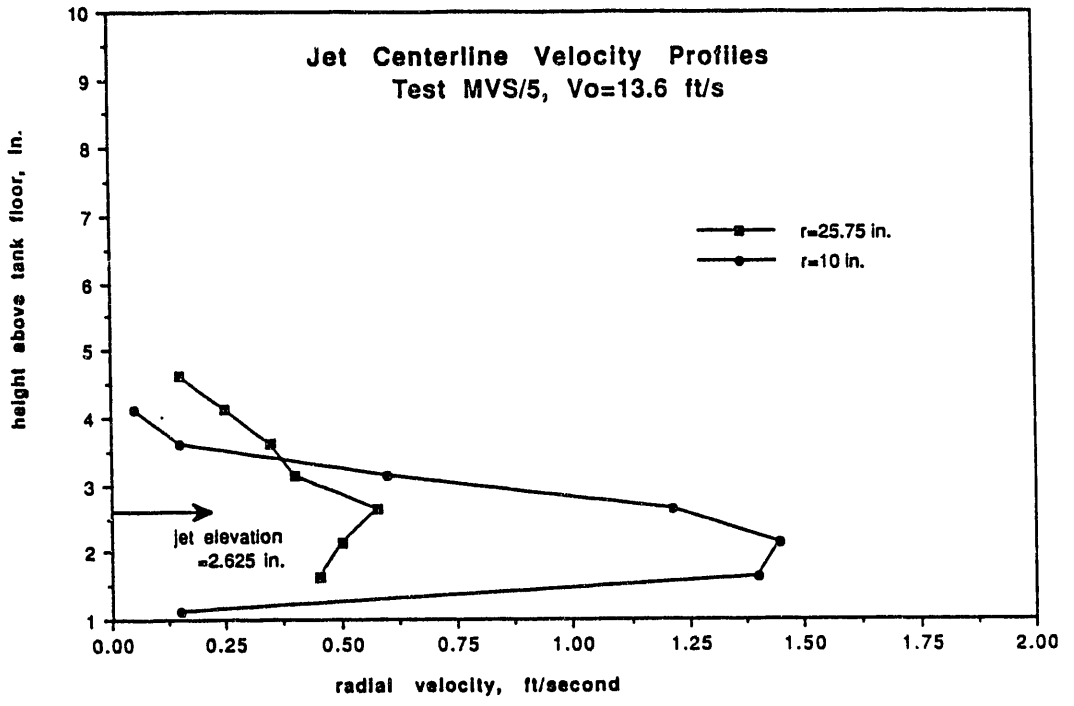

FIGURE B.17. Jet Centerline Velocity Profiles from MVS/5

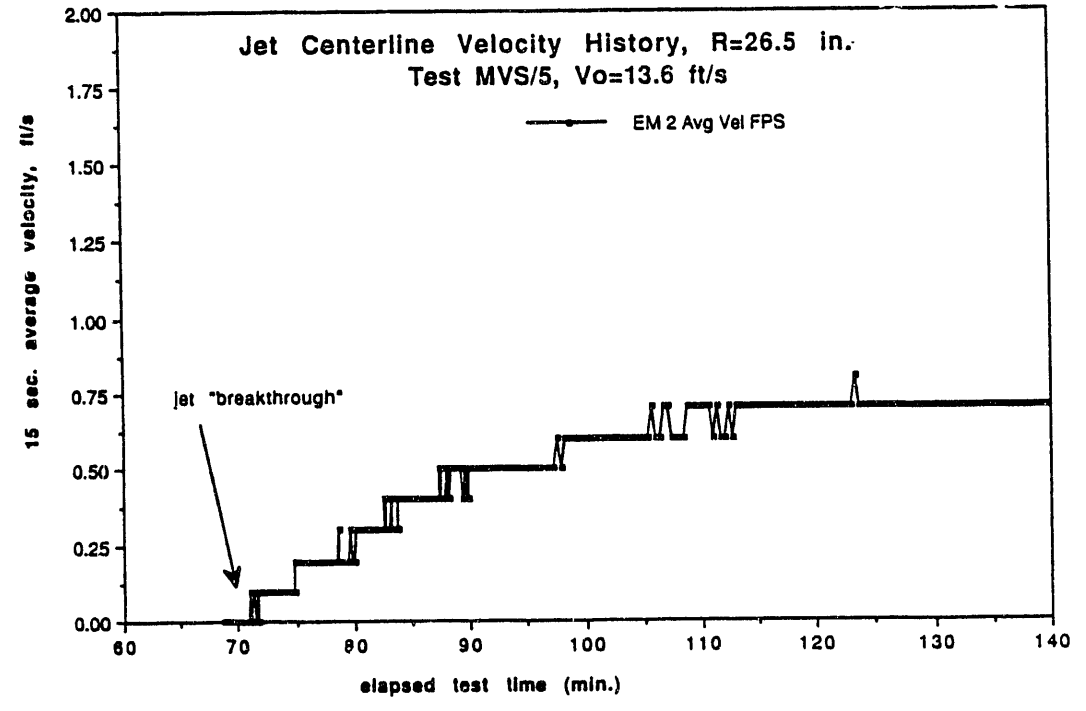

FIGURE B.18. Jet Centerline Velocity History from MVS/5

TABLE B.9. Slurry Interface Heights Measured in MVS/5

Elapsed Time hr:min	Interface Depth Below the Surface
0:00	
0:45	4½ to 4¾
3:55	6
4:50	6½
7:36	7½
9:06	7¼

Discrete Concentration Data - Data taken in WVS/5 are shown in Table B.10.

TABLE B.10. Discrete Concentration Data for MVS/5

Elapsed Time, min	Mixing Pump Orientation, degree	Probe Elevation from Tank Bottom, in.				Probe Location
		28.33	23.33	13.33	3.33	
		Density, g/cm^3				
~0	0	1.270	1.289	1.305	1.788	north
130	0	1.072	1.332	1.348	1.353	
310	0	1.189	1.347	1.345	1.357	
400	0	1.111	1.346	1.341	1.328	
~0	0	1.263	1.289	1.308	1.759	west
175	0	1.112	1.352	1.334	1.592	
310	0	1.114	1.340	1.348	1.743	
420	0	1.111	1.337	1.337	1.714	

These data are shown plotted in Figure B.19.

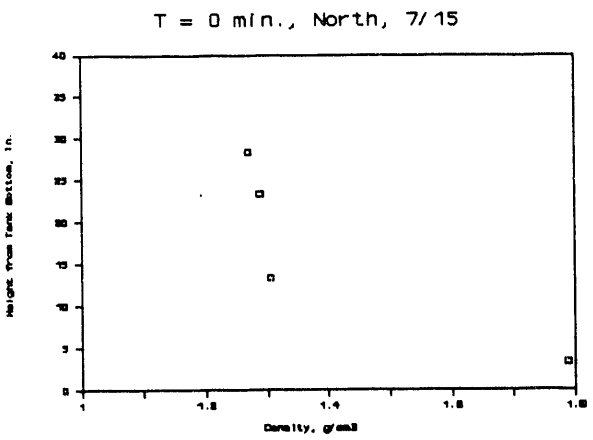

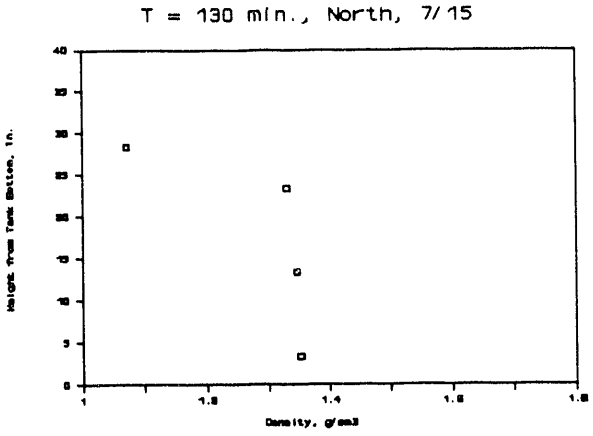

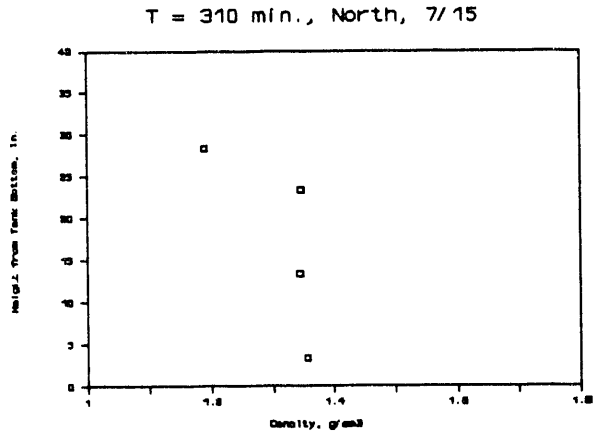

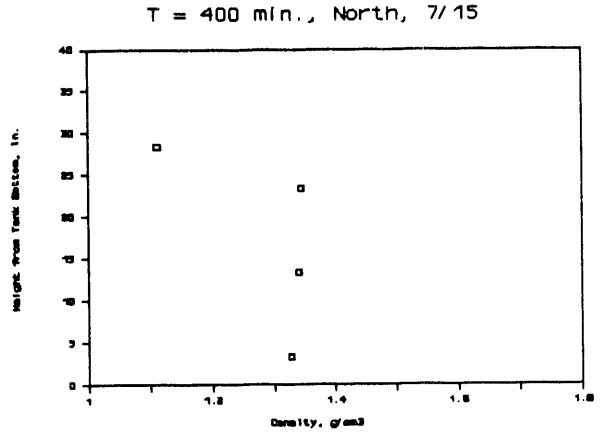

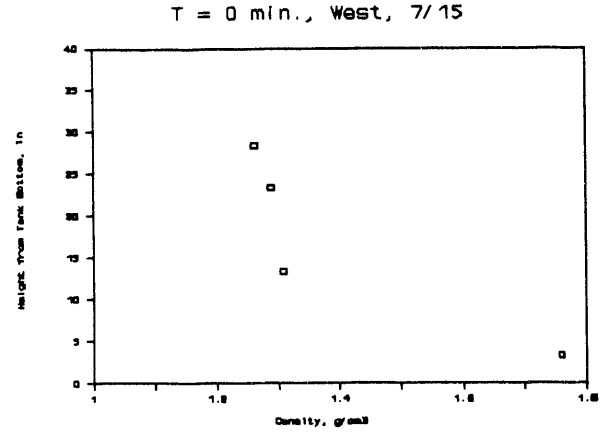

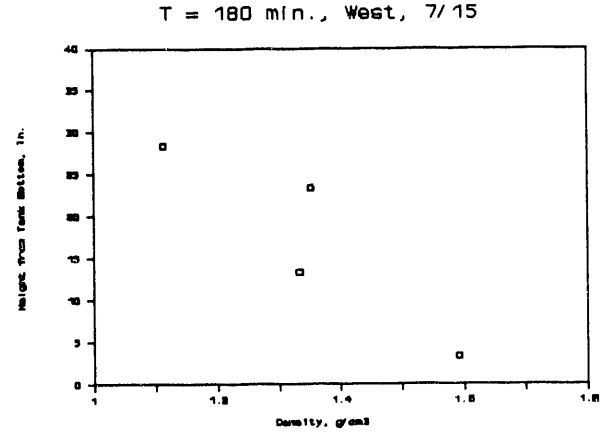

FIGURE B.19. Discrete Concentration Data for MVS/5

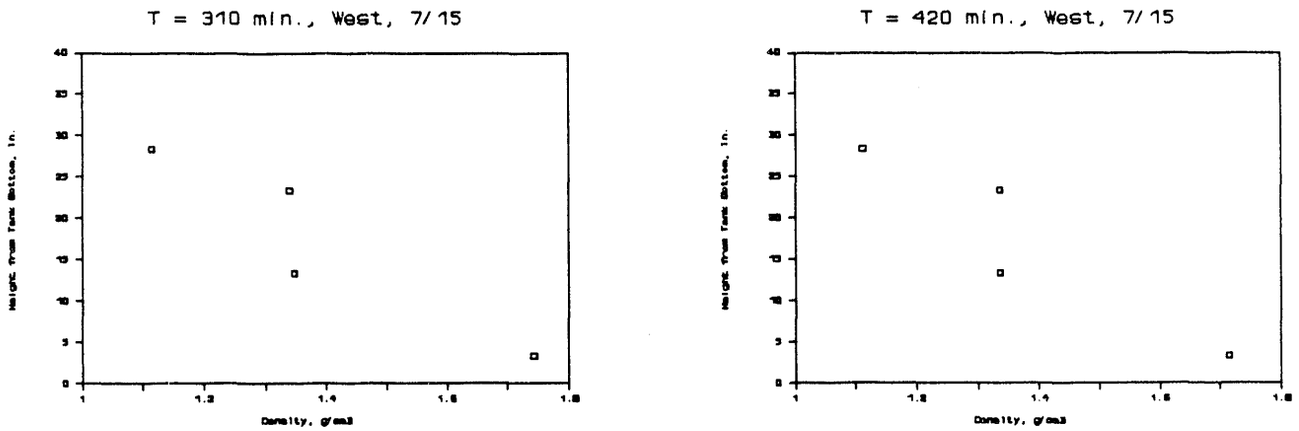

FIGURE B.19. (contd)

Ultrasonic Concentration Data - Figure B.20 shows the change in wt% over time of the slurry (actually, the sludge layer) in the plane of the jet, which was about 2.6 in. from the bottom. The signal at 2 MHz was consistently small enough that the signal noise introduced a fair amount of uncertainty in the measurement. Therefore, the slight changes in wt% shown in the plot may or may not indicate actual changes in wt%.

Figure B.21 shows three traverses, the first of which was taken before the jet was turned on and after overnight settling. The horizontal line extending off the plot at about 10 in. indicates that the RS amplitude at 2 MHz dropped to zero below that point. The rest of the points appear to confirm our expectations that the wt% would increase from the lower-middle to near the top of the tank, but decrease at the very bottom of the tank. However, the top of the tank remained at a relatively low and constant wt% for many hours after the jet was turned on.

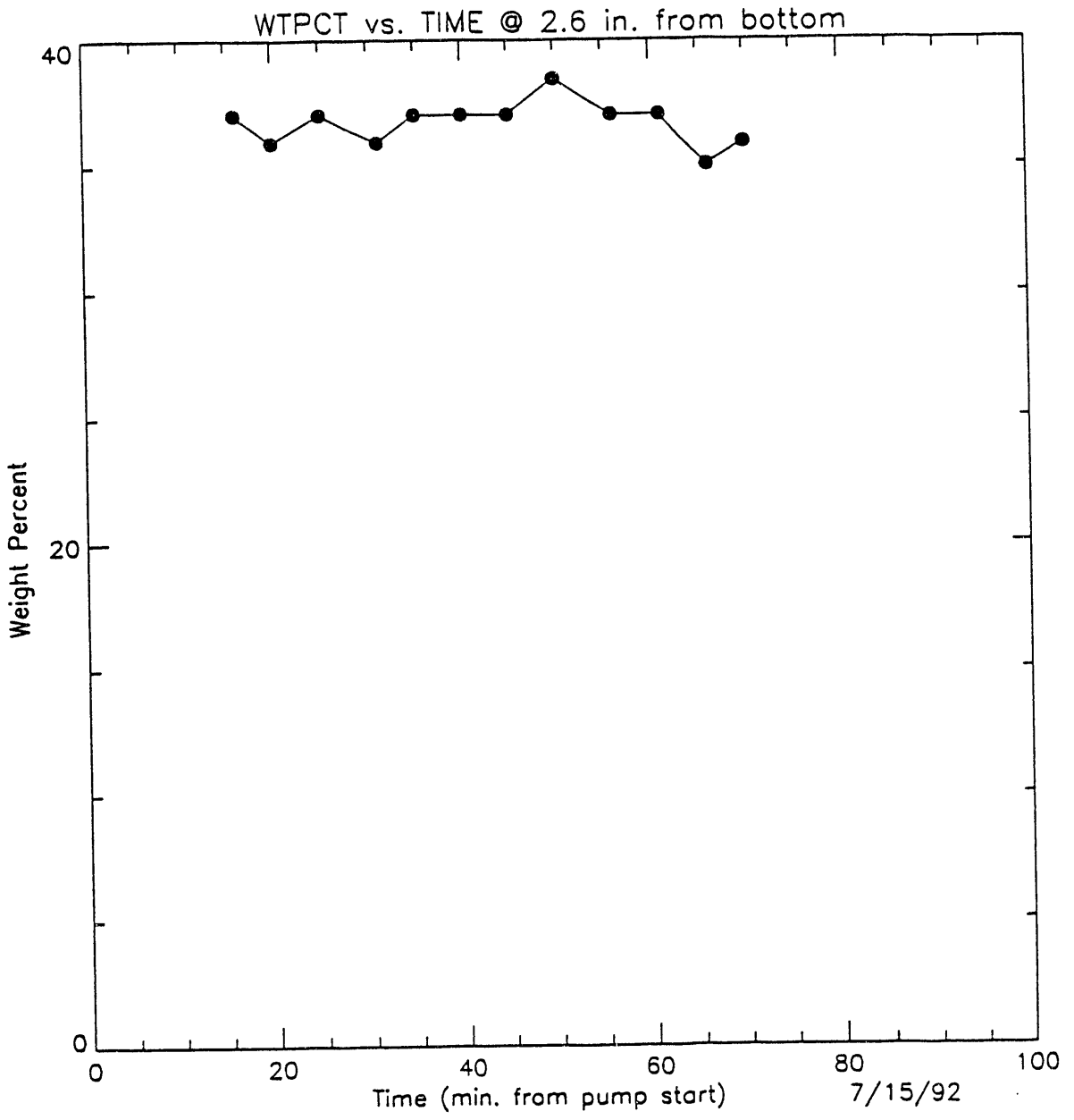

FIGURE B.20. Wt% Concentration Versus Time at a Height of 2.6 in. Test MVS/5

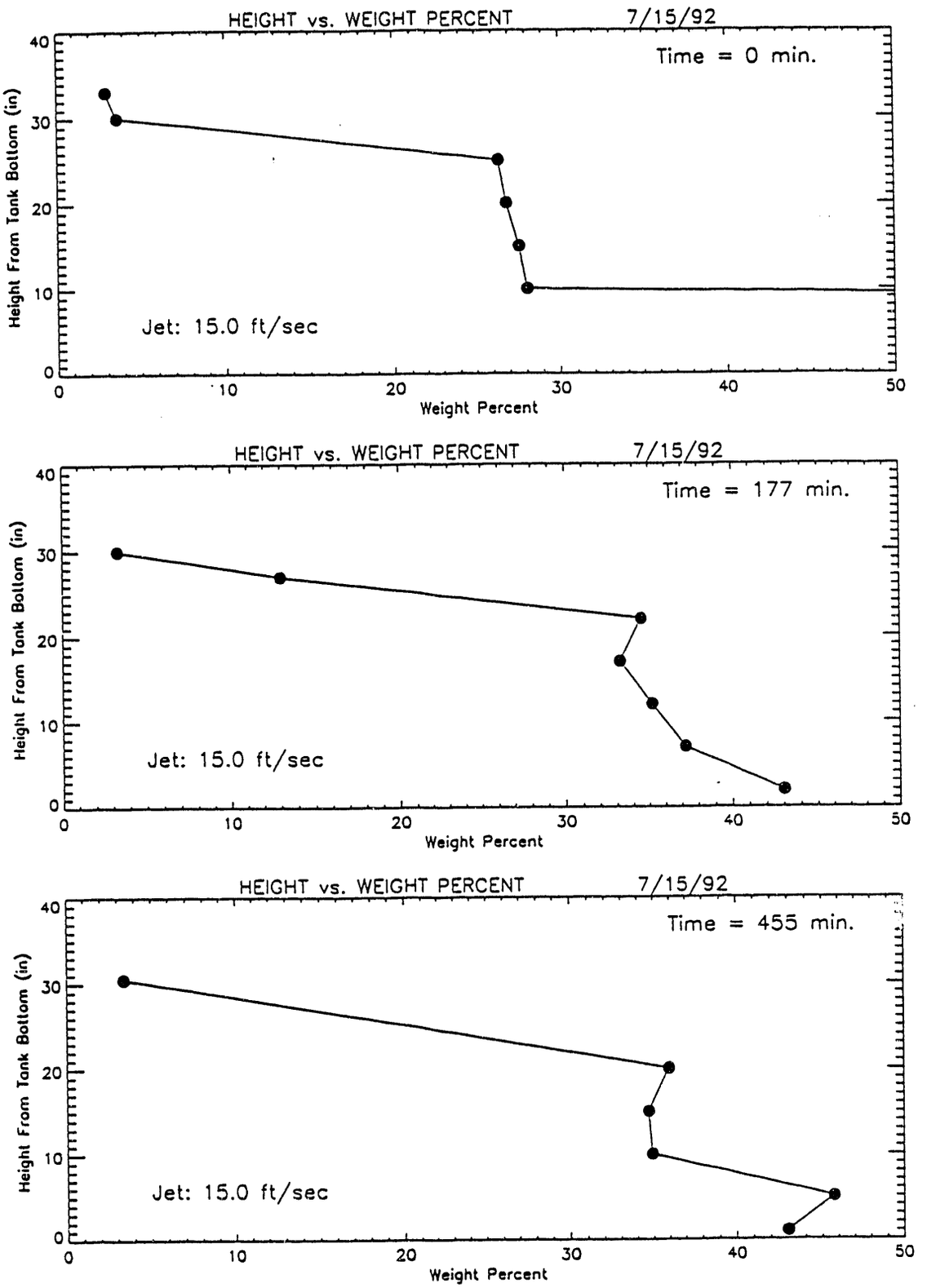

FIGURE B.21. Height Versus Wt% Concentration for MVS/5

Test No. MVS/6 **Test Date:** July 17, 1992

Description: Steady-state velocity profiling at a jet velocity of 25 ft/s. Locations 4 and 5 recorded. This test was conducted to replace data taken in tests MVS/3 and MVS/4, which may be unreliable for positions 4 and 5.

Measurements: Velocity profiles are shown in Figure B.22.

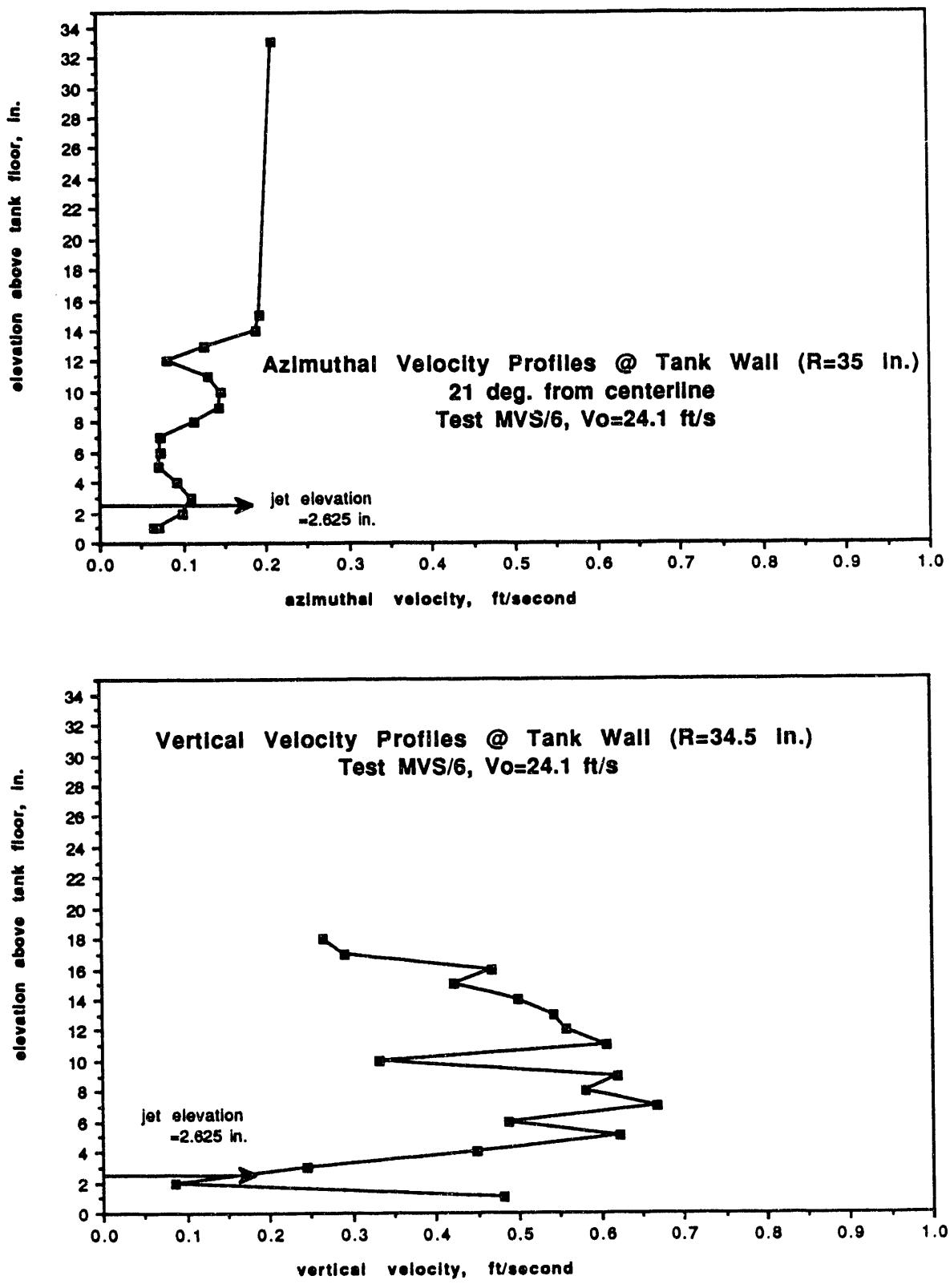

FIGURE B.22. Velocity Profiles Measured in Test MVS/6

B.4.3 Low Viscosity Simulant-Based Tests

Test No: MVLS/1,2 **Test Date:** July 23, 1992

Description: Transient test with low viscosity simulant and initial jet velocity of 25.4 ft/s (MVLS/1). Velocity profiles taken during test at locations 2, 3, 4, and 5. After reaching steady state, jet velocity was increased to 50 ft/s and velocity profiles were repeated at all locations (MVLS/2). Density profiles were measured at N and W locations.

Observations:

Measurements:

Pre-Test Settling - Tank contents had been allowed to settle for approximately 11 h after being fully mixed. Density was measured with the Statham densitometer during this settling process and the results are given in Figure B.23.

Sludge Interface Location - Measurements of interface height after initiating test MVLS/1 are given in Table B.11.

Velocity Data - Jet centerline profiles for the developing flow field are given for MVLS/1 in Figure B.24. Vertical and azimuthal velocity profiles at the wall for MVLS/1 are shown in Figure B.25. Unfortunately, the flow rate had been increased during these wall traverses. The plots are included for completeness.

Velocity profiles for MVLS/2 are given in Figure B.26.

Discrete Concentration Data - Discrete Concentration Data are given in Table B.12. The data in Table B.12 are shown plotted in Figure B.27.

Ultrasonic Concentration Data - The four plots in Figure B.28 again show a gradual convergence of slurry to uniform wt%. However, the first traverse was not taken before the jet was turned on (as in the previous plots).

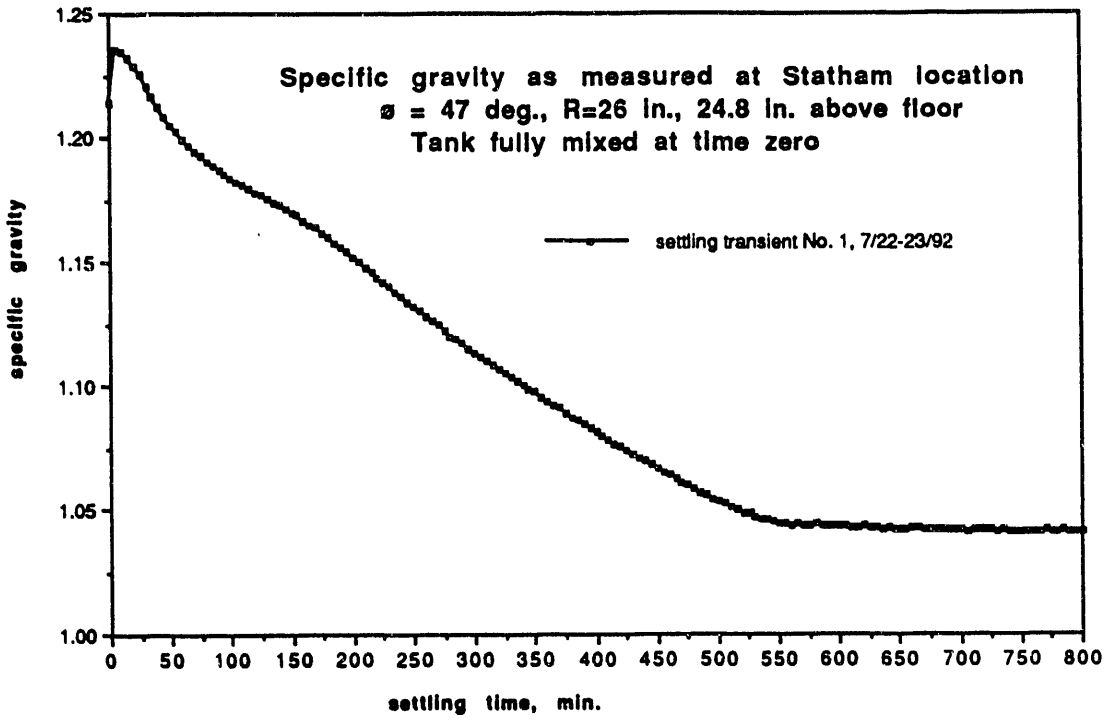

FIGURE B.23. Density History During Settling Prior to MVLS/1

TABLE B.11. Slurry Interface Heights Measured in MVLS/1

Elapsed Time hr:min	Interface Depth Below the Surface
0:00	20
0:40	7
1:07	3½
1:30	2⅛
1:59	3
2:12	2
3:02	1½ to 2
3:46	1 to 1¼
4:42	¼ to ⅛
5:07	¼
6:05	<¼
7:26	@ surface

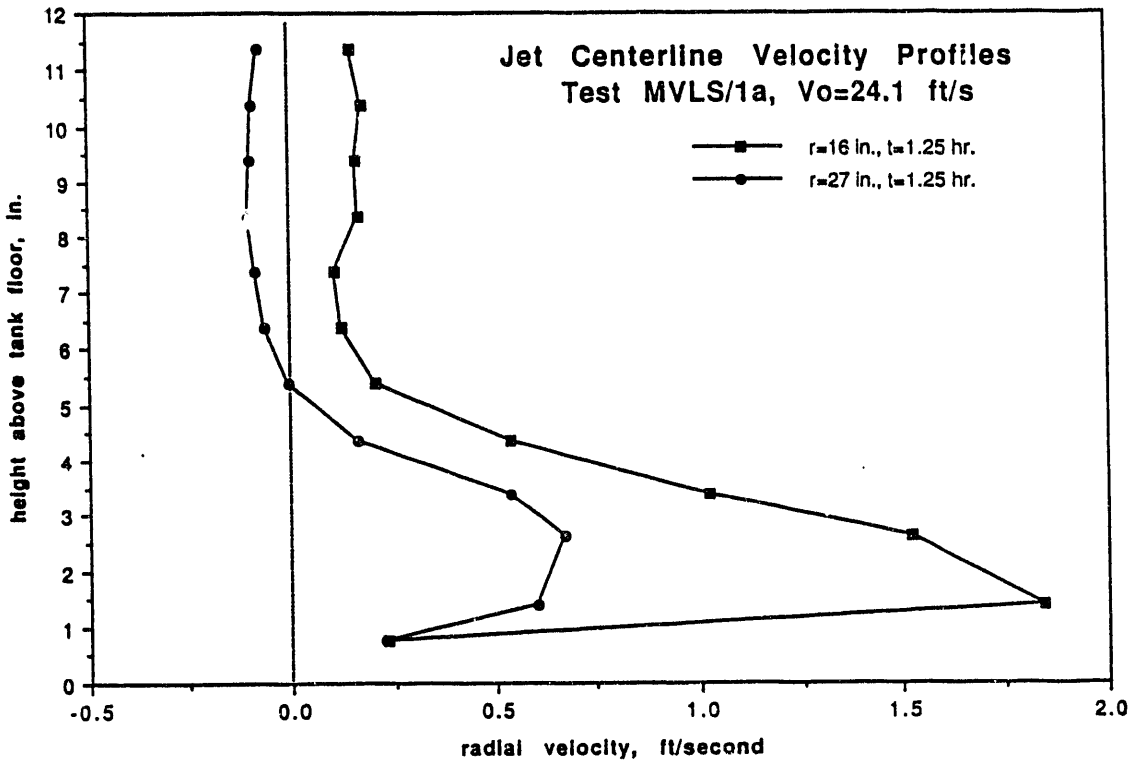

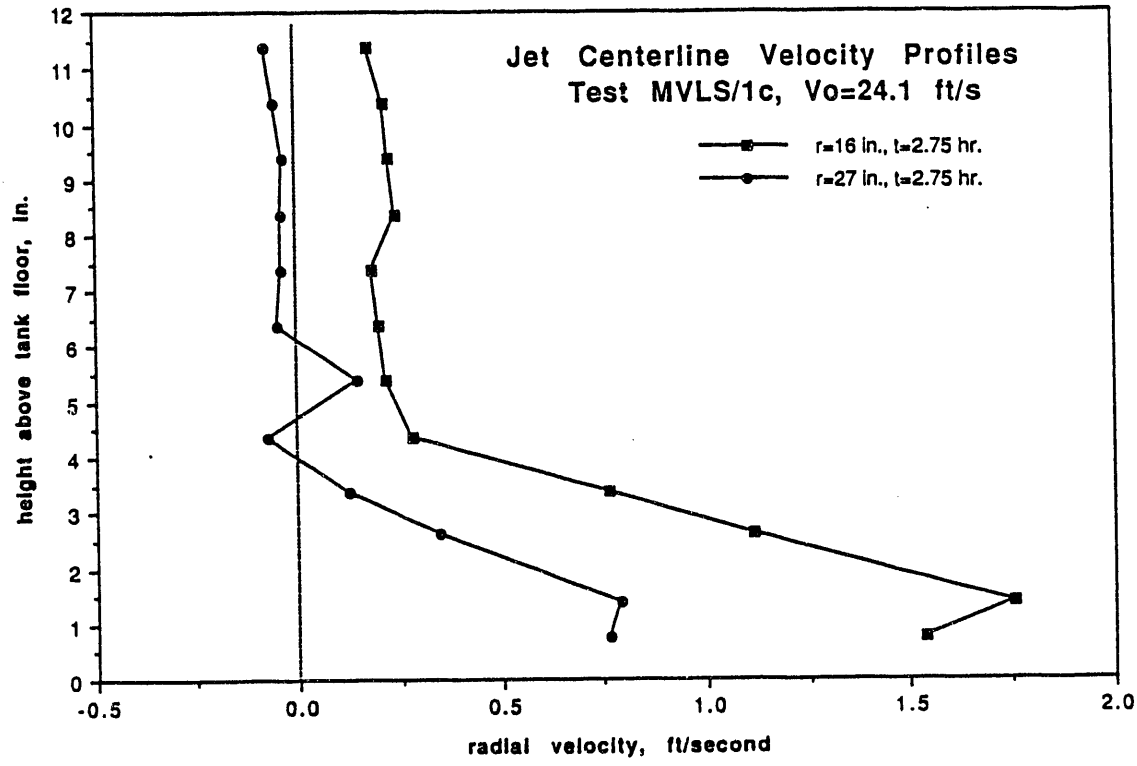

FIGURE B.24. Centerline Velocity Profiles for MVLS/1

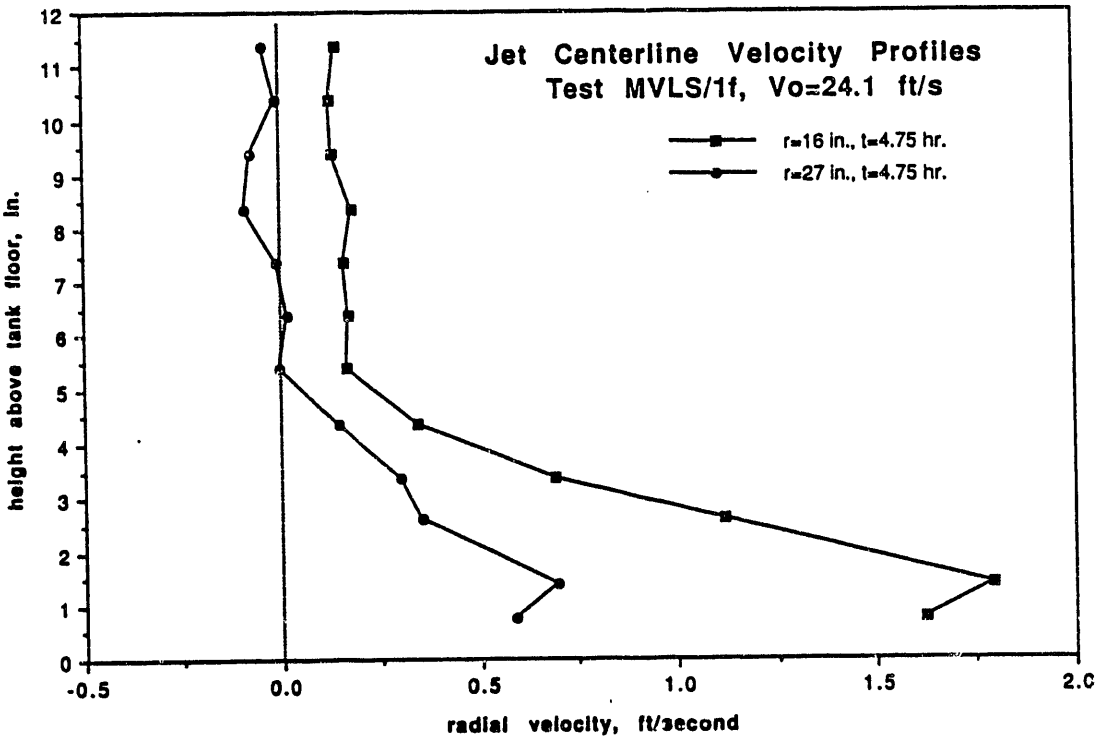

FIGURE B.24. (contd)

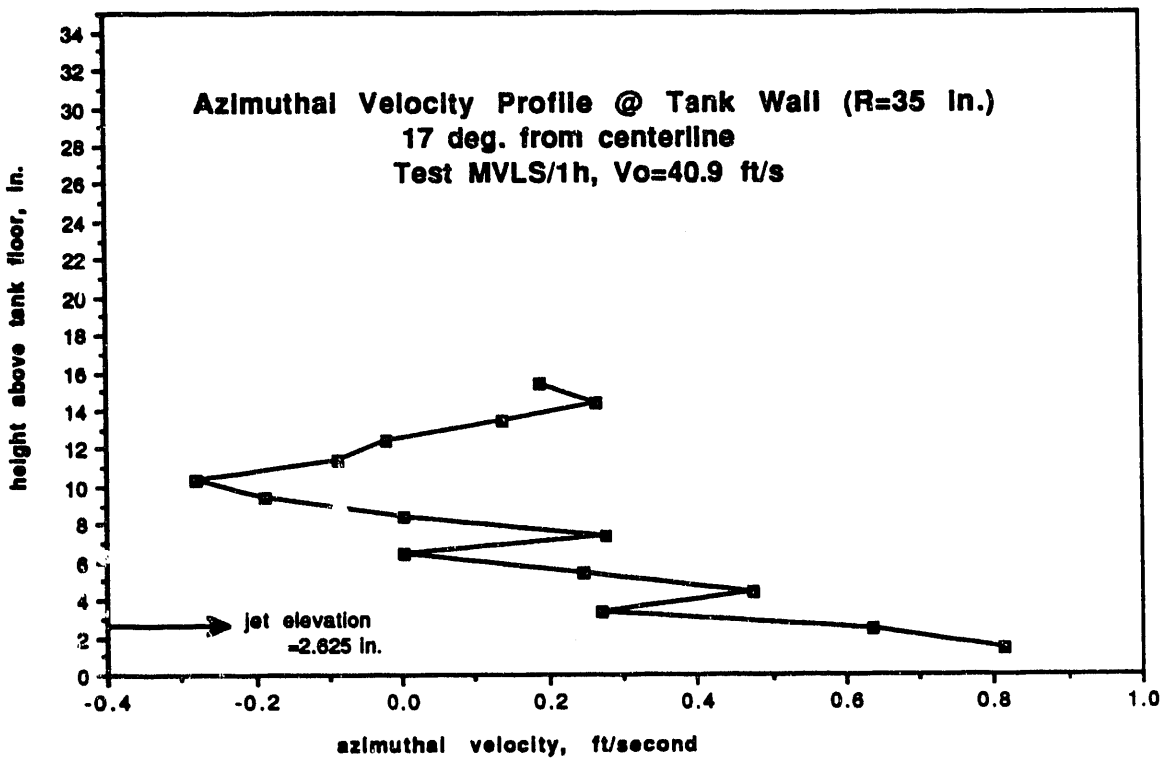

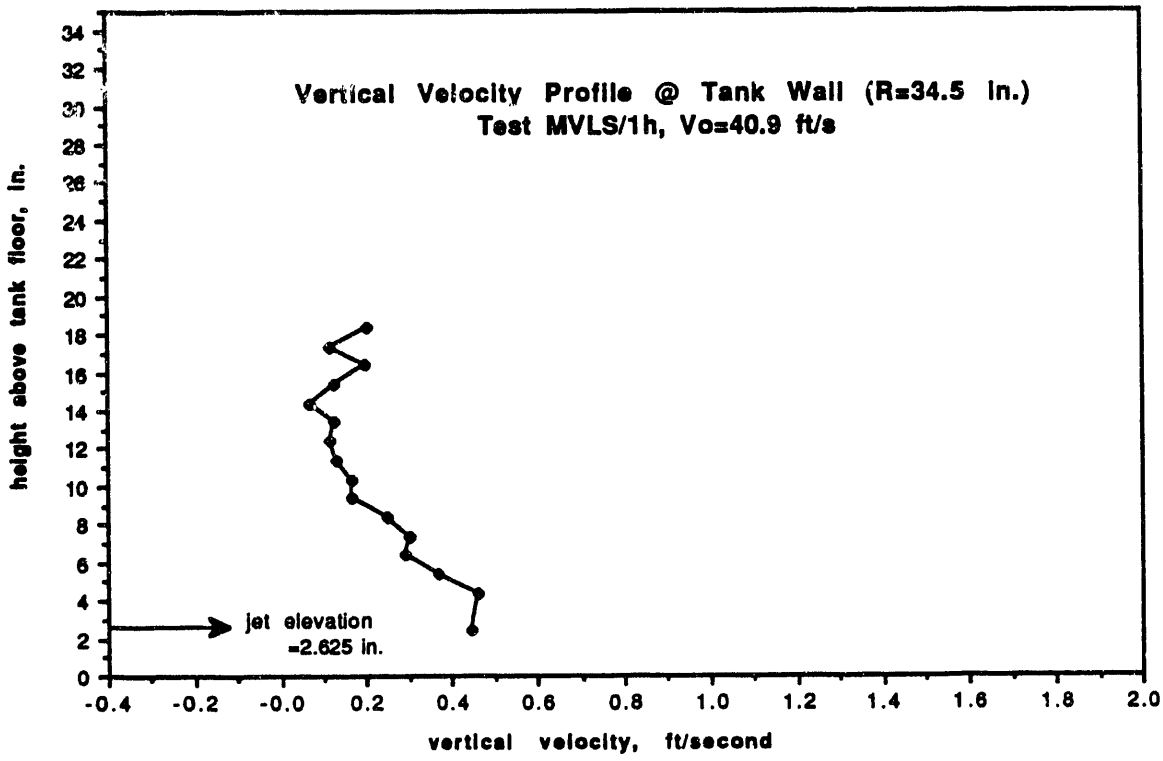

FIGURE B.25. Velocity Profiles at Wall for MVLS/1

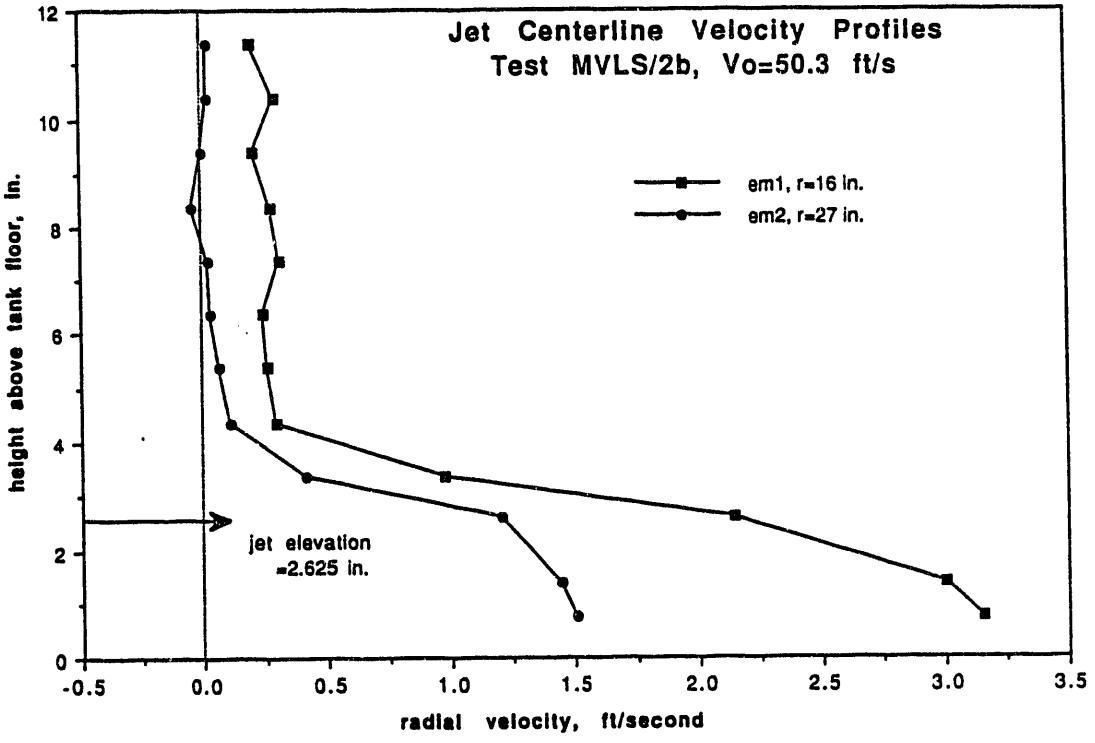

FIGURE B.26. Centerline Velocity Profiles for MVLS/2

TABLE B.12. Discrete Concentration Data from MVLS/1,2

Elapsed Time, min	Mixing Pump Orientation, degree	Probe Elevation from Tank Bottom, in.				Probe Location
		28.33	23.33	13.33	3.33	
		Density, g/cm^3				
W_0 = 25.4 ft/s						
~0	0	1.015	1.013	1.106	1.644	north
126	0	1.163	1.155	1.178	1.165	
208	0	1.152	1.177	1.170	1.151	
321	0	1.157	1.168	1.160	1.162	
488	0	1.156	1.168	1.174	1.173	
W_0 = 50 ft/s						
546	0	1.174	1.192	1.184	1.182	
W_0 = 25.4 ft/s						
~0	0	1.022	1.022	1.111	1.640	west
82	0	1.132	1.147	1.156	1.667	
206	0	1.154	1.166	1.171	No good	
316	0	1.144	1.156	1.143	1.563	
483	0	1.159	1.160	1.171	1.576	
W_0 = 50 ft/s						
541	0	1.171	1.177	1.177	1.332	
621	0	1.177	1.169	1.174	1.421	

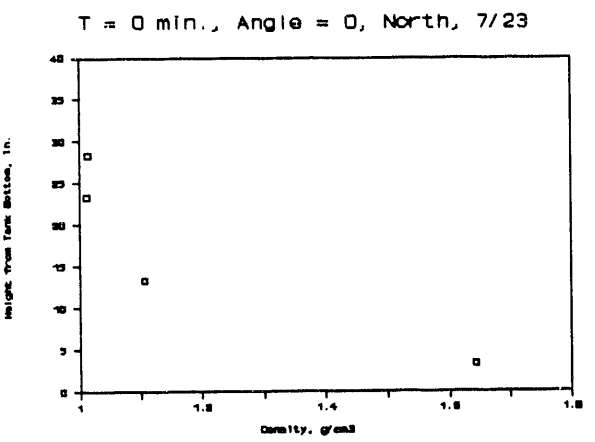

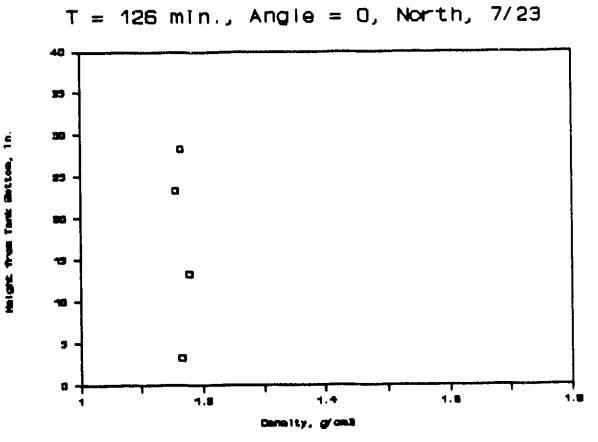

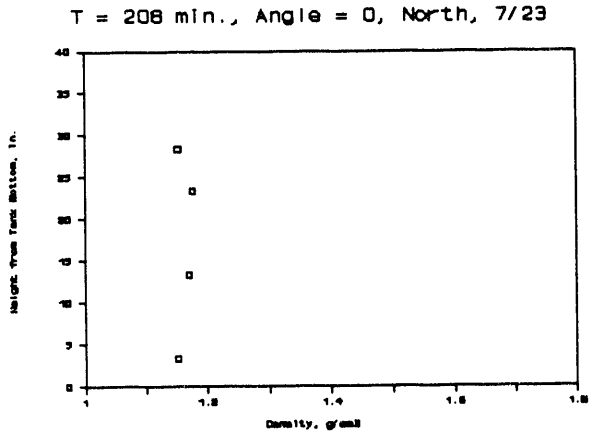

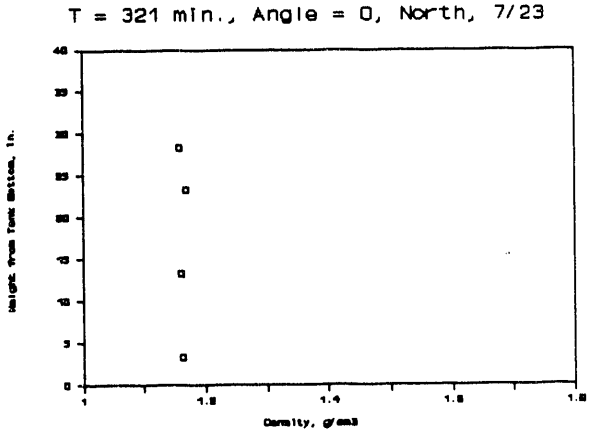

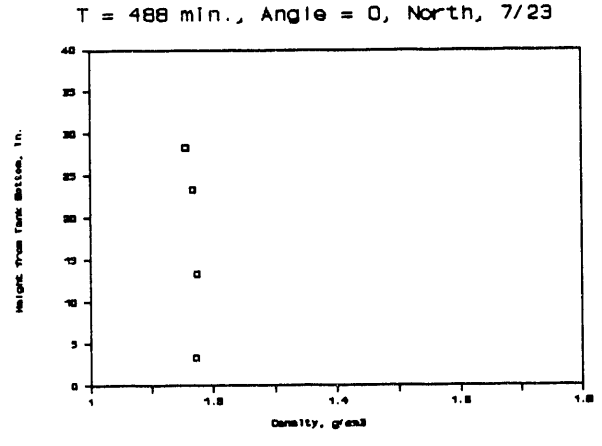

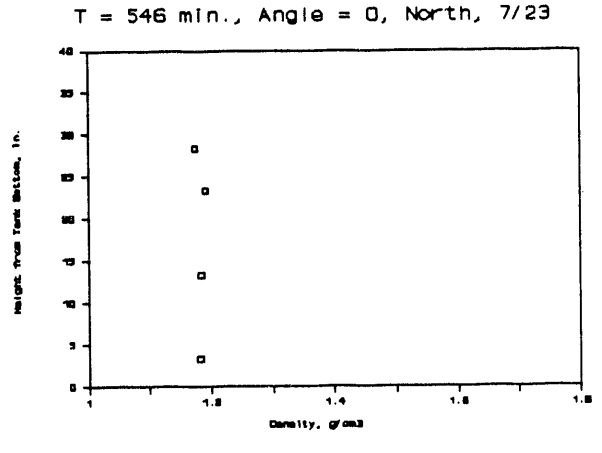

FIGURE B.27. Discrete Concentration Data from MVLS/1,2

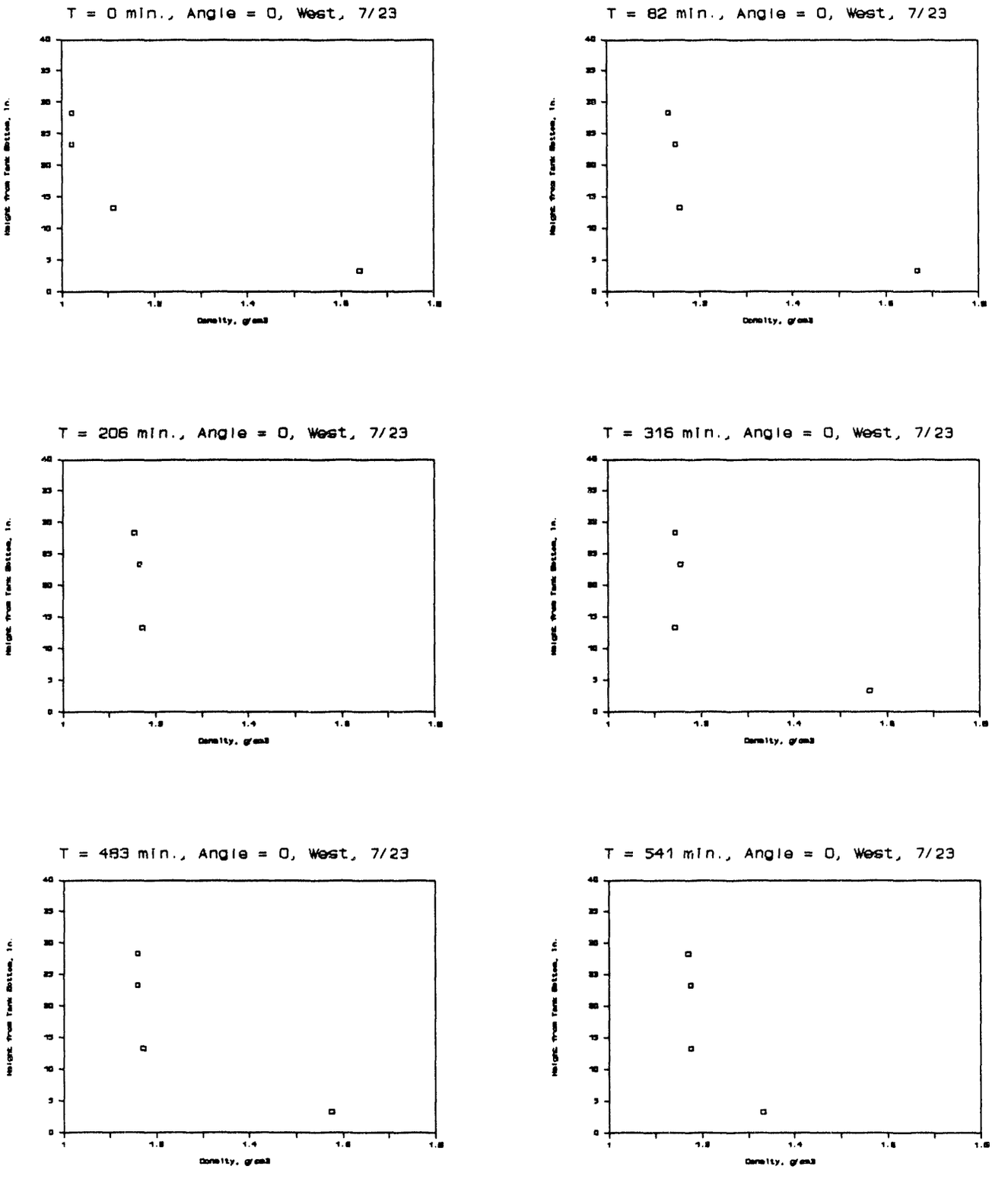

FIGURE B.27. (contd)

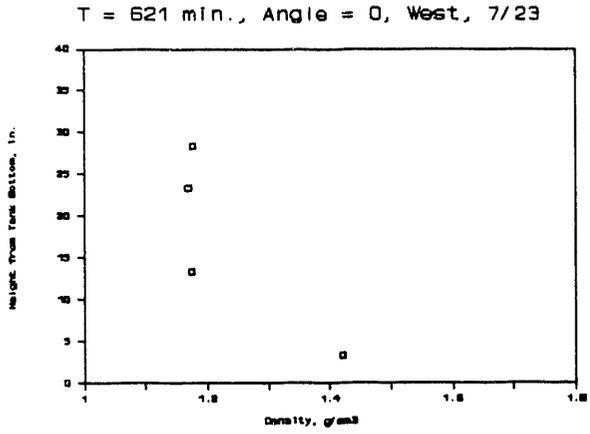

FIGURE B.27. (contd)

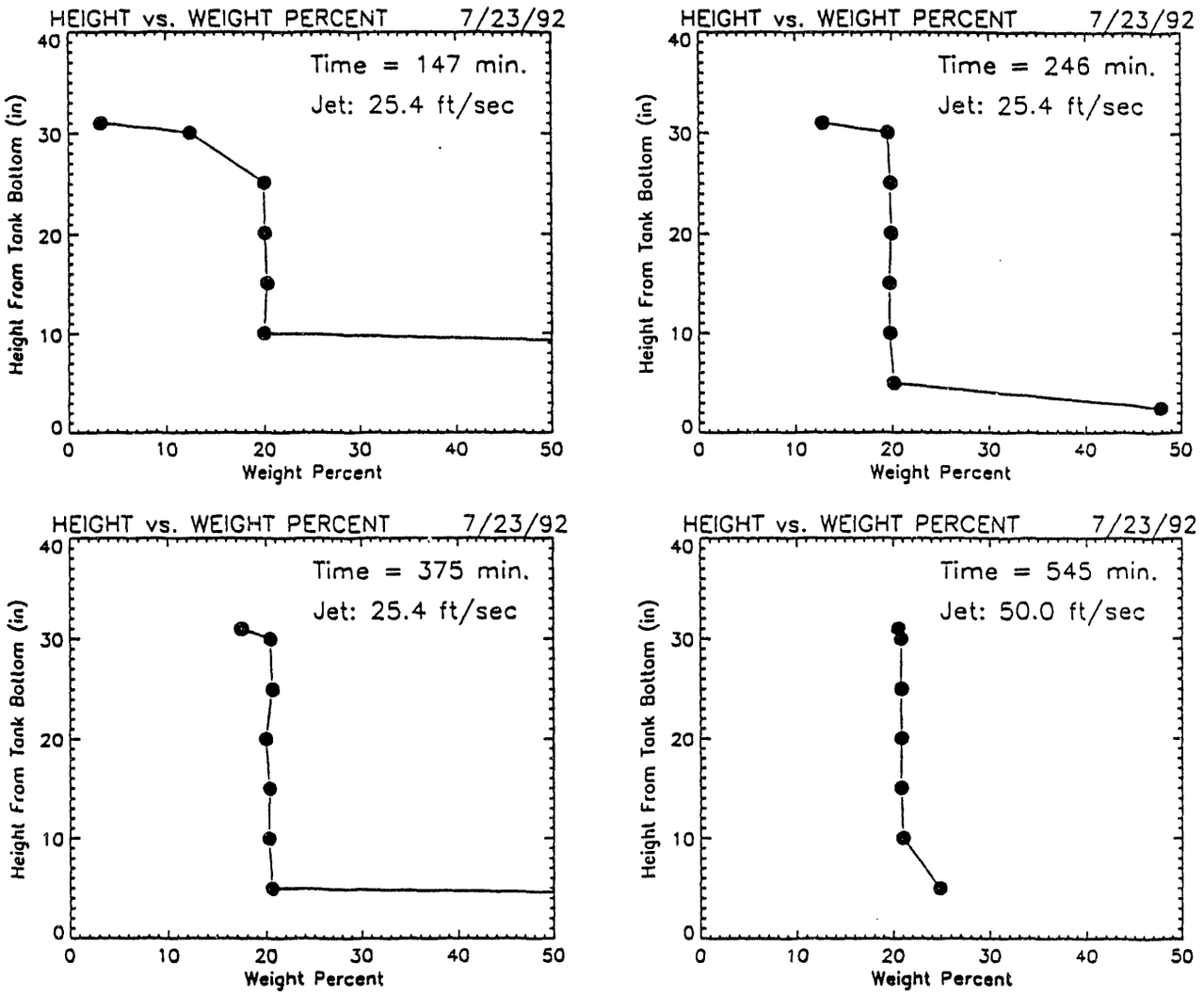

FIGURE B.28. Wt% Versus Height for MVLS/1

Test No: MVLS/3 **Test Date:** July 24, 1992

Description: Velocity profiling on jet centerline at jet velocity just below that at which jet attachment occurs, 67 ft/s.

Observations: This test was performed immediately after OPLS/2 was completed and the jet was repositioned.

Measurements: Centerline velocity profiles are shown in Figure B.29.

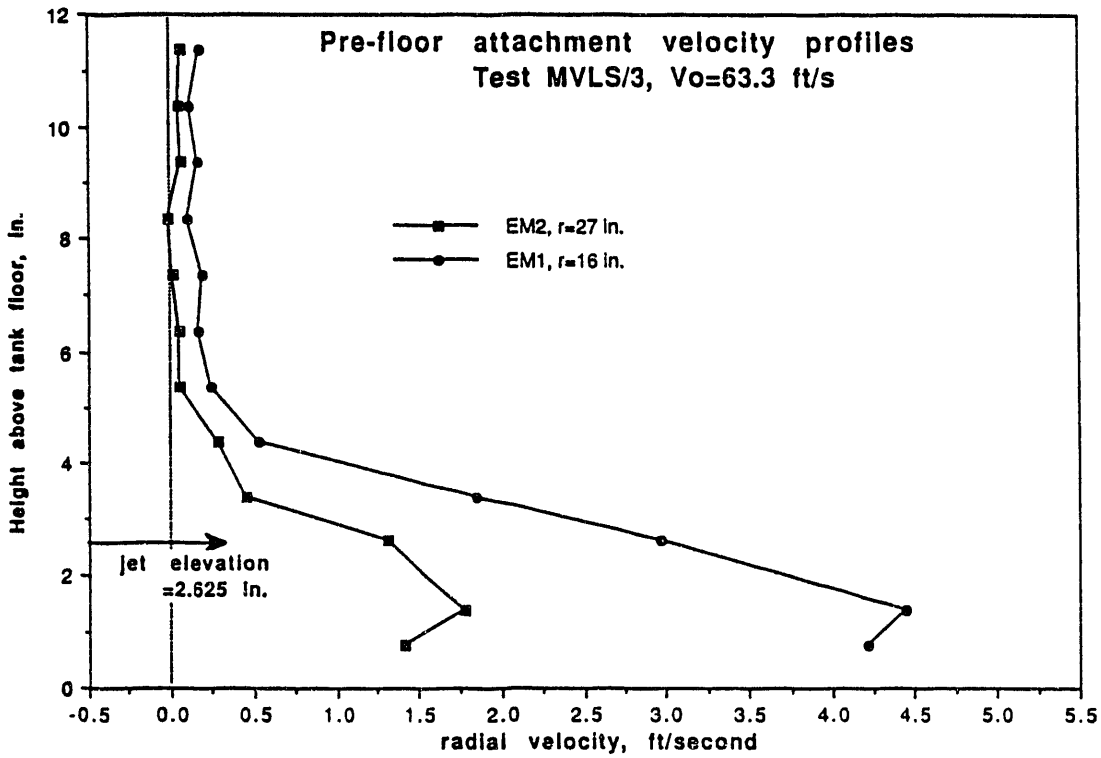

FIGURE B.29. Centerline Velocity Profiles for MVLS/3

Test No: MVLS/4 **Test Date:** July 24, 1992

Description: Velocity profiling on jet centerline at jet velocity just above that at which jet attachment occurs, 69 ft/s.

Observations: This test was performed following completion of MVLS/3. The jet velocity was increased from 63 to 69 ft/s and allowed to run for 15 min before making velocity measurements.

Measurements: Centerline velocity profiles are shown in Figure B.30.

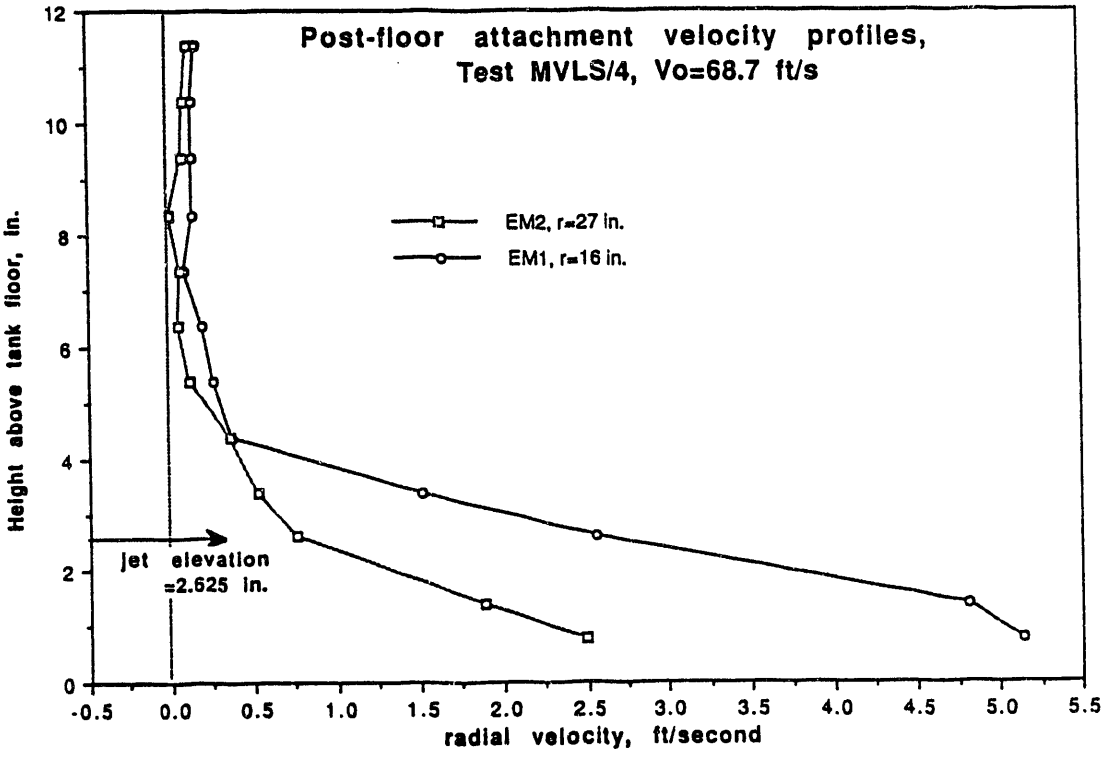

FIGURE B.30. Centerline Velocity Profiles for MVLS/4

B.5 OPERATING PARAMETER TESTS

This section describes locations of instruments for OP tests (e.g., EMs at 0 and 60 degrees).

B.5.1 High Viscosity Simulant-Based Tests

Test No: OPS/1 **Test Date:** July 17, 1992

Description: Operating parameter test with high viscosity simulant and 25.4 ft/s jet velocity. Density profiles taken at north position.

Measurements:

Sludge Interface Location - Tank contents had been allowed to settle after being fully mixed at 6:00 p.m. on July 15 (about 38 h prior to beginning this test). The mixing process involved moving the jet in 10 degrees increments around the tank, holding each position until the solids had been removed from the floor all the way to the wall. Measurements of interface height are given in Table B.13.

TABLE B.13. Slurry Interface Heights Measured in OPS/1

Elapsed Time hr:min	Interface Depth Below the Surface
0:00	13½
2:38	5¾
2:55	5
4:20	2 to 2½
4:43	1½ to 1¾

Statham Densitometer Data - Density history measured with the Statham densitometer is shown in Figure B.31.

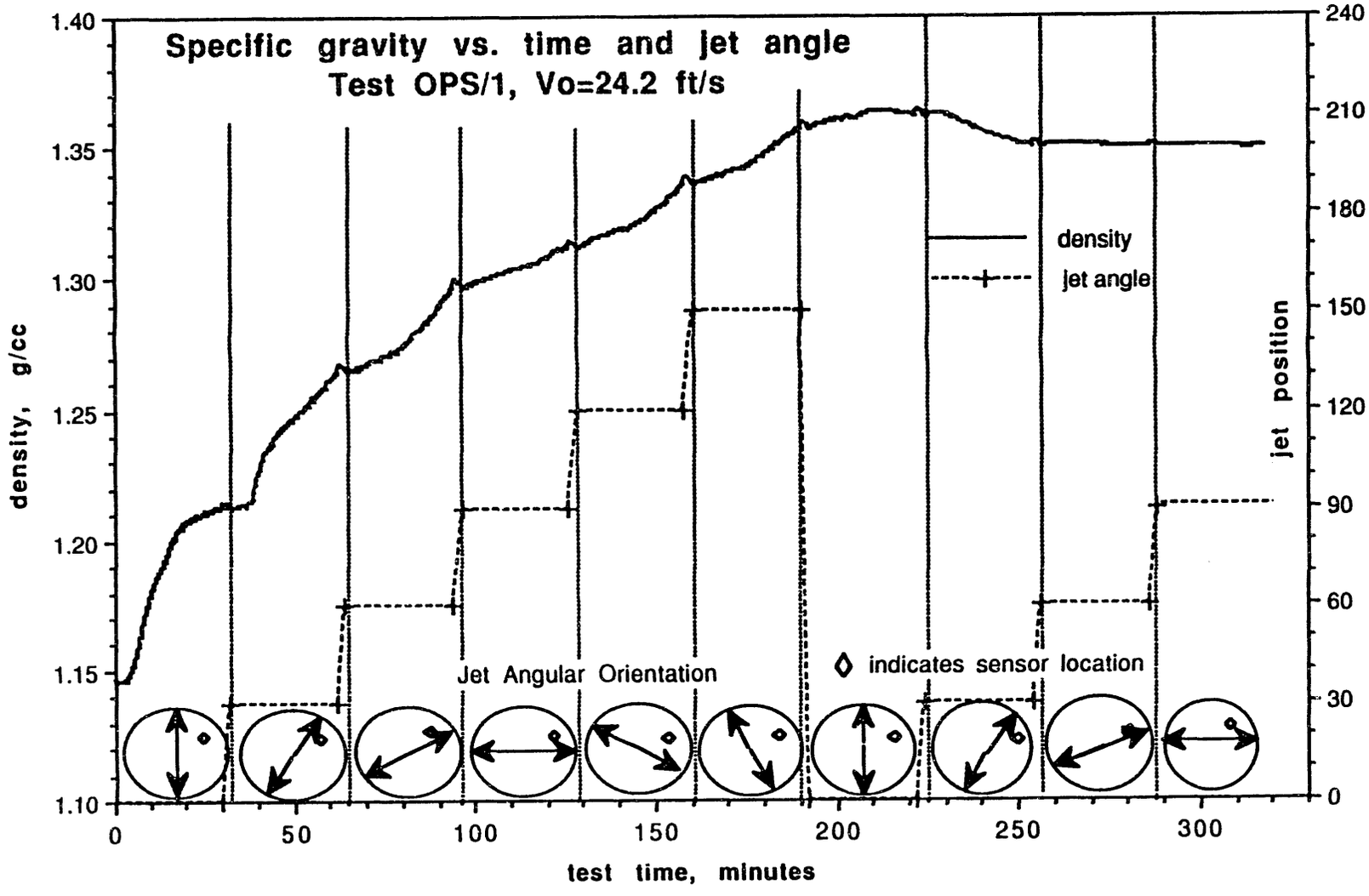

FIGURE B.31. Density History Recorded with Statham Densitometer for OPS/1

Discrete Concentration Data - Measurement data taken are given in Table B.14.

TABLE B.14. Discrete Concentration Data Taken 7/17/92

Elapsed Time, min	Mixing Pump Orientation, degree	Probe Elevation from Tank Bottom, in.				Probe Location
		28.33	23.33	13.33	3.33	
		Density, g/cm^3				
0	0	1.123	1.120	1.338	1.722	north
		1.126	1.126	1.342	1.725	west
32	30	1.113	1.211	1.378	1.377	north
64	60	1.119	1.351	1.343	1.351	north
96	90	1.117	1.337	1.339	1.329	north
128	120	1.118	1.337	1.348	1.339	north
160	150	1.340	1.332	1.332	1.443	north
192	0	1.324	1.338	1.320	1.328	north
224	30	1.322	1.327	1.312	1.316	north
256	60	1.324	1.189	1.317	1.353	north
288	90	1.311	1.317	1.318	1.315	north

After the end of the test, a sample of sludge was taken at the tank bottom, at north location at a radius of 34 in. ρ_{sludge} = 1.15 g/cm^3. The discrete concentration data are shown plotted in Figure B.32.

Ultrasonic Concentration Data - Figure B.33 clearly shows the point when the slurry-supernate interface reached 23.5 in. from the bottom. The time is about 50 min from pump start. The fact that the initial values of the wt% appear as negative values, as opposed to zero or positive values, is merely a result of the uncertainty in our data and in our calibration-line coefficients.

The four plots in Figure B.34 provide the same information as the previous plots, but each traverse is plotted separately for clarity. Here the slurry had been allowed to settle over two nights instead of only one, and it is clear from the first plot that the extra day allowed more particulate to

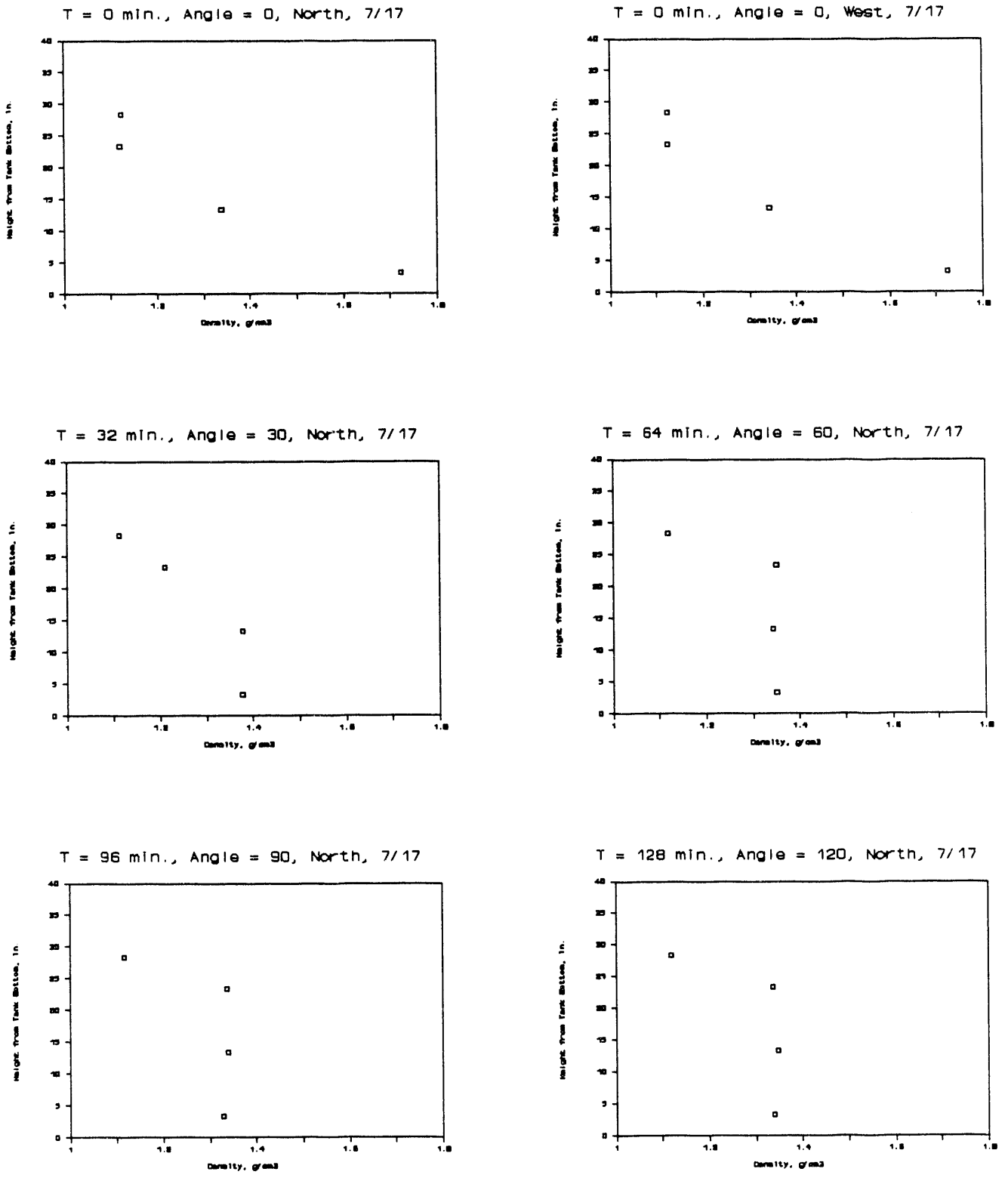

FIGURE B.32. Discrete Concentration Data for OPS/1

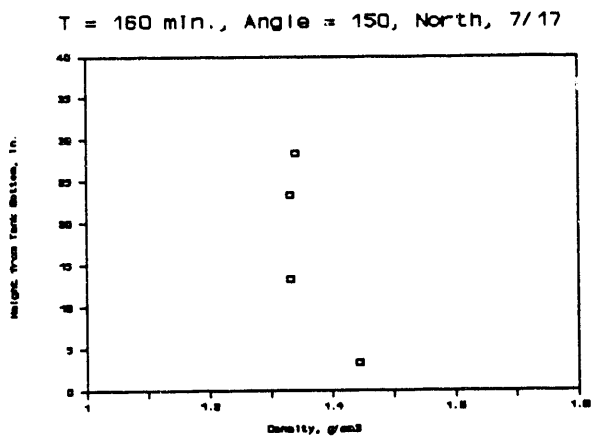

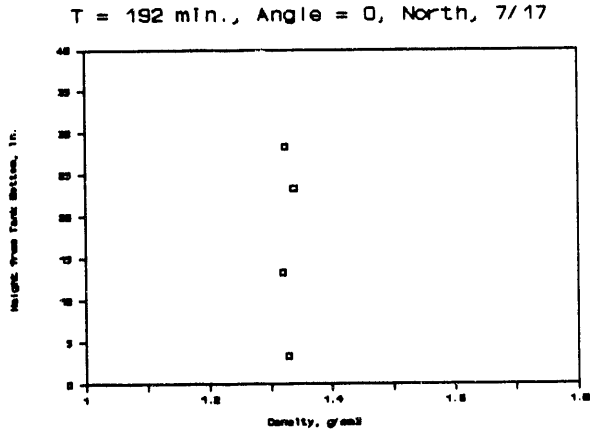

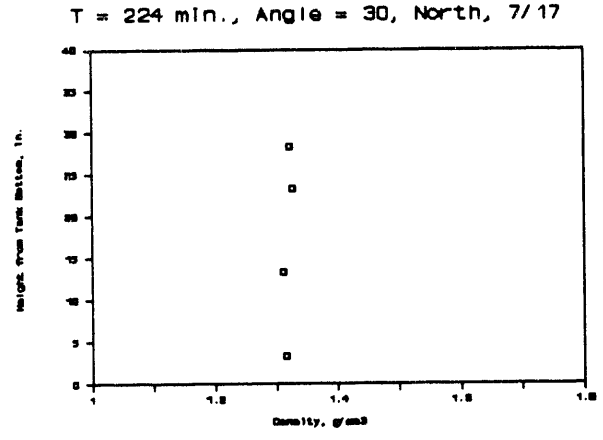

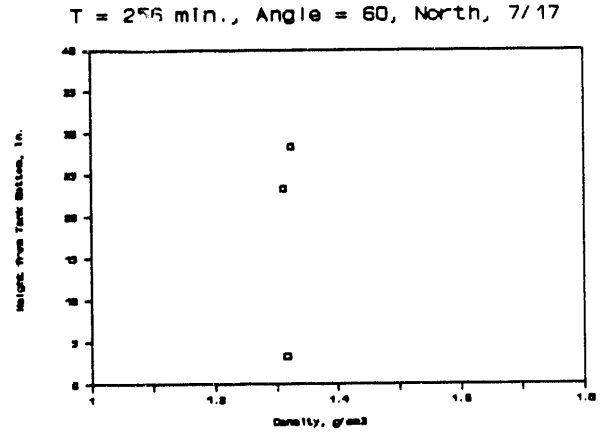

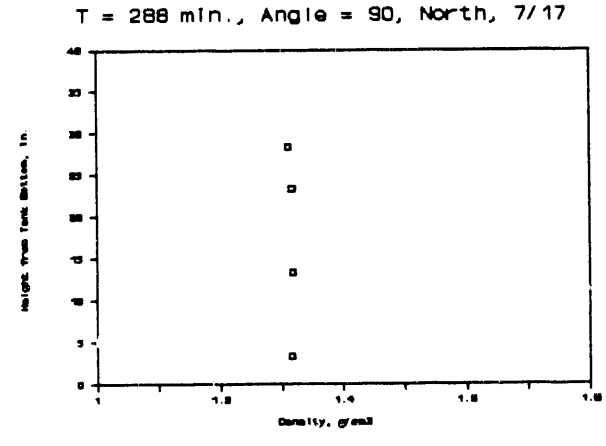

FIGURE B.32. (contd)

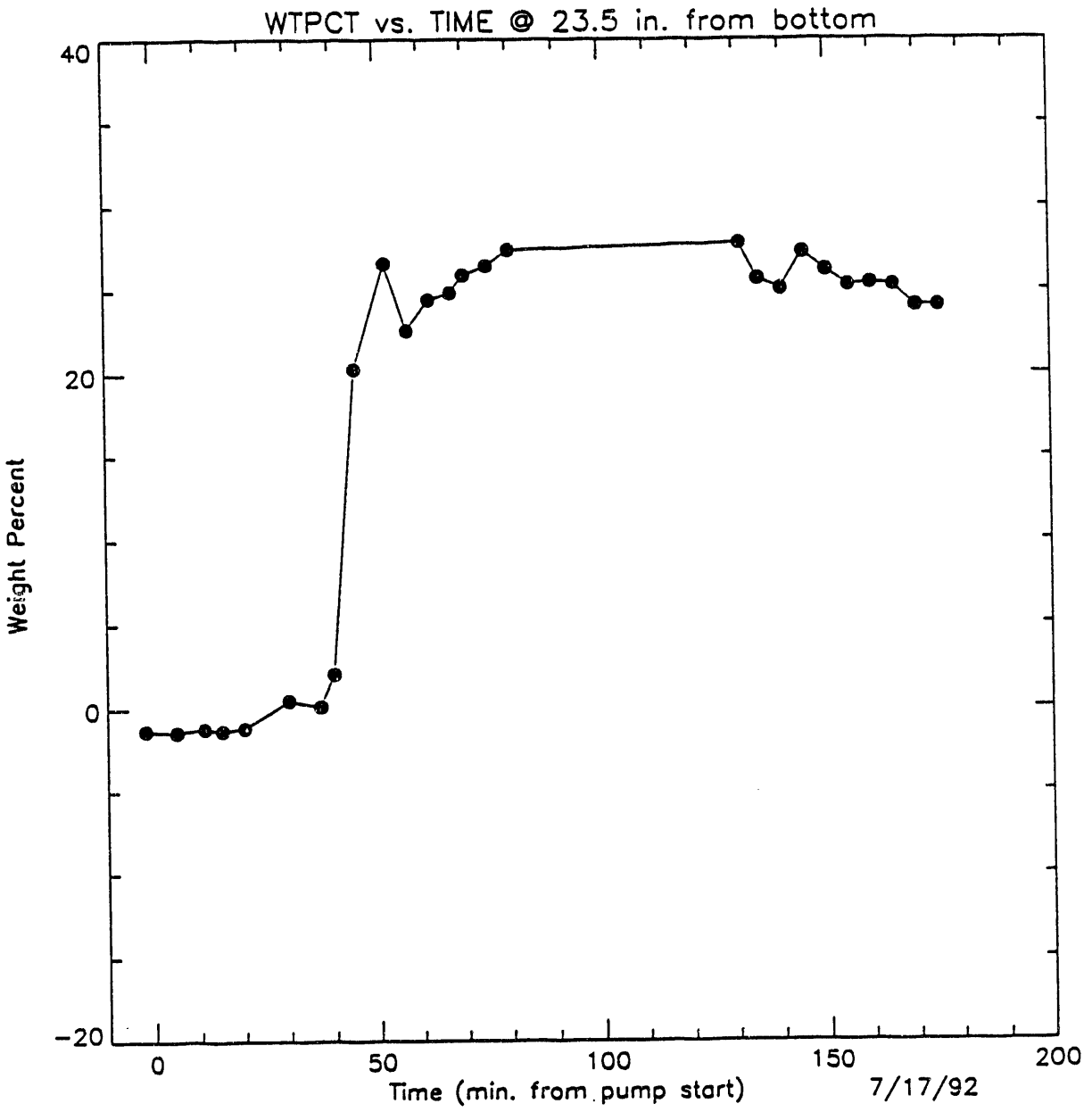

FIGURE B.33. Wt% Versus Time at a Height of 23.5 in. for OPS/1

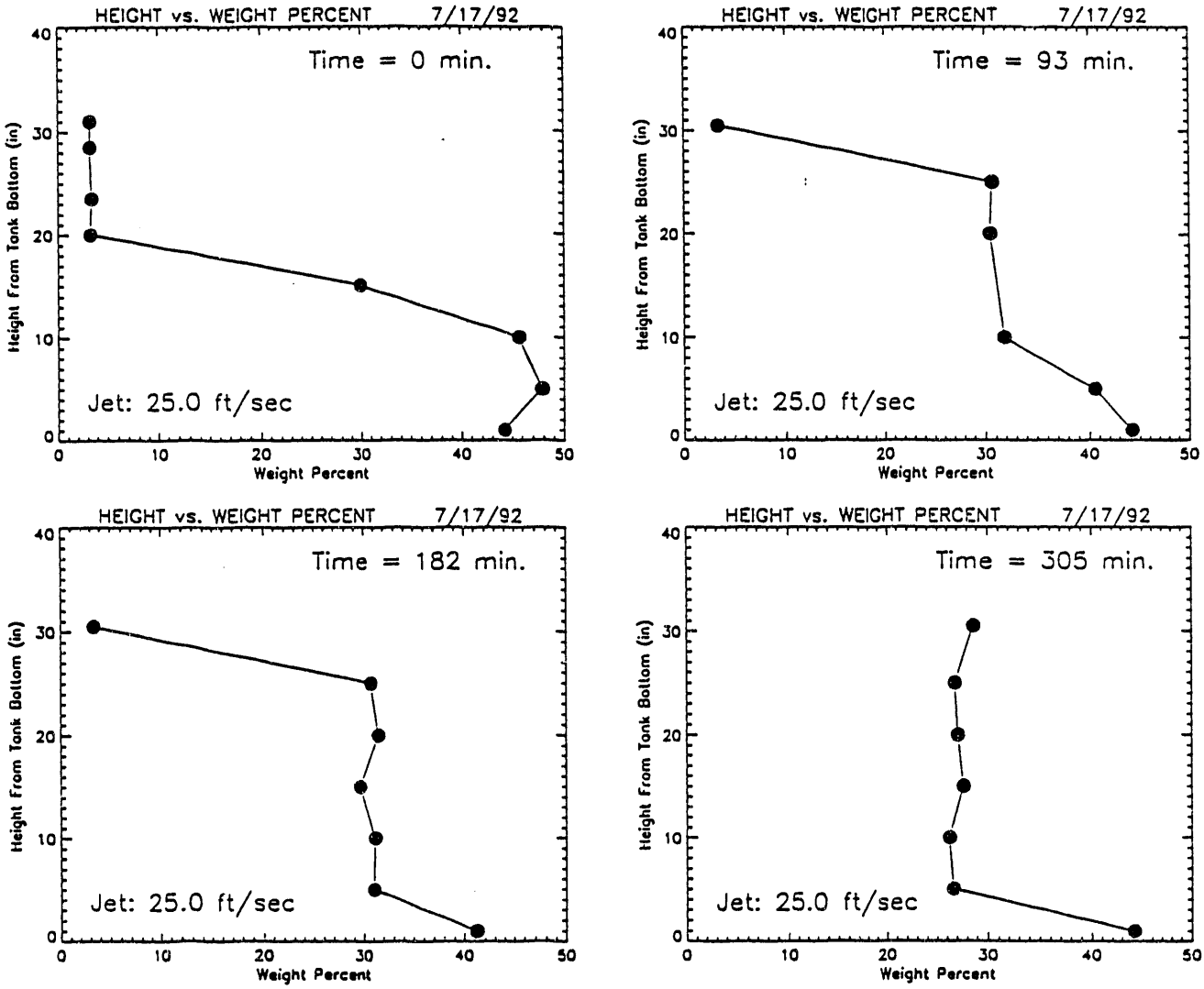

FIGURE B.34. Height Versus Wt% for OPS/1

settle to greater depths. The second plot shows that as the jet stirred the slurry, the middle of the tank became more concentrated, while the third plot shows the decrease in wt% of the point just above the tank's sludge layer (height = 5 in.). Interestingly, the fourth plot shows that the wt% is just about constant for all heights but in the sludge layer. Note also that as the wt% top of the slurry increases in wt% between the third and fourth plots, the wt% of those heights below the top decreases slightly.

B.5.2 Low Viscosity Simulant-Based Tests

Test No: OPLS/1 **Test Date:** July 22, 1992

Description: Operating parameter test with low viscosity simulant and 25.4 ft/s jet velocity. Jets moved in 30 degrees increments, held for 30 min at each position with a 2-min pause to reposition.

Observations: The low viscosity supernate is much more transparent than the high viscosity supernate. At the beginning of this test, the bottom of the Statham densitometer was clearly visible. Jet action in interface is visible at wall and appears more vigorous than in the high viscosity simulant.

The sludge layer depth was probed after completing one complete rotation of the jets. This was at 3 h and 47 min into the test. The top of the heavy sludge layer was approximately ¼ in. off the bottom at the 0 degrees position just after moving the jets to the 30 degrees position. At the 90 degrees position, the sludge layer is approximately 1¼ in. deep. Both of these measurements were made at 15 to 20 in. out from the center of the tank.

Measurements:

Sludge Interface Location - Tank contents had been allowed to settle after being fully mixed at 6:15 p.m. on July 20 (about 38 h prior to starting this test). Measurements of interface height are given in Table B.15. Interface height and jet position are shown plotted against elapsed time in Figure B.35.

Statham Densitometer Data - Density and jet position are plotted against time in Figure B.36.

Discrete Concentration Data - Measurement data are given in Table B.16.

Ultrasonic Concentration Data - The 10 plots shown in Figure B.38 correspond to 10 traverses and are plotted separately for clarity. Again the slurry was allowed to settle for two nights, and the first plot shows that the settling seems greater than that encountered in the high-viscosity slurry in OPS/1. Perhaps the lower viscosity of this slurry facilitates particle settling. The next nine plots show the gradual convergence of the entire slurry, except the sludge layer, toward a uniform wt%. The data points in the

TABLE B.15. Slurry Interface Heights Measured in OPLS/1

Elapsed Time hr:min	Interface Depth Below the Surface
0:00	23
0:50	10
1:17	9½
1:50	8
2:32	6¾
2:54	6¼
3:28	5
3:47	3¾
4:38	2
5:07	1½
5:30	½

sludge layer have a large uncertainty associated with them because the jet seems to allow certain areas at the bottom of the tank to collect particulate, while clearing out other areas. This irregular profile along with the relatively large attenuation at the bottom of the tank may explain the inconsistency of the wt% there.

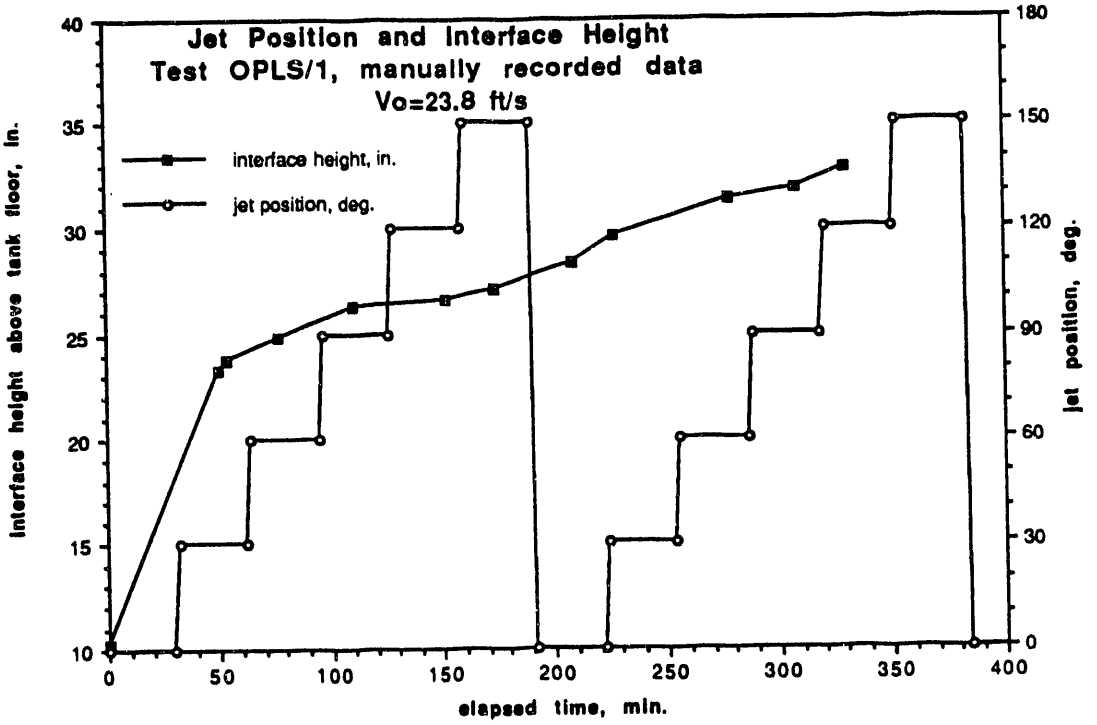

FIGURE B.35. Jet Position and Interface Height History for OPLS/1

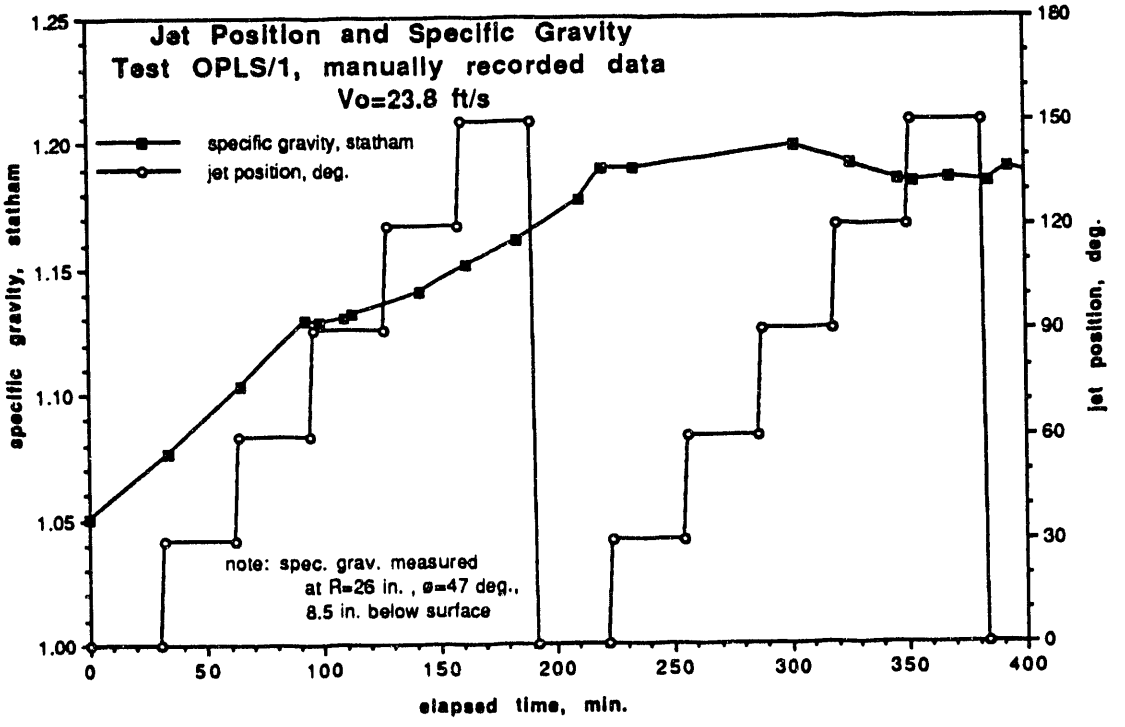

FIGURE B.36. Jet Position and Density History for OPLS/1

TABLE B.16. Discrete Concentration Data for OPLS/1

Elapsed Time, min	Mixing Pump Orientation, degree	Probe Elevation from Tank Bottom, in.				Probe Location
		28.33	23.33	13.33	3.33	
		Density, g/cm^3				
0	0	1.021	1.027	1.026	1.640	north
		1.027	1.017	1.019	1.645	west
32	30	1.031	1.024	1.134	1.322	north
64	60	1.020	1.130	1.152	1.145	north
96	90	1.026	1.150	1.156	1.212	north
128	120	1.014	1.152	1.168	1.267	north
160	150	1.022	1.175	1.181	1.431	north
192	0	1.031	1.164	1.177	1.422	north
224	30	1.136	1.173	1.173	1.175	north
256	60	1.176	1.175	1.191	1.183	north
288	90	1.169	1.177	1.186	1.194	north
320	120	1.170	1.180	1.178	1.177	north
352	150	1.173	1.178	1.184	1.440	north
384	0	1.164	1.158	1.176	1.187	north

These data are shown plotted in Figure B.37.

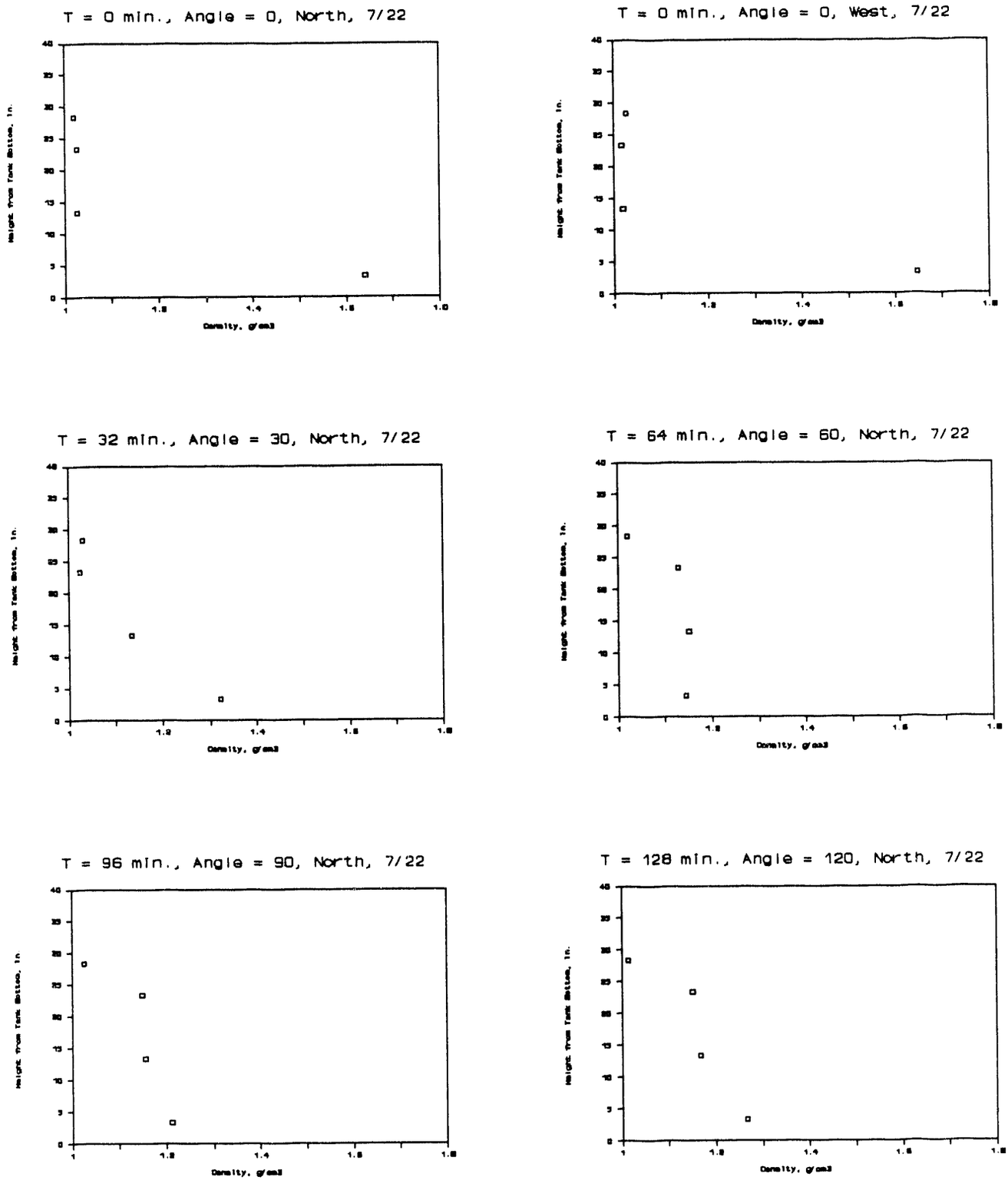

FIGURE B.37. Discrete Concentration Data for OPLS/1

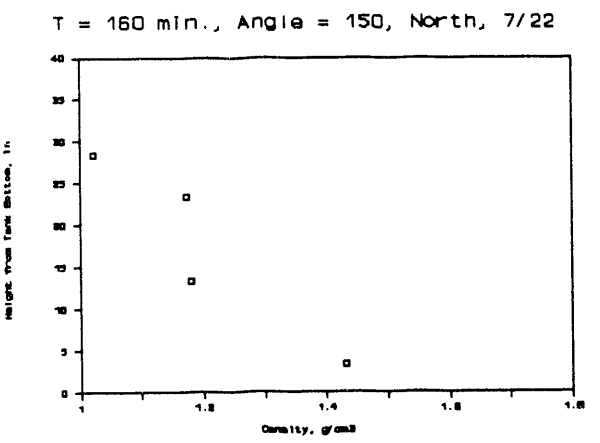

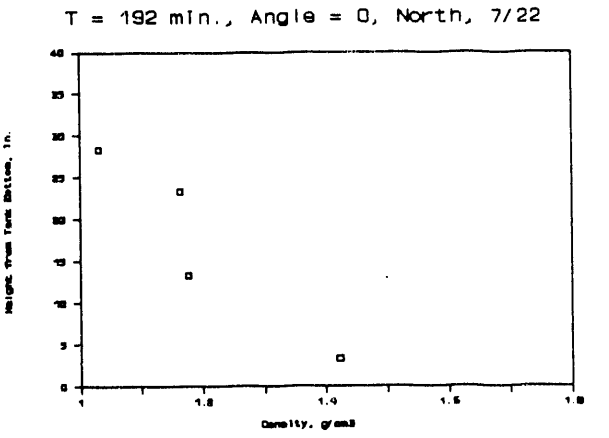

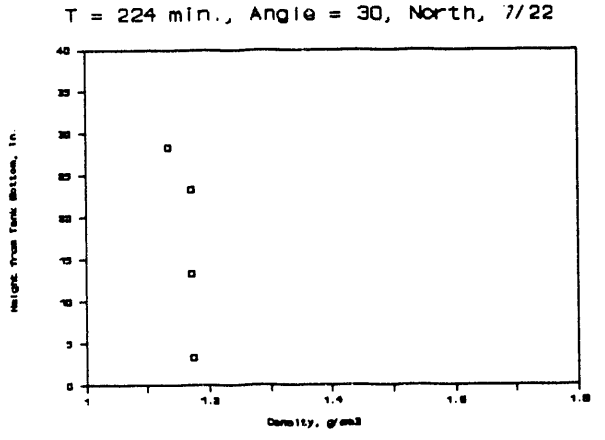

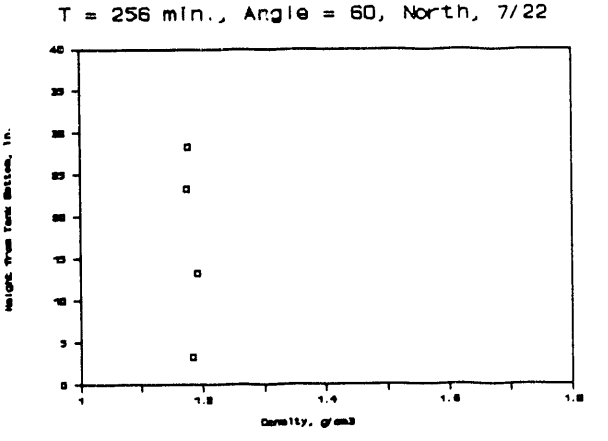

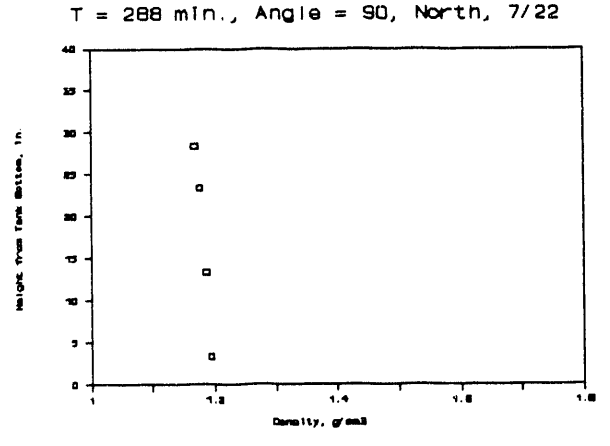

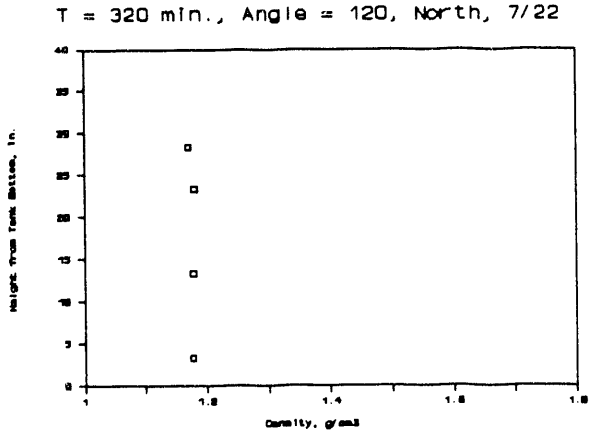

FIGURE B.37. (contd)

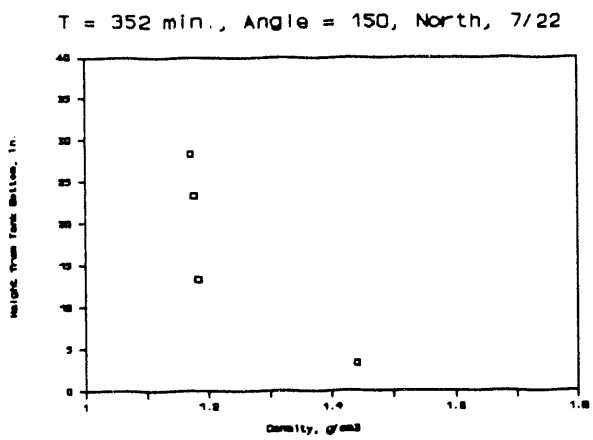

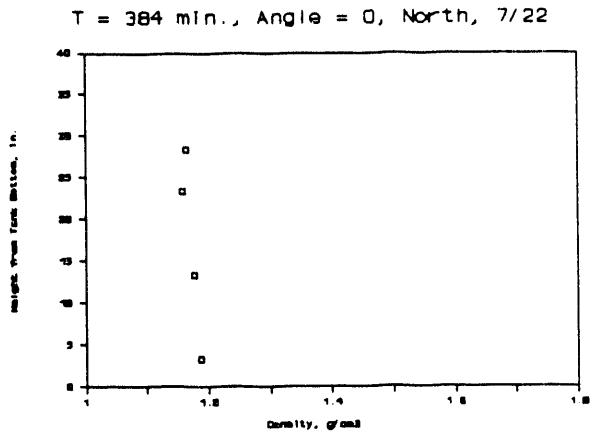

FIGURE B.37. (contd)

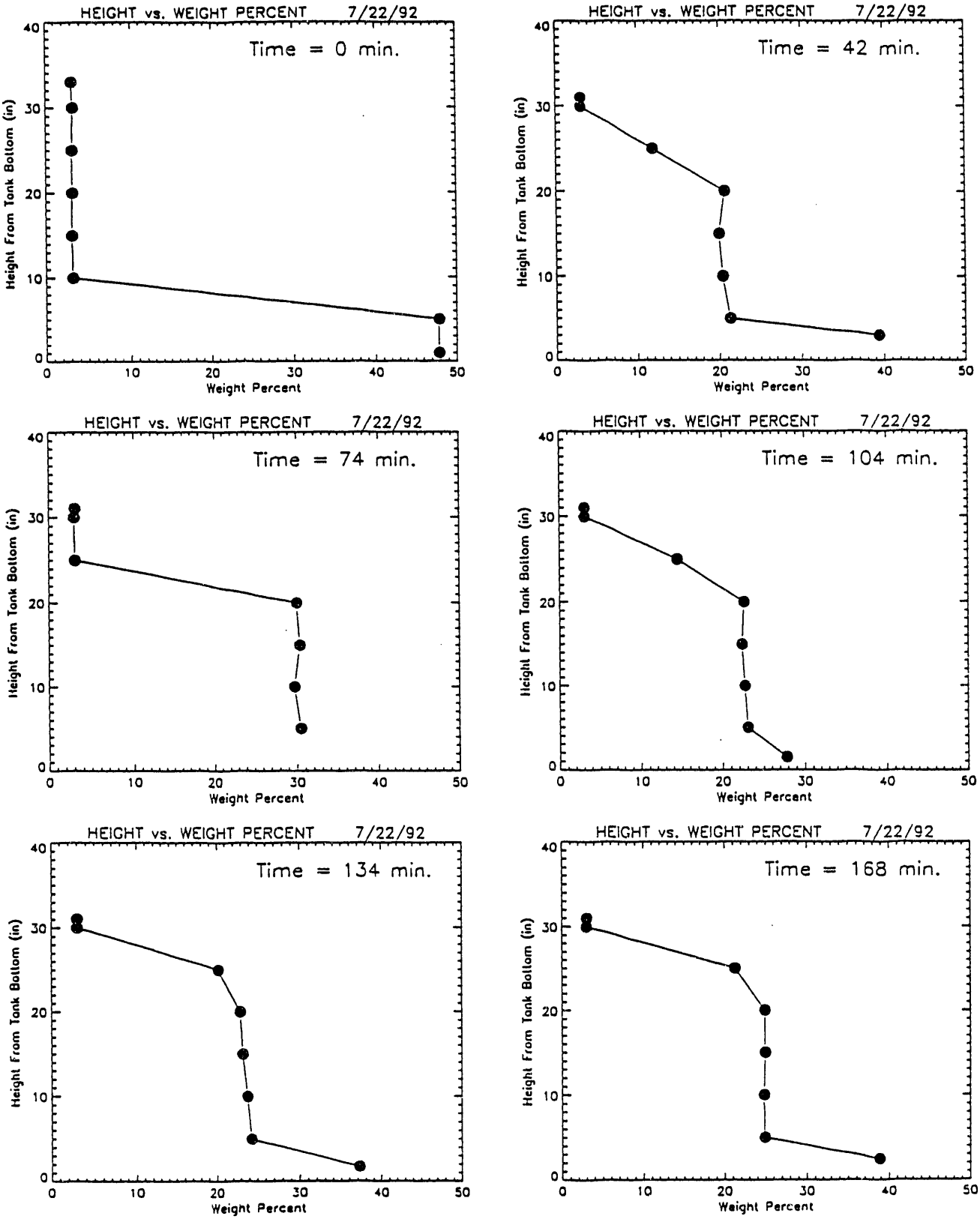

FIGURE B.38. Height Versus Wt% Concentration for OPLS/1

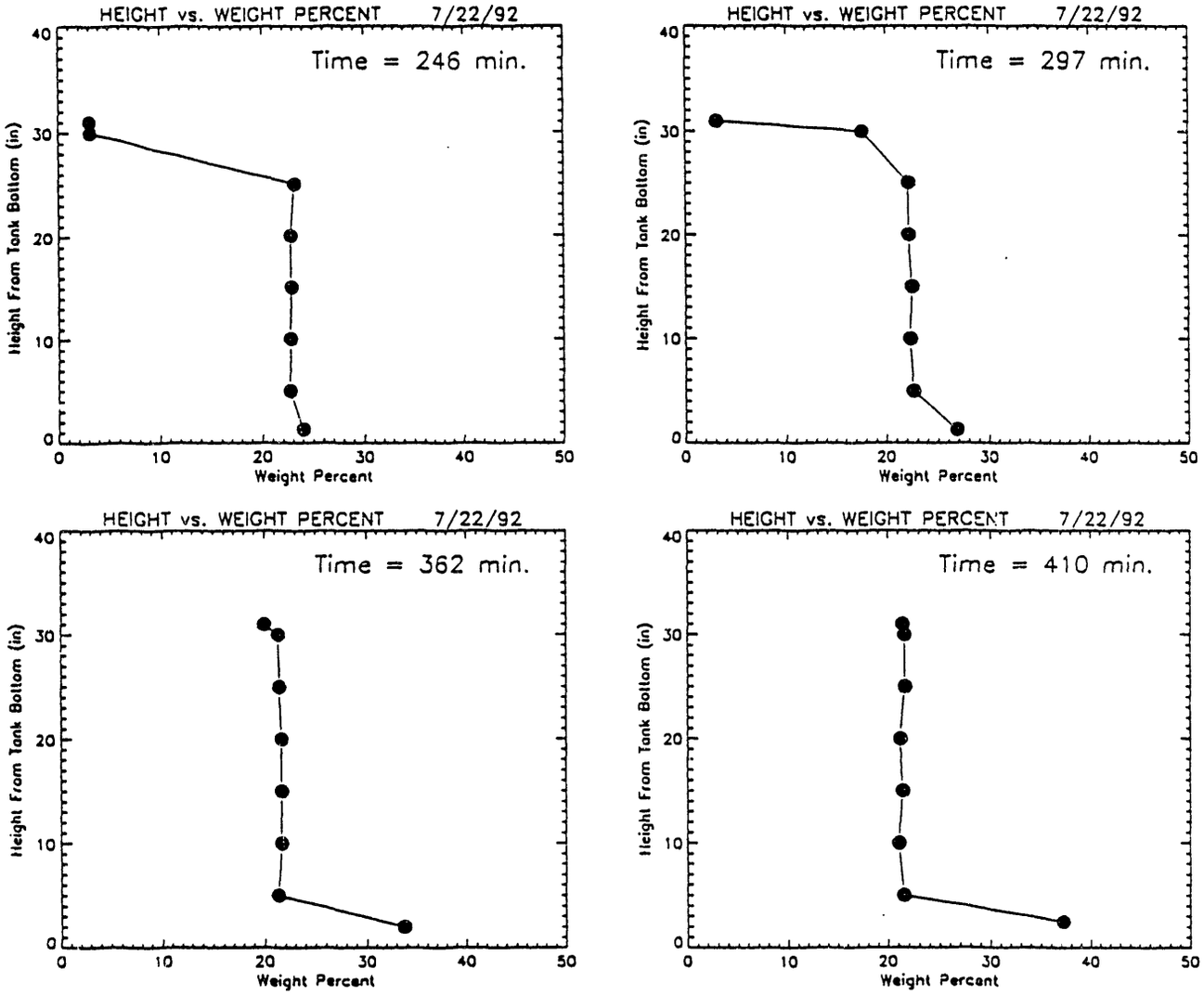

FIGURE B.38. (contd)

Test No: OPLS/2 **Test Date:** July 24, 1992

Description: Operating parameter test with low viscosity simulant and 50 ft/s jet velocity. Jets moved in 30 degrees increments, held for 30 min at each position with a 2-min pause to reposition.

Measurements:

Pre-Test Settling - Tank contents had been allowed to settle for 14 h after being fully mixed. Density was measured with the Statham densitometer during this settling process and the results are given in Figure B.39.

Sludge Interface Location - Measurements of interface height after initiating test OPLS/2 are given in Table B.17.

Velocity Measurements - EM probes buried in the sludge were used to measure the rate that the jet would penetrate through the settled sludge layer. These breakthrough times at the two jet postions are illustrated in Figure B.40.

Statham Densitometer Data - Density measured with the Statham densitometer is shown plotted along with jet position in Figure B.41.

Discrete Concentration Data - Measurement data are given in Table B.18. These data are also shown plotted in Figure B.42.

Ultrasonic Concentration Data - Figure B.43 again shows the gradual convergence of the slurry to uniform wt%.

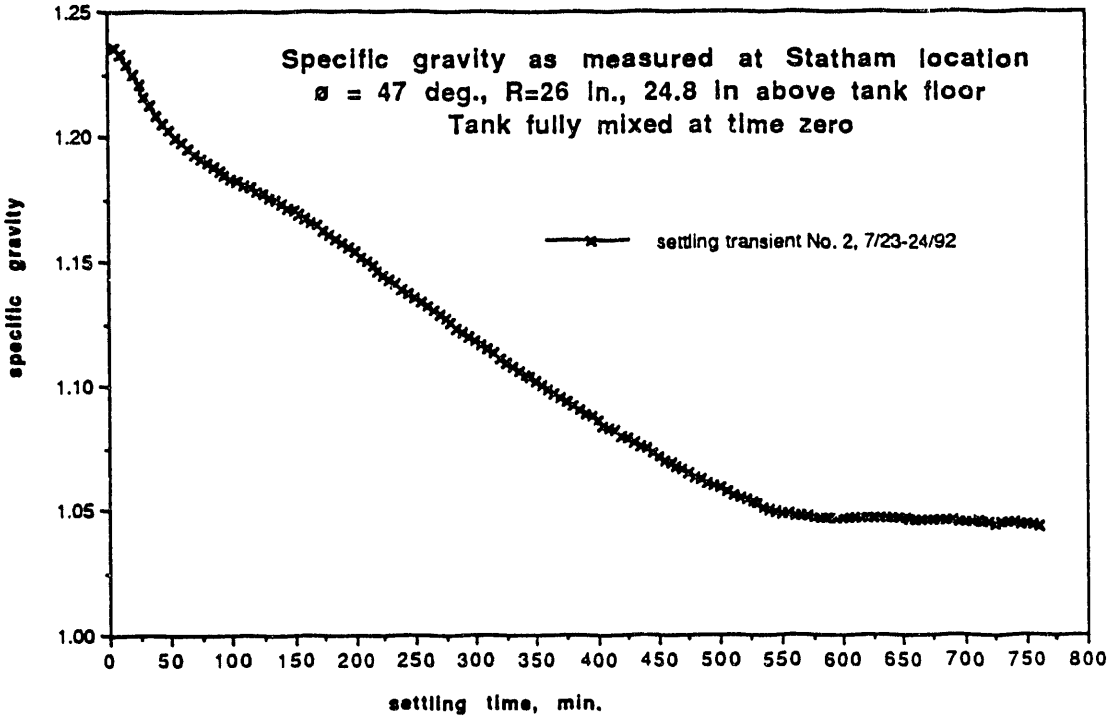

FIGURE B.39. Density History During Settling Prior to OPLS/1

TABLE B.17. Slurry Interface Heights Measured in OPLS/2

Elapsed Time hr:min	Interface Depth Below the Surface
0:00	19½
0:24	@ surface

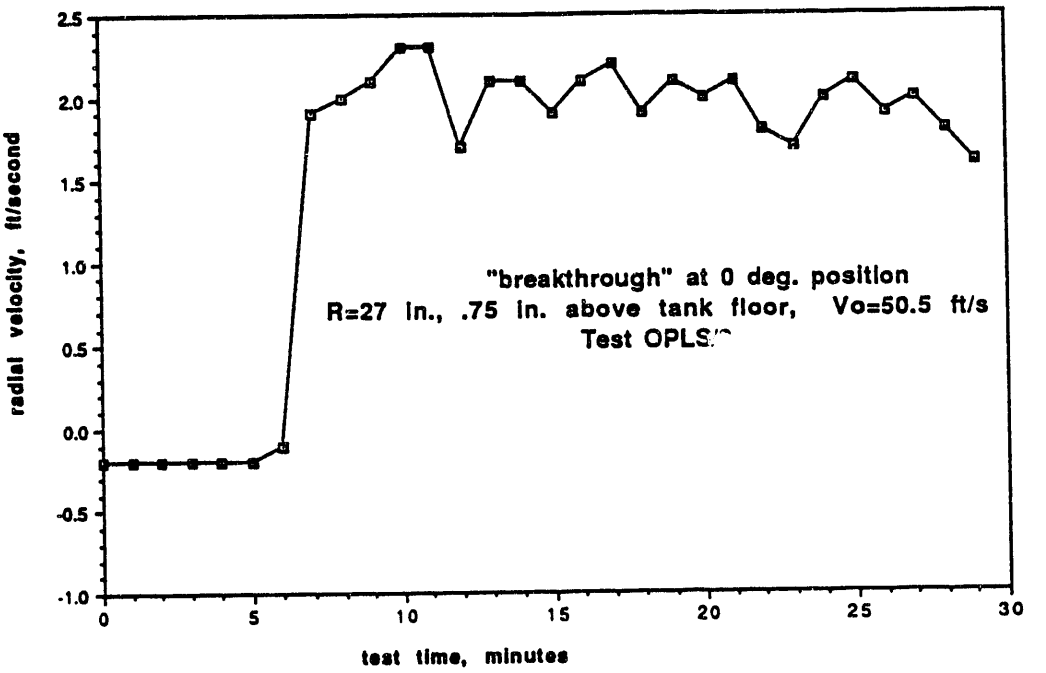

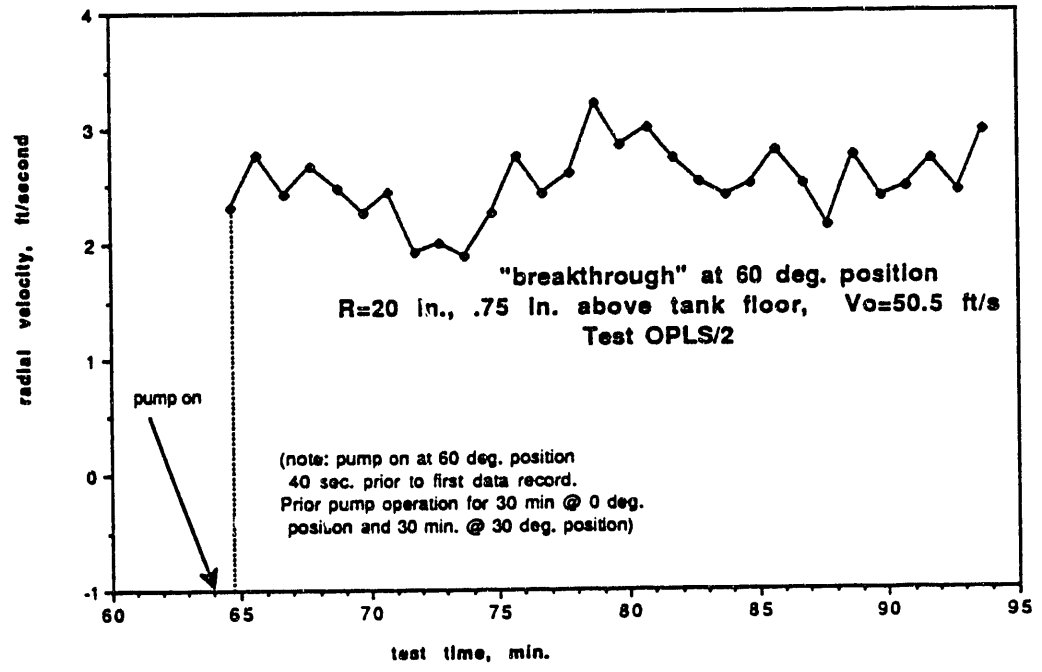

FIGURE B.40. Breakthrough Times at Buried Probe Positions for OPLS/2

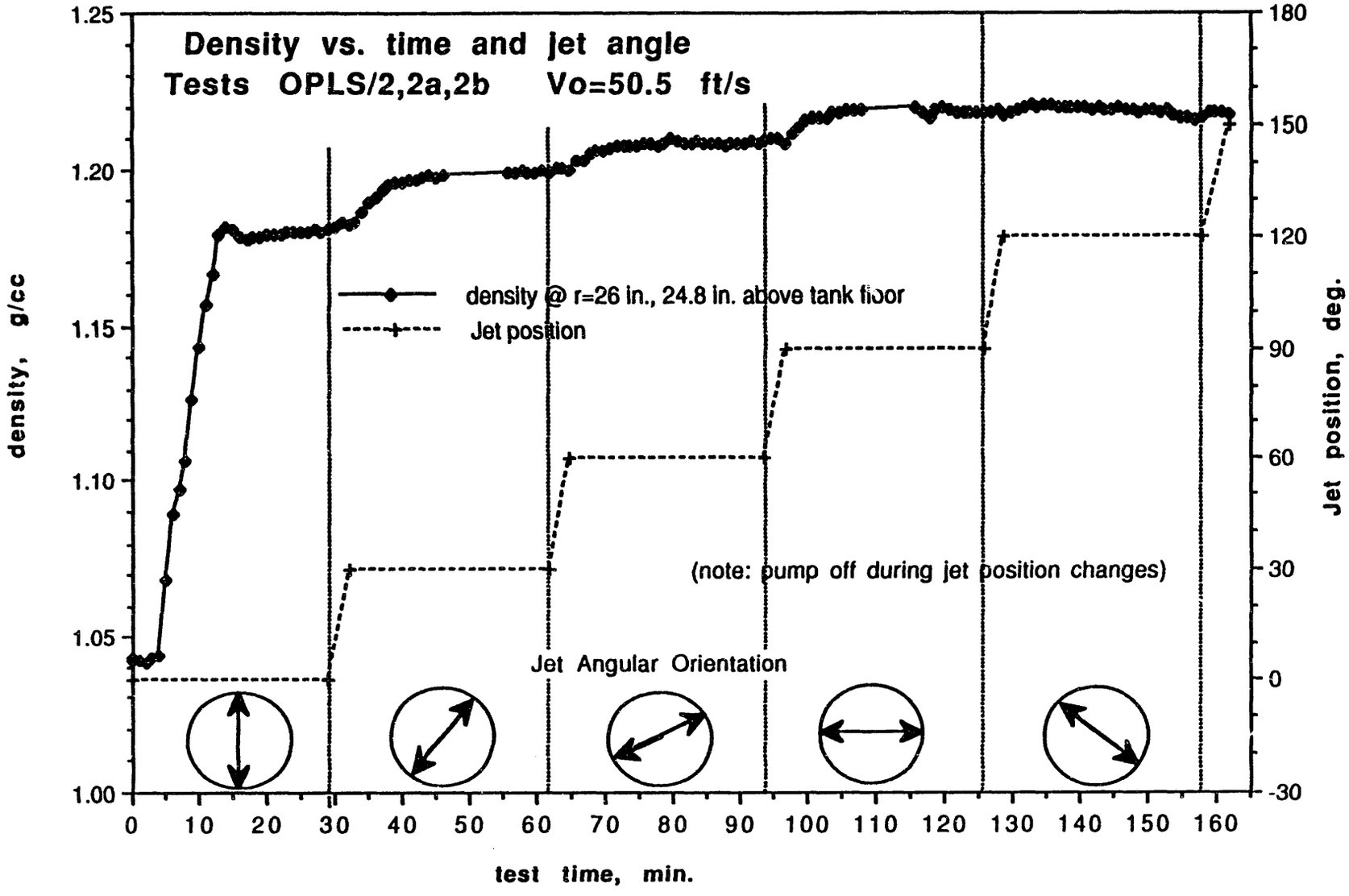

FIGURE B.41. Jet Position and Density History for OPLS/2

TABLE B.18. Discrete Concentration Data for OPLS/2

Elapsed Time, min	Mixing Pump Orientation, degree	Probe Elevation from Tank Bottom, in.				Probe Location
		28.33	23.33	13.33	3.33	
		Density, g/cm^3				
~0	0	1.038	1.039	1.035	1.650	north
54	30	1.188	1.211	1.195	1.192	north
112	90	1.206	1.227	1.220	1.220	north
~0	0	1.029	1.032	1.090	1.664	west
46	30	1.186	1.188	1.199	1.448	west
105	90	1.208	1.194	1.201	1.204	west
154	120	1.204	1.209	1.225	1.215	

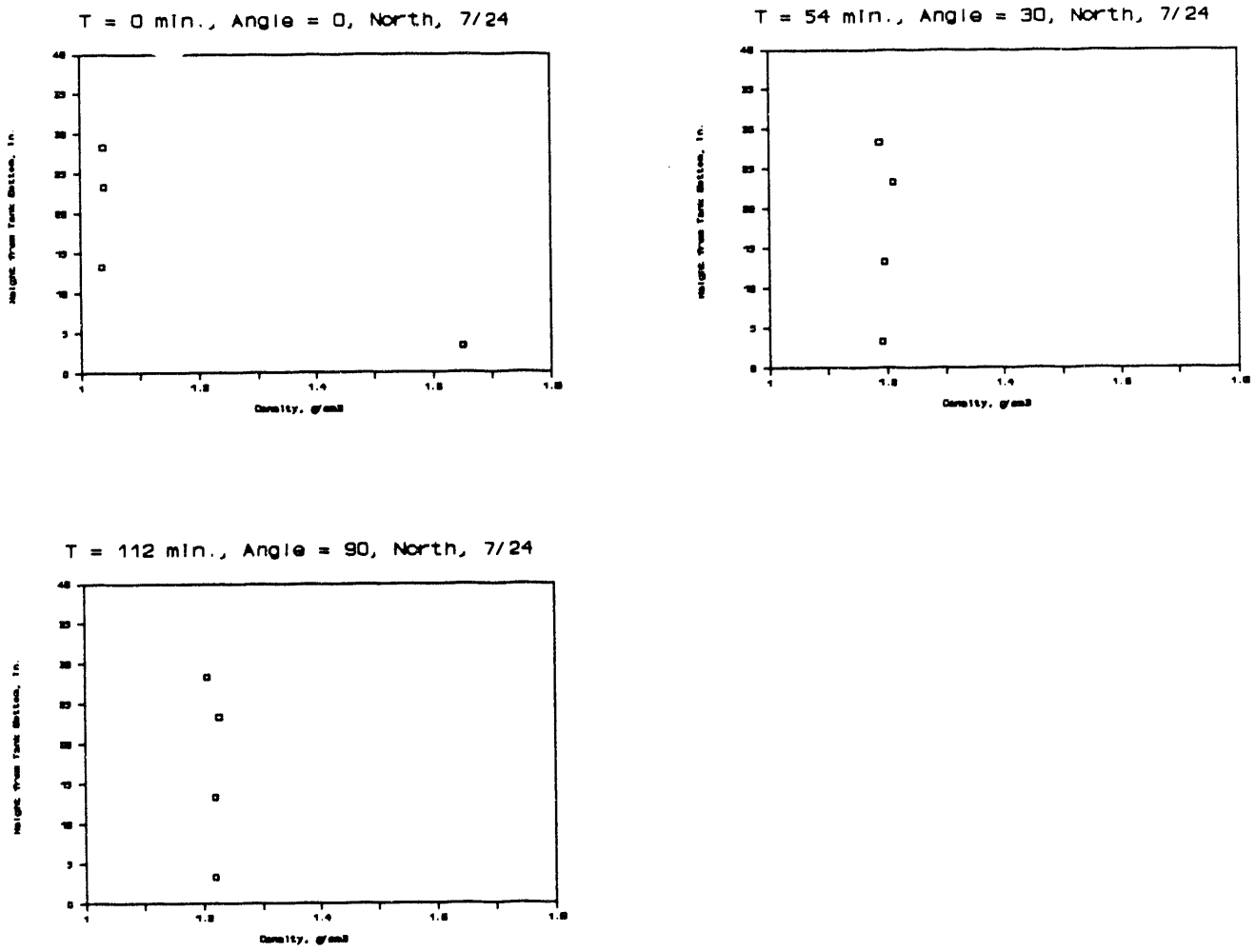

FIGURE B.42. Discrete Concentration Data for OPLS/2

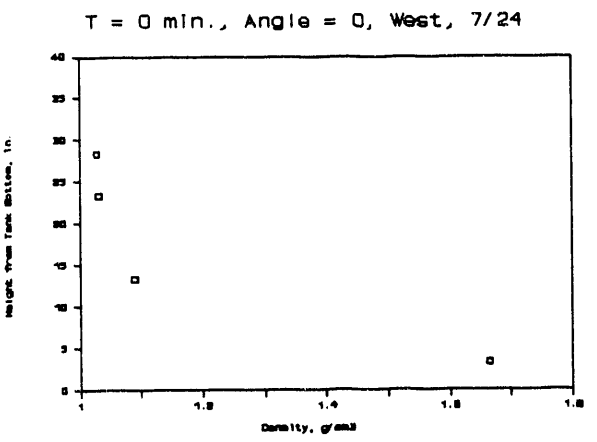

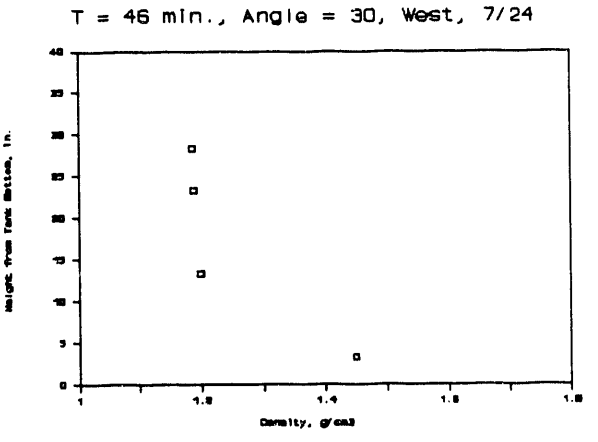

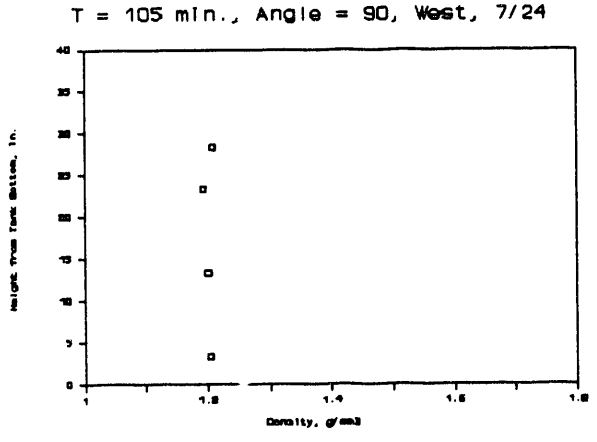

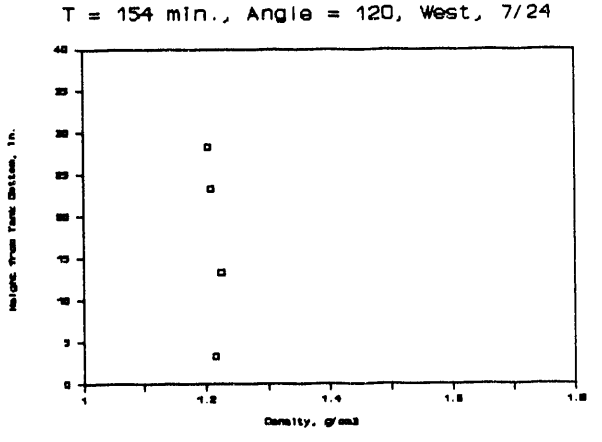

FIGURE B.42. (contd)

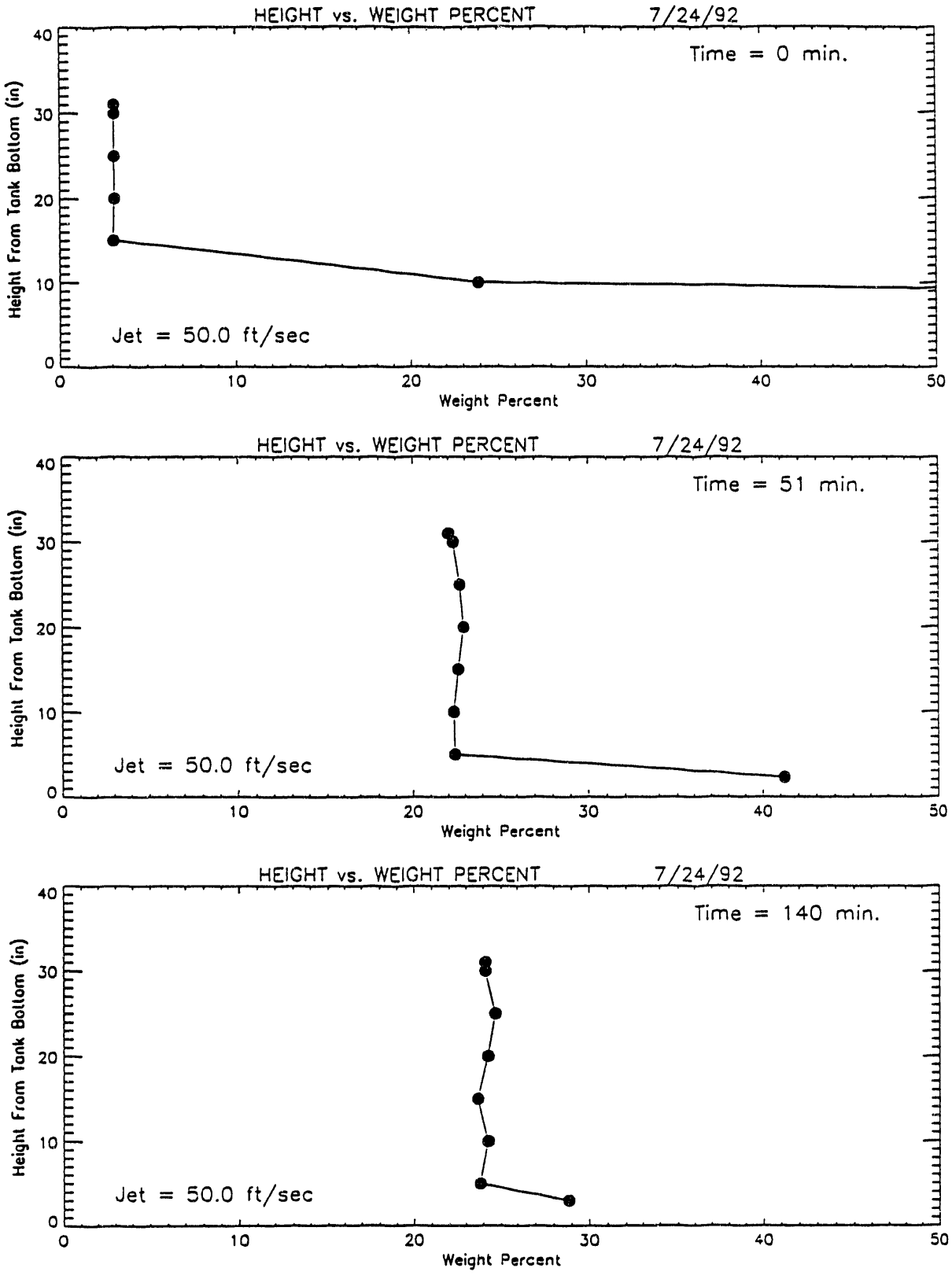

FIGURE B.43. Height Versus Weight Data for OPLS/2

APPENDIX C

UNCERTAINTY OF INSTRUMENTATION AND DATA REDUCTION RESULTS

APPENDIX C

UNCERTAINTY OF INSTRUMENTATION AND DATA REDUCTION RESULTS

Section C.1 describes the uncertainty related to each set of final data reduced from the initial experimental data. The uncertainty associated with instrumentation is included in the discussions of final data uncertainty.

C.1 UNCERTAINTY RESULTS

Each subsection discusses the uncertainty of a single reduced parameter. The uncertainties of the experimental measurements associated with a reduced parameter are included in the discussion. All of the experimental data was recorded by the data acquisition system (DAS), which used an OMEGA, 12-byte A/D converter analog input card, model WB-FA1-M2-16. The uncertainty resulting from the card was $\pm 2.4 \times 10^{-4}$ of the recorded value.

Nozzle Exit Velocity

The nozzle exit velocity was determined by measuring the flow rate to the jet mixer pump and accounting for the cross-sectional area of the nozzles with a fixed diameter of 0.224 in. The flow rate was measured using a Krohne, Delta Flux - F2000, electromagnetic flowmeter. The specified accuracy of the flow meter's current output was ±1% of the reading.

The flowmeter was calibrated using the 1/12-scale system's equipment. The instrumentation used for the calibration included a Fairbanks load cell with a ±1-lb uncertainty and the DAS's clock. Because of the calibration method, the timing was assumed to have an uncertainty of ±1 sec. The uncertainty in the calculated nozzle exit velocity was the larger of 2.5 percent or .25 ft/s.

Specific Gravity of Supernate Measured with Statham Densitometer

The specific gravity of the upper supernatent liquid was measured using a Statham MD-3018 densitometer. The specified accuracy of the densitometer's output current was ±0.25% of the span (4 to 20 ma). The resistors used by the

DAS to determine the signal current had a specified accuracy of ±0.01% of the specified resistance (approximately 25 ohms). The calculated value of the specific gravity had an uncertainty of ±0.04 S.G.

Specific Gravity Measured via Syringe Sampling

A 10-ml syringe was used to extract samples from the tank at various depths. The samples were weighed using a Mettler Electronic Balance, PC-4400. The accuracy listed by the Westinghouse Standards Laboratory was ±1.6 mg; however, measurements were made to an accuracy of ±0.01 g. The uncertainty of the measured sample volumes was ±0.05 ml. The uncertainty of the measured specific gravity was ±0.006 S.G.

Jet Velocities Using Stagnation Tubes

Jet velocities in water were measured using 3/16-in. stagnation tubes. Honeywell transducers were used to measure the dynamic pressures of the stagnation tubes. The accuracy of the transducers given by the Westinghouse Standards Laboratory was ±0.5% of span (4 to 20 ma). An initial zero reading of the transducers was taken prior to each test. This zero reading was used in the transfer equation for calculating the jet velocities.

The transfer function did not account for density differences in the fluid caused by temperature differences. However, the temperature gradients within the tank were measured using ANSI standard thermocouples with a specified uncertainty of ±2°F. Using the maximum temperature gradient measured in the tank along with the thermocouple uncertainty resulted in an uncertainty of ±0.001 slugs/ft^3 in the water's density. The maximum estimated uncertainty in the calculated velocities was 0.23 ft/s.

Velocity Measured with Electromagnetic Flowmeter

Marsh-McBirney, Model 2000, electromagnetic flowmeters were used to measure jet velocities in both water and simulant. The specified accuracy of the flowmeters was ±2 percent of reading plus the zero stability. The zero stability was listed at ±0.05 ft/s.

Another factor that may have added additional uncertainty to the velocity measurements was the probe configuration. The probe's front is a

half sphere with a 1.5-in. dia. The back of the probe is a truncated cone with a 1.5-in.-dia. base tapering to a 0.625-in.-dia. top. The height of the cone is approximately 1.5 in. This obstructive shape can add additional uncertainty in areas where the 1.5-in.-wide face of the probe may be exposed to high velocity gradients. It is for this reason that velocity measurements were not made with the EM meters within 16 in. of the nozzle exits.

Probe Position

The probe positions are considered to be the data with the greatest uncertainty. The uncertainty in position is related to two major factors. All position measurements were taken with respect to the tank bottom and the location of the nozzles. To take relative measurements with the tank full of fluid required reference points to be transferred to positions above the tank. The error associated with the positioning of the reference points was a major source of uncertainty.

The second major source of uncertainty came from the equipment used to hold the probes in position. The vertical shafts of the probes were fixed into position using horizontal steel beams placed across the top of the tank and clamps. After the probes were secured in the clamps, their vertical alignment was adjusted with the aid of an 8-in. torpedo level. Because of the play in the clamps, the adjustment of the vertical alignment could be made without loosening the clamps. With a probe at the nozzle centerline height, a 0.7-degree offset of the probe's vertical alignment would result in a 0.5-in. change in horizontal position.

The uncertainty associated with probe location was $\pm$0.25 in. in vertical position and $\pm$0.75 in. in horizontal position.

Shear Strength

The shear strength was measured using a ⅛-in., four-blade shear vane with a HAAKE VR-100 viscometer coupled to an M-500 measuring head. Based on technical literature and values of the measured shear strength (close to instrument mid range), the uncertainty of the shear strength measurements is estimated at 20 percent. At the higher and lower ends of the instrument's

range, the estimate of uncertainty would likely be greater than the 20 percent estimated at mid range.

Viscosity

Slurry viscosities were measured with Canon-Fenske type capillary viscometers. The specified uncertainties for these viscometers are 0.5 percent or less for "transparent" fluids. It is unknown whether the addition of particles in the fluid increases the uncertainty. Because of the small size of the particles, they may add no additional uncertainty. Multiple measurements were made for each viscosity sample with negligible differences.

C.2 TABULATED UNCERTAINTIES OF REPORTED PARAMETERS

This information is illustrated in Table C.1.

TABLE C.1. Uncertainties of Final Data

Parameter	Uncertainty
Nozzle exit velocity	Larger of ±2.5% or 0.25 ft/s
Specific gravity (Statham densitometer)	±0.04 S.G.
Specific gravity (syringe sampling)	±0.006 S.G.
Jet velocity (stagnation tubes)	±0.23 ft/s
Jet velocity (electromagnetic flowmeter)	±0.05 ft/s
Probe position (horizontal plane)	±0.25 in.
Shear strength	±20%
Viscosity	Approximately ±0.5%

APPENDIX D

SIMULANT PARTICLE SIZE DISTRIBUTIONS PERTAINING TO MIXING EFFICIENCY

APPENDIX D

SIMULANT PARTICLE SIZE DISTRIBUTIONS PERTAINING TO MIXING EFFICIENCY

The solid phase of the simulant consisted of a range of particle sizes. Density measurements taken during testing yielded information about the percent of solid material being swept from the tank bottom and suspended in the supernate; however, the size distribution of the particles is indeterminate from these measurements. An important factor to be considered in the mixing of a slurry is the size distribution of particles being suspended or mobilized compared to the bulk slurry's size distribution.

This appendix contains the size distribution data generated from various mixture samples. The size distribution of suspended particulate related to mixing velocity is also discussed.

D.1 SAMPLE DESCRIPTIONS

Eleven samples were taken for the purpose of particle size distribution analysis. Descriptions of the samples taken follow.

Sample	Description
Initial 1	Sample taken from sack of dry particulate prior to any mixing or testing.
Initial 2	Same as Initial 1 except taken from a separate sack.
Initial 3	Same as Initial 1 except taken from a third sack.
Sample 1	Sample taken near tank center approximately 3 in. below liquid surface at the completion of test MVLS/1. Tank contained low viscosity simulant and had been mixing for 8.5 hrs at a nozzle exit velocity of 25 ft/s. During the 8.5 hrs of mixing, the jets had remained stationary.

Sample	Description
Sample 2	Same as Sample 2 except sample taken near tank wall 3 in. below the liquid surface just above the point at which the jet impacted the tank wall.
Sample 3	Sample taken near tank wall approximately 3 in. below liquid surface, above the point were the jet impacted the tank wall, after the completion of test MVLS/2. Tank contained low viscosity simulant and had been mixing for 8.5 h at a nozzle exit velocity of 25 ft/s followed by 2 h at 50 ft/s with the jets held stationary. This mixing was followed by 50 min of mixing with the jets rotating and an exit velocity of 80 ft/s.
Sample 4	Same as Sample 3 except sample taken near tank center 3 in. below the liquid surface.
Sample 7	Sample taken near tank wall approximately 3 in. below liquid surface, above the point were the jet impacted the tank wall, after the completion of test OPLS/2. Tank contained low viscosity simulant and had been mixing for 3 h at a nozzle exit velocity of 50 ft/s. Mixing was performed by holding the jet stationary for 30 min and then rotating the nozzles 30 degrees. Nozzle rotations were performed with all flow stopped. The total flow pause time was 2 min.
Sample 8	Same as Sample 7 except sample taken near tank center 3 in. below the liquid surface.
Sample 9	Sample taken from settled sludge after supernate had been decanted off at the completion of the simulant tests.
Sample 10	Same as Sample 9.

NOTE: Samples 5 and 6 were not taken for the purpose of sizing analysis. All samples were analyzed for both probability volume and number densities.

D.2 RESULTS

The mean diameter and standard deviation for both the number and volume densities are presented in Table D.1 for each sample. Plots of the results are shown in Figures D.1 to D.11. Each figure contains plots of the number and volume density data for its corresponding sample.

TABLE D.1. Results of Particle Size Analyses

Sample	Velocity (ft/s)	Volume Density		Number Density	
		Mean (μm)	S.D. (μm)	Mean, (μm)	S.D. (μm)
Initial 1	--	13.47	11.09	1.25	1.24
Initial 2	--	10.26	8.80	1.25	1.17
Initial 3	--	7.76	5.82	1.26	1.11
Sample 1	25	14.64	14.98	1.73	1.71
Sample 2	25	17.44	23.22	1.90	1.82
Sample 3	80	17.59	13.90	2.03	2.15
Sample 4	80	16.53	10.91	1.90	2.01
Sample 7	50	11.55	9.29	1.35	1.25
Sample 8	50	10.99	7.47	1.41	1.27
Sample 9	--	27.13	19.08	2.14	2.59
Sample 10	--	17.20	20.85	1.90	1.82

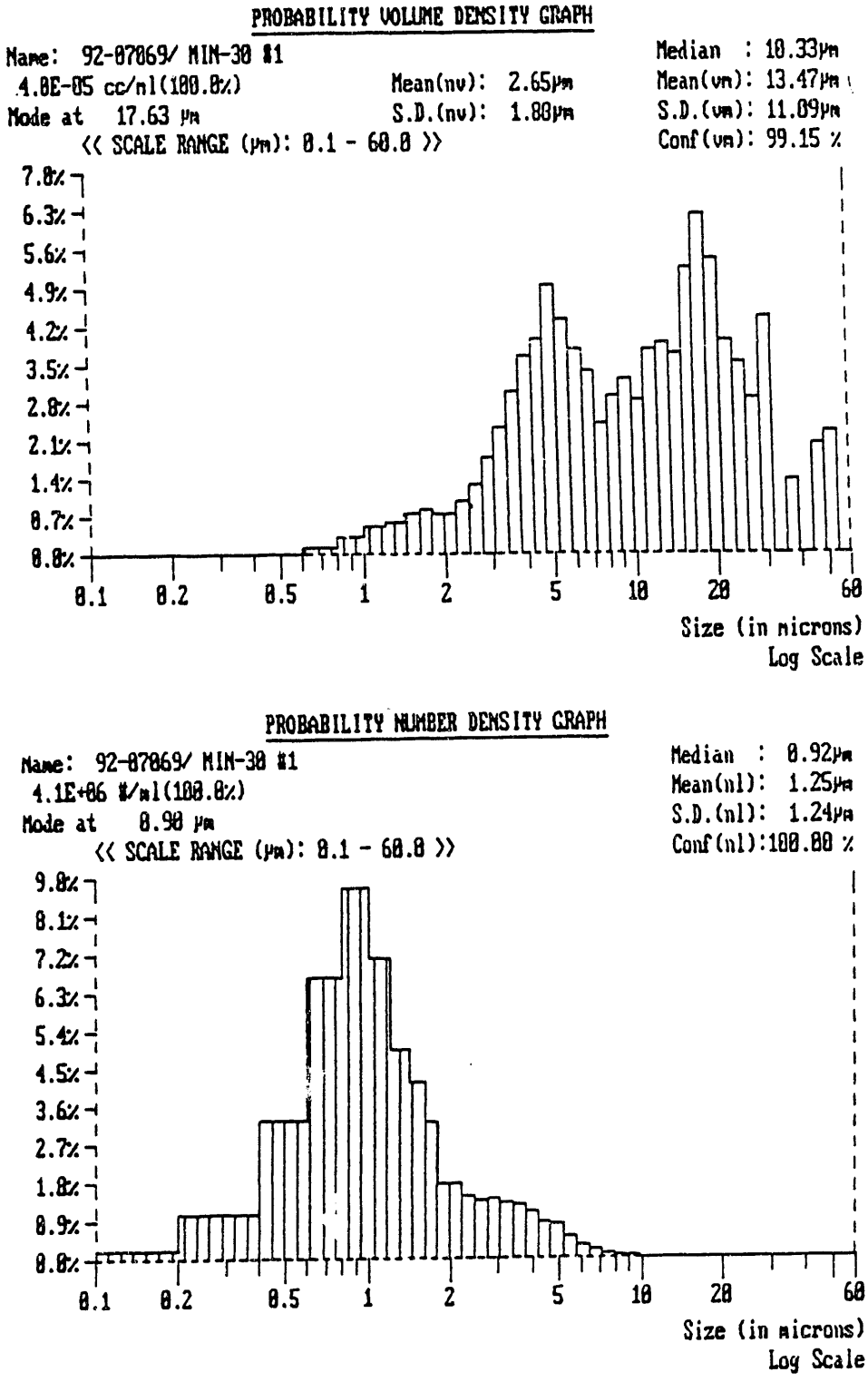

FIGURE D.1. Particle Size Distribution Plots for Initial 1

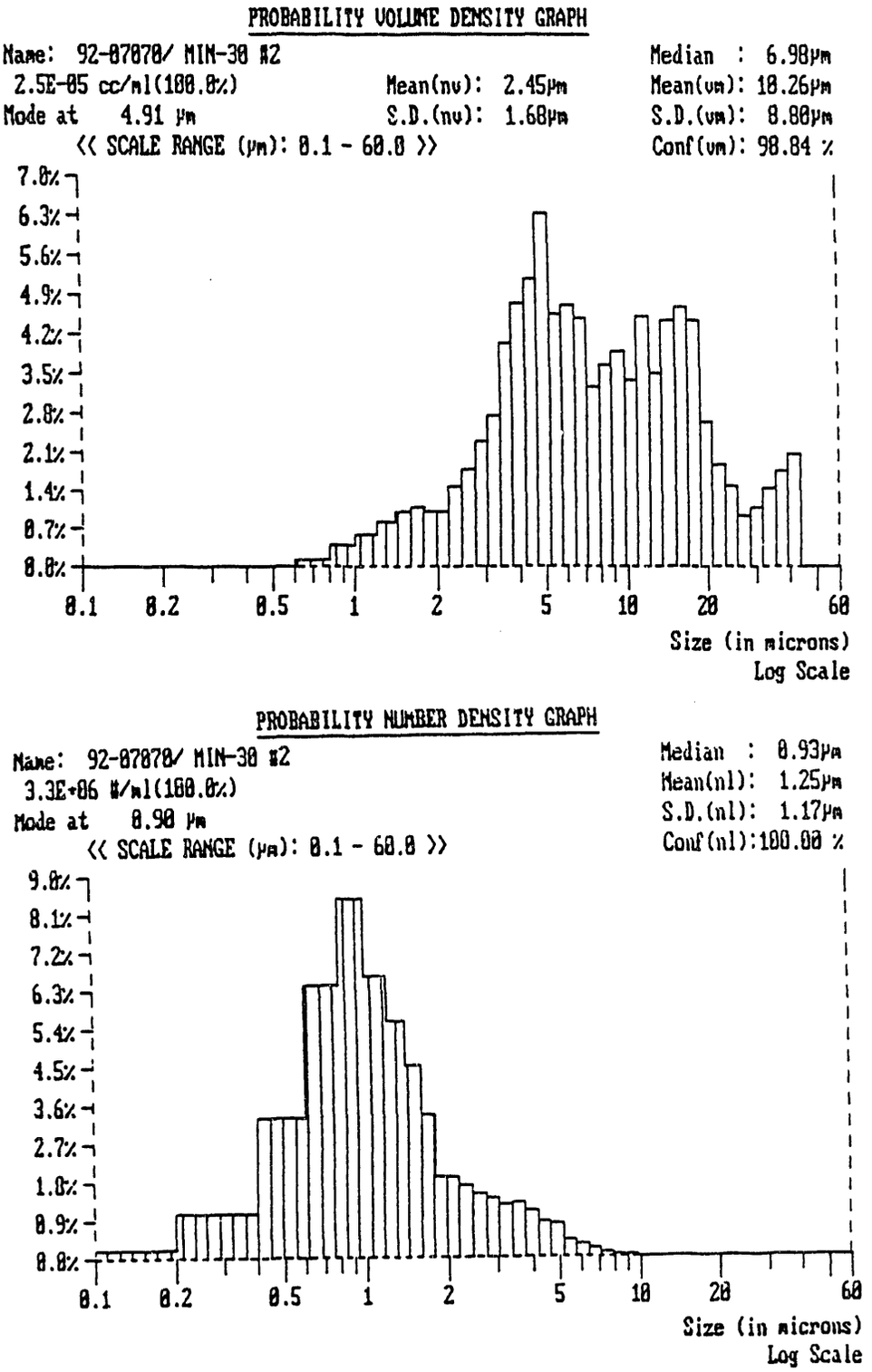

FIGURE D.2. Particle Size Distribution Plots for Initial 2

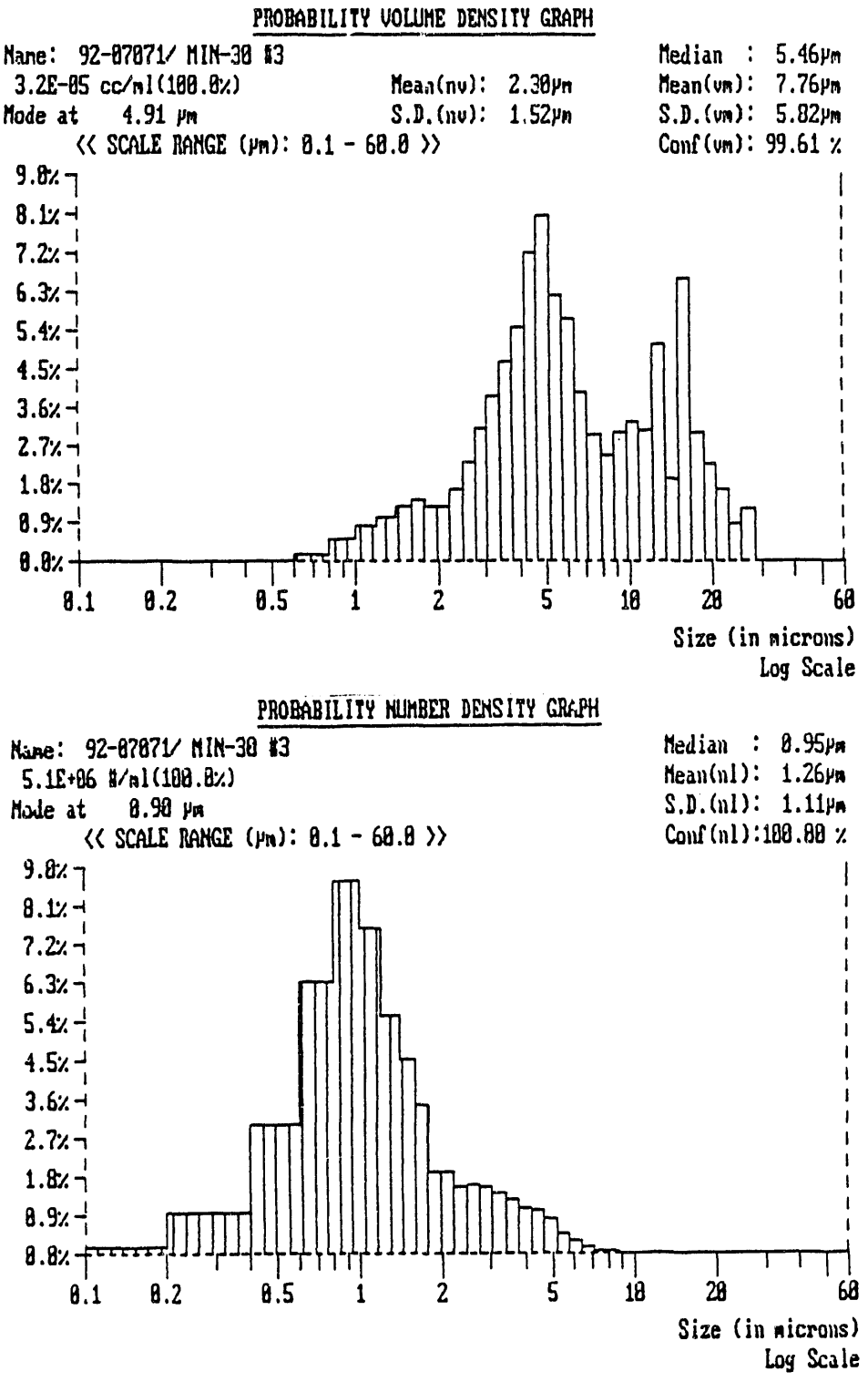

FIGURE D.3. Particle Size Distribution Plots for Initial 3

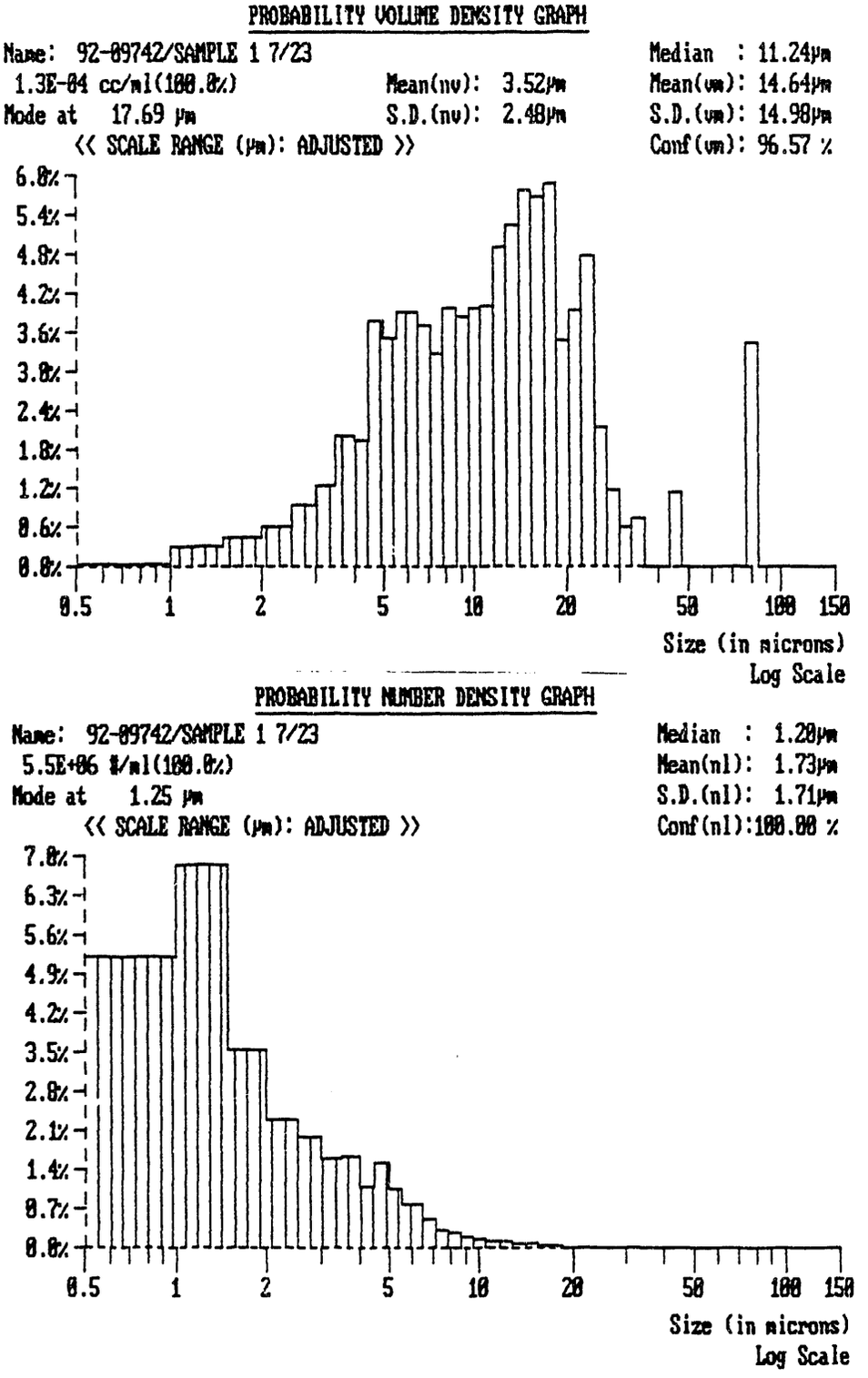

FIGURE D.4. Particle Size Distribution Plots for Sample 1

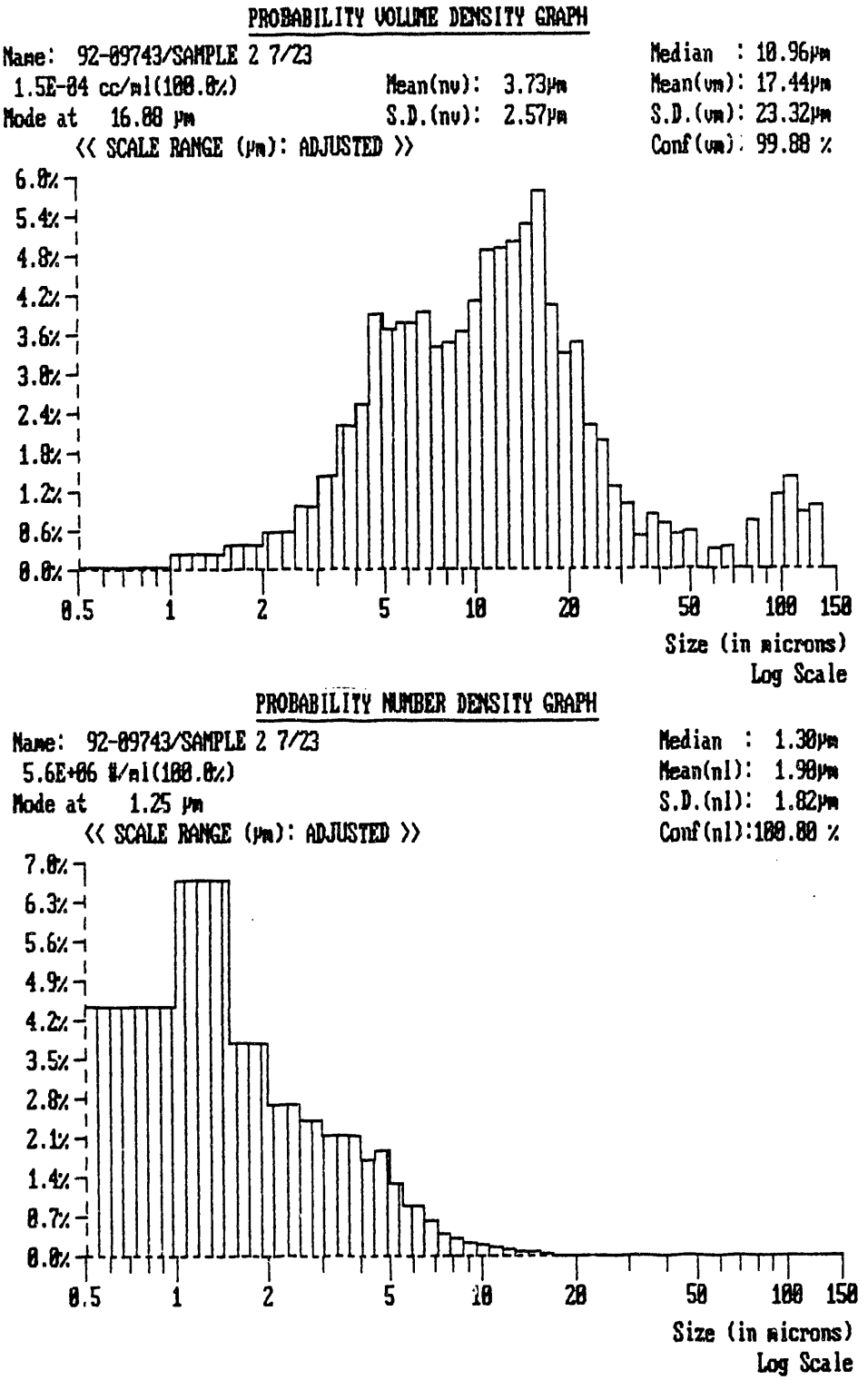

FIGURE D.5. Particle Size Distribution Plots for Sample 2

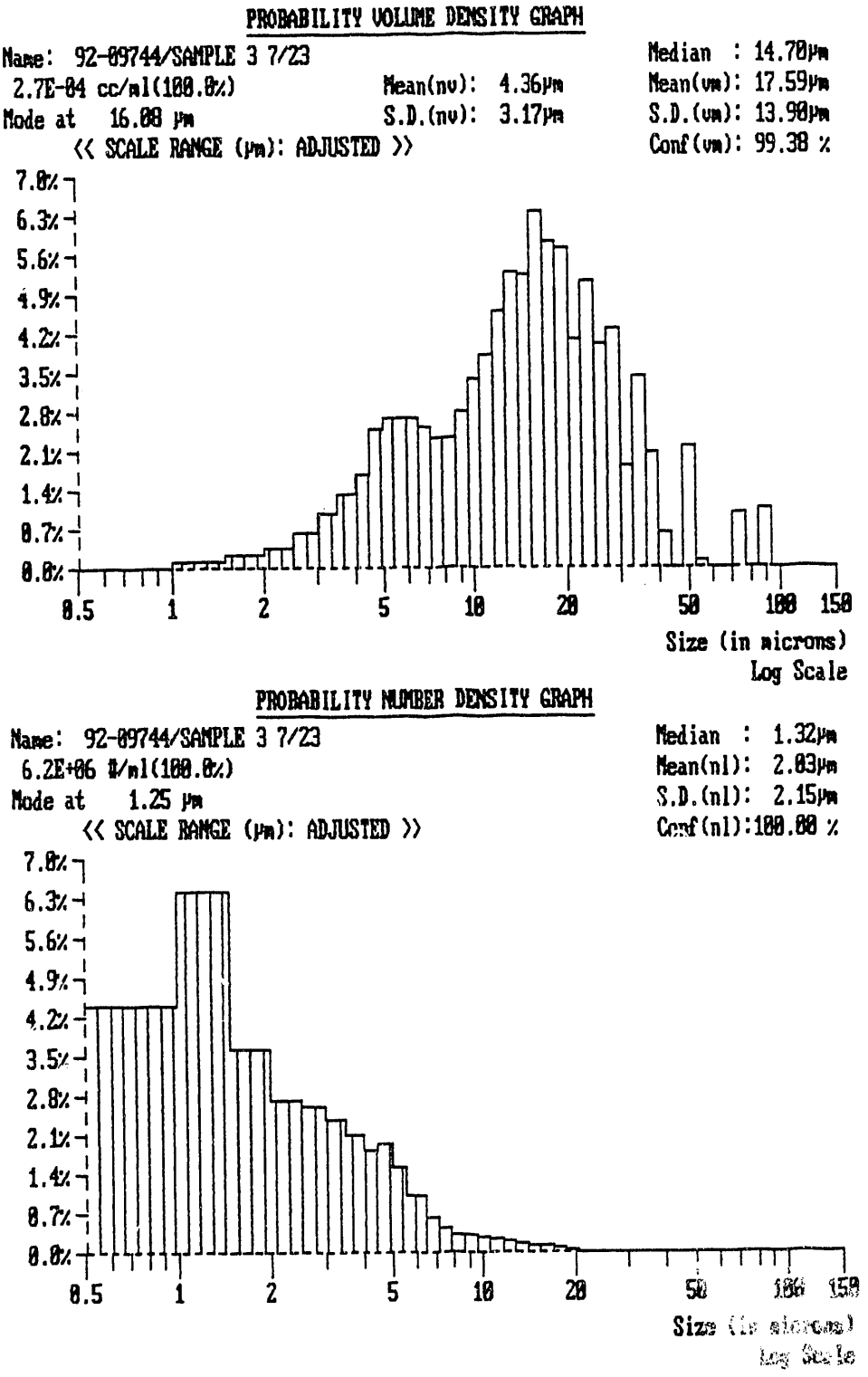

FIGURE D.6. Particle Size Distribution Plots for Sample 3

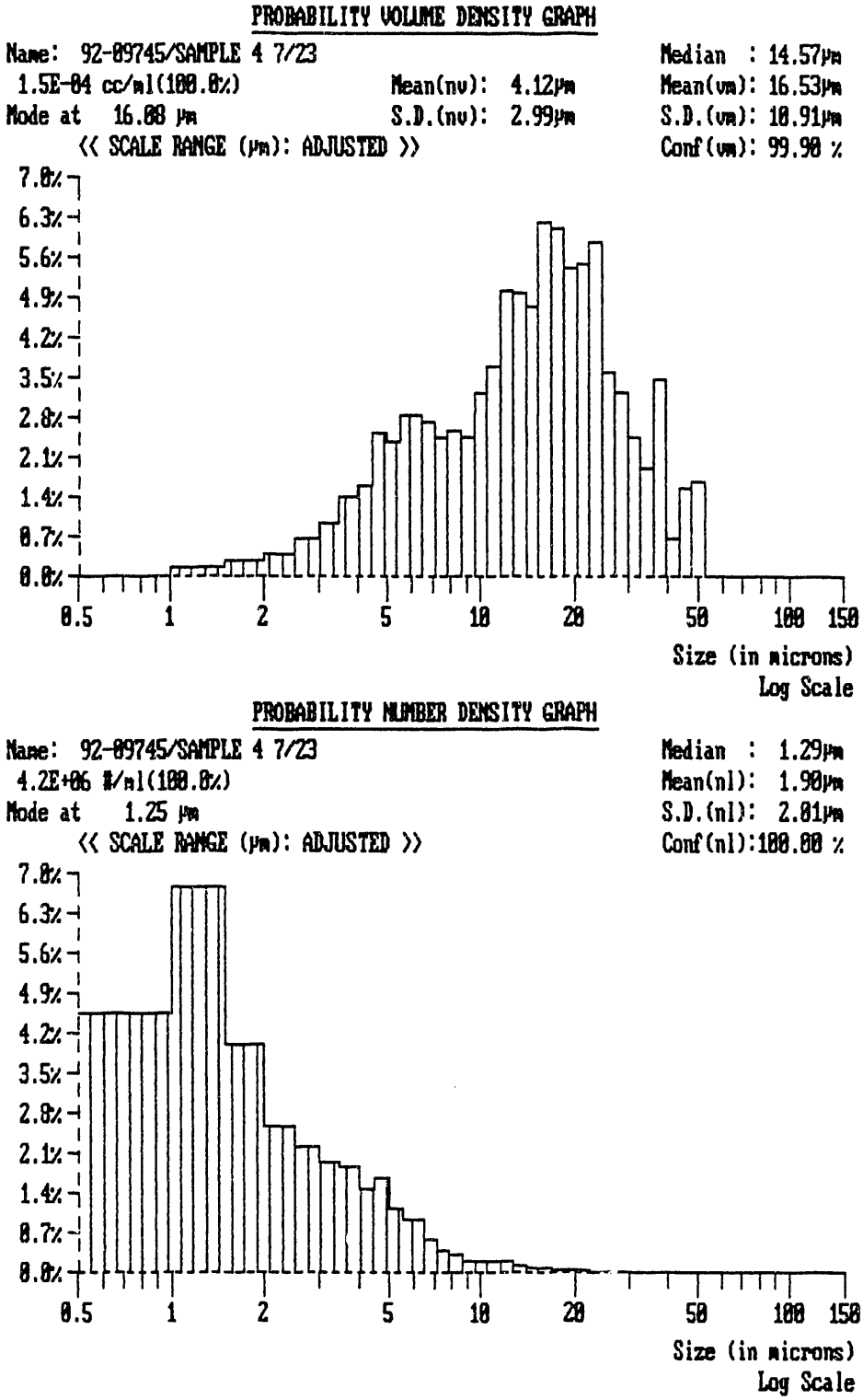

FIGURE D.7. Particle Size Distribution Plots for Sample 4

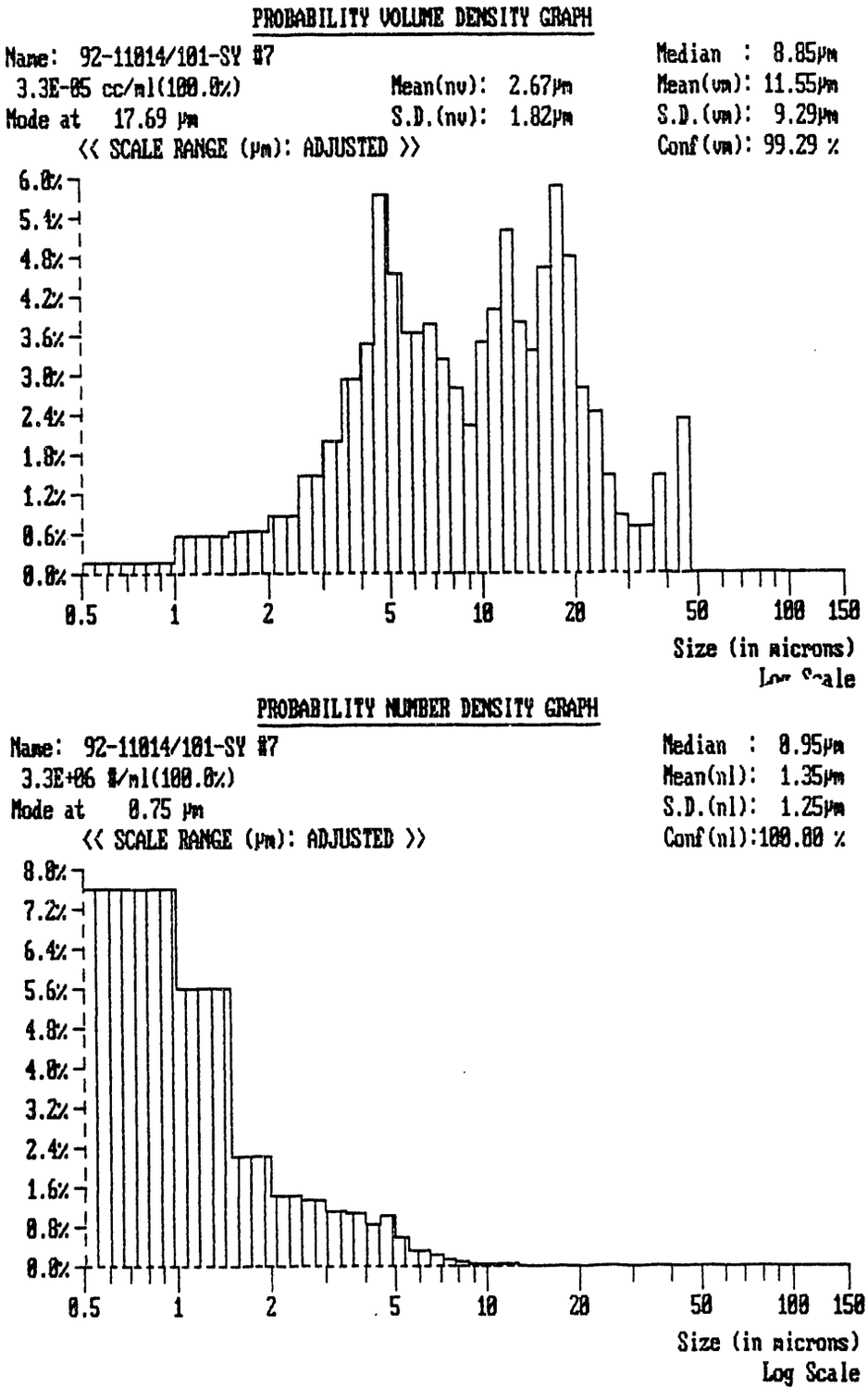

FIGURE D.8. Particle Size Distribution Plots for Sample 7

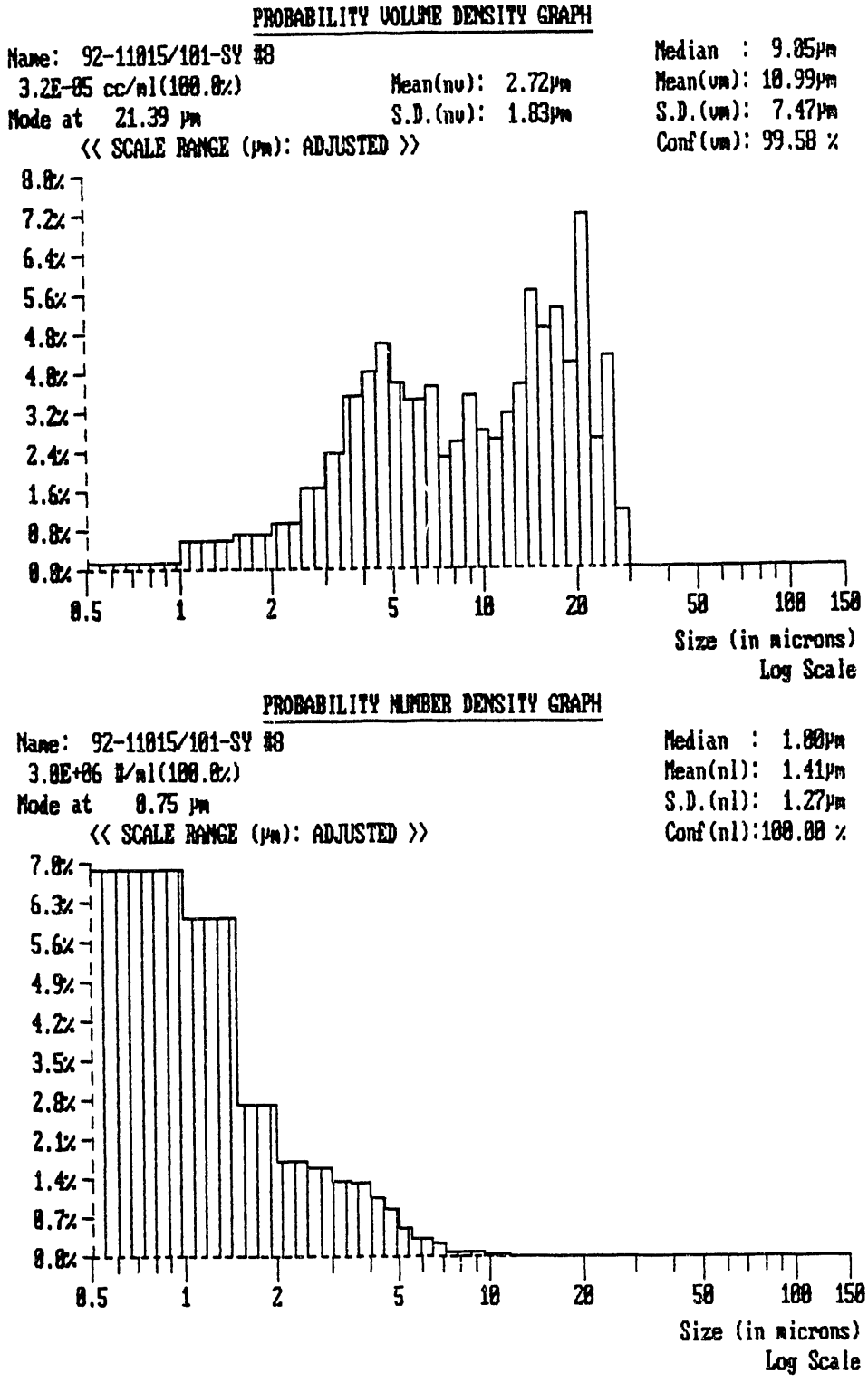

FIGURE D.9. Particle Size Distribution Plots for Sample 8

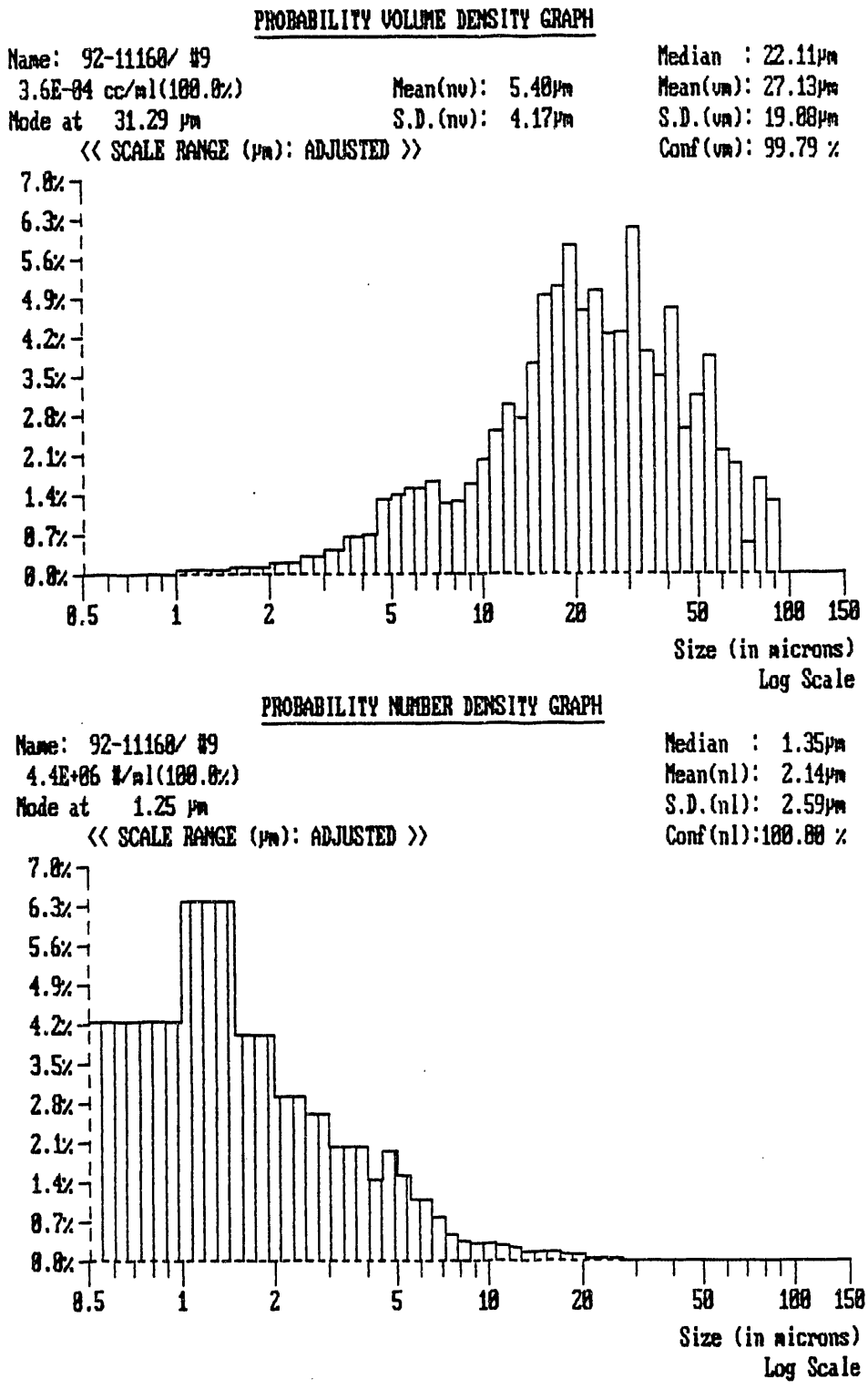

FIGURE D.10. Particle Size Distribution Plots for Sample 9

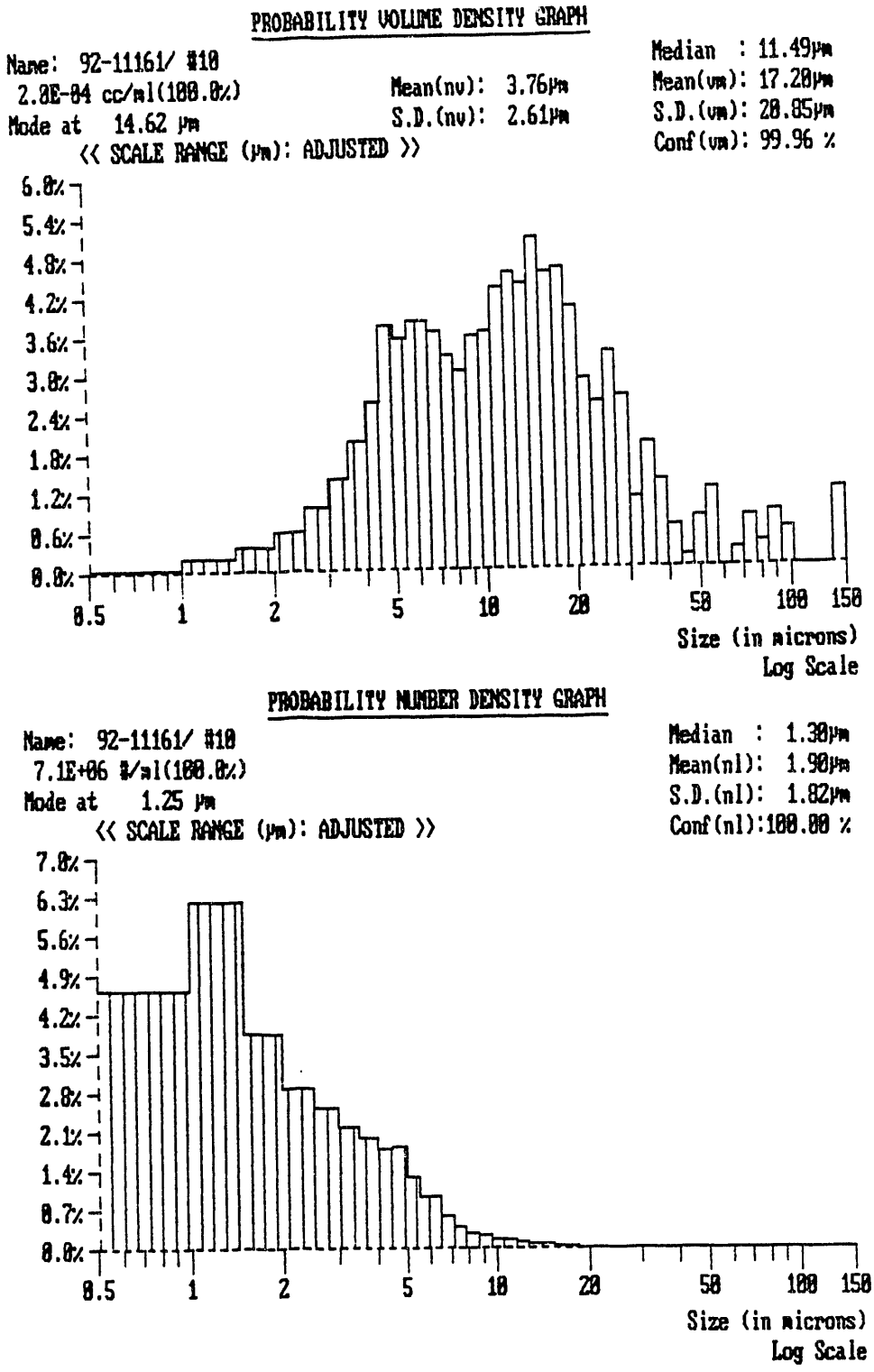

FIGURE D.11. Particle Size Distribution Plots for Sample 10

D.3 CONCLUSIONS

Looking at the results for Samples 1 through 4, 7, and 8, it appears there was no clear relationship between the mixing velocity and the mean particle size suspended. The mean diameter for volume density was higher for the wall samples while the wall number density results yielded higher diameters for two of the three velocities sampled. The limited samples and large size distributions make it difficult to draw any firm conclusions about size variation between the tank center and wall.

The mean diameters of all of the samples are larger than those of the three initial samples. Samples 1 through 4 and 7 through 10 were taken during or after the low viscosity simulant tests. At the completion of testing with the high viscosity simulant, the supernate was decanted and disposed. It appears the decanting process removed many of the smallest size particles thus resulting in a higher mean particle diameter. Prior to the taking of Samples 9 and 10 the supernate was again decanted. The effects of this decanting process are again observed in the increased mean diameter particle sizes for Samples 9 and 10.

Another factor possibly accounting for the larger mean diameters measured is sample contamination. In the initial three samples taken prior to the mixing of the simulant, there were no particles larger than 60 μm. Some of the plotted data for samples taken during testing show readings for particles as large as 120 μm. Surface samples were more likely to be affected by contamination caused by dust and debris that fell or settled into the tank. Some of the fine debris that fell into the tank was buoyant and floated on the surface making it more likely to be collected by surface sampling. Foreign particulate was also introduced to the tank from old simulant residue present in the system piping. Another possible factor contributing to the increase in the mean diameter seen in Samples 9 and 10 was the recrystallizing of sugar in the sludge after the supernate had been decanted.

The variation that exists between mean diameters may not be as influenced by velocity as by mixing method. The lower mean diameters of the 50 ft/s test might be a result of the various mixing methods represented. The 25 ft/s test had been running for a considerable amount of time with the jets

stationary. The jets had swept the floor clean and scoured out a channel. Its possible that the larger particles suspended had been sloughed down into the jet from sludge built up at the edges of the channel. The 80 ft/s test mixed the tank by continually rotating the jet. The larger size particles may have been suspended because of the higher velocity.

In the case of the 50 ft/s test, the jet was held stationary for 30 min and then rotated to a new position. These step changes in jet position may have resulted in the larger particles being moved around the tank without a mechanism to suspend them. The jet may never have been held stationary long enough for a clear channel to be swept out allowing particles to be sloughed into the jet. It may also be that the mean particle diameter was time dependent for each jet position. When the nozzles were first repositioned at a new location, the jet may have suspended the larger particles only to have them settle to the bottom during the course of the 30 min residence time at a single jet orientation.

The particle sizing data strongly suggests that the mixing jets were suspending a particle distribution similar to that of the bulk solids. The particle size distribution did not appear to vary significantly for the velocity range sampled. It should also be noted that both the mixing velocity and mixing method were altered among the sampled tests.

APPENDIX E

NOZZLE DEFORMITY

APPENDIX E

NOZZLE DEFORMITY

After all of the testing was completed, the mixing pump nozzles were removed and inspected. Both nozzles showed visible signs of erosion. Each nozzle barrel was eroded symmetrically except at the nozzle exit. The erosion resulted in the nozzles being nonuniformly tapered outward around the circumference of the nozzle exits. At the nozzle exits, axes of maximum erosion were clearly defined.

Post tests were conducted in fresh water to obtain velocity profiles for the eroded nozzles. These profiles were taken for comparison against the profiles produced by the original nozzle geometry. This appendix contains, pump run time histories for simulant tests, measurements of nozzle erosion, and post-test velocity profiles.

E.1 BACKGROUND

After the fresh water flow visualization tests and the initial system tests, the mixer pump jet nozzles were replaced with new nozzles. The new nozzles had diameters of 0.224 in. and were used throughout the model validation and operation tests. At the completion of the fresh water tests, the nozzles' diameters were measured as 0.224 in. and no apparent wear was visible at the exits.

The high viscosity simulant was mixed and pumped into the 1/12-scale tank and then the simulant was mixed in the tank using the mixing jets. The pump run time was not recorded for this mixing. The first simulant test, MVS/1, consisted of 3.5 h run time at a nozzle exit velocity of 25 ft/s and approximately 0.5 h at 53 ft/s. The nozzle diameters were again measured at 0.224 in. The remaining high viscosity simulant tests were conducted before another measurement of the nozzle diameters was taken. Figure E.1 shows a plot of the nominal nozzle exit velocity versus pump run time for the tests performed after MVS/1 until the next nozzle diameter measurement. The

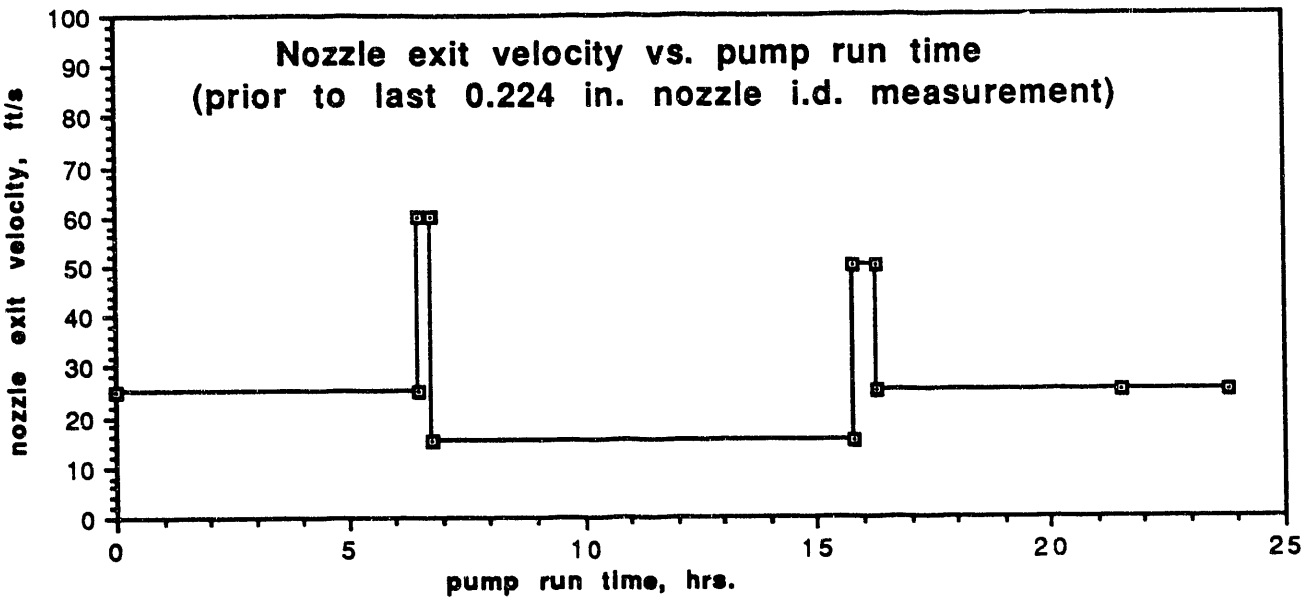

FIGURE E.1. Plot of Nozzle Exit Velocity Versus Pump Run Time for Tests MVS/2 through MVS/6

measurement at the end of the high viscosity simulant tests (after MVS/6) yielded a diameter of 0.224 in. No evidence of erosion was visible.

The nozzle diameter was not measured again until all testing was finished. Figure E.2 shows a plot of the nominal nozzle exit velocity verses pump run time for the tests performed after MVS/6. Prior to the final observation tests (after OPLS/2, MVLS/3, and MVLS/4) there was a considerable amount of high velocity mixing conducted without run times being recorded. These velocities ranged from 50 to 80 ft/s and the run time is estimated to be between 3 to 6 h. It is difficult to estimate these unrecorded run times.

E.2 EROSION MEASUREMENTS

It was difficult to determine the actual cross-sectional area of the eroded nozzles because of the nature of the erosion. The eroded barrels were out of round and the cross section varied along the nozzles' lengths. The nozzle barrels were eroded fairly uniform in the radial direction and still looked to be round. The barrel diameters varied some in the axial direction. The minimum barrel diameter was measured using a hole gage. Two measurements

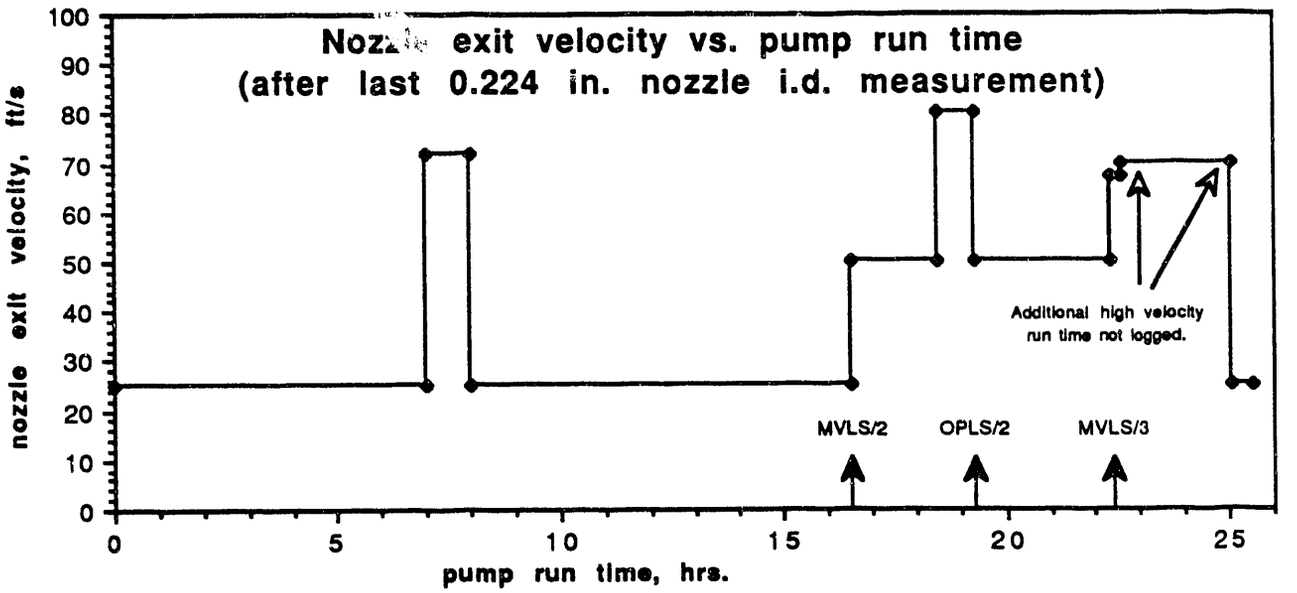

FIGURE E.2. Plot of Nozzle Exit Velocity Versus Pump Run Time for Tests After MVS/6

were taken to determine a range for the minimum barrel diameter. The low range measurement is determined by the maximum hole gage diameter that will pass through the nozzle in any orientation. The high range measurement was obtained from the maximum gage diameter that will pass through the nozzle in a single orientation.

The nozzle exits were not eroded in any uniform fashion and showed distinct grooves of maximum erosion. Some of the grooves reached 1/4 in. into the nozzle. Three measurements were taken to characterize the erosion at the nozzle exits: vertical diameter, horizontal diameter, and maximum diameter of erosion. The measurements were taken using dial calipers at a distance of 1/8 in. in from the nozzle exit. The orientation of the maximum diameter was the same for both nozzles, occurring on a line rotated 20 degrees clockwise from vertical and passing through the nozzle center. Significant erosion was evident on both ends of the line defining the maximum diameter of erosion. Table E.1 shows the measurements taken for both the north and south nozzles.

TABLE E.1. Nozzle Dimensions After Erosion

Measurement Location	South Nozzle	North Nozzle
Minimum barrel diameter	0.238 to 0.246 in.	0.240 to 0.243 in.
Vertical exit diameter	0.295 in.	0.267 in.
Horizontal exit diameter	0.264 in.	0.262 in.
Maximum diameter of erosion	0.352 in.	0.315 in.

E.3 POST-TEST PROFILING

The post-test profiling consisted of nine tests abbreviated PTMV/1-9. The tests were carried out in water and the method of testing was the same as that used for tests MV/2 through 7. In addition to vertical traverses, horizontal traverses were made of both jets at the center line height. Table E.2 shows the test matrix for the post tests. The position numbers are the same as those defined in Appendix B.

TABLE E.2. Post-Test Test Matrix

Test No.	Nominal Jet Velocity, ft/s	South Jet (traverse/ position)	North Jet, (traverse/ position)
PTMV/1	25	---	Vert/3
PTMV/2	25	Vert/3	Vert/2
PTMV/3	25	Vert/2	Vert/1
PTMV/4	25	Vert/1	---
PTMV/5	25	Horiz/1	Horiz/1
PTMV/6	50	Horiz/1	Horiz/1
PTMV/7	50	Vert/1	Vert/1
PTMV/8	50	Vert/2	Vert/2
PTMV/9	50	Vert/3	Vert/3

Data packages are included in this section and follow in the order that the tests appear in Table E.2.

Test No. PTMV/1 **Test Date:** Sept. 11, 1992

Description: Freshwater velocity profiling at 24 ft/s and r = 29 in. in the north jet.

Measurements: Vertical velocity profile is shown in Figure E.3.

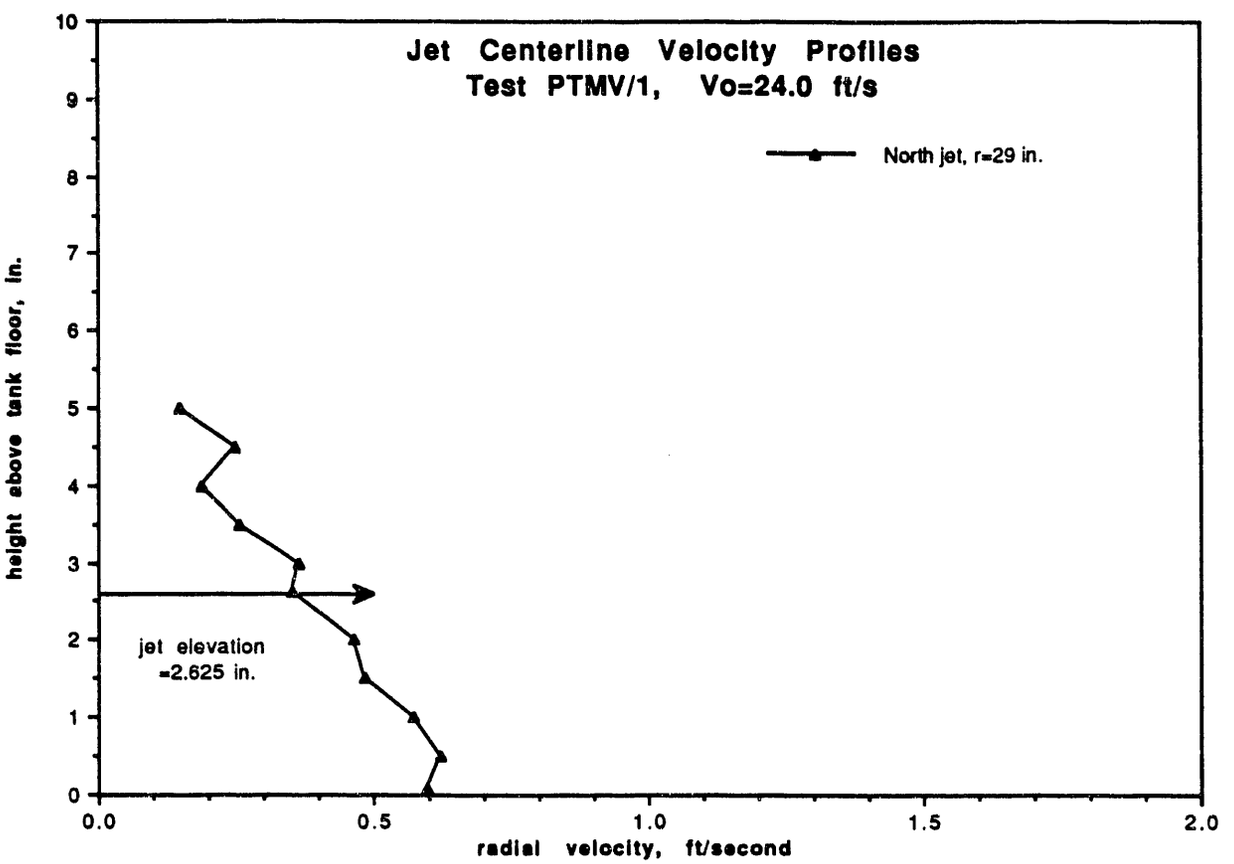

FIGURE E.3. Velocity Profile Measured in Test PTMV/1

Test No. PTMV/2 **Test Date:** Sept. 11, 1992

Description: Freshwater velocity profiling at 24 ft/s, r = 20 in. in the north jet, and r = 28.5 in. in the south jet.

Measurements: Vertical velocity profiles are shown in Figure E.4.

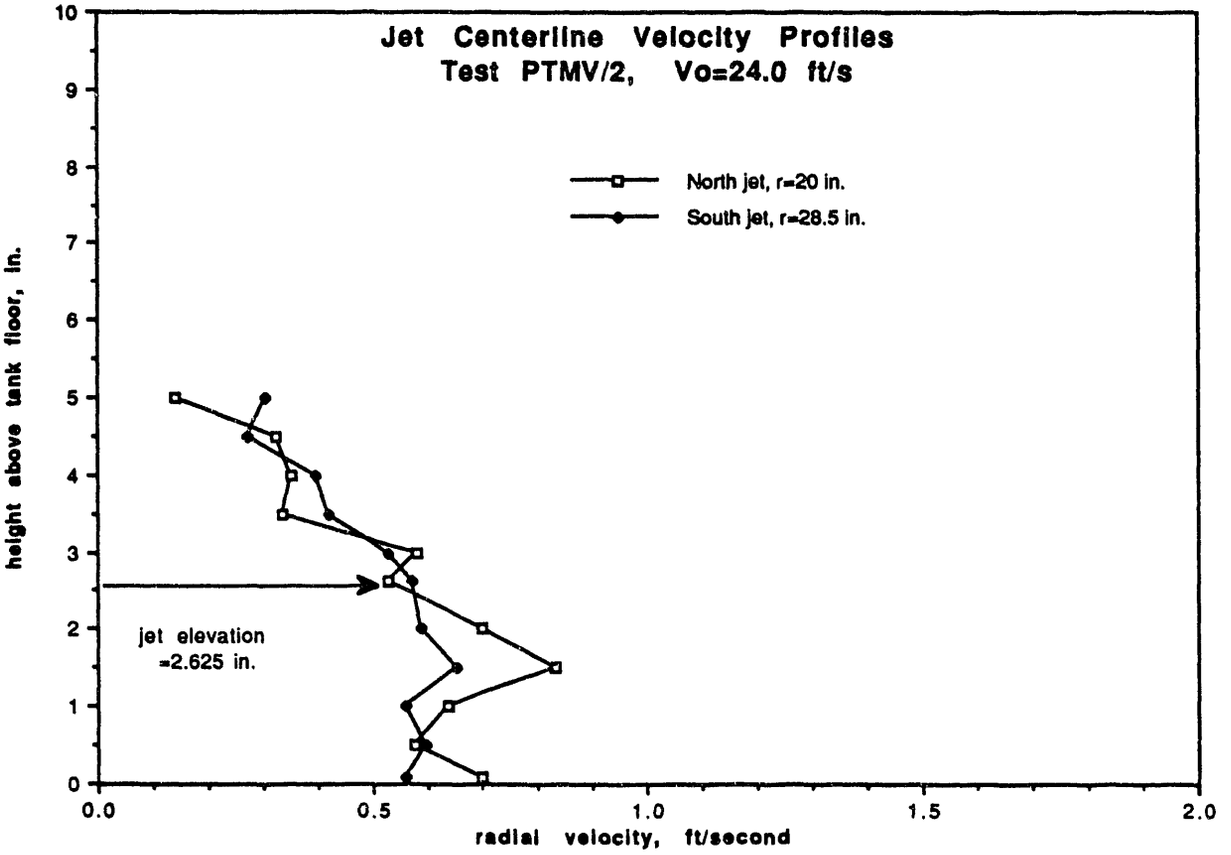

FIGURE E.4. Velocity Profiles Measured in Test PTMV/2

Test No. PTMV/3 **Test Date:** Sept. 11, 1992

Description: Freshwater velocity profiling at 24 ft/s, r = 10 in. in the north jet, and r = 20 in. in the south jet.

Measurements: Vertical velocity profiles are shown in Figure E.5.

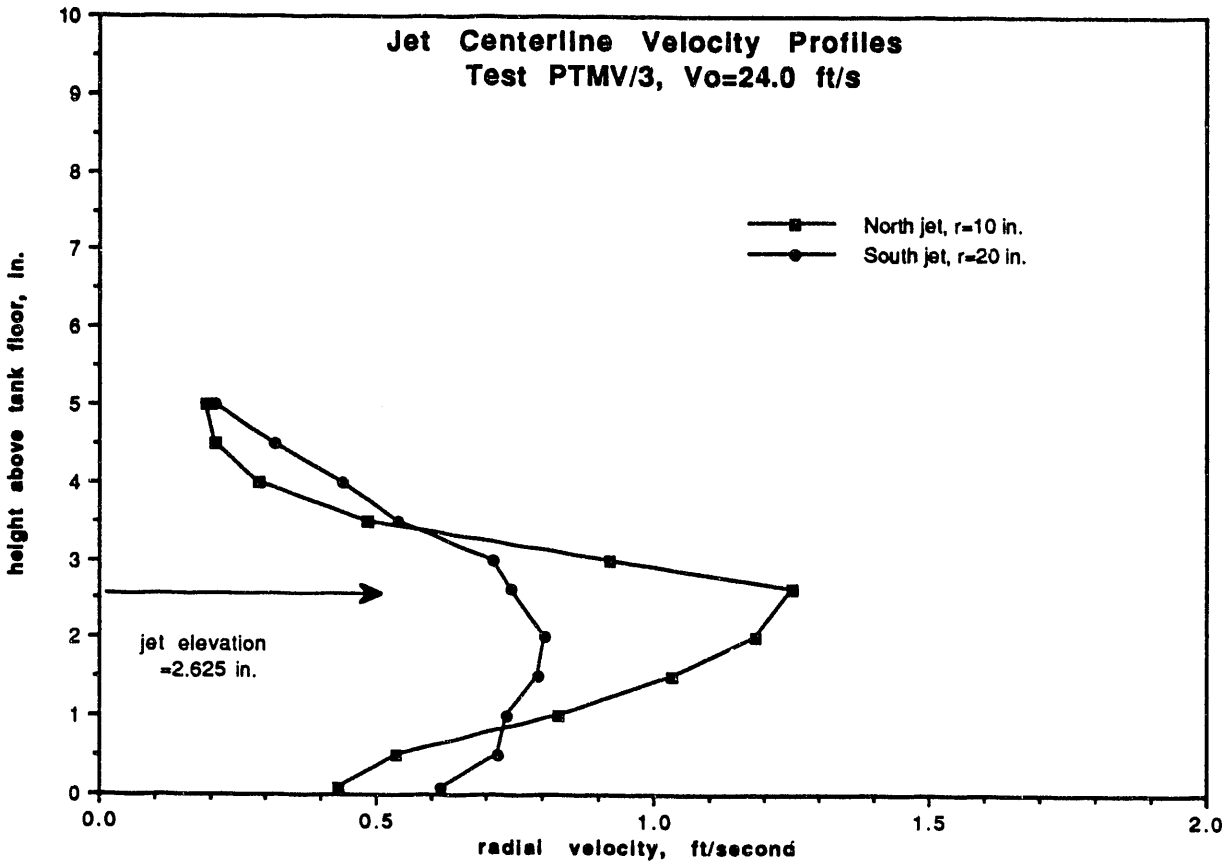

FIGURE E.5. Velocity Profiles Measured in Test PTMV/3

Test No. PTMV/4 **Test Date:** Sept. 15, 1992

Description: Freshwater velocity profiling at 24 ft/s and r = 10 in. in the south jet.

Measurements: Vertical velocity profile is shown in Figure E.6.

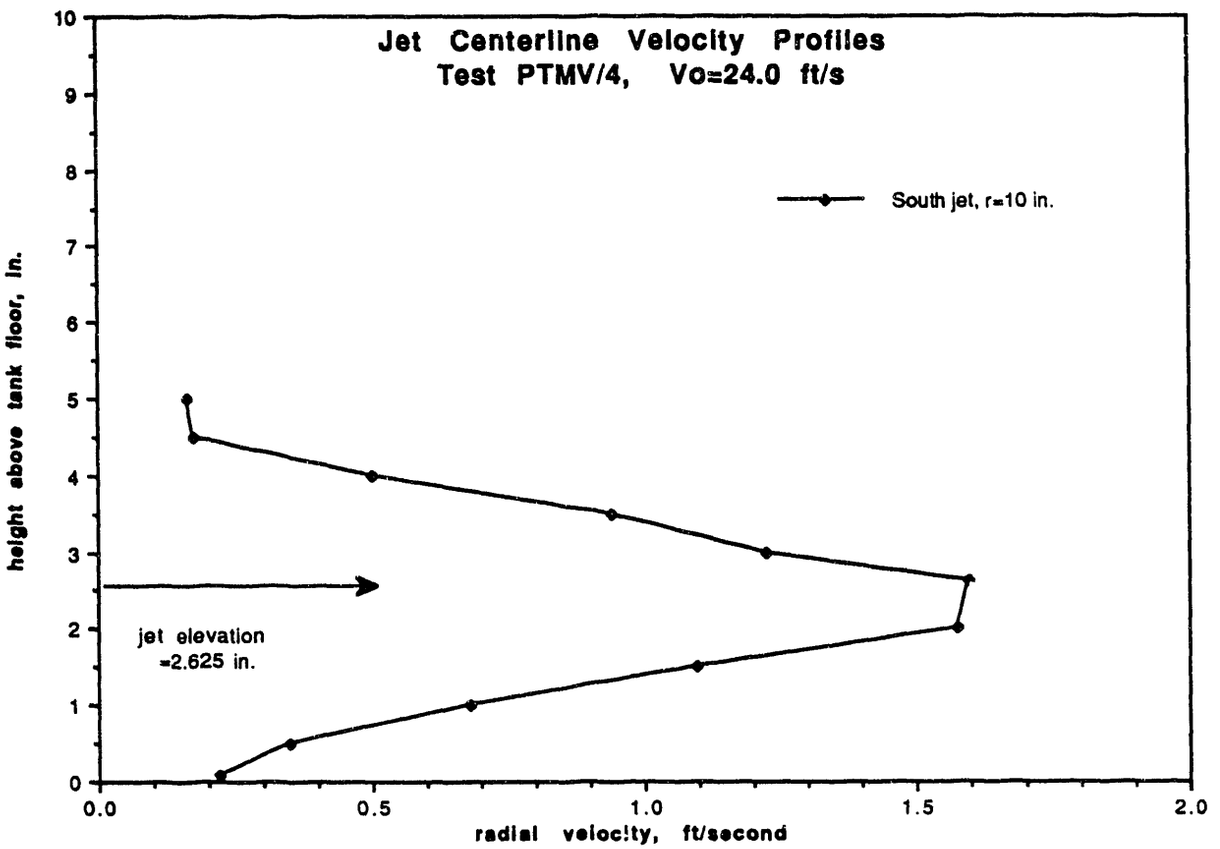

FIGURE E.6. Velocity Profile Measured in Test PTMV/4

Test No. PTMV/5 **Test Date:** Sept. 15, 1992

Description: Freshwater velocity profiling at 24 ft/s, r = 10 in. in the south jet, and r = 10 in. in the north jet.

Measurements: Horizontal velocity profiles are shown in Figure E.7.

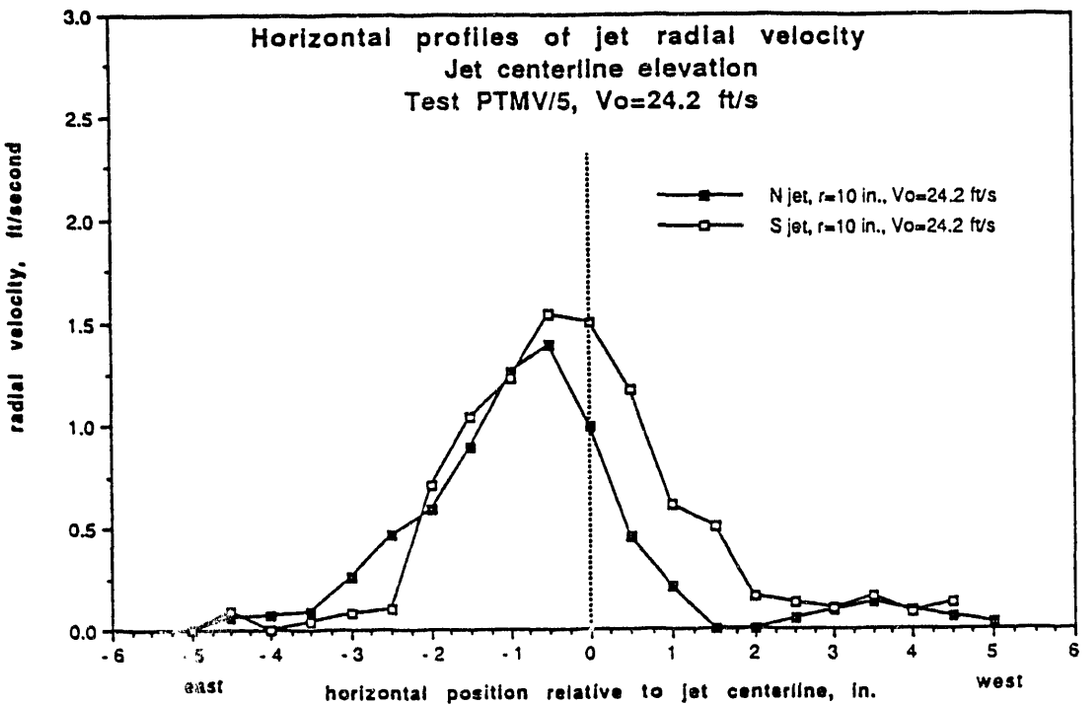

FIGURE E.7. Velocity Profiles Measured in Test PTMV/5

Test No. PTMV/6 **Test Date:** Sept. 15, 1992

Description: Freshwater velocity profiling at 52 ft/s, r = 10 in. in the south jet, and r = 10 in. in the north jet.

Measurements: Horizontal velocity profiles are shown in Figure E.8.

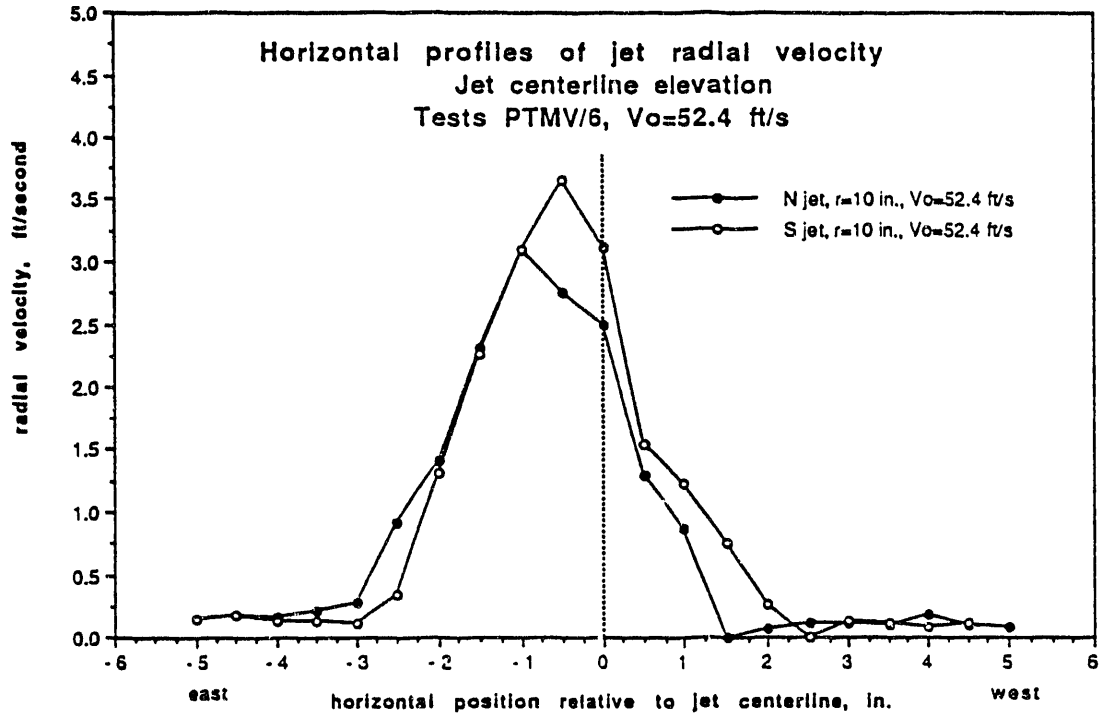

FIGURE E.8. Velocity Profiles Measured in Test PTMV/6

Test No. PTMV/7 **Test Date:** Sept. 15, 1992

Description: Freshwater velocity profiling at 52 ft/s, r = 10 in. in the south jet, and r = 10 in. in the north jet.

Measurements: Vertical velocity profiles are shown in Figure E.9.

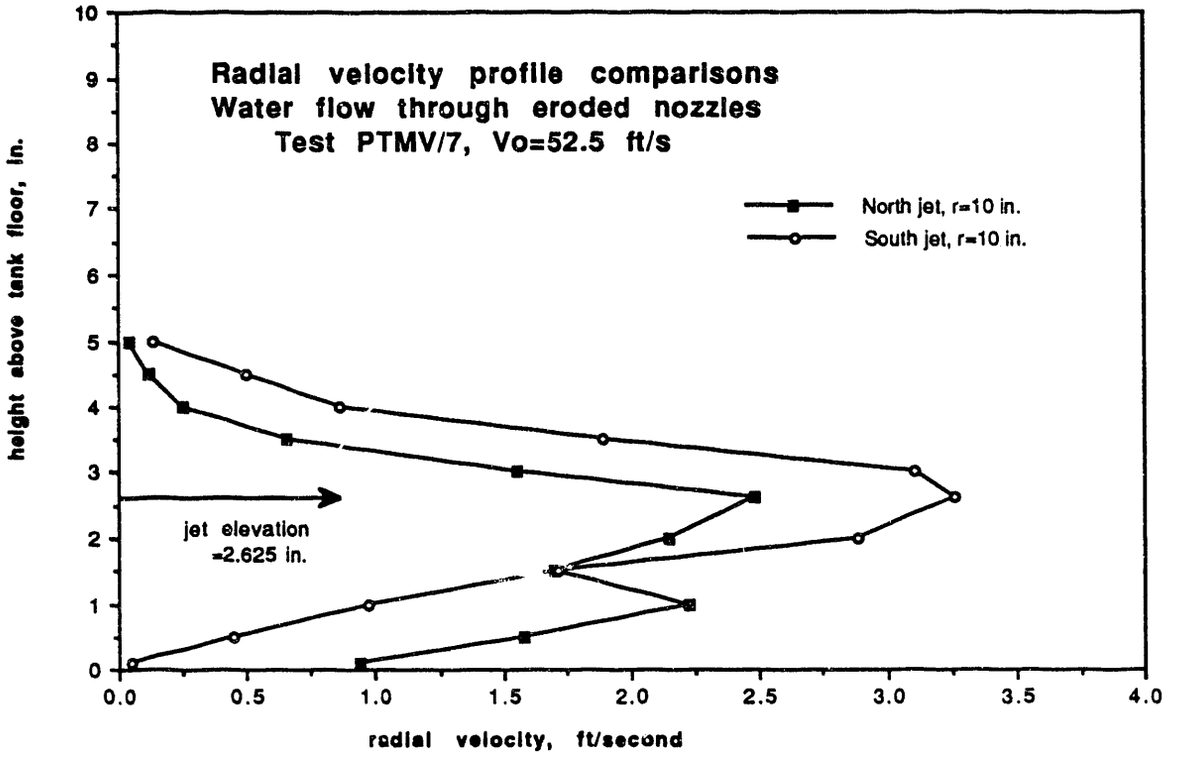

FIGURE E.9. Velocity Profiles Measured in Test PTMV/7

Test No. PTMV/8 **Test Date:** Sept. 15, 1992

Description: Freshwater velocity profiling at 52 ft/s, r = 20 in. in the south jet, and r = 20 in. in the north jet.

Measurements: Vertical velocity profiles are shown in Figure E.10.

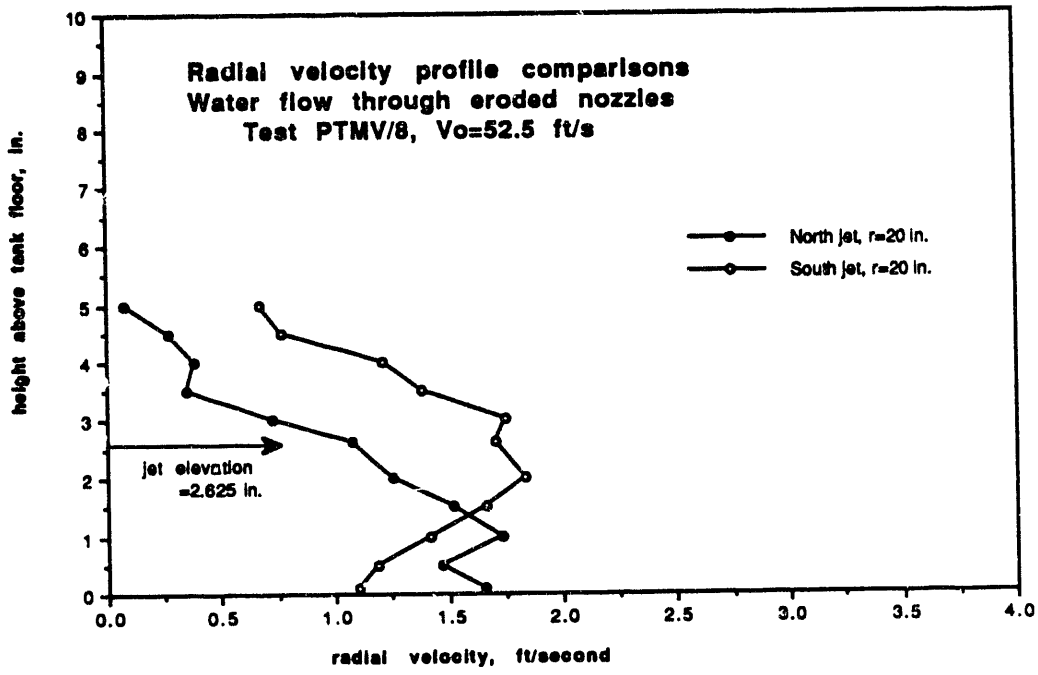

FIGURE E.10. Velocity Profiles Measured in Test PTMV/8

Test No. PTMV/9 Test Date: Sept. 15, 1992

Description: Freshwater velocity profiling at 52 ft/s, r = 20 in. in the south jet, and r = 20 in. in the north jet.

Measurements: Vertical velocity profiles are shown in Figure E.11.

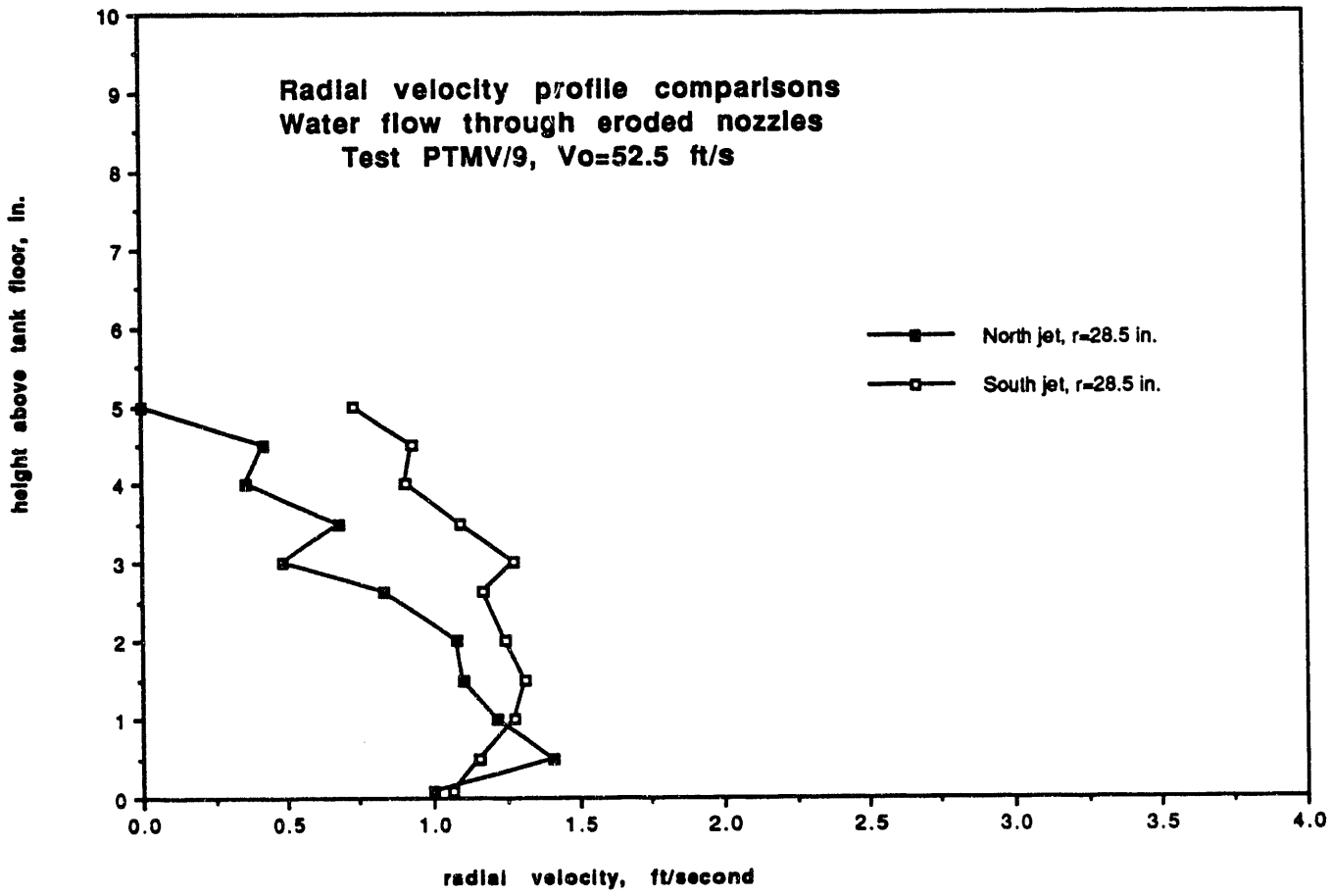

FIGURE E.11. Velocity Profiles Measured in Test PTMV/9

E.4 PROFILE COMPARISONS

This section presents comparisons between the velocity profiles obtained from the post tests and those from the fresh water model validation tests. In the model validation (MV) tests no distinction was made between the north and south jets because the assumption was made that the two jets were similar based on the results of the jet comparison tests. Velocity profiles for a particular position were made in only one jet; however, the individual jet identities were logged during the MV tests and are specified in the comparison plots that follow.

Figure E.12 shows all of the 24 ft/s vertical profiles obtained from the post tests. The profiles of the north and south jets appear fairly similar with the south jet yielding slightly higher velocities. Figure E.13 compares the post-test 24 ft/s profiles with that from the MV tests for r = 10 in. The post-test profiles have lower peak velocities and higher velocities at the top and bottom of the profiles indicating the post-test jets are spreading faster.

Profiles for r = 20 in. and r = 28.5 in. at 24 ft/s are shown in Figures E.14 and E.15, respectively. Again, flatter profiles exist for the post-test jets. At r = 20 in. the MV test's profile yields greater velocities over the entire profile. At r = 30 in., the peak velocities are relatively equal.

All of the 52 ft/s vertical profiles from the post tests are shown in Figure E.16. The profiles shown here have the same basic shapes as those measured at 24 ft/s, Figure E.12. The differences in peak velocities for the north and south jets are proportional to the increase in the jet exit velocity from 24 ft/s to 52 ft/s.

Figures E.17 through E.19 compare post-test 52 ft/s profiles to MV test profiles for the radii of 10, 20, and 28.5 in., respectively. In all three cases, the peak velocity from the MV tests was at a lower tank height than it was in the case of the 24 ft/s profiles. This phenomenon is not as clearly defined in the post-test profiles. The 10-in. profiles show no change in peak

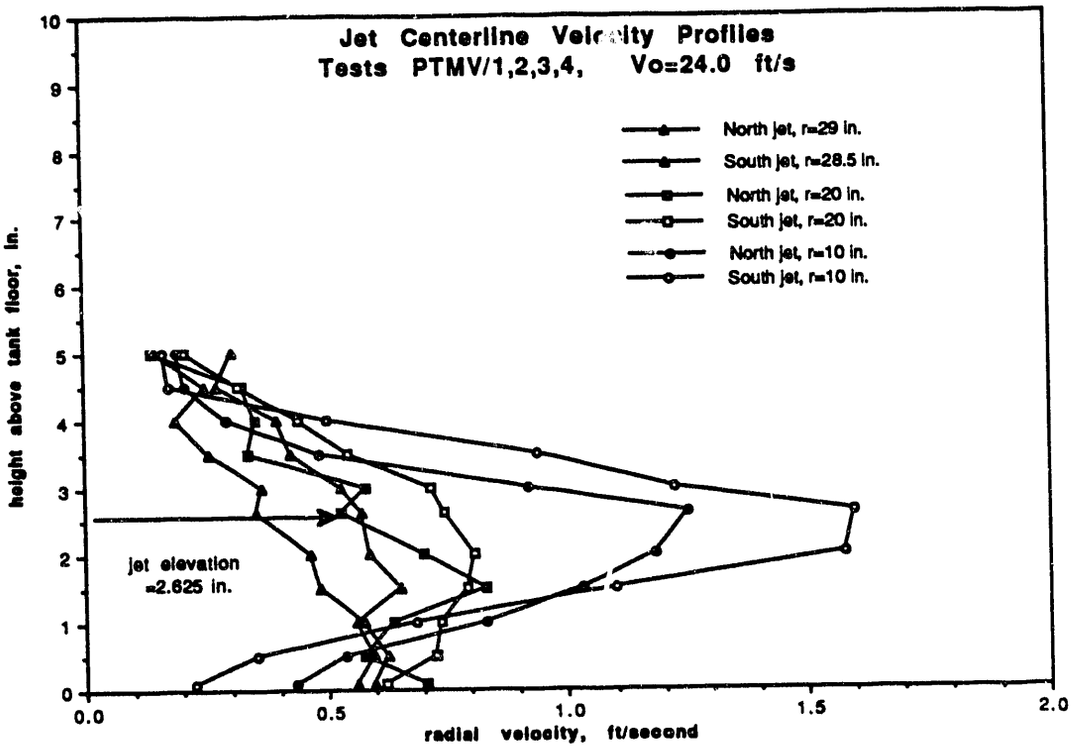

FIGURE E.12. Post-Test Vertical Velocity Profiles Obtained with a Nozzle Exit Velocity of 24 ft/s

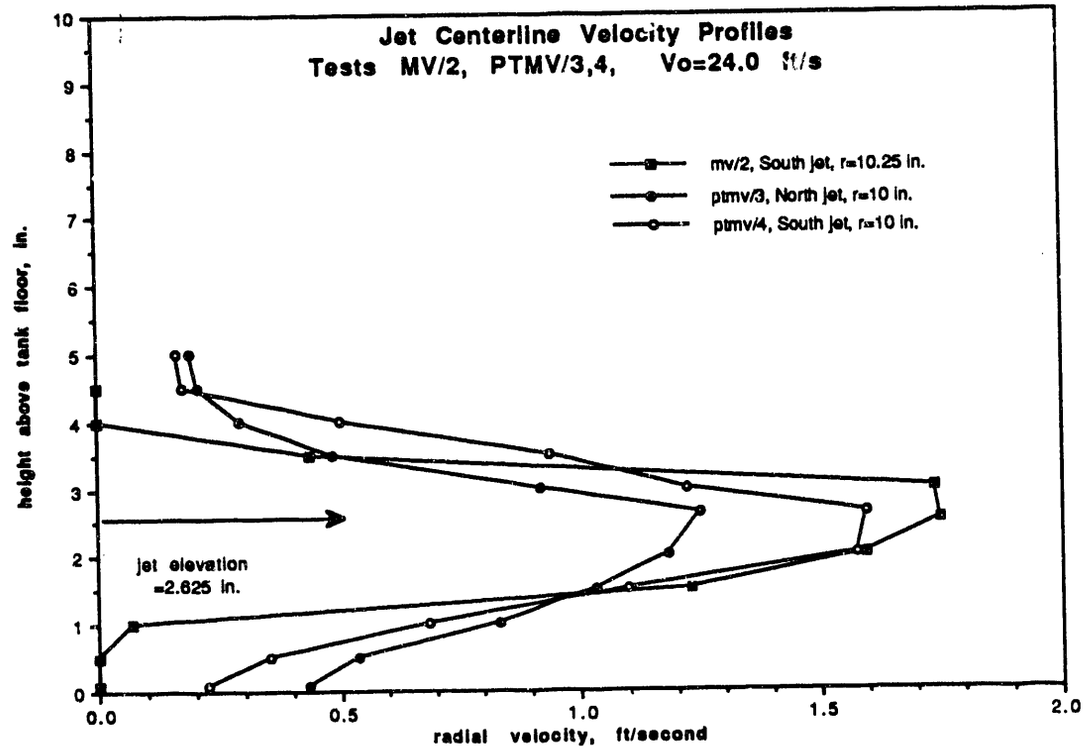

FIGURE E.13. Comparison of Vertical Velocity Profiles at a Radius of 10 in. and an Exit Velocity of 24 ft/s

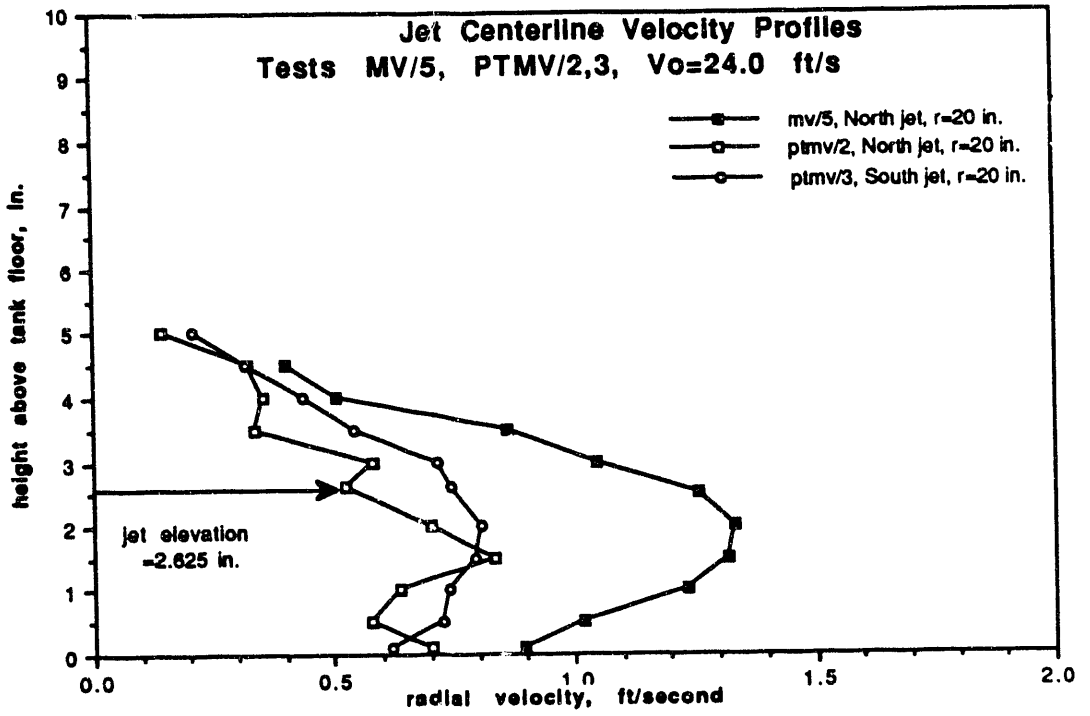

FIGURE E.14. Comparison of Vertical Velocity Profiles at a Radius of 20 in. and an Exit Velocity of 24 ft/s

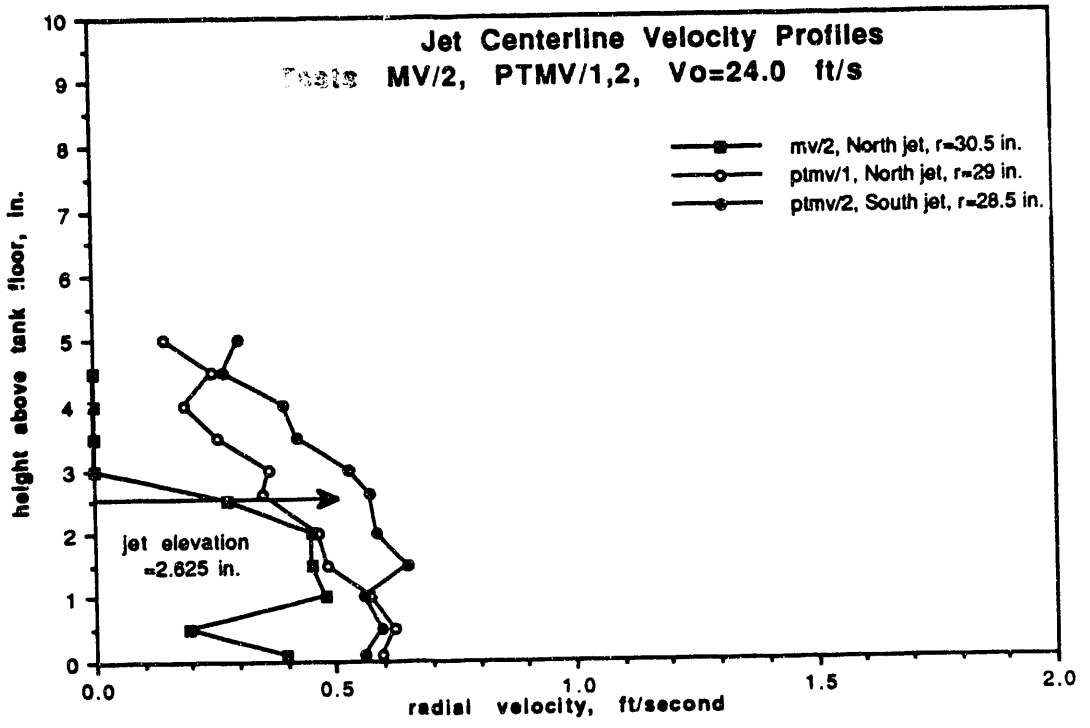

FIGURE E.15. Comparison of Vertical Velocity Profiles at a Radius of 28.5 in. and an Exit Velocity of 24 ft/s

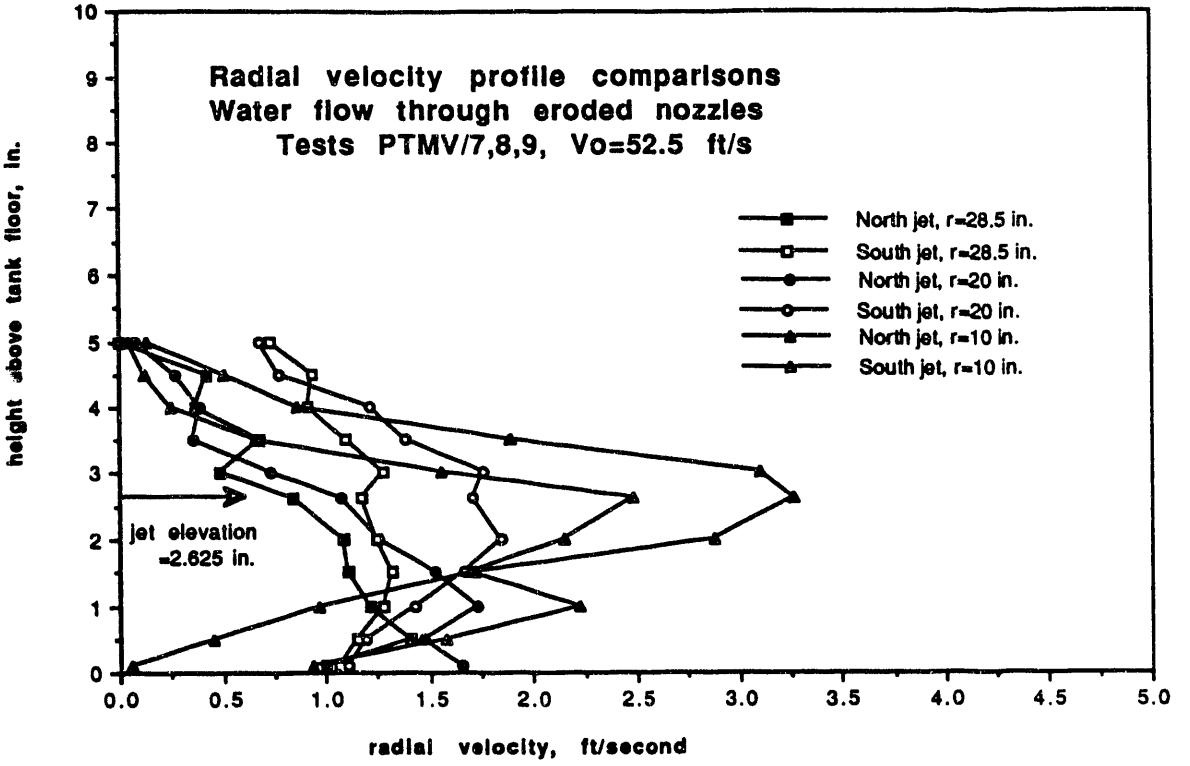

FIGURE E.16. Post-Test Vertical Velocity Profiles Obtained with a Nozzle Exit Velocity of 52.5 ft/s

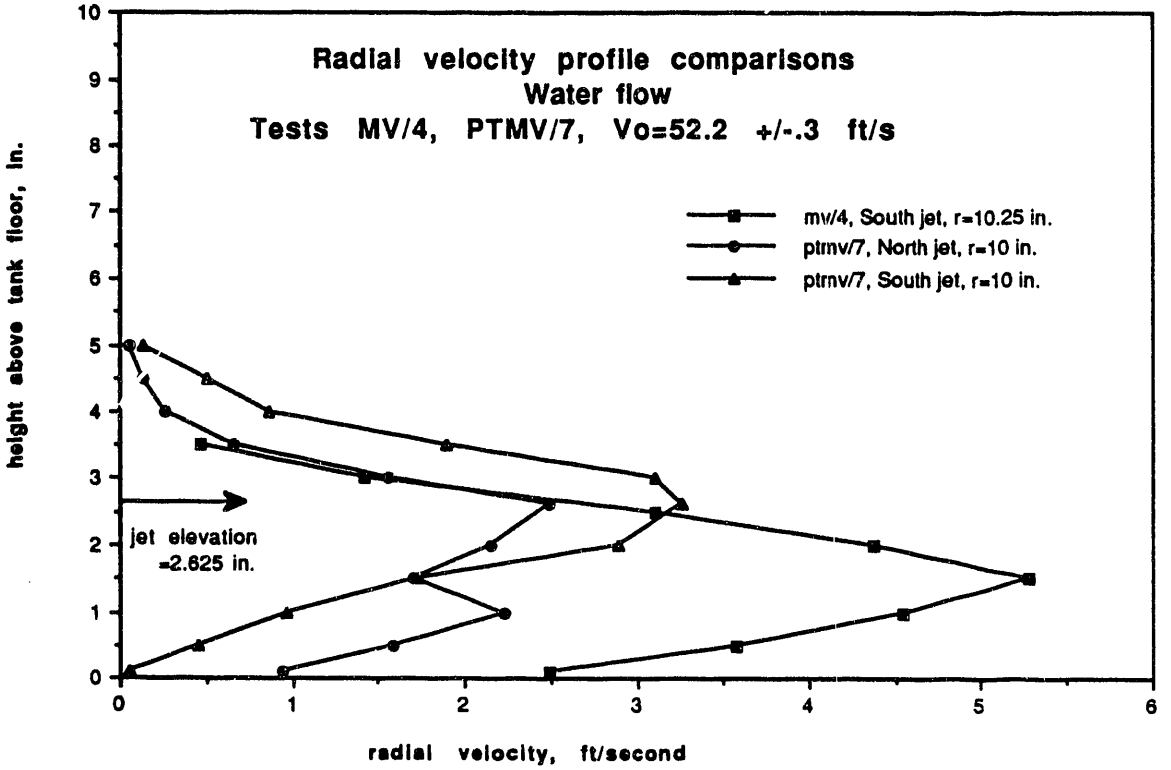

FIGURE E.17. Comparison of Vertical Velocity Profiles at a Radius of 10 in. and an Exit Velocity of 52.5 ft/s

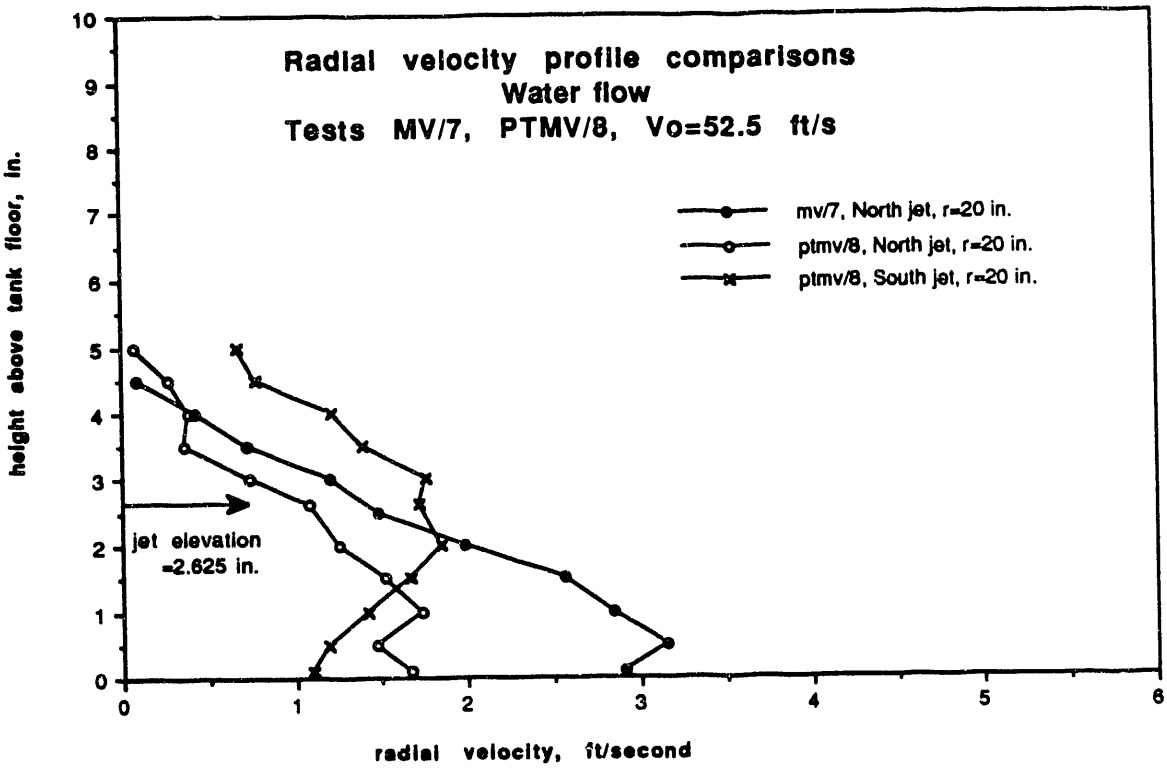

FIGURE E.18 Comparison of Vertical Velocity Profiles at a Radius of 28.5 in. and an Exit Velocity of 52.5 ft/s

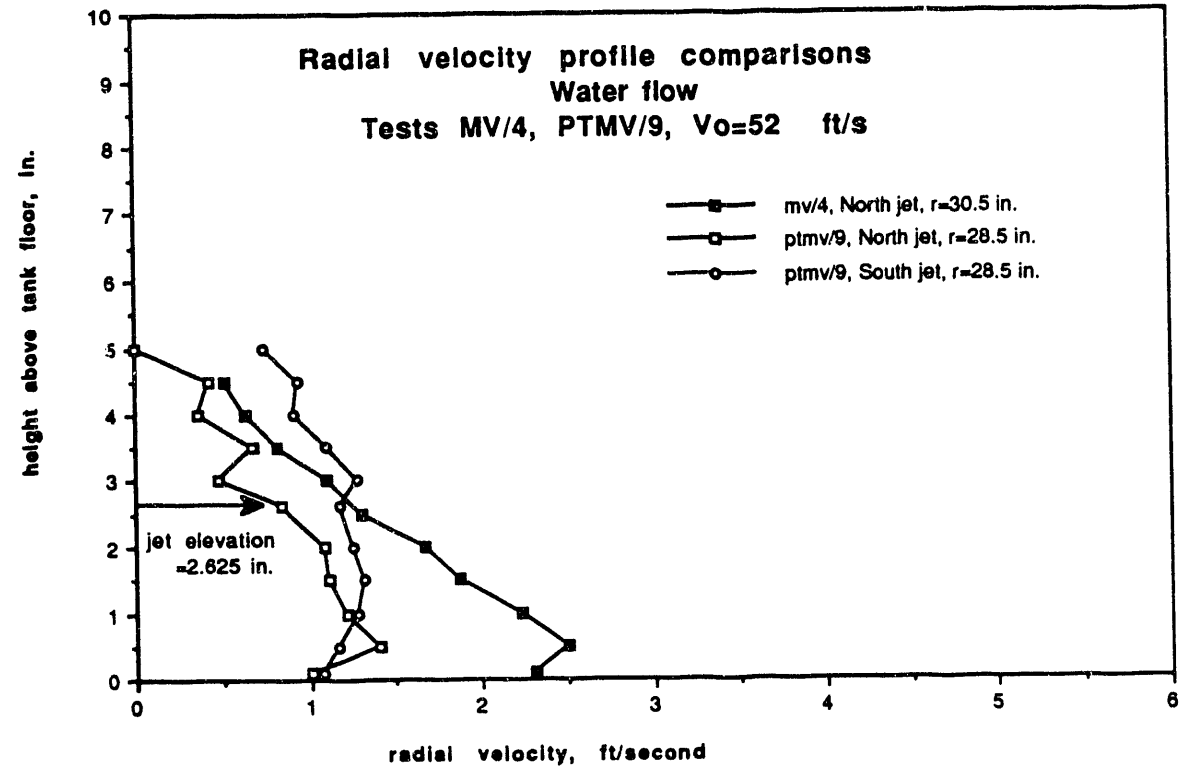

FIGURE E.19 Comparison of Vertical Velocity Profiles at a Radius of 28.5 in. and an Exit Velocity of 52.5 ft/s

velocity height. Only the north jet appears to have a drop in the peak velocity height at 20 and 30 in. and this drop is not as well defined as in the original MV tests' profiles.

Figure E.20 compares the horizontal velocity profiles of both jets for both 24 and 52 ft/s. The profiles are similar for the north and south jets. There are no horizontal profiles from the MV tests. It is evident that the peak velocities of the horizontal profiles don't fall on the tank and nozzle centerlines. It appears that both nozzles have been shifted east. Without previous horizontal profiles, it is unclear whether this is the result of erosion. After the post tests, the center position of the nozzles was checked in an attempt to account for the 0.5-in. offset of the peak velocities. The nozzles were found to be within 1/16 in. of the tank centerline. The horizontal profiles do indicate that the jets are fairly symmetrical.

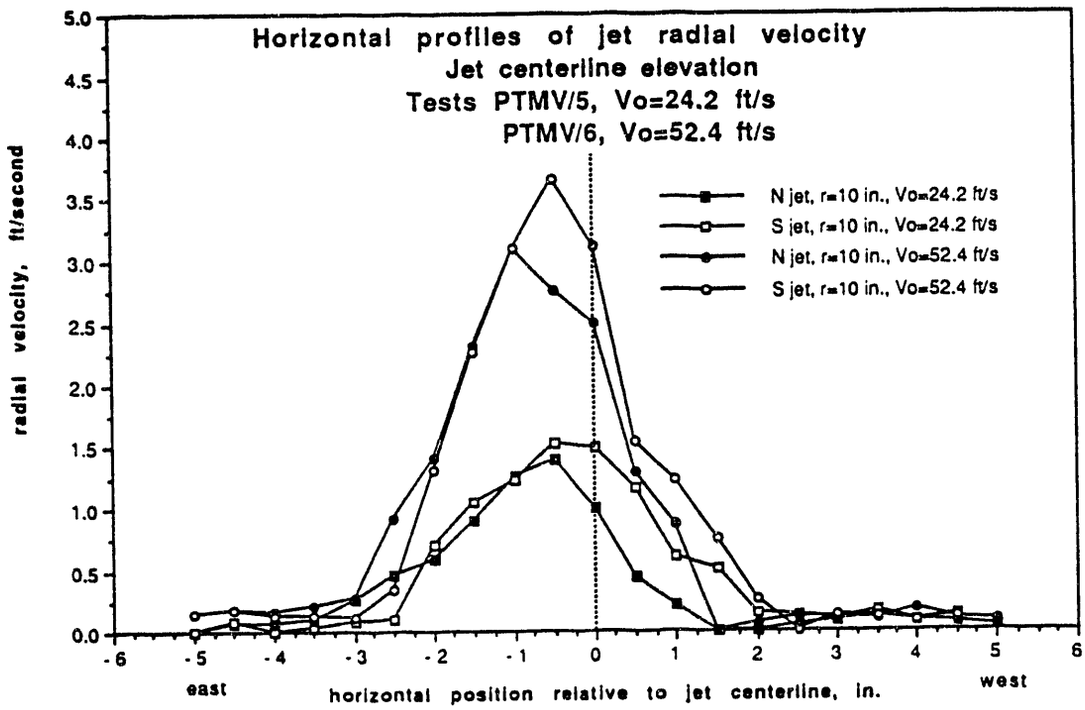

FIGURE E.20. Comparison of Post-Test Horizontal Velocity Profiles

It appears the nozzle deformity has had some effect on the jet flow fields. The north and south jet profiles are similar, but a comparison of velocity values shows the jet comparison is not as good as that observed from the jet comparison tests. The jet profiles indicate the jets spread more in the vertical plane resulting in smaller peak velocities.

Another indication of the effects of erosion is the lack of changes in height of the peak velocities with respect to exit velocities. Throughout testing a sudden downward shift in the height of the peak velocity was observed at a critical velocity. During the MV tests, the critical velocity for water was determined to be approximately 50 ft/s. A well defined shift was not observed during the post tests; however, the flow rate of the MV tests was duplicated in the post tests and the erosion of the nozzles may have resulted in lower nozzle exit velocities.

E.6 CONCLUSIONS

A comparison of the post test profiles with those from the MV tests indicates erosion has had some effect on the jet flow fields. This is observed in the velocity measurements and the critical velocity for peak velocity elevation shift. The nozzle erosion may have resulted in lower exit velocities or the change in geometry may have resulted in a change in the critical velocity.

The profiles measured are similar in shape, but it is difficult to quantify the effects of erosion caused by the lack of data from the original nozzle flow field. The lower velocities may just be the result of a shift in the jet axis to the east.

While it is difficult to quantify the effects of the erosion it is possible to predict the start of erosion and, thus, identify those tests that may contain measurements affected by the erosion. The plot of exit velocity versus pump run time shown in Figure E.1 indicates that velocities of 25 ft/s and less contribute little to erosion. Figure E.2 shows the exit velocity versus pump run time from the last time that the nozzle diameter was measured at 0.224 in. If a velocity of 25 ft/s causes negligible erosion, the nozzles should have been intact at the start of MVLS/2.

After the start of MVLS/2, almost all of the pump run time consisted of velocities greater than 50 ft/s with some as high as 80 ft/s. Based on the velocity comparisons presented in Section E.4, it appears some erosion could have been tolerated with negligible effects on the jet flow fields. It is believed by the authors that OPLS/2, MVLS/3, and MVLS/4 are the only tests that might have been affected by the nozzle erosion. Based on the high velocity run times conducted after MVLS/4, it should be safe to assume that less than half of the erosion had occurred by the completion MVLS/4.

DISTRIBUTION

No. of Copies

12 DOE Office of Scientific and Technical Information

C. S. Abrams
1987 Virginia
Idaho Falls, ID 83404

E. C. Ashby
225 North Avenue
Boggs Chemistry Building
Georgia Institute of Technology
Atlanta, GA 30332

N. E. Bibler
Westinghouse Savannah River Co.
Bldg. 773A, Room B132
Box 616
Aiken, SC 29802

D. Campbell
102 Windham Road
Oak Ridge, TN 37830

F. N. Carlson
6965 North, 5th West
Idaho Falls, ID 83401

G. R. Choppin
Department of Chemistry B-164
The Florida State University
Tallahassee, FL 32306

M. First
Harvard School of Public Health
665 Huntington Avenue
Boston, MA 02115

C. W. Forsberg
Oak Ridge National Laboratory
MS-6495, P.O. Box 2008
Oak Ridge, TN 37831-6495

No. of Copies

C. Grelecki
Hazards Research Corporation
200 Valley Road, Suite 301
Mt. Arlington, NJ 07856

E. P. Horwitz
Chemistry Division
Argonne National Laboratory
9700 Cass Avenue
Argonne, IL 60439-4831

B. C. Hudson
Lawrence Livermore National Laboratory
Nuclear Test Containment Program
P.O. Box 808, L-221
East Avenue
Livermore, CA 94550

B. R. Kowalski
Chemistry Department BG-10
University of Washington
Seattle, WA 98195

6 Los Alamos National Laboratory
P.O. Box 1663
Los Alamos, NM 87545
Attn: L. H. Sullivan, K557
J. R. White, K555
S. W. Eisenhawer, K557
J. Edwards, K557
J. Hanson, H5-09
T. E. Larson, P915

J. L. Mai
723 45th Avenue
San Francisco, CA 94121

D. Meisel
Chemistry Department
Argonne National Laboratory
9700 Cass Avenue
Argonne, IL 60439-4831

No. of
Copies

F. L. Parker
Vanderbilt University
P.O. Box 1596, Station B
Nashville, TN 37235

G. Powers
Design Science Inc.
163 Witherow Road
Sewickley, PA 15143

G. A. Russell
Professor of Chemistry
Iowa State University
Gilman Hall
Ames, IA 50011-3111

A. Schneider
Massachusetts Institute of Technology
Department of Nuclear Engineering
Room 24-1098
77 Massachusetts Avenue
Cambridge, MA 02139

W. W. Schulz
727 Sweetleaf Drive
Wilmington, DE 19808

D. D. Siemer
WINCO
IRC MS 2207
Idaho Falls, ID 83403

S. E. Slezak
Sandia National Laboratories
1515 Eubank NE
Division 6424
P.O. Box 5800
Albuquerque, NM 87185

W. J. Thomson
Dept. of Chemical Engineering
Washington State University
Pullman, WA 99164

No. of
Copies

J. Tseng
U.S. Department of Energy
EM-35
Trevion II
Washington, D.C. 20585-0002

G. Wallis
Associate Dean
Thayer School of Engineering
Dartmouth College
Hanover, NH 03755

ONSITE

4 DOE Richland Field Office

R. F. Christensen, A4-02
R. E. Gerton, A5-21
J. M. Gray, A4-02
G. W. Rosenwald, A5-21

31 Westinghouse Hanford Company

H. Babad, B2-15
T. R. Beaver, H0-33
T. R. Benegas, H5-09
H. R. Brager, L5-03
T. M. Burke, H0-34
R. J. Cash, R2-31
S. [illegible] Chang, H0-34
C. DeFigh-Price, R2-31
J. C. Fulton, R2-31
K. A. Gasper, B3-68
M. N. Hall, H5-68
C. E. Hanson, H5-09
G. D. Johnson, L5-03
N. W. Kirch, R2-11
W. L. Knecht, H0-34
J. W. Lentsch, R2-31
R. D. Marusich, H5-32
G. J. Miskho, R2-50
C. P. Molteni, R1-51
D. Ogden, H0-34
M. A. Payne, R2-50
R. W. Reed, R1-51
D. A. Reynolds, R2-11

No. of Copies

Westinghouse (contd)

D. C. Richardson, R2-31
K. Sathyanarayana, H0-34
M. H. Shannon, B1-35
D. D. Stepnewski, N1-31
T. I. Stokes, H5-09
J. D. Thomson, R1-30
R. E. Vandercook, S6-07
D. D. Wodrich, R2-23

No. of Copies

34 Pacific Northwest Laboratory

R. T. Allemann, K5-19
J. A. Bamberger, K7-15
J. M. Bates, K7-15
J. B. Colson, K5-10
M. R. Elmore, P7-19
C. W. Enderlin, K7-15
E. J. Eschbach, K7-15
L. L. Eyler, K7-15
J. A. Fort, K7-15 (5)
M. S. Greenwood, K2-31
M. S. Hanson, K1-51
B. M. Johnson, Jr., K5-02 (3)
M. R. Kreiter, K7-90 (3)
L. M. Liljegren, K7-15
N. J. Lombardo, K7-02
T. E. Michener, K7-15
R. D. Scheele, P7-25
D. M. Strachan, K2-44
D. S. Trent, K1-82
H. H. Van Tuyl, P7-22
Publishing Coordination
Technical Report Files (5)

END

DATE FILMED

5/24/93